Development of Cell-Based Assays for Adenine Receptors and Selected Purine Receptor Subtypes:
Receptor Characterization and Search for Novel Ligands

Dissertation

zur

Erlangung des Doktorgrades (Dr. rer. nat.)

der

Mathematisch-Naturwissenschaftlichen Fakultät

der

Rheinischen Friedrich-Wilhelms-Universität Bonn

vorgelegt von

Aliaa Mahmoud Mohamed Eltayb Abdelrahman

aus

Ägypten

Bonn 2010

Angefertigt mit Genehmigung der Mathematisch-Naturwissenschaftlichen Fakultät der Rheinischen Friedrich-Wilhelms-Universität Bonn

1. Referent: Prof. Dr. Christa E. Müller
2. Referent: Prof. Dr. Michael Wiese

Tag der Promotion: 20.07.2010

Erscheinungsjahr: 2010

To My Parents,

To Ali, Aia and Khaled

Table of contents

1. Introduction

1.1. Purinergic receptor and its subtypes

Purinergic receptors were first defined in 1976.[1] Later on they were divided into two families, P1 and P2 (for adenosine and nucleotides, respectively).[2] The P1 (adenosine (**1**)) receptors were divided into four receptor subtypes (A_1, A_{2A}, A_{2B}, A_3) and the P2 receptors were subdivided in two big families (P2X and P2Y receptors).[3,4] The P2Y receptors comprise eight subtypes ($P2Y_{1,2,4,6,11-14}$) which are G protein-coupled receptors (GPCR) activated by ADP (**2**), ATP (**3**), UDP (**4**), UTP (**5**) or UDP-glucose respectively.[5-7] The P2X receptors are seven ligand-gated ion channel subunits ($P2X_{1-7}$) and activated by ATP (**3**)[8,9] (Figure 1 and 2; Table 1). Both, P2XR and P2YR subtypes, can form homomers and heteromers.[10] The combinations of different receptor subtypes can result in different receptor characteristics regarding agonist and antagonist potencies and selectivities, signaling and desensitization properties. Beside P1 and P2, P0 receptors were recently suggested as a third family of purinergic receptors which are GPCRs activated by the nucleobase adenine (**6**) (Figure 1 and 2).[5]

1.1.1. P2 Receptors

1.1.1.1. P2X receptors

P2X receptors define a third major family of ionotropic receptors (besides Cys-loop channels and glutamate-gated channels) and consist of 379–595 amino acids, possessing tertiary structures with two transmembrane domains, intracellular N- and C-terminus, and post-translational modifications including glycosylation and phosphorylation. Most of the conserved regions are in the extracellular loop, with the transmembrane domains being less conserved. The extracellular loop of cloned $P2X_{1-7}$ receptors has 10 conserved cysteine residues, 14 conserved glycine residues and 2–6 potential N-linked glycosylation sites. It is believed that disulfide bridges in the extracellular loop may form the structural constraints needed to couple the ATP-binding site to the ion pore. Alignment of the sequences of the cytoplasmic C-terminal regions of P2X subunits shows that a motif (a tyrosine and a lysine separated by three amino acids) present in 39 of the 41 full-length receptor sequences in the database is conserved, and that this motif is responsible for appropriate cell surface expression and polarization of $P2X_{2-6}$ receptors.[11]

The first crystal structure of an ATP-gated $P2X_4$ ion channel in a closed, resting state, provided atomic-resolution evidence that these receptors are trimeric in subunit stoichiometry,

with each subunit being composed of two continuous, transmembrane α-helices, intracellular termini and a large disulphide-bond-rich extracellular domain.[12]
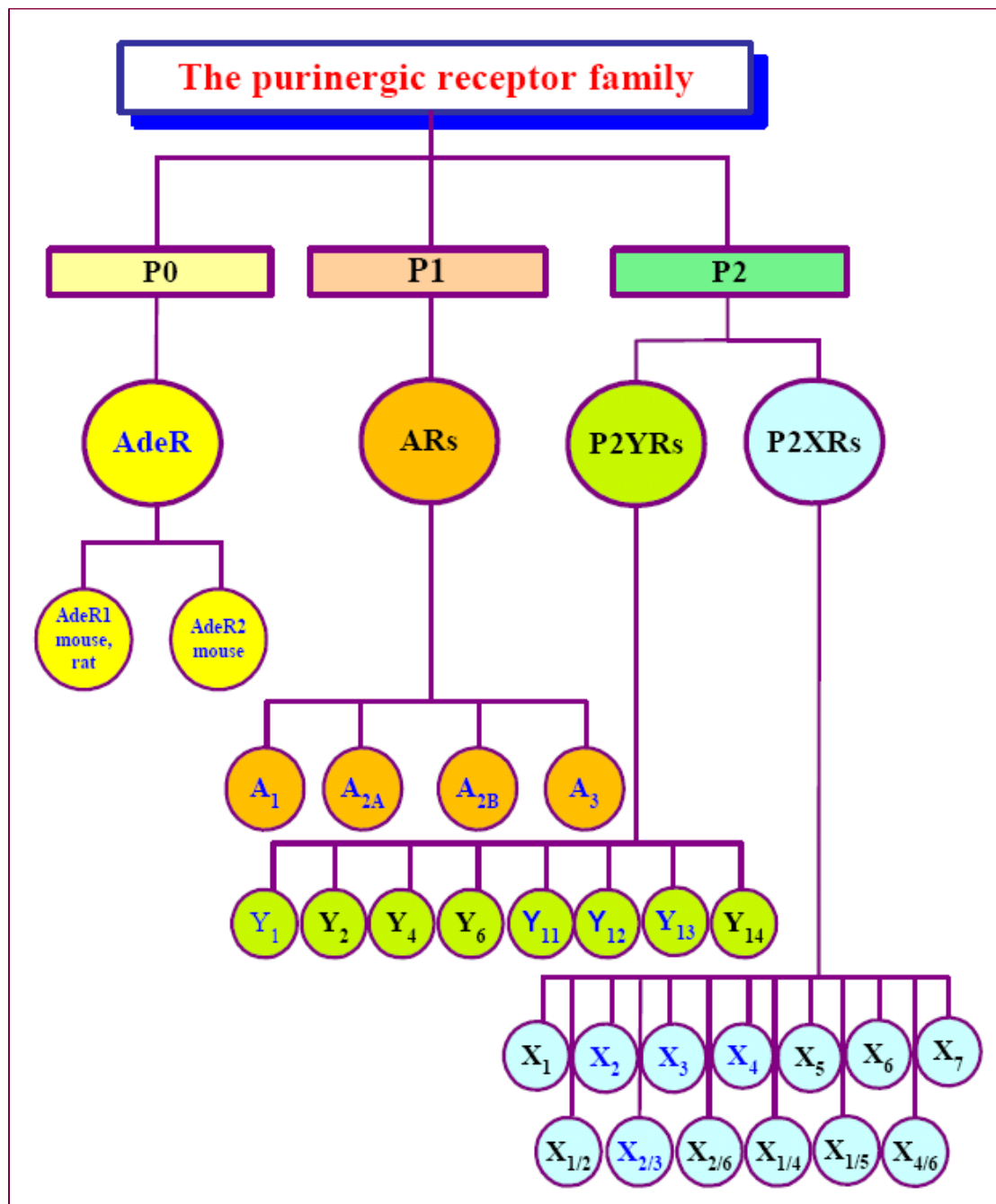
Figure 1. The purinergic receptor family.

The location of the ATP-binding site remains unknown. However it was proposed that ATP binds to a non-canonical site, 45 Å from the ion channel domain, in a deep cleft, inducing conformational changes within and between subunits. These changes are spread to the ion channel by conserved residues located at the interface between the transmembrane domain and the extracellular domain, opening the ion channel pore.[12]
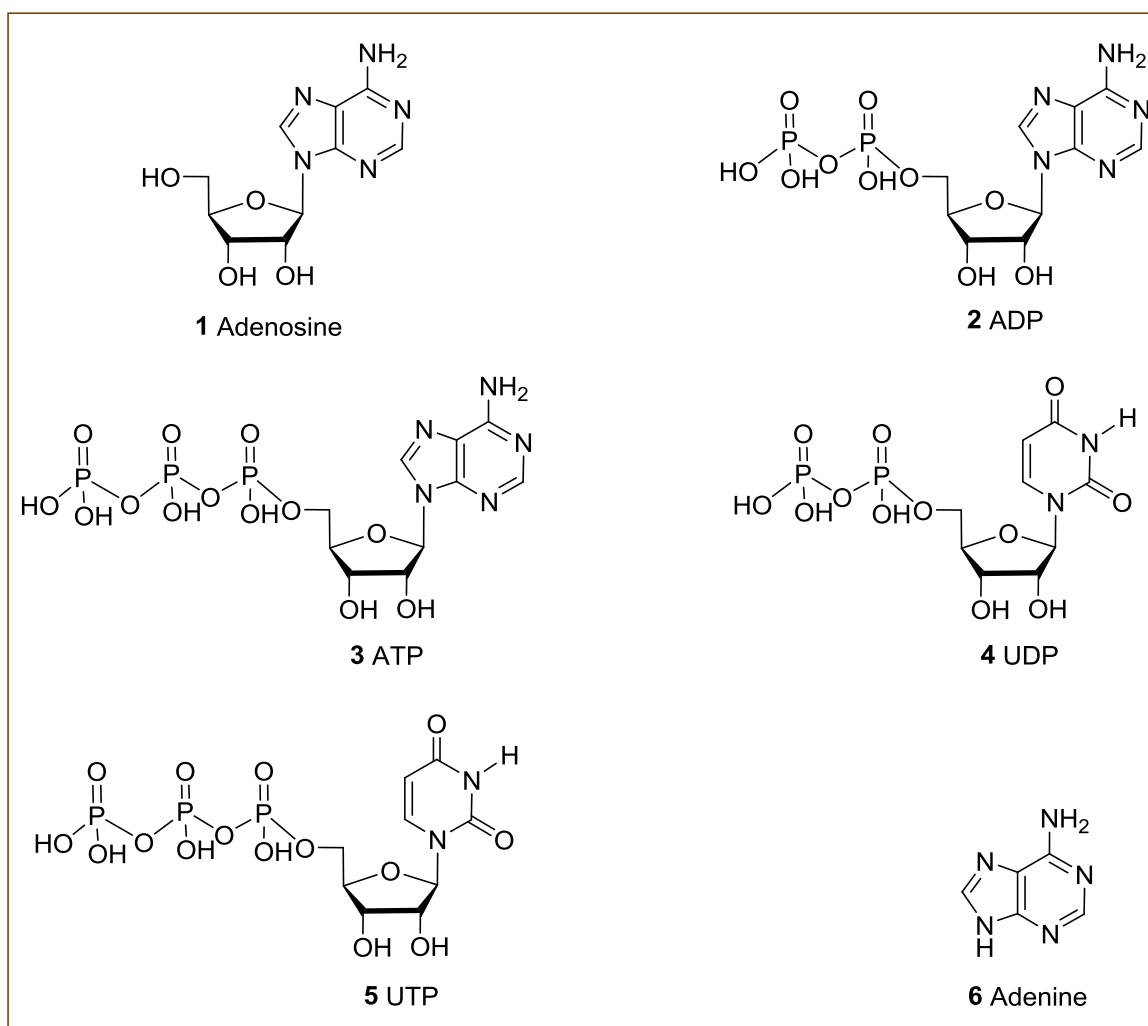
Figure 2. Physiological agonists for selected purinergic receptor subtypes.

Desensitization takes place for all P2XRs. Some of the P2XR subtypes are desensitized very fast ($P2X_1$ and $P2X_3$ receptors), whereas in others it occurs 100–1000 times more slowly (slow desensitization: $P2X_{2, 4-7}$ receptors) (Table 1).[11]

A common property to all P2X subtypes is a direct influx of extracellular Ca^{2+} (as well as Na^+), promoted by purines through the receptor channel itself. This entry is the first event in the purinergic machinery, and represents a significant source of the overall intracellular Ca^{2+} pool. This transduction mechanism does not depend on production and diffusion of second messengers within cytosol or membrane and, therefore, the cellular response-time is generally within 10 ms.[11]

Table 1. A summary of the molecular, biophysical, functional and cellular properties of recombinant homomeric P2X receptors

	P2X$_1$	P2X$_2$	P2X$_3$	P2X$_4$	P2X$_5$	P2X$_6$	P2X$_7$
Molecular properties							
Amino acids[13-20]	399	472	393	389	455	379	595
Membrane expression[13-20]	Good	Good	Good	Good	Poor	No expression in most cases	Good
Desensitization (complete in)[13-20]	Fast (<1 s)	Slow (>20 s)	Fast (<1 s)	Slow (>20 s)	Slow (>20 s)	-	Slow (>20s)
Pharmacological agonist EC$_{50}$ values (μM)[20-26] (Figure 3)							
ATP (**3**)	0.07	1.2	0.5	10	10	12	100
2-MeSATP (**7**)	0.07	1.2	0.3	10	10	9	100
α,β-MeATP (**8**)	0.3	> 300	0.8	> 300	> 300	> 100	> 300
BzATP (**9**)	0.003	0.75	0.08	7	> 500	-	20
Antagonist IC$_{50}$ values (μM)[20-26] (Figure 4)							
Suramin (**11**)	1	10	3	> 500	4	> 100	500
NF279 (**12**)	9	30	50	> 100	-	-	20
PPADS (**13**)	1	1	1	> 500	3	> 100	50
TNP-ATP (**16**)	0.006	1	0.001	15	-	-	> 30
A-317491 (**15**)	> 10	> 100	0.10	> 100	-	> 100	> 100
RO-3 (**17**)	> 100	> 100	0.10	> 100	>100		> 100
IP$_5$I (**20**)	0.003	> 300	2.8	-	-	-	-
MRS2179	80	> 100	> 100		-	-	> 100
NF449	0.8	> 100	> 100	> 100	-	-	> 100
Modulator EC$_{50}$ values (μM)[27-31]							
Ivermectin	-	> 30	> 30	0.25	-	-	> 30
Cibacron Blue	IC$_{50}$ (μM) = 0.7	-	Potentiation	Potentiation and block	-	-	-

	P2X$_1$	P2X$_2$	P2X$_3$	P2X$_4$	P2X$_5$	P2X$_6$	P2X$_7$
Zn^{2+}	-	Increase	-	Increase	-	-	
Ca^{2+}	No effect	Block	Block	-	Decrease	-	Decrease
Physiology and pathophysiology							
Major cellular expression[32]	Smooth muscle	Neurons	Pain sensing neurons	Microglia	Skeletal muscle	Broad expression	Immune cells
Major role[32]	Neuroeffector transmission	Taste, pre- and post-synaptic responses	Bladder reflexes, Chronic pain, taste	Vascular remodeling, neuropathic pain	-	-	Bone reabsorption, chronic pain
Model native cell type	Vas deferens myocytes	Superior cervical ganglia (SCG) and myenteric plexus neurons	Small dorsal root ganglion (DRG) neurons	Macrophages	Skeletal myocytes	-	Monocytes, macrophages microglia
KO available ?[32]	Yes	Yes	Yes	Yes	-	-	Yes
Major disease indication	Male infertility	-	Bladder function, pain	Neuropathic pain	-	-	Arthritis, brittle bones, pain

1.1.1.1.1. Homomeric P2X$_2$ receptor

Homomeric P2X$_2$ receptors are widely distributed throughout the peripheral and central nervous system, and on many non-neuronal cell types, where they play a role in sensory transmission and modulation of synaptic function.[23]

P2X$_2$ channels are the only homomeric P2X subtype potentiated by acidic conditions; they are also potentiated by Zn^{2+}, but inhibited by other divalent cations at high concentrations. The P2X$_2$ receptor can be activated with ATP (**3**), ATPγS, and 2-MeSATP (**7**) which are the most potent agonists, with similar EC$_{50}$ values.[21, 33-36]

Ap$_4$A is the only diadenosine polyphosphate capable of gating P2X$_2$ channels (EC$_{50}$ = 15.2 μM).[37,38] There are no known selective or highly potent antagonists for P2X$_2$ (Table 1). PPADS, TNP-ATP and reactive blue-2 are equipotent antagonists for P2X$_2$, while suramin has a tenfold lower potency than these antagonists.[23]
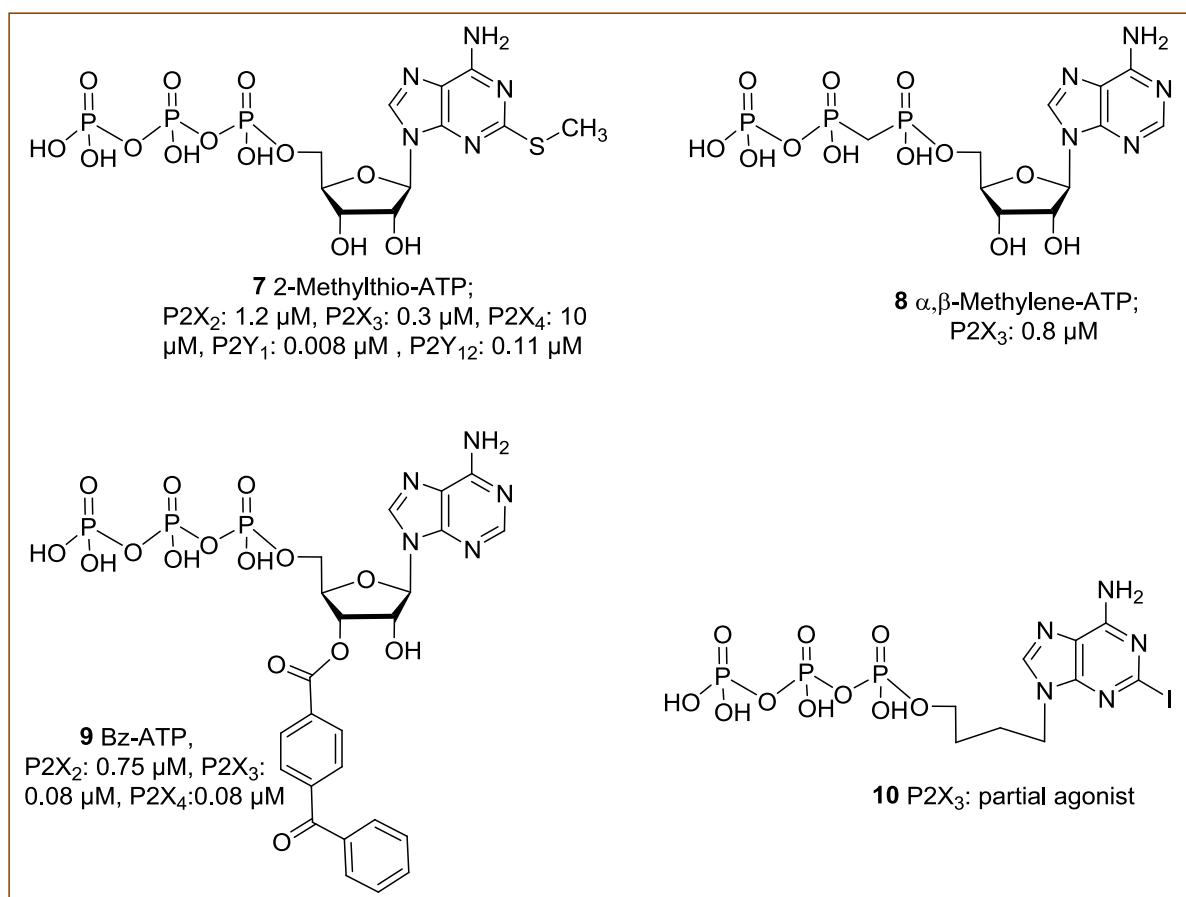
Figure 3. Chemical structures of common P2X agonists.

1.1.1.1.2. Homomeric P2X$_3$ and heteromeric P2X$_{2/3}$ receptors

P2X$_3$ and P2X$_{2/3}$ channels are predominantly localized on peripheral and central terminals of unmyelinated C-fiber and thinly myelinated Aδ sensory afferents, where they mediate sensory neurotransmission. P2X$_3$ and P2X$_{2/3}$ channels are pharmacologically similar, they are selectively gated by α,β-MeATP (**8**). These channels differ, however, in their desensitization kinetics and in their sensitivity to extracellular ions. α,β-MeATP (**8**) shows high affinity for homomeric native and recombinantly expressed P2X$_3$ channels with a rapidly desensitizing inward current (pEC$_{50}$=5.7–6.3).[21,36,39-43]

When α,β-MeATP (**8**) was tested side-by-side in the same assay systems with ATP (**3**) and 2-2-MeSATP (**7**), **3** and **7** have been shown to be slightly more potent than α,β-MeATP.[21,23,36] BzATP (**9**) is the most potent agonist at homomeric P2X$_3$ channels, with the concentration required to elicit half-maximal responses being approximately five-fold lower than that required for ATP or 2-MeSATP.[21, 36]

A series of acyclic nucleotides based on the adenine skeleton and bearing in the 9-position a phosphorylated four-carbon chain was evaluated on rat P2X$_3$ receptors (Figure 3, **10**).[44] The results showed that certain acyclic nucleotide analoges are partial agonists on P2X$_3$ receptors. This is an interesting property which can depress the function of P2X$_3$ receptors, whose activation is believed to be involved in a number of chronic pain conditions including neuropathic pain and migraine.[44]

IP$_5$I (**20**) blocked α,β-MeATP-evoked P2X$_3$ responses in a concentration-dependent manner with an IC$_{50}$ value in the micromolar range and it is a noncompetitive antagonist which binds to a site at the desensitized conformation of P2X$_3$ receptors. [45]

The heteromeric P2X$_{2/3}$ channel shares many of the activation characteristics of homomeric P2X$_3$ including selective gating by α,β-MeATP (**8**) and a similar rank order of agonist potencies.[21,41,46] However, the key difference is that α,β-MeATP-evoked inward currents through recombinant or natively expressed (nodose ganglion neurons) P2X$_{2/3}$ channels are slowly desensitizing.[39,41]

The activation of P2X$_3$ and P2X$_{2/3}$ channels by α,β-MeATP (**8**) is sensitive to inhibition by TNP-ATP (**16**). Nanomolar concentrations of TNP-ATP (**16**) can inhibit α,β-MeATP-evoked

inward currents and Ca^{2+} influx in cell lines expressing recombinant rat $P2X_3$ ($pIC_{50} = 9.0$) and $P2X_{2/3}$ ($pIC_{50} = 8.3–8.5$) channels,[47,48] representing an approximately 1,000-fold or greater selectivity over the homomeric $P2X_2$ receptors. α,β-MeATP (**8**) evoked currents through natively expressed rat $P2X_3$ (DRG neurons) and $P2X_{2/3}$ (nodose ganglion neurons) channels are also inhibited by TNP-ATP (**16**) with $pIC_{50}s$ of 9.1–9.5 and 7.7, respectively.[40,49]

R = CH$_3$ **11** Suramin, P2X$_2$: 10 μM,
P2X$_3$: 3 μM
R = H   **12** NF279   P2X$_2$: 30 μM,
P2X$_3$: 50 μM
R = F   **12a** NF157   P2Y$_{11}$: 0.0447 μM

13 PPADS, P2X$_2$: 1 μM,
P2X$_3$: 1 μM

14 Reactive Blue 2

15 A-31491, P2X$_3$: 0.10 μM
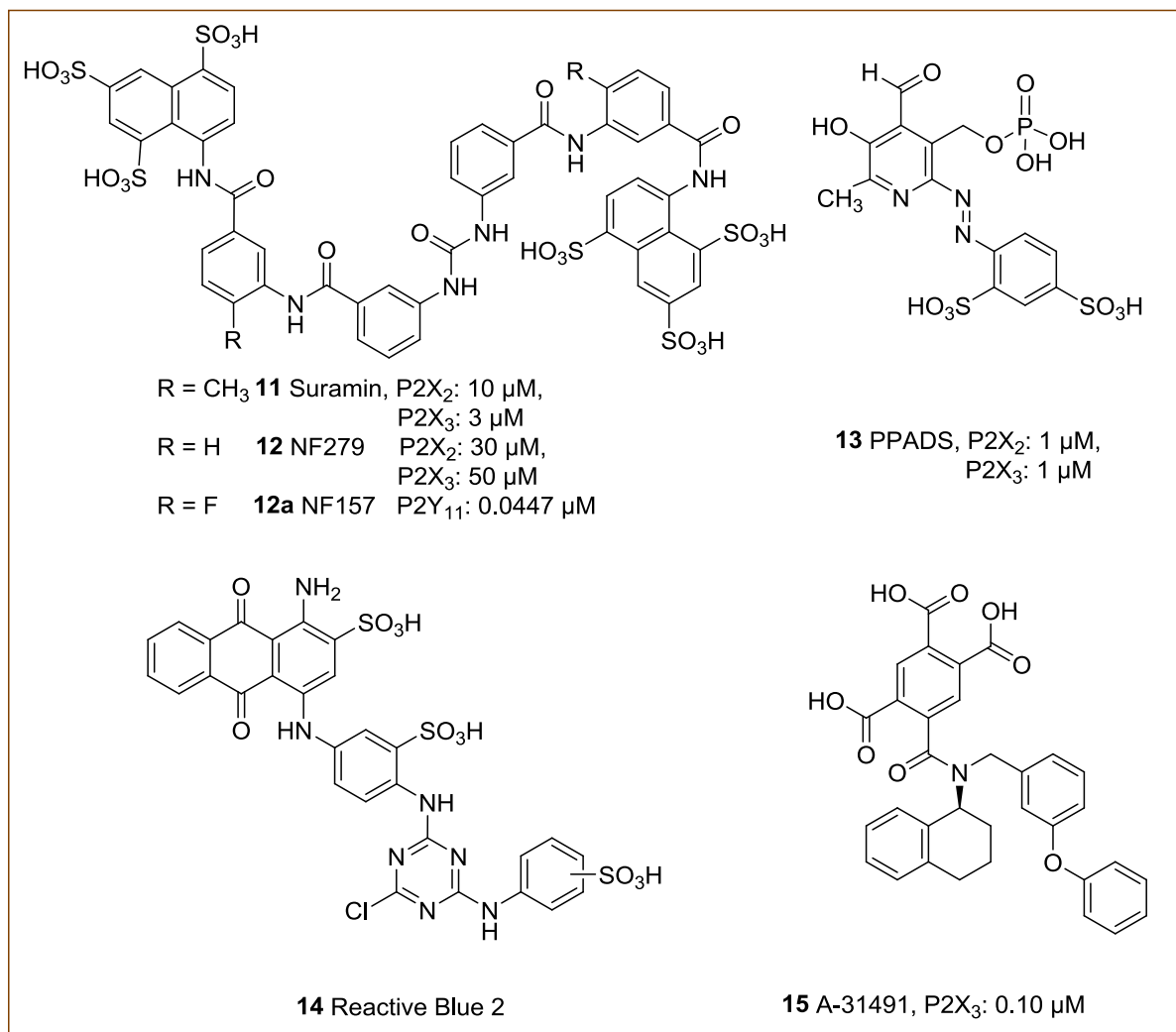
Figure 4. Chemical structures of P2X antagonists with multiple acidic functional groups leading to poor *in vivo* pharmacokinetic properties.

A-317491(**15**) is a non-nucleotide competitive antagonist of $P2X_3$ and $P2X_{2/3}$ receptor activation. A-317491 (**15**) blocked recombinant human and rat $P2X_3$ and $P2X_{2/3}$ receptor-mediated calcium flux (Ki = 22-92 nM). RO-3 (Figure 5, **17**) is identified as an antagonist for $P2X_3$ receptors (pIC_{50}-7.0, IC_{50}: 0.1 μM) and $P2X_{2/3}$ receptors (pIC_{50}=5.9, IC_{50}: 1 μM). RO-4 (**18**) is a potent, selective and drug-like dual $P2X_3$/$P2X_{2/3}$ antagonist for the treatment of pain.[50]

1.1.1.1.3. Homomeric P2X$_4$ receptors

P2X$_4$ subunits are widely distributed within neuronal and non-neuronal tissues. P2X$_4$ channels localized on activated microglia have been implicated in chronic inflammatory and neuropathic pain. Homomeric P2X$_4$ channels generally produce a slowly desensitizing inward current in response to ATP (**3**).[23]

The rat P2X$_4$ receptor is different from other P2X channels due to its relative insensitivity to classic, non-selective P2X antagonists, such as suramin (**11**) and PPADS (**13**), even at high concentrations of 100–500 μM.[51-53] It has been reported that suramin (**11**), PPADS (**13**), and cibacron blue at some concentrations can potentiate ATP-evoked currents in rat and mouse P2X$_4$.[54-56]
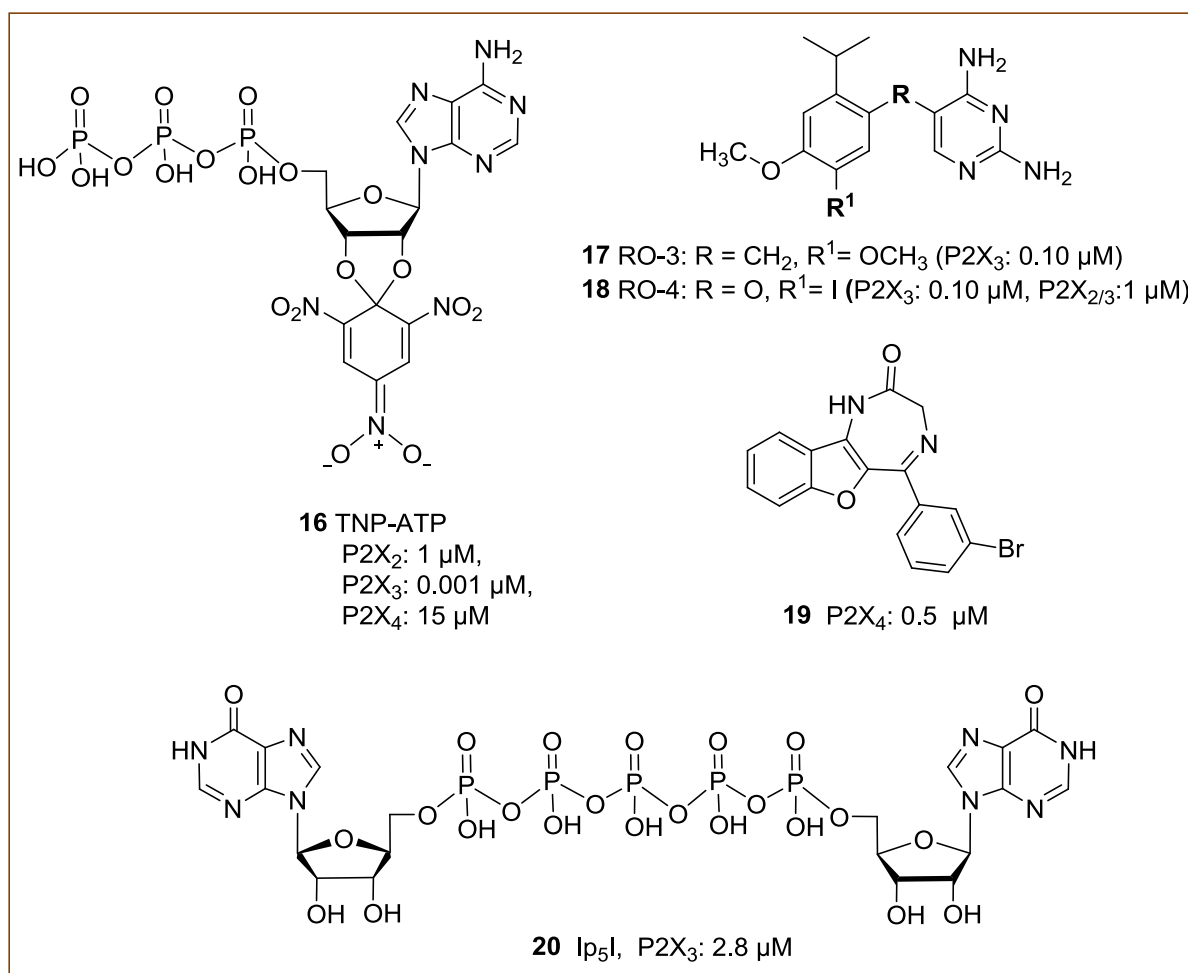
Figure 5. Commonly used P2X antagonists: Nucleotides related to the structure of ATP: TNP-ATP is an antagonist. RO-3 and RO-4 are a selective antagonist with improved "drug-like" properties (e.g., oral bioavailability, improved metabolic stability);benzofuro-1,4-diazepin-2-one (selective P2X$_4$ antagonist); dinucleotide Ip$_5$I.

However, the rat $P2X_4$ may be uniquely insensitive as moderate sensitivity of the human $P2X_4$ has been reported for several antagonists, including PPADS (**13**) (human $P2X_4$ pIC_{50}=4.6–5.0; rat $P2X_4$ $pIC_{50} < 3.3$), suramin (**11**) (human $P2X_4$ $pIC_{50} = 3.7$; rat $P2X_4$ $pIC_{50} <$ 3.3), bromphenol blue (human $P2X_4$ $pIC_{50} = 4.1$; rat $P2X_4$ $pIC_{50} < 3.5$), and cibacron blue (human $P2X_4$ $pIC_{50} = 4.4$; rat $P2X_4$ $pIC_{50} = 3.9$), and the mouse $P2X_4$ has also been reported to be inhibited by PPADS (**13**) at a concentration of 10 μM with a potency similar to that seen at the human $P2X_4$.[13,52] The lack of selective $P2X_4$ antagonists has hindered the pharmacological validation of the role for $P2X_4$ receptors in pain. 5-(3-bromophenyl)-1,3-dihydro-2*H*-benzofuro-[3,2-*e*]-1,4-diazepin-2-one (Figure 5, **19**) was shown to block $P2X_4$-mediated currents expressed in Chinese hamster ovary cells with an IC_{50} value of 0.5 μM.[22]

Neuropathic pain is characterized by pain hypersensitivity to innocuous stimuli (tactile allodynia) that is nearly always resistant to known treatments such as non-steroidal anti-inflammatory drugs or even opioids. Some antidepressants are effective for treating neuropathic pain. However, the molecular mechanisms are not well understood. Paroxetine exhibited inhibition of calcium influx via rat and human $P2X_4$ receptors, with IC_{50} values of 2.45 μM and 1.87 μM, respectively. The inhibition on $P2X_4$ receptors may clarify the analgesic effect of paroxetine, and it is possible that some antidepressants clinically used in patients with neuropathic pain show antiallodynic effects, at least in part via their inhibitory effects on $P2X_4$ receptors.[57]

1.1.1.2. P2Y receptors

Metabotropic P2Y receptors (P2YRs) consist of 308–379 amino acids, with a mass of 41–53 kDa after glycosylation. They possess tertiary structures with seven transmembrane domains, an extracellular N-terminus and an intracellular C-terminus. Basic residues near the extracellular surface may be involved in ligand binding and coordination of the polyphosphate chain of the endogenous ligands.[11]

Eight different subtypes have been cloned (Table 2) of the $P2Y_{(1,2,4,6,11-14)}$ receptor family. The missing numbers represent either non-mammalian orthologs or receptors having some sequence homology to P2Y receptors but without functional evidence of responsiveness to nucleotides.[11]

Based on phylogenetic and structural considerations (i.e., protein sequence), P2Y receptors can be subdivided into at least two groups by a relatively high level of sequence difference (Figure 6):[6]

1)P2Y$_1$-like receptors including P2Y$_1$, P2Y$_2$, P2Y$_4$, P2Y$_6$, P2Y$_{11}$

2)P2Y$_{12}$-like receptors including P2Y$_{12}$, P2Y$_{13}$ and P2Y$_{14}$.
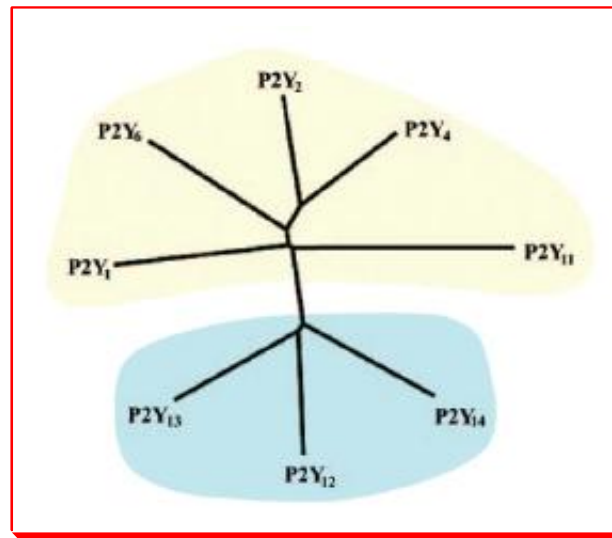
Figure 6. A phylogenetic tree (dendrogram) showing the relationships among the current members of the P2Y receptor family. The P2Y receptors can be divided into two subgroups, shown with green and blue backgrounds. Sequences were aligned using CLUSTALX, and the tree was built using the TREEVIEW software.[6]

Pharmacologically the P2Y receptors can be subdivided into four groups:[11]

- Adenine nucleotide-activated receptors sensitive to ADP (**2**) and ATP (**3**). This group includes P2Y$_1$, P2Y$_{12}$, and P2Y$_{13}$, and P2Y$_{11}$ (which has been reported to also respond to UTP (**5**)[57]);

- uracil nucleotide-receptors; this group includes P2Y$_4$ and P2Y$_6$ responding to either UDP (**4**) or UTP (**5**);

- Mixed selectivity receptors (human and rodent P2Y$_2$, rodent P2Y$_4$ and, may be, P2Y$_{11}$); and

- Receptors activated by the sugar nucleotides UDP-glucose and UDP-galactose (P2Y$_{14}$).

P2Y receptor subtypes can also form heteromeric complexes,[58] and recently, adenosine A$_1$ receptors have been shown to form a heteromeric complex with P2Y$_1$ receptors.[60,61] Dopamine D$_1$ and adenosine A$_1$ receptors have also been shown to form functionally interactive heteromeric complexes.[62] Only recently hetero-oligomerization between P2Y$_1$ and P2Y$_{11}$ receptors has been described.[63] An interesting functional consequence of the interaction between the P2Y$_{11}$ receptor and the P2Y$_1$ receptor was found: it promotes an agonist-induced internalization of the P2Y$_{11}$ receptor. This is remarkable because the P2Y$_{11}$ receptor expressed alone is not able to undergo endocytosis.[63]

Table 2. Overview of P2Y receptors subtypes[5,6&64]

Subunit	Amino acids	Agonist	Signal transduction	In vitro test systems		Main distribution	Main functions
				Radioligand binding studies	**Functional studies**		
$P2Y_1$	373	ADP	G_q, PLC	[^{3}H]MRS2279; [^{33}P]MRS2179	IP_3 accumulation and $[Ca^{2+}]_i$ mobilization	Epithelial and endothelial cells, platelets, immune cells, osteoclasts, glial cells	Smooth muscle relaxation & mitogenic actions; platelet shape change & aggregation; bone resorption
$P2Y_2$	376	UTP, ATP	G_q, PLC	None	IP_3 accumulation and $[Ca^{2+}]_i$ mobilization	Immune cells, epithelial and endothelial cells, kidney tubules, osteoblasts, astrocytes	Vasodilatation through endothelium & vasoconstriction through smooth muscle; mitogenic actions; mediates surfactant secretion; epithelial cell Cl^- secretion; bone remodelling
$P2Y_4$	365	UTP	G_q, PLC	None	IP_3 accumulation and $[Ca^{2+}]_i$ mobilization	Endothelial and epithelial cells, intestine, pituitary, brain	Regulates epithelial Cl^- transport; vasodilatation through endothelium; mitogenic actions
$P2Y_6$	328	UDP	G_q, PLC	None	IP_3 accumulation and $[Ca^{2+}]_i$ mobilization	Some epithelial cells, placenta, T cells, thymus, spleen, kidney, activated microglia	NaCl secretion in colonic epithelium; role in epithelial proliferation

P2Y$_{11}$	371	ATP	G$_s$, cAMP G$_q$, PLC	None	cAMP measurement; $[Ca^{2+}]_i$ mobilization; IP$_3$ accumulation	Spleen, intestine, brain, granulocytes	Role in maturation & migration of dendritic cells; granulocytic differentiation
P2Y$_{12}$	342	ADP	G$_i$, cAMP	[^{33}P]2-MeSADP; [^{3}H]PSB-0413	cAMP measurement in stably transfected cells; cAMP measurement in platelets	Platelets, glial cells, spinal cord	Platelet aggregation; role in dense granule secretion
P2Y$_{13}$	333	ADP	G$_i$, cAMP	[^{33}P]2-MeSADP	IP$_3$ measurement in 1321N1 astrocytoma cells that express recombinant receptor; cAMP measurement; [^{35}S] GTPγs binding	Spleen, brain, lymph nodes, bone marrow, liver, pancreas, heart	Function largely unknown, but present in both the immune system and brain
P2Y$_{14}$	338	UDP-glucose	G$_i$, cAMP	None	cAMP measurement	Placenta, adipose tissue, stomach, intestine, discrete brain regions, spleen, lung, heart, bone marrow, peripheral immune cells	Chemoattractant receptor in bone marrow hematopoietic stem cells; dendritic cell activation

1.1.1.2.1. $P2Y_1$ receptors

The $P2Y_1$ receptor is coupled to $G_{\alpha q}$, thus receptor activation leads to an increase in intracellular IP_3 levels and the release of Ca^{2+} from intracellular stores ($[Ca^{2+}]_i$). ADP (**2**, $K_i = 0.92$ μM) is the physiological agonist for this receptor and 2-MeSADP (**18**) is more potent than the parent compound with a K_i value of 0.0099 μM.[65,66]

The most potent agonist known for $P2Y_1$ is the *N*-methanocarba analog of 2-MeSADP which is called MRS2365.[67] ATP (**3**) is a partial agonist at the $P2Y_1$ receptor [68] and so at low levels of receptor expression will act as an antagonist.[69,70] MRS2179 (2'-deoxy-N^6-methyladenosine 3',5'-bisphosphate) is a highly selective and potent antagonist at $P2Y_1$ receptors with antithrombotic activity ($IC_{50} = 330$ nM),[71,72] and MRS2279 (2-chloro-N^6-methyl-(*N*) methanocarba-2'-deoxyadenosine-3',5'-bisphosphate) is a competitive antagonist at $P2Y_1$ receptors ($pK_B = 8.1$, $K_B = 7.94$ nM).[73]

Binding studies showed that [^{3}H]MRS2279 bound specifically to the human $P2Y_1$ receptor, with a K_D of 3.8 nM. The binding was displaced by 2-MeSADP (**18**) > ADP (**2**) = 2-meSATP (**7**) > ATP (**3**) and by MRS2279 = MRS2179 > adenosine-3'-phosphate-5' -phosphosulfate (A_3P_5PS).[65,66]

18 2-Methylthio-ADP;
$P2Y_1$: 0.014 μM, $P2Y_{12}$: 0.097 μM

19 ADPβS;
$P2Y_{12}$: 0.191 μM
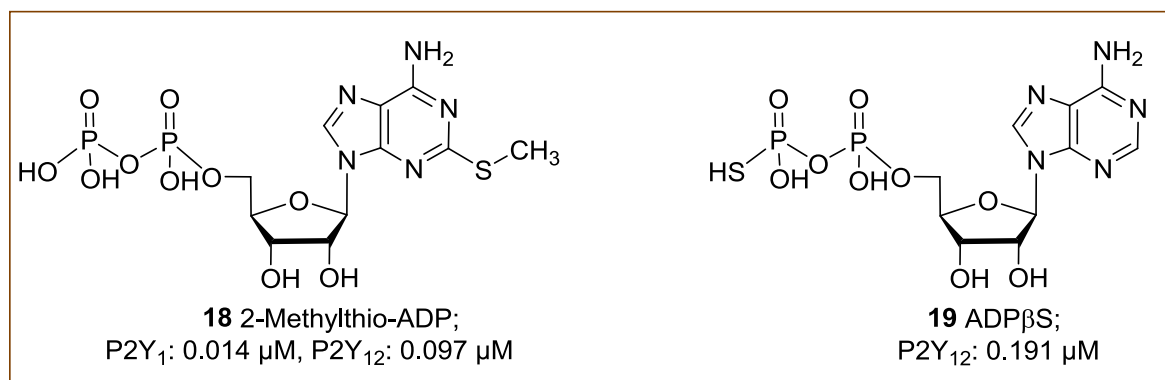
Figure 7. Chemical structures of selected P2Y receptor agonists.

1.1.1.2.2. P2Y₁₁ receptors

The human $P2Y_{11}$ receptor is distinguished from the other P2Y receptor subtypes by the following characteristics:

1)the natural agonist ATP (**3**) has a low potency for it; and

2)it is dually coupled to PLC and adenylyl cyclase stimulation;

3)there is no rodent ortholog of $P2Y_{11}$.

This means that this receptor subtype is quite different from the other members of the family. At the recombinant human $P2Y_{11}$ receptor, the rank order of potency with which nucleotides increase either cAMP or IP_3 is ARC67085MX (**20**) ≥ ATPγS ≈ BzATP (**9**) > ATP (**3**) > ADP (**2**).[74-76]

The EC_{50} of ATP is in the 5 to 100 μM range, whereas in the same expression systems (i.e., 1321N1 or CHO cells), the EC_{50} characterizing the activation of the other P2Y subtypes by their respective ligands is in the 10 to 500 nM range. Suramin (**10**) behaves as a competitive antagonist of the human $P2Y_{11}$ receptor with a K_i close to 1 μM.[75] $P2Y_{11}$ receptor antagonists derived from suramin exhibit nanomolar potency. NF157 (**12a**) has a K_i value of 0.0447 μM at the $P2Y_{11}$ receptor and displays selectivity over $P2Y_1$, $P2Y_2$, $P2X_2$, $P2X_2$, $P2X_3$, $P2X_4$, and $P2X_7$ receptors.[58]

Activation of $P2Y_{11}$ receptors leads to an increase of both cAMP and IP_3. The use of various pharmacological tools, inhibition of PLC or prostaglandin synthesis, chelation of intracellular calcium, and down-regulation of PKC showed that the cAMP increase is not an indirect consequence of rises in IP_3, $[Ca^{2+}]_i$, and PKC activity.[76,77]

Proteinkinase C (PKC) activation plays some role and amplifies the stimulation of adenylyl cyclase. In addition, it has been reported that UTP (**5**) acts via the human $P2Y_{11}$ receptor to induce an IP_3-independent Ca^{2+} mobilization that is sensitive to pertussis toxin (PTX) inhibition, but the ATP (**3**) response is unaffected.[78]

1.1.1.2.3. P2Y₁₂ receptors

ADP is the natural agonist of this receptor. For diphosphates, the rank order of agonist potency in all cases reported is 2-MeSADP (**18**) >> ADP (**2**) > ADPγS. In platelets there have been reports that ATP (**3**) and a wide range of its triphosphate analogs behave as antagonists of ADP (**2**) which induces adenylyl cyclase inhibition.[79] This has been confirmed: ATP (**3**)

and its triphosphate analogs are antagonists of the $P2Y_{12}$ receptor both in human and mouse platelets, provided care is taken to remove contaminants and to prevent enzymatic production of ADP (**2**) or 2-MeSADP (**18**).[80]

The $P2Y_{12}$ receptor is mostly expressed in the megakaryocyte/platelet lineage in which it is the molecular target of the active metabolite of the antiplatelet drug clopidogrel (**25**).[6] This metabolite covalently binds cysteine residues of the extracellular loops resulting in inhibition of ligand binding.[81]

Ticlopidine (**24**) and clopidogrel (**25**) are efficient antithrombotic drugs of the thienopyridine family of compounds. CS-747 or prasugrel (**26**) is a third antithrombotic thienopyridine recently approved as a drug.[82] Clinical studies using clopidogrel (**25**) demonstrate a significantly reduced risk of peripheral artery disease, myocardial infarction, ischemic stroke, or vascular death compared with aspirin therapy.[83]

Potent direct competitive antagonists which are all ATP analogs at $P2Y_{12}$ receptors have also been described including ARC69931MX (**21**), also named cangrelor, as well as other AR-C compounds (Figure 8).[84]
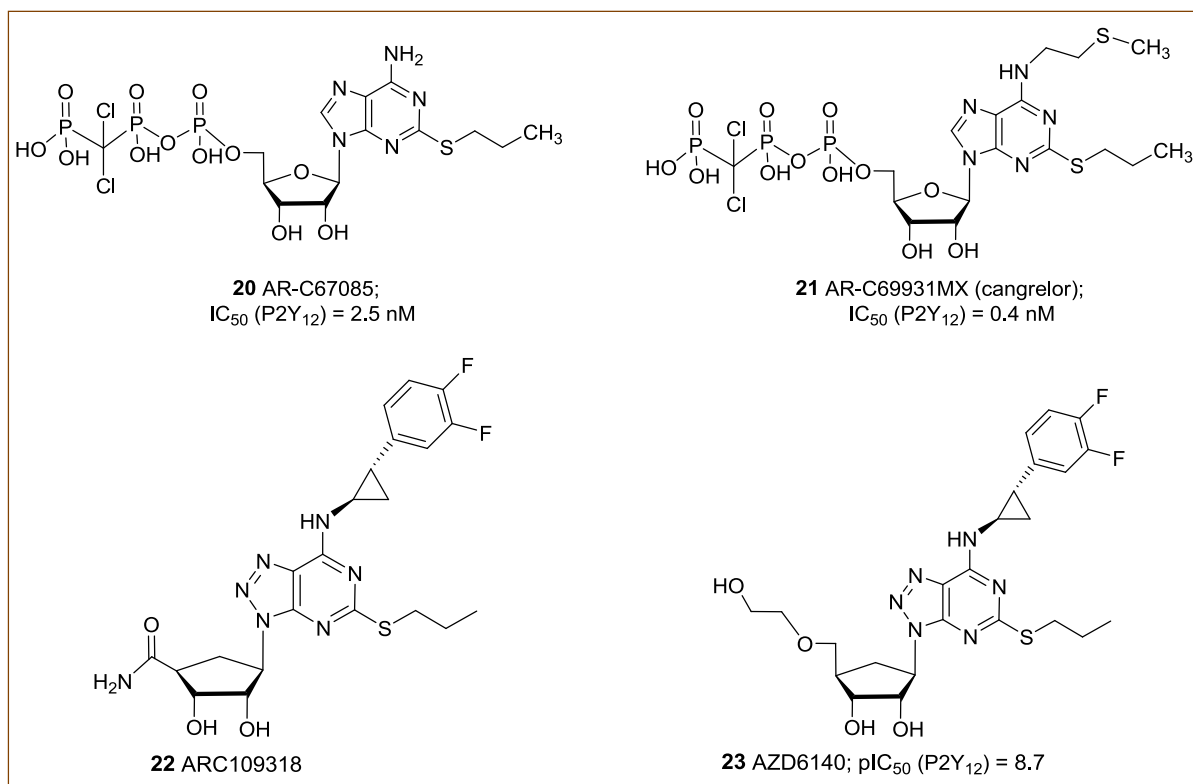
Figure 8. Chemical structures of common $P2Y_{12}$ ligand.

Unlike clopidogrel (Plavix TM) (**25**), which is a pro-drug, cangrelor (**21**) is an active drug not requiring metabolic conversion.[84] Phase II studies of intravenous AR-C69931MX (**21**) in patients with acute coronary syndromes show that this agent has a rapid onset of action, rapidly achieving steady-state inhibition of platelet aggregation with a half-life of only a few minutes.[83,85] The nonphosphorylated AZD6140 (**23**) is an orally active compound currently under clinical evaluation. To increase oral bioavailability, the structure of AZD6140 (**23**) was modified from ARC109318 (**22**).[86]

P2Y$_{12}$ knockout mice seem normal, but they exhibit prolonged bleeding times, and their platelets aggregate poorly in response to ADP and display a reduced sensitivity to thrombin and collagen.[87]
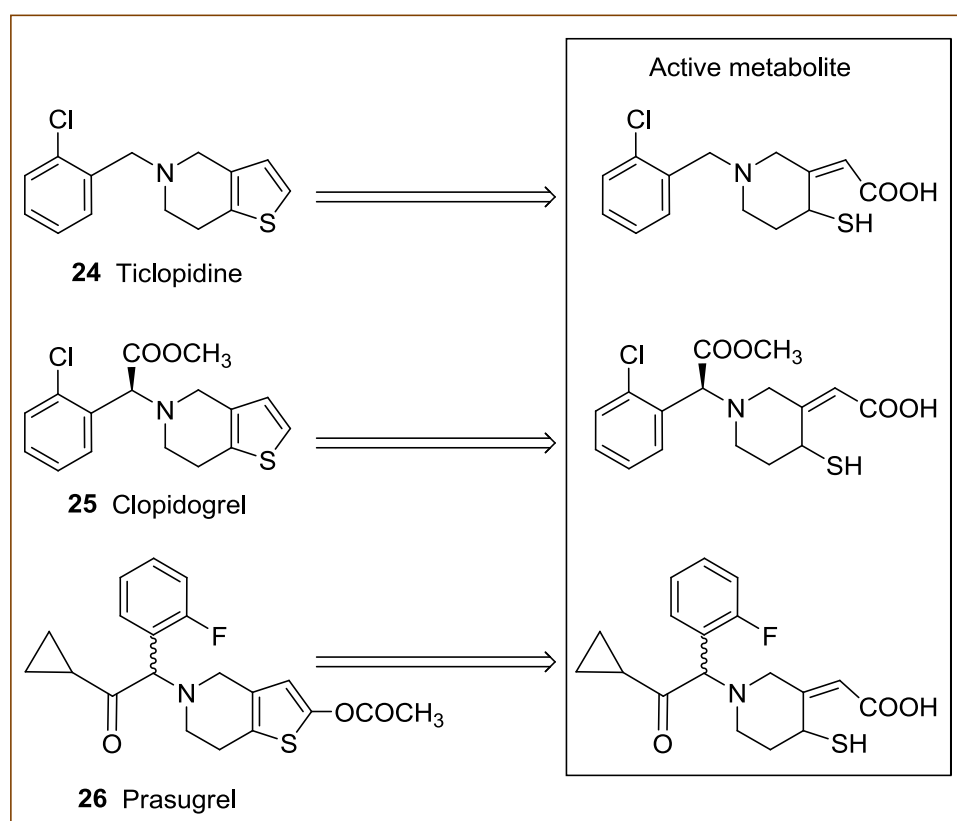
Figure 9. Thienopyridines and their active metabolites.

1.1.1.2.4. P2Y$_{13}$ receptors

ADP (**2**) and Ap$_3$A are naturally occurring agonists of the P2Y$_{13}$ receptor. When contaminating ADP (**2**) was enzymatically removed and testing was performed over a short period, ATP (**3**) behaved as a weak partial agonist.[88] The relative potencies of ADP (**2**) and 2-MeSADP (**18**) differed according to the assays used. 2-MeSADP was more potent than ADP

in competing with $[^{33}P]$2-MeSADP on intact 1321N1 cells expressing human $P2Y_{13}$ and in stimulating binding of $[^{35}S]$GTPγS to membranes of the same cells, whereas ADP was more potent than 2-MeSADP (**18**) on the rat $P2Y_{13}$.[89] In CHO-K1 cells expressing human $P2Y_{13}$, ADP (**2**) and 2-MeSADP (**18**) produced an equipotent inhibition of cAMP accumulation.

These results suggest that the $P2Y_{13}$ receptor might exist in multiple active conformations characterized by differences in affinity for 2-MeSADP (**18**) versus ADP (**2**), kinetics, and preference for G proteins.[89]

The effect of clopidogrel (**25**) as antithrombotic is mediated by an active metabolite. That metabolite has been shown to inhibit the binding of $[^{33}P]$2-MeSADP to human $P2Y_{12}$ with an IC_{50} of 100 nM,[90] but it had no effect on human $P2Y_{13}$ up to 2 μM.[88]

AR-C69931MX (Cangrelor) (**21**) which is an antagonist of the human $P2Y_{12}$ receptor with an IC_{50} value of 2.4 nM is also an antagonist of human and rat $P2Y_{13}$ receptors in nanomolar concentrations.[84] Two other $P2Y_{12}$ antagonists, Ap_4A and 2-MeSAMP, are also antagonists of the $P2Y_{13}$ receptor.[88]

The $P2Y_{13}$ receptor is primarily coupled to a $G_{i/o}$ protein. Effects of ADP mediated by the recombinant $P2Y_{13}$ receptor were inhibited by PTX. Furthermore ADP results in:

- ✓ increased binding of $[^{35}S]$GTPγS,
- ✓ inhibition of cAMP formation,
- ✓ ERK1/2 phosphorylation,
- ✓ and accumulation of IP_3 in cells co-expressing $G_{α16}$.[88,91]

However, increased cAMP formation was observed at high ADP (**2**) concentrations and that may be as a result of promiscuous coupling to G_s. This phenomenon has also been observed with other recombinant $G_i/_o$-coupled receptors, such as the $α_2$-adrenergic receptor.[91] Further evidence for the coupling to $G_{i/o}$ derives from the measurement of $[Ca^{2+}]_i$ increases in HEK cells co-expressing various chimeric G proteins.[92]

Major problems in investigations at P2 receptors are:[5]

1) the lack of selective ligands (agonists and antagonists) for the majority of P2 receptor subtypes,
2) the frequently moderate degree of purity of commercial nucleotides,

3) the fast degradation of nucleotides by a number of phosphate-hydrolyzing ecto-enzymes,

4) phosphorylation by ecto-kinases; the enzyme pattern varies in different cell types, tissues and organs.

5) A further problem constitutes the fact that cells can release nucleotides when they are being stressed, e.g. by physical movement (stirring, shaking), subsequent to change of incubation medium, or by changes of the pH value.[92,94] ATP (and other nucleotides) may be released from the cells via connexins, maxi-channels, p-glycoproteins or specific transporters. Efforts are currently under way to elucidate the mechanisms of ATP release and possible reuptake in various cellular systems.[95]

1.1.2. P1 receptors

There are four subtypes of P1 receptors that have been cloned, A_1, A_{2A}, A_{2B}, and A_3.[20,96&97] The P1 adenosine receptors are coupled to G proteins. They contain seven transmembrane (TM) domains of hydrophobic amino acids. Each TM is composed of 20–27 amino acids (Figure 10) connected by three extracellular loops and three intracellular ones. The NH_2 terminus of the protein lies on the extracellular side, and the COOH terminus lies on the cytoplasmic side of the membrane. The first crystal structure of a human A_{2A} adenosine receptor bound to an antagonist was recently identified.[98] The intracellular segment of the receptor interacts with the appropriate G protein, with subsequent activation of the intracellular signal transduction mechanism.
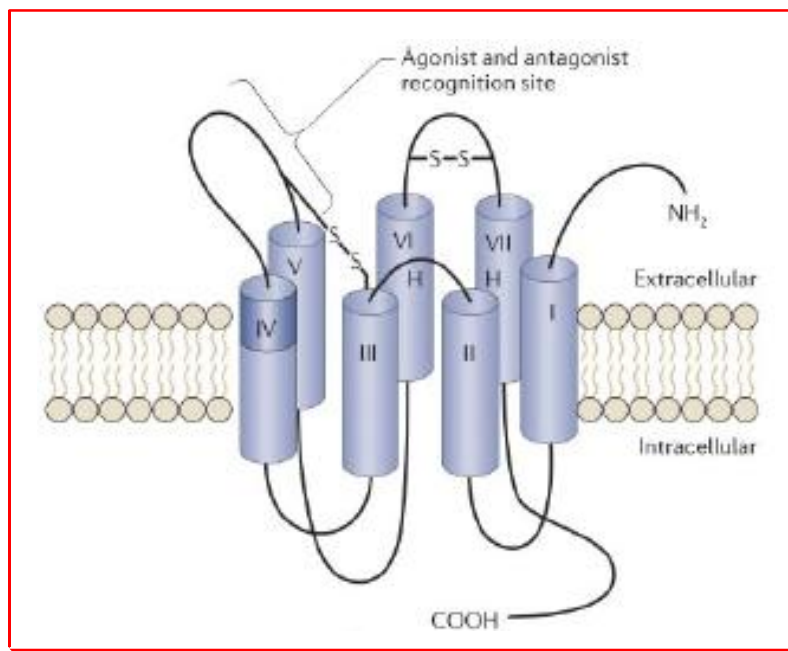
Figure 10. Membrane receptors for extracellular adenosine: the P1 family of receptors for extracellular adenosine are G protein-coupled receptors (S-S; disulfide bond).[20]

The summary of the pharmacological properties of the mammalian adenosine receptors and their subtypes are summarized in table 3.

Table 3: Pharmacological properties of mammalian adenosine receptors[64, 99-101]

Subtypes	Amino acid	Signal transduction	Agonist	Antagonist	In vitro test systems		Functional studies	Main distribution	Main functions
					Radioligand binding studies				
					Agonist radioligand	Antagonist radioligand			
A_1	326	G_i, G_o	CPA, CCPA, S-ENBA, GR7 9236, CVT-510	DPCPX, WRC-0571 PSB-036	[^{3}H]CCPA, [^{3}H]PIA, [^{3}H]NECA*	[^{3}H]DPCPX	GTP-shift cAMP	Brain, spinal cord, testis, heart, autonomic nerve terminals	Sedation, anticonvulsive, anxiolytic; cardiac depression
A_{2A}	328	G_S, G_{olf}	CGS 21680, HENECA ATL-146e, CVT-3146	SCH420814, ZM241385, KW-6002, MSX-2, MSX-3, MSX-4	[^{3}H]NECA*, [^{3}H]CGS21680	[^{3}H]SCH58261, [^{3}H]MSX-2, [^{3}H]ZM241385	cAMP	Brain (striatum), heart, lungs, spleen	Facilitates neurotransmission; smooth muscle Relaxation
A_{2B}	409	G_S, G_q	Bay 60-6583, MRS3997	MRS 1754, MRS 1706, PSB 1115, Enprofylline, MRE 2029-F20, PSB-603		[^{3}H]MRS 1754, [^{3}H]PSB 298, [^{3}H]PSB 603	cAMP, Ca^{2+} assay	Large intestine, bladder, mast cells	Role in allergic and inflammatory disorders; vasodilatation
A_3	318	G_i, G_q	2-Cl-IB-MECA, IB-MECA, VT 160	MRS 1220, VUF 5574, MRS 1523, MRS 1191, VUF 8504, PSB-10, PSB-11	[^{3}H]NECA*, [^{125}I]AB-MECA	[^{3}H]MRE-3008F20, [^{3}H]PSB-11	cAMP	Lung, liver, brain, testis, heart	Facilitates release of allergic mediators; cardio- & cytoprotective

* non-selective.

1.1.3. P0 Receptors

The recently discovered adenine receptors (AdeRs) belong to the family of purinergic receptors, referred to as P0 receptors.[5] Adenine has been identified as the endogenous ligand of an orphan rat G_i protein-coupled receptor by a reverse pharmacology approach.[102] The highest expression of mRNA for this receptor is in the small neurons of the dorsal root ganglia, pointing out that the AdeRs plays a role in nociception, and adenine may be a neuronal signalling molecule.[102] The *in vivo* experiments showed that spinally administered adenine facilitated electrically-evoked neuronal responses in a rat model of inflammation indicating a pronociceptive role of adenine in nociceptive sensory transmission.[103] Rat AdeR mRNA was also detected at lower expression levels in brain cortex, hypothalamus, lung, peripheral blood leukocytes, and ovaries.[102] Binding sites for [³H]adenine were detected in brain cortical and striatal membrane preparations,[104] and in synaptosome-rich fractions.[103] In *in vitro* studies at cultured rat cerebellar Purkinje cells adenine showed concentration-dependent neurotrophic effects; it was the most potent compound among a series of physiological nucleobases, nucleosides and nucleotides.[106,107] Recent studies demonstrating the specific binding of [³H]adenine to membrane preparations provided further evidence for the expression of the adenine receptor in rat neuronal tissues as well as a number of cell lines of neuronal origin.[104]

It was shown that adenine exhibited a G_i protein-mediated and A_1 adenosine receptor-independent inhibitory effect on Na^+-ATPase activity in the basolateral membranes of the proximal tubule isolated from adult pig kidneys, thus adenine appears to be involved in renal function.[108] Increased plasma adenine concentrations have been observed to correlate with the progress of chronic renal failure in humans[109] confirming the significance of adenine in renal function.[108]

Functional experiments showed that the rat Ade1R expressed in Chinese hamster ovary (CHO) cells[102] is coupled to adenylate cyclase via G_i protein.

A mouse ortholog (mMrgA10), but no human ortholog, of rat Ade1R could be identified by sequence analysis and comparison.[102] Adenine receptors are expressed in high density in the rat brain and native cell lines. Functional coupling to inhibition of adenylate cyclase has been found in a native cell line (NG108-15).

RT-PCR experiments indicated that NG108-15 cells do not express a rat, but a mouse mRNA sequence encoding for an adenine receptor.[104] The mouse sequence found in mouse brain and NG108-15 cells is clearly distinct from the mouse ortholog (mMrgA10) of the rat adenine receptor.[110]

Furthermore, there is evidence for the existence of human AdeR, since human cell and tissue membrane preparations have shown high affinity binding sites for [^{3}H]adenine.[104] Active and passive transport systems for nucleobases have been described to exist in various species including mammals.[111,112] A saturable transport system for adenine across basolateral membranes of the sheep choroid plexus has been characterized.[113] Recently, it was shown that [^{3}H]adenine is taken up into primary cultured rat cortical neurons via a saturable Na^+-independent mechanism indicating that efficient mechanisms for the removal of adenine from the extracellular fluid exist. Such systems are required for limiting the duration of receptor activation.[114]

1.2. Radioligand binding studies

Radioligand binding assays are important tools which are used for mapping the distribution of receptors in different areas of the body, as well as the effects of physiological conditions on the expression of the receptors, and to evaluate ligands for a specific receptor. The radioligand is a radioactively labelled compound which can interact with a receptor.[115] Natively expressed and cloned receptors have been used in radioligand binding studies for the characterization of ligands.

1.2.1. Basic concepts in receptor binding studies

The basis of the receptor binding study is the binding of a ligand **(L)** to the receptor **(R)** to form a ligand-receptor complex **(LR)**. The unbound ligand is identified as **Free** which means the amount of ligand that is free and able to interact with the receptor, while the amount of ligand bound to the examined receptor is defined as **Bound**. Radioligand binding studies are based on a chemical equilibrium process (Figure 11) that is defined by the law of mass action.

$$\textbf{Receptor (R) + Ligand (L)} \underset{\textbf{k}_{-1}}{\overset{\textbf{k}_{+1}}{\rightleftharpoons}} \textbf{Ligand Receptor Complex (LR)}$$
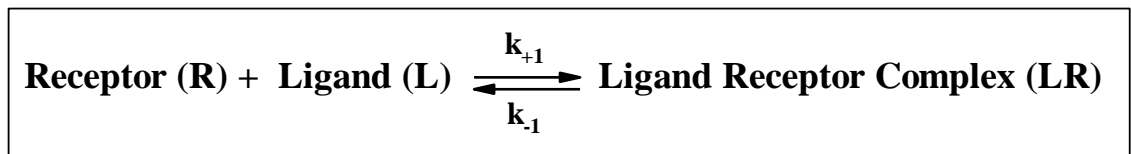
Figure 11. Ligand-receptor complex (LR) which is formed as a result of ligand binding between the receptor (R) and the ligand (L).

The binding of a ligand (L) to a receptor (R) to form a ligand-receptor complex (LR) is describing in general a reversible binding phenomena. At equilibrium or steady state, the rate of the forward reaction equals the rate of a reverse reaction (not a static process). It is viewed as a kinetic process of a ligand moving toward and away from receptors at different states.

The equilibrium binding constant is defined as an association binding constant (K_A) or as a dissociation binding constant (K_D). In biological chemistry this equilibrium is expressed in terms of the dissociation reaction K_D rather than the association reaction K_A. The K_D is obtained by a rearrangement of the law of mass action (equation 1).

$$K_D = \frac{k_{-1}}{k_{+1}} = \frac{[L][R]}{[LR]}$$

Equation 1. The law of mass action, where K_D is the dissociation equilibrium constant, [L] is the concentration of the unbound ligand, [R] the concentration of the unbound receptor and [LR] the concentration of the receptor-ligand complex.

K_D is a measure of the affinity of a ligand for a receptor and is equal to k_{-1} / k_{+1}, where k_{+1} is the rate constant for association and k_{-1} is the rate constant of dissociation, [L] is the concentration of the unbound ligand, [R] the concentration of the unbound receptor and [LR] the concentration of the receptor-ligand complex (equation 1).

At equilibrium, when the concentration of the ligand equals the K_D, half of the receptors are occupied. If the receptors have a high affinity for the ligand, the K_D will be low, as it will take a low concentration of ligand to bind half of the receptors, while if the K_D is large it means the receptor has a low affinity for the ligand.

The law of mass action is not valid under all conditions. It can only be used under certain conditions:

1. all receptors are equally accessible for the ligand;
2. all receptors are either free or bound by the ligand;
3. not more than one affinity state exists;
4. binding is reversible;
5. neither ligand nor receptor is altered by binding.

1.2.2. Basic types of receptor binding experiments

1.2.2.1. Saturation experiments

The saturation experiments measure, at equilibrium, the specific radioligand binding at various concentrations of the radioligand, which are used to determine the affinity $1/K_D$ of a radioactive ligand for a receptor and the B_{max} of the receptor in specific tissues or samples. Such experiments are based on the one binding site equation (equation 2).

$$\text{Bound} = \frac{B_{max} \text{ x Free}}{K_D + \text{Free}}$$

Equation 2. Binding equation, where Bound is the concentration of the drug-receptor complex, Free is the concentration of the free radioactive ligand, K_D is the affinity of the radioactive ligand for the receptor and B_{max} is a measure of the density of the receptor in that tissue.

These experiments are called saturation experiments because at higher radioligand concentrations all the binding sites are occupied (saturated) by a radioactive ligand. In a typical saturation experiment, the radioligand concentration should be between 1/10 and 10 times the possible K_D (Figure 12).[116]
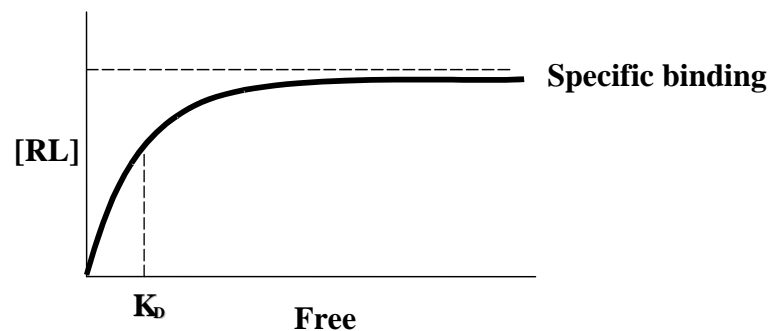
Figure 12. Typical graph of a saturation hyperbole.

Specific versus non-specific binding

Unfortunately, radioactive ligands bind also to other sites (non specific sites) than to those of interest. The whole amount of the radioactive ligand bound is referred to as total binding, whereas the specific binding is the difference between the total binding and the non-specific binding.

Specific binding (S) = Total binding (TB) – Non-specific binding (NS)

The non-specific binding sites may be receptors in the same family or in other receptor families which recognize similar chemical structures, other constituents of the tissue (they could be trapped in the lipid membrane) as well as the assay tools, such as glass fibre filters and test tubes.

The non-specific binding must be determined in each experiment. If it exceeds 50%, the experiment cannot be considered reliable. The optimal result should be between 10% and

30%.[117,118] To reduce non-specific binding, a very clean membrane homogenate should be used, the filtration time should be optimized, filter can be "pre-soaked" before the filtration and finally the right radioligand concentration ($1/10\ K_D$ - $10\ K_D$) should be used.

1.2.2.2. Competition experiments

In competition experiments the affinity of an unlabelled ligand for the receptor can be determined indirectly by measuring its ability to compete with the binding of a known radioactive ligand to its receptor. In the experiment, a fixed concentration of the radiolabeled ligand is used against different concentrations of the unlabelled ligand which compete with the radioligand for the binding to the receptor,[116] leading to a decrease in the concentration of the free receptor and accordingly the concentration of radioligand receptor complex.[116]

From the experiment, the concentration of the unlabelled ligand that inhibits the binding of the radioactive ligand by 50 % (IC_{50} value) is determined.

The value of the **IC_{50}** depends on:

- the affinity of the radioactive ligand for the receptor;
- optimization of the radioactive ligand concentration which should ideally be approximately 0.8 times the K_D.

If a higher concentration of the radioactive ligand is used, then higher concentrations of unlabelled ligand will be required to inhibit the binding of the radioactive ligand, and accordingly the value of Cheng-Prusoff correlation (equation 3) will be quite large. If a lower radioactive ligand concentration is used, it may lead to no sufficient binding and therefore no reliable data can be obtained.[116]

The dissociation constant (**K_i**) for an unlabeled ligand (agonist or antagonist) for the receptor is obtained from the competition experiment. If the K_i value is low, the affinity of unlabeled ligand for the receptor will be high. The K_i value can be obtained from the IC_{50} value using Cheng-Prusoff equation (equation 3).

$$\mathbf{K_i = IC_{50}\ /\ (1 + L\ /\ K_D)}$$

Equation 3. Cheng-Prusoff equation

Where L is the concentration of the radioactive ligand used and K_D is the affinity of the radioligand for the receptor.[119]

1.2.2.3. Kinetic experiments

1.2.2.3.1. Dissociation rate

A dissociation binding experiment measures the "k_{-1}" or k_{off} for a radioligand dissociating from the receptor. The aim of dissociation experiments is to:

- fully characterize the interaction of the ligand and the receptor;
- confirm that the law of mass action applies;
- help to design the experimental protocol.

If the dissociation is fast, the filtration and washing of the samples should be quick so that negligible dissociation occurs. Lowering the temperature of the buffer used to wash the filters, or using another method such as centrifugation might be done. While, if the dissociation is slow, the filtration of the samples can be done more slowly.

To perform a dissociation experiment, first, the ligand and receptor are allowed to bind to equilibrium. At that point, the further binding of the radioligand to the receptor should be blocked. After initiating the dissociation, the binding is measured over time (typically 10-20 measurements) to determine how rapidly the ligand dissociates from the receptors.[120]

1.2.2.3.2. Association rate

Association binding experiments are used to determine the association rate constant. This is useful to characterize the interaction of the ligand with the receptor. It is also important as it allows the determination of how long it takes to reach equilibrium in saturation and competition experiments. In this method, the radioligand is added and specific binding at various time intervals is measured.

The observed rate constant (k_{ob}) is determined from the association experiment (equation 4), and it is a measure of how quickly the incubation reaches equilibrium, and it depends on three factors:

- o the association rate constant, this needs to be determined;
- o the concentration of radioligand;

o the dissociation rate constant.

$$k_{+1} = \frac{k_{ob} - k_{-1}}{[\text{Radioligand}]}$$

Equation 4. Association rate constant where the k_{ob} is determined from the experiment

At equilibrium, the rate of the forward binding reaction equals the rate of the reverse dissociation reaction. If the radioligand dissociates quickly from the receptor, equilibrium will be reached faster, but there will be less binding at equilibrium. If the radioligand dissociates slowly, equilibrium will be reached more slowly and there will be more binding at equilibrium.[120]

The analyses of association experiments assume:

- no ligand depletion. A small fraction of the radioligand binds to receptors, so the concentration of free radioligand equals the amount you added and does not change over time;
- no cooperativity;
- the binding is for a specific receptor.

1.2.2.3.3. Combining association and dissociation data

Once the values of k_{-1} and k_{+1} were separately determined, the K_D can be calculated from the combination of them (equation 5).

$$K_D = \frac{k_{-1}}{k_{+1}}$$

Equation 5. Combining association and dissociation data, K_D obtained by k_{-1} and k_{+1}.

If binding follows the law of mass action, the K_D calculated this way should be the same as the K_D calculated from a saturation binding curve.

1.3. G protein-coupled receptors

G protein-coupled receptors (GPCR) are a family of proteins which plays an important role in signal transduction in the cells. GPCRs have grown to be one of the most important areas of research in the pharmaceutical industry. Analysis has indicated that ~ 45% of currently marketed medicines are targeted to this type of receptors.[121,122]

GPCRs interact with heterotrimetric G proteins. The G_α proteins regulate the activity of the GPCRs. Guanosine diphosphate (GDP) binds to G_α proteins in their inactive state, in which they are non-covalently associated with the $G_{\beta\gamma}$ subunits and a corresponding GPCR.
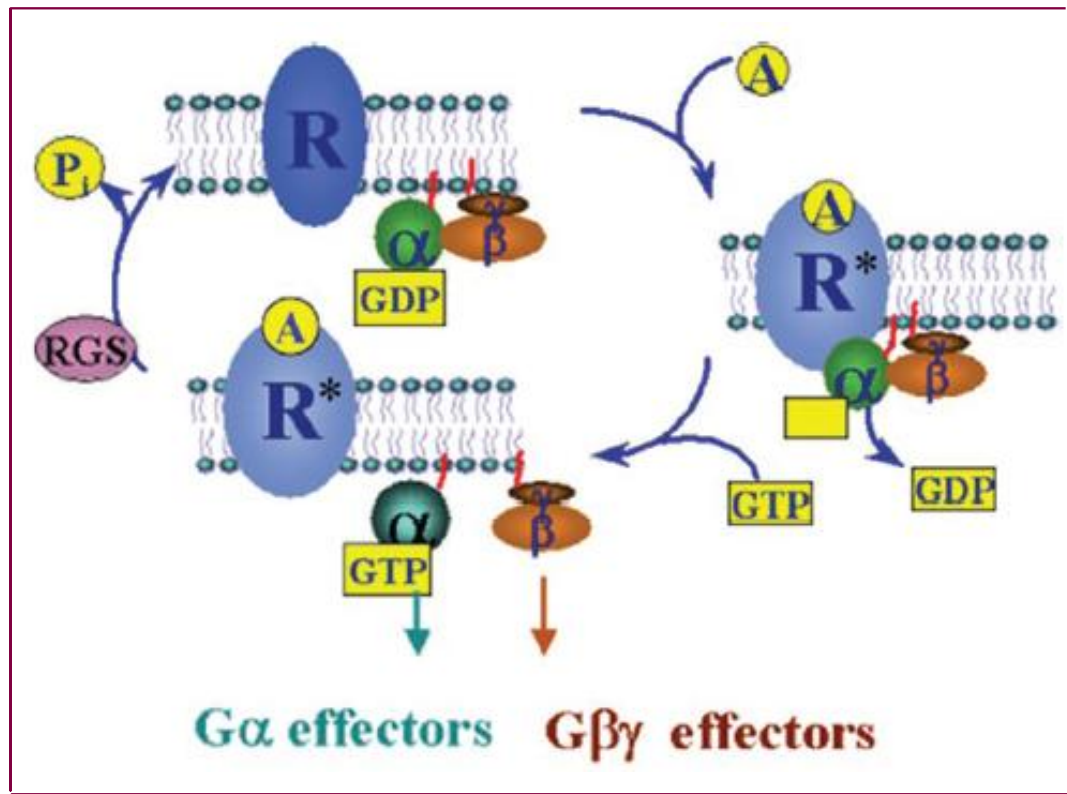
Figure 13. Receptor-mediated G protein activation. The interaction of an endogenous ligand with its cell surface receptor (R) facilitates the coupling of the activated receptor (R*) with intracellular heterotrimeric G proteins. The R*-G protein coupling promotes the exchange of GDP for GTP on the G_α-subunit. G_α-GTP then dissociates from $G_{\beta\gamma}$ and R*. Both subunits are free to modulate the activity of a wide variety of intracellular effectors. Termination of the signal occurs when the γ-phosphate of GTP is removed by the intrinsic GTPase activity of the G_α-subunit, leaving GDP in the nucleotide binding pocket on G_α. G_α-GDP then reassociates with $G_{\beta\gamma}$ and the cycle is complete.[123]

The activation of GPCR leads to allosteric conformational changes in the receptor, leading to exchange of GDP from the G_α subunit for guanosine triphosphate (GTP) and dissociation of the G protein heterotrimeric subunits. The $G_{\beta\gamma}$ form a single subunit which performs various functions independently of the G_α constituent (Figure 13). The G protein cycle is completed by the hydrolysis of the GTP bound to the G_α subunit by its intrinsic GTPase activity. Thus, the G_α subunit returns to the original state, which leads to reassociation again with the $G_{\beta\gamma}$ subunits and finally binding of the heterotrimer to the GPCR (Figure 13).[124]

The G_α subunit nomenclature is used to classify GPCRs with regard to their primary signal transduction pathway. There are 16 forms of α subunits known, which have been grouped into 4 subclasses (Figure 14):

1. $G_{\alpha i}$ which leads to decreased cAMP though the inhibition of adenylate cyclase,
2. $G_{\alpha q}$ which leads to a rise in intracellular calcium by activating the PLC pathway,
3. $G_{\alpha s}$-coupled receptors lead to increased levels of cAMP via the adenylate cyclase pathway and
4. $G_{\alpha 12}$ interacts with Cl^- channels.

The dissociated βγ subunit can also modulate several signaling pathways, including stimulation or inhibition of adenylate cyclases, activation of phospholipases, and regulation of potassium and calcium channels.[125]
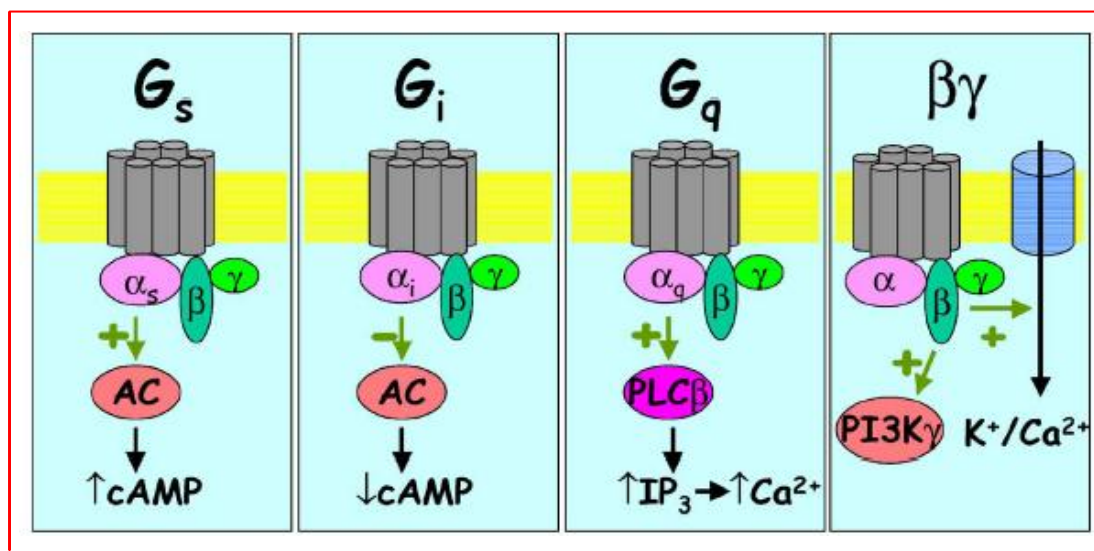
Figure 14. The principle mechanisms involved in different G protein signalling pathways. G_s and G_i proteins are coupled to adenylate cyclase (AC) whereas G_q is coupled to phospholipase β (PLCβ) and inositol-1,4,5-trisphosphate (IP_3) production. In addition βγ affects activity of phosphoinositol-3-kinaseγ (PI3Kγ) as well as certain ion channels.[126]

GPCR signalling is a multistep process composed of:

- agonist binding,

- conformational change of the receptor leading to G protein activation and

- subsequent coupling to intracellular secondary messenger mechanisms.

Each of these three steps gives possibilities for the development of a screening strategy:

1. The first point in the process that could be used is the binding of a ligand to the receptor. If suitable tracer compounds are available a variety of approaches could be exploited for developing a screening assay.

2. The second step that could be exploited is agonist-mediated stabilization of the receptor in an active conformation resulting in nucleotide exchange (GTP for GDP) on an associated hetero-trimeric G protein. This step could be exploited for screening purposes using GTPγS binding technologies.

3. The third step depends on the type of G protein coupled to receptor.[126]

In principle the simplest assay is competition binding, however, this has the disadvantage that it primarily addresses the initial event, potentially missing receptor regulation through allosteric mechanisms. A functional assay where a receptor functions through its cognate G protein offers the best choice for identifying all compounds that alter receptor function.[126]

1.4. Functional studies

Functional assays are used for the following purposes:

- they facilitate early and direct pharmacological characterization of compounds;
- they expedite the separation of antagonist and agonist compounds and
- enable the identification of novel compounds such as allosteric modulators, weak-affinity and high-potency agonists.[127]

In *in vitro* screening there are several methods used to quantify functional effects at a number of points along the GPCR signalling cascade. In the following chapters, selections of the commonly used methods are reviewed.[128]

1.4.1. Regulation of intracellular 3',5'-cyclic adenosine monophosphate levels

The production of cAMP is controlled through the adenylyl cyclase (AC) family of enzymes, which convert adenosine triphosphate (ATP) to cAMP and inorganic diphosphate (Figure 15). These enzymes are activated or inhibited by direct interaction with G protein α-subunits and, for some isoforms, with Ca^{2+} and calmodulin.[129, 130]

- ✓ Following G_s-coupled GPCR activation, agonists exert a positive effect on AC catalysis. The produced cAMP is able to bind to protein kinases in the cell, initiating phosphorylation events that regulate target enzymes and transcription factors.
- ✓ Following G_i-coupled receptor activation, $G_{αi}$ is activated and a negative effect is exerted on the enzyme.

Degradation of cAMP is controlled by the cAMP phosphodiesterase (PDE) enzymes, which catalyse the hydrolysis of the 3′-ester bond of cAMP to form 5′-adenosine monophosphate (AMP). There are various PDE isoforms, which are involved in the breakdown of either cAMP or cGMP. There are several mechanisms which lead to activation of PDE enzymes. The most widely observed mechanism for activation of the cAMP PDEs is phosphorylation by cAMP-dependent protein kinases. The cAMP PDE enzymes act as an important negative-feedback system on the receptor-mediated signalling cascade, regulating the extent of changes in intracellular cAMP concentrations.[131]
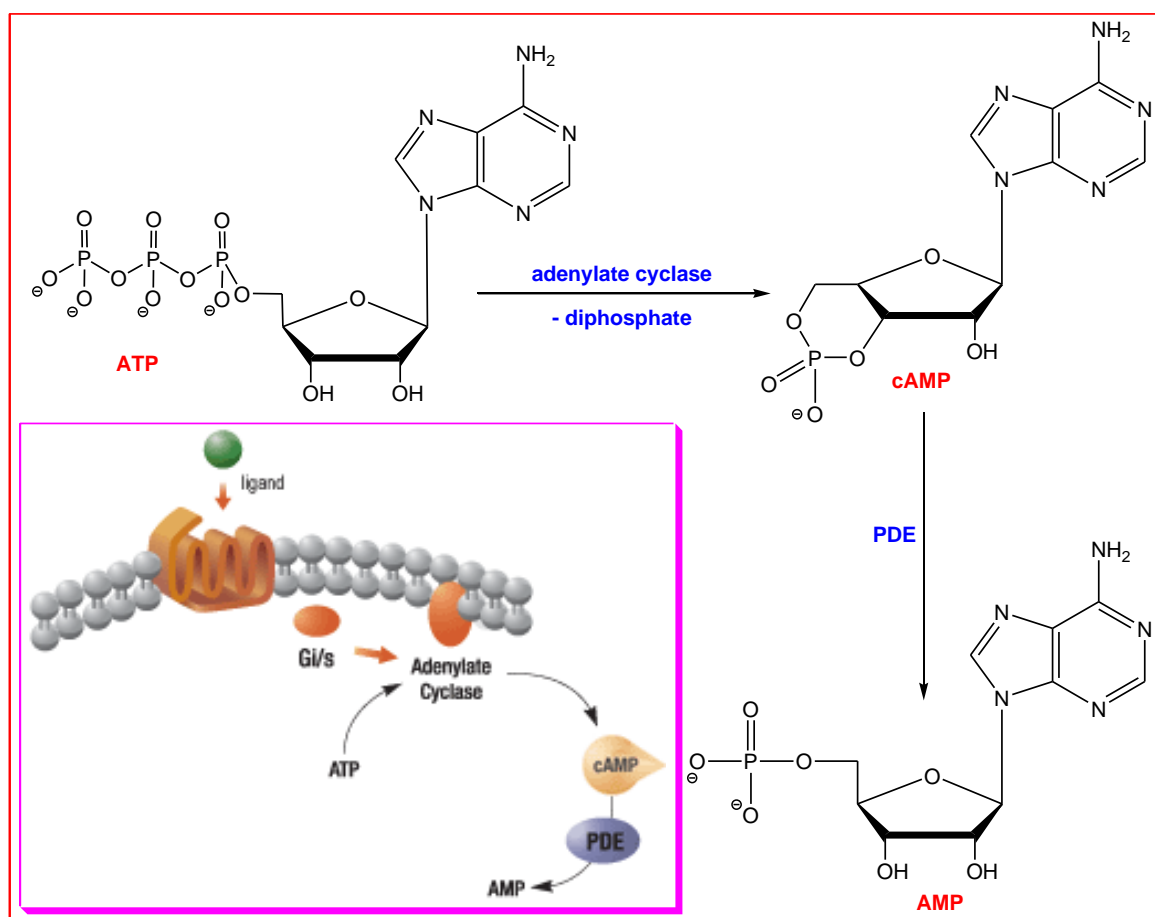
Figure 15. Ligand-receptor interaction and intracellular regulation of cAMP levels.

1.4.1.1. Quantitative analysis of 3',5'-cyclic adenosine monophosphate levels

1.4.1.1.1. Accumulation assays

➢ **Radiometric competitive binding assays**

These are the most widely used techniques for cAMP measurement. These methods follow a general principle, in which changes in intracellular cAMP are detected by the competition between cellular cAMP and a labelled form of cAMP for binding to an anti-cAMP antibody or anther cAMP-binding protein.

➢ **Non-radiometric assays**

Examples for these types of assays are the application of fluorescence polarization (FP)[132] for detection of cAMP. Time-resolved fluorescence resonance energy transfer (TR-FRET) has also been applied to the measurement of cAMP as well as homogeneous time-resolved fluorescence (HTRF).

Three new technologies have been developed which aim to provide non-radiometric high-sensitivity assays:[128]

1. ALPHA screen (amplified luminescent proximity homogeneous assay),
2. an enzyme complementation technology and [133]
3. electrochemiluminescence detection.

The selection of a given technology might also require evaluation of other parameters, such as detection limits, cost and the number of addition steps.[128]

1.4.1.1.2. Reporter-gene assays for 3',5'-cyclic adenosine monophosphate detection

A reporter gene is a sequence of DNA whose product is synthesized in response to activation of the signalling cascade under investigation. The DNA sequence consists of a promoter, where transcription factors bind to control transcription, a reporter gene and a transcription stop signal. The choice of promoter element dictates the sensitivity and specificity of the reporter. The reporter must have:[134]

- low basal expression and a large transcriptional response following receptor activation,
- offer a unique property to the cell system being studied,
- have a short half-life to minimize basal accumulation and
- be easily measurable by simple, cheap assays.

Reporter-gene assays follow a general principle, in which receptor-mediated changes in intracellular cAMP concentrations are detected through changes in the expression level of a particular gene (the reporter), the transcription of which is regulated by the transcription factor cAMP response-element binding protein (CREB) binding to upstream cAMP response elements (CREs) (Figure 16).[134]

Several protocols and different numbers of CREs are used for reporter assays. The choice of reporter gene and the particular method for measuring activity of that reporter gene must be done carefully. Although all reporter genes share common properties in that they are absent from the cell type of interest and a small number of active molecules are required for detection, they represent the most significant factor when considering which assay system to choose.[128]
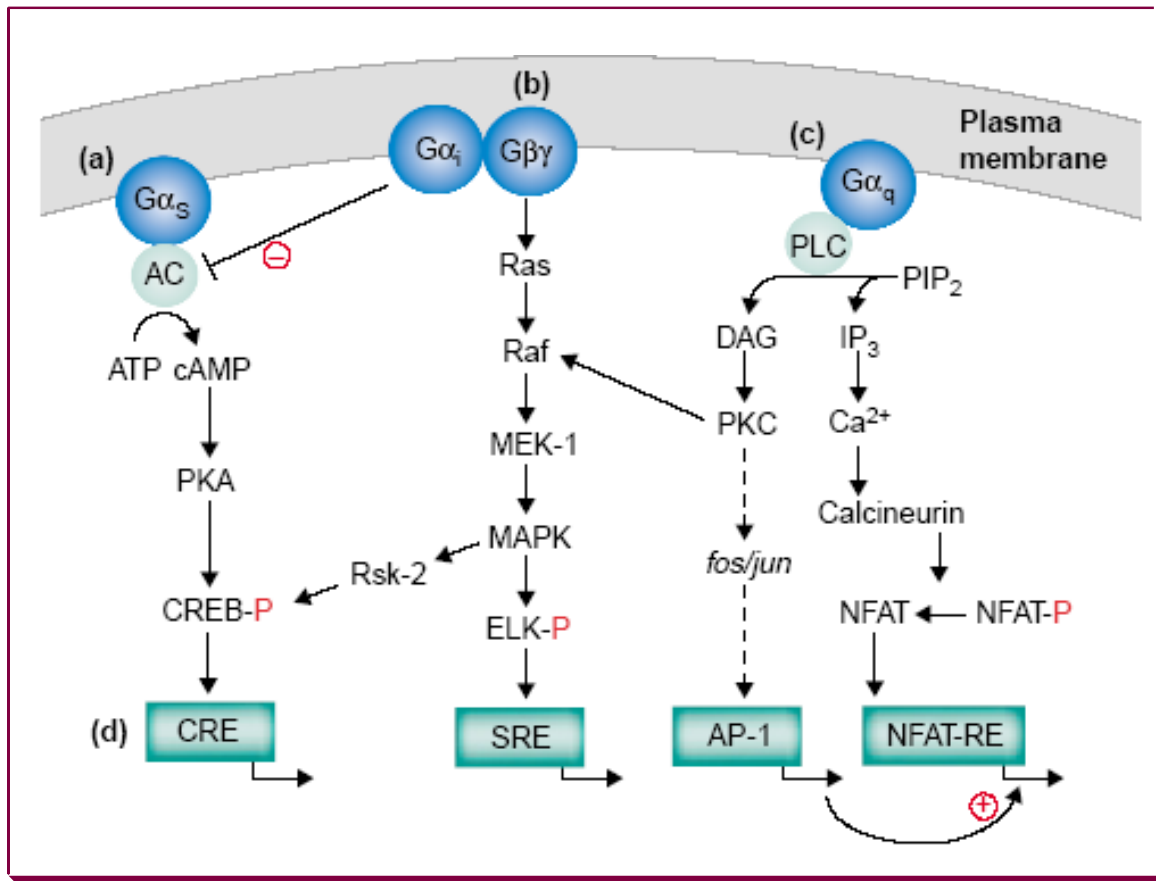
Figure 16. A schematic diagram showing how, after stimulation of the GPCR and dissociation of the G protein subunits, the major G protein families signal by the different intracellular second messenger pathways to communicate with nuclear promoter elements. **(a)** $G_{\alpha s}$-coupled receptors stimulate AC, which synthesizes cAMP from ATP. In contrast $G_{\alpha i}$-coupled receptors inhibit AC and so reduce cAMP formation. **(b)** The βγ subunits from $G_{\alpha i}$ and other G proteins are able to activate the MAP kinase pathways and PLCβ. **(c)** GPCRs coupled to the $G_{\alpha q}$ family of G proteins stimulate PLC$_\beta$, which cleaves membrane phospholipids to produce IP_3, which mobilizes intracellular calcium, and DAG, which activates PKC. **(d)** Second messenger pathways then activate a range of effector systems to change cell behaviour; in many cases this includes the regulation of gene transcription. The dotted line shows a more indirect pathway. MAPK, MAP kinase, MEK, MAP kinase kinase; P, phosphate; PIP_2, phosphatidylinositol-4, 5-bisphosphate.[134] Abbreviations, cAMP response element (CRE), serum response element (SRE), activator protein 1 (AP-1) nuclear factor of activated T cells response element (NFAT-RE).

Various reporter genes have been used in *in vitro* and *in vivo* studies, including:[134-137]

- β-galactosidase,
- green fluorescent protein (GFP),
- luciferase,
- β-lactamase.

Luciferase enzymes have shorter half-lives than β-galactosidase and GFP, providing some advantage and making them a popular choice in screening assays.[138]

The most commonly used luciferase enzyme is that from the firefly (Photinus pyralis), which catalyzes the oxidation of luciferin to produce oxyluciferin and light (Figure 17). The advantage of using this particular enzyme is that there are various reagents available to detect these effects. Some of these reagents can prolong the life time of the light emitted, making it detectable for several hours and improving automation compatibility. However, it is noted that luciferin analogues, which are present in the compound collection, will interfere with the assay in spite of reagent choice.[128]
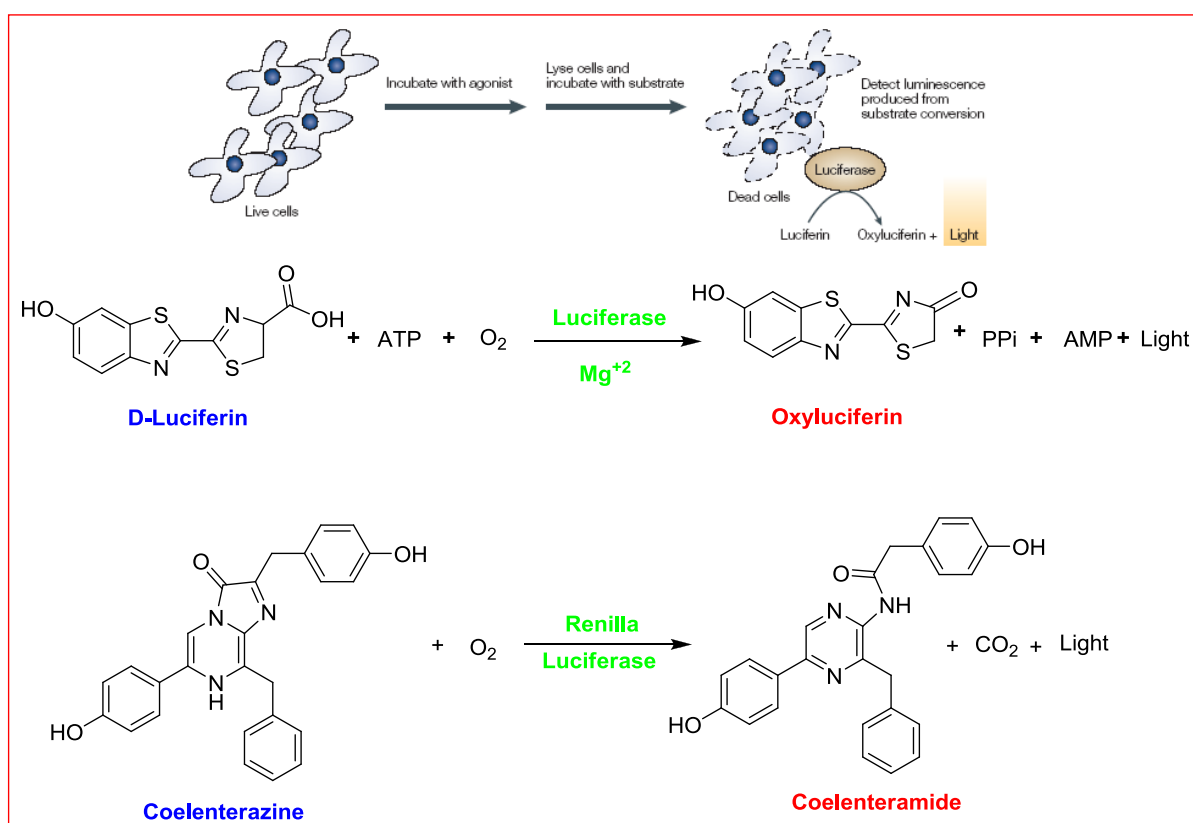
Figure 17. Schematic representation of the luciferase reporter-gene technologies. Cells containing the luc gene under the control of cAMP regulatory elements (CREs) are incubated with agonist. Following this receptor activation, increases in cAMP activate the cAMP-dependent protein kinase (PKA), which then phosphorylates the transcription factor CRE-binding protein (CREB). Phosphorylated CREB binds to the CREs, mediates transcription and functional luciferase is created. However, the cells need to be lysed to detect the activity of the luciferase enzyme. Following this lysis and addition of substrate, the enzyme catalyses a mono-oxygenation reaction, which produces oxyluciferin and light (550–570 nm) that can be measured. The light produced is naturally short-lived; however, reagents are available that prolong this lifetime, making it suitable for automated high-throughput screening.[128]

The sea pansy (Renilla reniformis) luciferase enzyme, which catalyses the oxidation of coelenterazine to coelenteramide and light (480 nm), can also be used as a reporter. It has been used in conjunction with the firefly enzyme as a means of controlling well-to-well variations or simultaneous screening of two different targets.[139]

Recently, the family of luciferase enzymes has been reviewed, highlighting key residues that are involved in both substrate binding and bioluminescence colour.[140] This could give us valuable information for the development of improved luciferase reagents that produce stable signals at alternative wavelengths and minimizing the potential for compound interference.

The cell lines most commonly used in reporter-gene assays are Chinese hamster ovary cells (CHO) and human embryonic kidney cells (HEKs).

Table 4. Advantages and disadvantages of accumulation and reporter-gene systems[128]

	Accumulation assays	**Reporter gene assays**
Advantage	Some technologies have been successful with membranes that can reduce the impact of false-positives (for example: FP) Molecular biology not required if endogenous receptors are used Might be more physiologically relevant than reporter systems (e.g. β2-adrenoceptor)[141]	Amplification might mean greater sensitivity to weak agonism Assays are generally cheaper than accumulation assays Assays are compatible with standard plate readers and automation Tissue-culture resource might be less than whole-cell accumulation assay
Disadvantage	Might be less sensitive to weak agonism Some technologies might require a specific reader Misleading data might arise due to large changes in cAMP producing small changes in raw data Accumulation technologies are generally more expensive than reporters	Amplification means that the compound activity detected might not be physiologically relevant Molecular biology required Misleading data might arise due to inducible cAMP early repressor (ICER) or accumulation assay receptor desensitization[142,143]

There are some factors that should be considered (Table 4) in order to indicate whether an accumulation or reporter-gene technology is more suitable for a certain test system. For example, if an agonist is required, a reporter-gene system might be more sensitive, through maximizing the potential of identifying activities. However, if a membrane-based accumulation assay can be developed, it might minimize the tissue culture resource required and could potentially minimize false-positives that would be observed as a result of downstream activity of compounds.[128]

1.4.1.2. General remark for 3',5'-cyclic adenosine monophosphate assays (accumulation or reporter)

The following points must be taken in consideration during the performance of cAMP assays:

1. Tolerance to organic solvents such as dimethylsulphoxide (DMSO), which is tolerated in the order of 1–10% for the cAMP assays mentioned before.[128]

2. In order to detect the negative regulation of AC by G_i-coupled GPCRs, the system must first be active. This is achieved by using the direct chemical modulator of AC, forskolin. The EC_{50} value for forskolin is different depending on the type of cell used and might also vary dependent on the type of assay format (that is, accumulation versus reporter gene).[144] Thus, it is important to determine the potency of forskolin for the system of choice. Also, forskolin can stimulate cells to produce changes in cAMP that are much greater than would be generated by receptor-mediated action. Therefore, care for evaluation of the concentrations used is required to ensure that optimum sensitivity is obtained.

3. Breakdown of cAMP by PDEs can also affect the data that are produced in assays that measure the AC pathway. For example, PDE inhibitors could appear as false-positives in a screen for agonists of a G_s-coupled GPCR. To control for such effects, the non-selective PDE inhibitor isobutylmethylxanthine (IBMX) can be included in the buffer. Dependent on the system, this might significantly increase basal levels of cAMP, but might also improve the observed potency of forskolin;[145] therefore, the effect of addition of IBMX on the assay sensitivity should be fully evaluated.

1.4.2. Measurement of intracellular calcium or inositol 1,4,5-trisphosphate levels (IP_3)

Activation of G_q-coupled receptors leads to release of calcium from intracellular $[Ca]_i$ stores through the generation of IP_3 as a consequence of PLC activation (Figure 14 and 16).

Functional assays of G_q-coupled receptors can be performed using both the IP_3 or calcium signal and are consequently cell-based screening strategies.

The detection of calcium can be achieved by fluorescent dyes and technologies such as fluorimetric imaging plate readers (FLIPR).[146] For example, in living cells, small, cell-membrane permeable molecules, such as fluorescent dyes can be used, which change their fluorescent properties after binding of Ca^{2+} (Figure 18). As high-throughput screening (HTS) test, this assay presents several advantages:[138,147,148]

(1) it is a sensitive nonradioactive fluorescence-based assay;

(2) it can be miniaturized to a 384 well plate level;

(3) it is easy to perform and can be automated;

(4) it provides a positive signal over the background.

The FLIPR technology is extensively used for high throughput screening even through fluorescent compounds can potentially interfere with the assay.[126]

In addition, it can be also used to study G_i-coupled receptors by using chimeric or promiscuous G proteins. These G proteins enable the system to be switched to the PLC/Ca^{2+} pathway or the stimulatory AC/cAMP pathway.[149-151] However, such strategies also need to be used with care because these alternative G proteins do not couple effectively to all receptor types, which can lead to either an altered pharmacological profile or to no signal being detected.[151-152]

An alternative approach is to use the aequorin technology. The use of the photoprotein aequorinwas reported as a sensitive detector of increases in [Ca^{2+}]$_i$ levels.[153, 154] Apoaequorin is a 21-kDa photoprotein, isolated from the jellyfish *Aequorea victoria*, which forms a bioluminescent complex when linked to the chromophore cofactor coelenterazine. The binding of [Ca^{2+}]$_i$ to this complex results in an oxidation reaction of coelenterazine, followed by the production of apoaequorin, coelenteramide, CO_2, and light (469 nm), which can be detected by luminometry.[155]

The calcium detection technologies provide one of the principal methods for G_q-coupled receptor screening.[126]
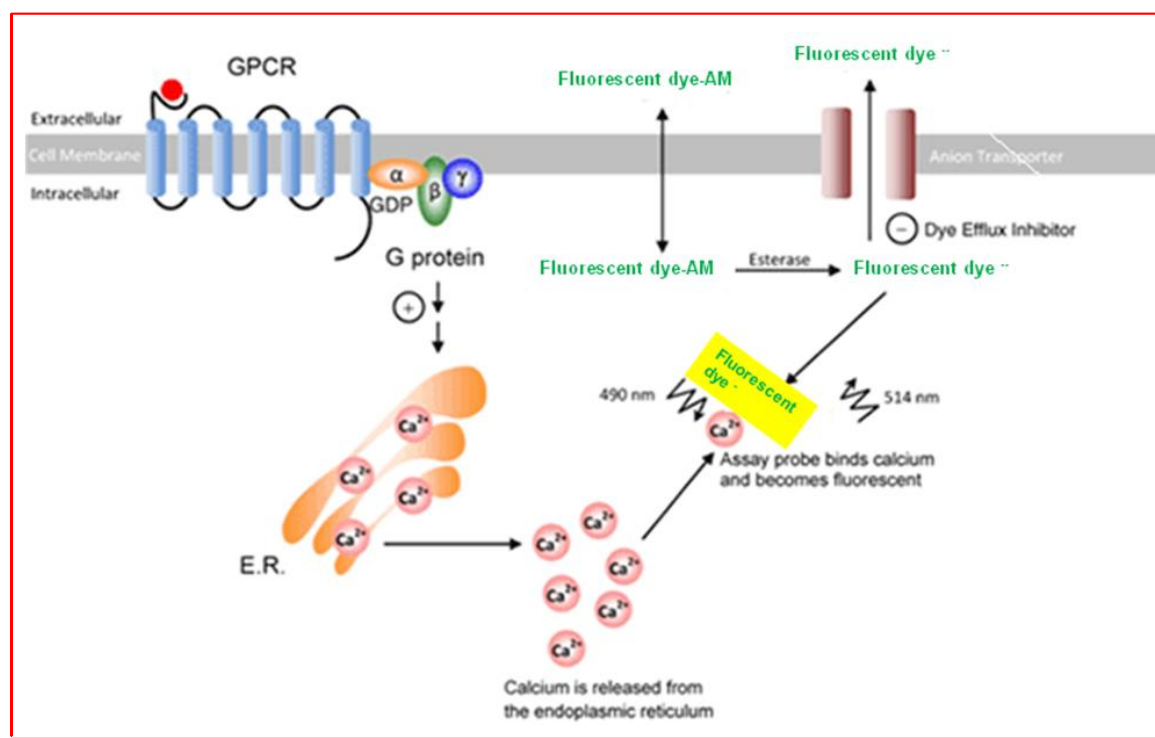
Figure 18. The fluorescent dye enters cells as a membrane-permeable acetoxymethyl (AM) ester. Once inside the cell, the fluorescent dye is hydrolyzed by intracellular esterases. The cell membrane-impermeable, negatively charged form of the fluorescent dye is now capable of binding with Ca^{2+}.[156]

Alternatively there are several methods for the screening of IP_3 levels. These methods are all cell-based and are a mixture of homogeneous and non-homogenous techniques. These methods should have rapid termination of the assay, a factor that introduces significant technical difficulties.

Practical experience has shown that calcium detection methodologies provide more robust assay options than those used to measure IP_3 accumulation. The measurement of IP_3 is necessary only when studying receptor inverse agonism.[126]

1.4.3. Measurent of extracellular signal-regulated kinase 1/2 levels (ERK$_{1/2}$)

Current methods employed in GPCR screening programs measure various cellular signaling events. As already described the most widely used include measuring the formation of cAMP, IP_3, and intracellular Ca^{2+} mobilization. cAMP assays are useful when the receptors are known to couple to G_i or G_s pathways, although they are limited in the irability to screen an orphan or G_q-coupled receptors. Ca^{2+} mobilization assays are widely used to measure activation of G_q-coupled receptors or in cell lines transfected with chimeric G proteins, which

redirect the normal signaling pathway through PLC and Ca^{2+} mobilization. Although this technology is widely used, it requires specialized instrumentation, and there are several limitations. The receptor must be $G_{\alpha q}$ coupled or be transfected with a chimeric G protein. The signal to baseline, and thus the dynamic range of the response, is often poor, and the time of flux is often brief, affording only a small window of time for measuring response. Finally, data output can be large due to the kinetic nature of the assay measurements forming large data sets.[157]

Because of these potential limitations, it is desirable to have another assay target as a measurement of cellular GPCR agonists and antagonists. The potential for using the phosphorylation of p42/44 MAP kinase (mitogen-activated protein kinase) (extracellular signal-regulated kinases 1 and 2 $ERK_{1/2}$) as a measure of GPCR activation became apparent in studies using COS-7 cells transfected with constitutively active mutants of $G_{\alpha s}$, $G_{\alpha q}$, or $G_{\beta \gamma}$. Transfection with these signaling mutants resulted in sustained activation of $ERK_{1/2}$[158,159] and demonstrated, at least in COS-7 cells, that activation of $ERK_{1/2}$ was possible from a variety of GPCR signaling inputs.

The $ERK_{1/2}$ cascade can be activated by a variety of different GPCRs, and the complex set of signaling pathways that are generated by GPCR stimulation converges at $ERK_{1/2}$, despite coupling to different G protein subclasses (Figure 19). Recent evidence has shown that these pathways are separated functionally by the presence of distinct pools of active $ERK_{1/2}$ throughout the cell.[160] Thus, activation of a GPCR in any given cell type may result in $ERK_{1/2}$ phosphorylation, and although the activated pool is located in the plasma membrane, focal adhesions, nucleus, or cytoplasm, $ERK_{1/2}$ can be used to measure the functional outcome of receptor stimulation.

Until recently, the use of $ERK_{1/2}$ activation as a measurement for GPCR activation has not been possible because a cell-based high throughput assay has not been available. Recent higher throughput assays for the detection of intracellular $ERK_{1/2}$ phosphorylation include electrochemiluminesence-based (Meso-Scale Discovery [MSD]) and infrared fluorescence-based (LICOR) detection systems. Using such detection systems, a 384-well ERK-based assay for the detection of agonist mediated dopamine D2 and D3 receptors has been described.[161]
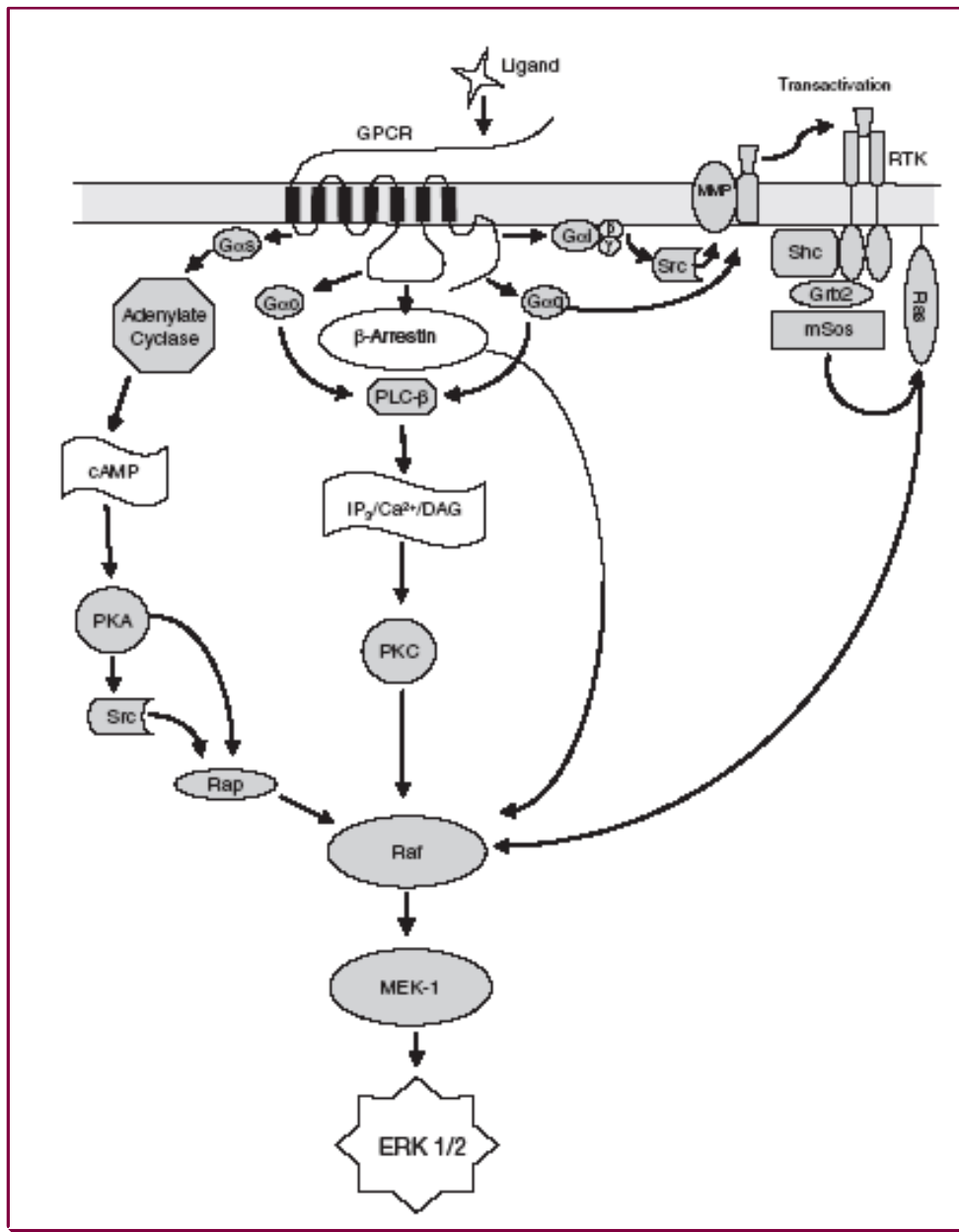
Figure 19. G protein–coupled receptor (GPCR) signaling pathways via ERK$_{1/2}$. ERK$_{1/2}$ can be activated by GPCRs, which couple to different protein subclasses and transduce the signal by different pathways. Functional separation of these signals is achieved by spatially distinct pools of ERK$_{1/2}$ within the cell.[160]

Common techniques for the detection of ERK$_{1/2}$, Western blotting or enzyme-linked immunosorbent assay (ELISA), are laborious and are medium throughput at best. The SureFire™ cellular ERK$_{1/2}$ assay measures activation of ERK$_{1/2}$ in a high-throughput format that is performed in 384-well microplates and can be fully automated with standard robotics. The assay was used to measure endogenous levels of ERK$_{1/2}$ phosphorylation in both transiently and stably transfected cell lines expressing G$_q$-coupled receptors and to measure the activation of endogenous GPCR receptor activation in several cell lines as well. The

measurements of GPCR activation indicated that ERK$_{1/2}$ activation is pharmacologically similar to previously established responses as measured by other assay formats.[157]

The serum response element (SRE) is activated by MAP kinases[162,163] which are activated by mitogenic signals from a number of receptors. At the SRE, a complex forms between the serum response factor and a ternary complex factor (e.g. Elk-1). A MAP kinase phosphorylates the ternary complex factor to allow the complex to initiate transcription. The βγ subunits from G$_i$ proteins have been shown to activate this pathway via Ras-dependent MAP kinase activation[159,164,165] (Figure 16 and 19). Stimulation of MAP kinases via G$_q$-coupled receptors results mainly from PKC activation.[159,164,166] Recent studies using SRE based reporter genes include investigation of the muscarinic M1 receptor,[167] Edg3 and Edg5 receptors for lysophosphatidic acid[168,169] and α1-adrenoceptors.[170]

ERK activation is related to the activation of the SRE-pathway.[171] The dopamine D2-receptor which is a G$_i$-coupled receptor has been previously shown to couple to the SRE-pathway.[172] The native P2Y$_{12}$-receptor mediates an activation of the extracellular signal-regulated protein kinase ERK[173,174] and recombinant hP2Y$_{12}$ was shown to activate the ERK through coupling to the SRE-pathway.[175] There is no information known about activation of the extracellular signal-regulated protein kinase ERK for the adenine receptors.

pSRE-Luc is designed for monitoring the induction of the serum response element (SRE) in a reporter gene assay. pSRE-Luc is designed to measure the binding of transcription factors to SRE, providing a direct measurement of activation for this pathway.[176] pSRE-Luc contains the firefly luciferase (luc) gene from Photinus pyralis.[177] After transcription factors bind SRE, transcription is induced and the reporter gene is activated. For example, the addition of serum or growth factors to the cell-culture medium induces the binding of transcription factors to SRE, which initiates transcription of the luciferase reporter gene. Luciferase is a highly sensitive enzymatic reporter that can be assayed by any standard luciferase-detection method, which provides quantitative data on induction levels. The pSRE-Luc vectors can be transfected into mammalian cells by any standard method.

1.4.4. ß-Arrestin assays

ß-Arrestin assays are high-throughput screening assays for monitoring GPCR activation following ligand stimulation, without an imaging instrument, fluorescent protein tag, or radioactivity. This assay method provides a suitable format for HTS automated screening. This GPCR assay system provide the means for discovering new therapeutic leads for known GPCRs and to potentially de-orphanize novel GPCRs with a high a sensitivity, specificity.[178,179]

1.4.4.1. Principle of ß-arrestin assay

GPCR activity can be monitored by detecting the interaction of arrestin with the activated GPCR using enzyme fragment complementation. In this system, the β-galactosidase enzyme is split into two inactive fragments. When these fragments are fused to two proteins that interact, the interaction of the two proteins forces the complementation of the fragments to restore enzyme activity. The figure 20 shows the system as applied to measuring GPCR activation. The larger portion of β-gal, termed Δω, is fused to the C-terminus of β-arrestin. The smaller complementing fragment of β-gal, the Δα, is expressed as a fusion protein with the GPCR of interest at the C-terminus. Upon activation, the GPCR is bound by β-arrestin. The interaction of β-arrestin and the GPCR forces the interaction of Δα and Δω, thus allowing complementation of the two fragments of β-gal and the formation of a functional enzyme capable of hydrolyzing substrate and generating a fluorescence signal (Figure 20).[178,179]

This assay eliminates interference from endogenous receptors on the parental cells because it measures a signal that is specifically generated by the tagged receptor and is immediately downstream of receptor activation.[179]

In general these important factors must be taken into consideration in the design of assays:
1) the low costs of assay development and assay reagents;
2) the ease of use and suitability of the assay format for automation;
3) the generation of an assay end-point suitable for miniaturization into 96-, 384-,1536-well and smaller microplate formats;
4) the generation of a suitable signal ratio in the assay to enable the rapid identification of any compound with activity.

An ideal assay would involve few requirements, no plate-to-plate transfers or washing steps, and would be suitable to full automation.
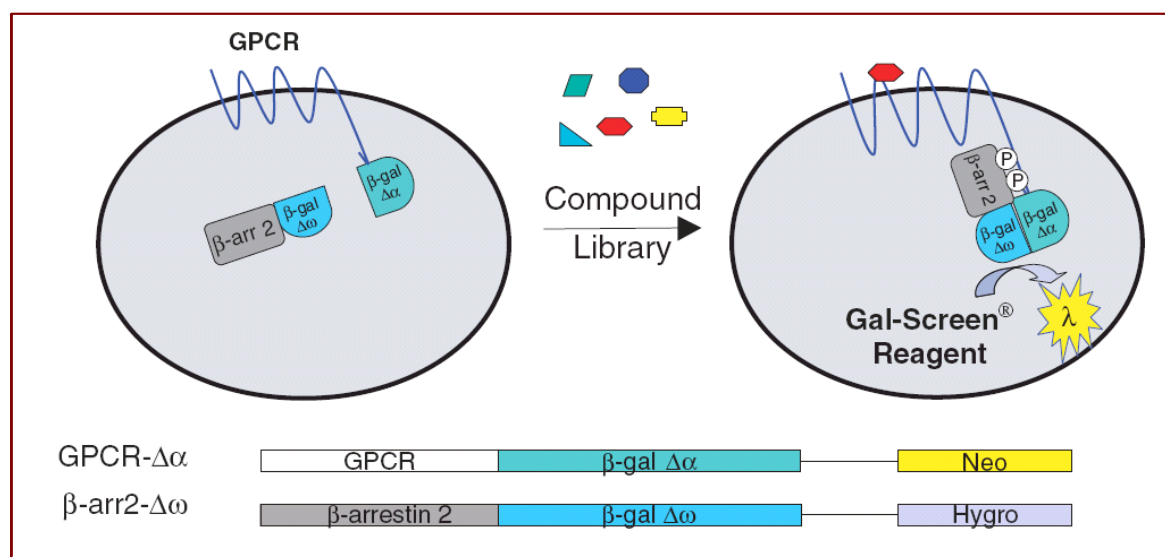
Figure 20. The inactive β-gal deletion mutants, Δα and Δω are fused to the carboxyl terminus of a GPCR and β-arrestin 2, respectively. Fusion proteins are stably expressed in cells following retroviral infection and clone selection. Interaction of ligand-activated GPCR with β-arrestin 2 drives complementation of the β-gal mutant fragments.[178]

1.5. Retroviral gene transfer technology principle

Current retroviral gene transfer technology is based on the coordinated design of packaging cell lines and retroviral expression vectors.[180,181] To develop a packaging cell line, the viral gag, pol, and env genes are stably integrated into the genome of the packaging cell line. The separate introduction and integration of the structural genes minimizes the chances of producing replication-competent virus due to recombination events during cell proliferation.[182,183] Retroviral expression vectors provide the packaging signal Ψ^+, transcription and processing elements, and a target gene. The viral env gene, expressed by the packaging cell line, encodes the envelope protein. Viral envelopes are classified according to the receptors used to enter host cells. For example,

1. ecotropic viruses can recognize a receptor found only on mouse and rat cells;
2. amphotropic viruses recognize a receptor found on a broad range of mammalian cell types;
3. dualtropic viruses recognize two different receptors found on a broad range of mammalian cell types;

4. a pantropic packaging cell line provides a major advancement in retroviral gene transfer, as this cell line produces viruses that can infect both mammalian and non-mammalian cells.[183] Using this cell line, virions are pseudo-typed with the envelope glycoprotein from the vesicular stomatitis virus (VSV-G). Unlike other viral envelope proteins, VSV-G mediates viral entry through lipid binding and plasma membrane fusion.[184]

Stable expression of the VSV-G envelope protein is toxic; thus, the packaging cell line only contains the viral gag and pol genes. Virus is produced by transiently cotransfecting a retroviral expression vector and pVSV-G into a pantropic packaging cell line.
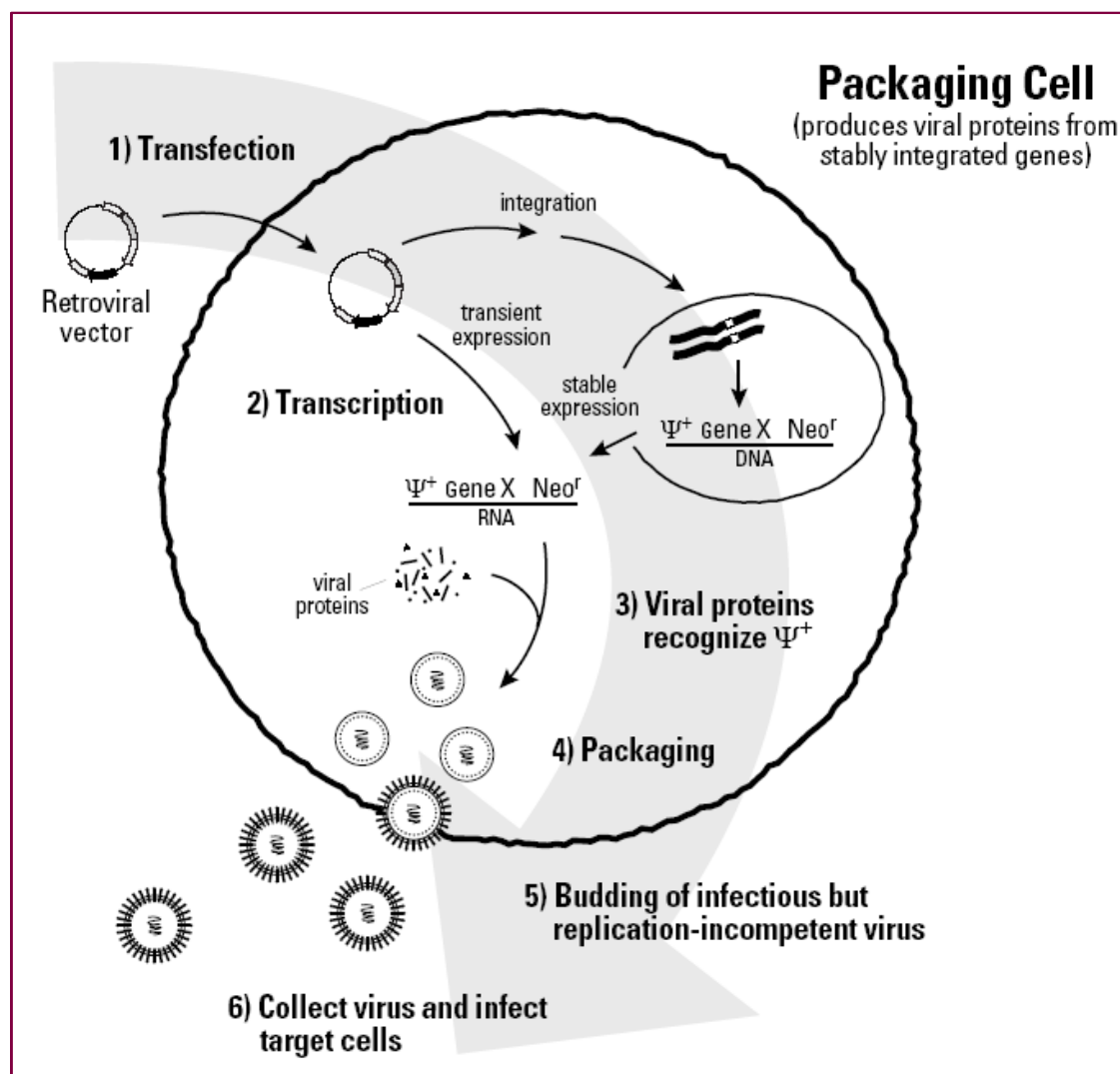
Figure 21. Virus production in packaging cell lines. The *gag, pol* and *env* genes required for viral production are integrated into the packaging cells genome. The vector provides the viral packaging signal, commonly denoted Ψ^+, a target gene, and drug-resistance marker.

Once a packaging cell line is transfected with a retroviral expression vector that contains a packaging signal, the viral genomic transcript containing the target gene and a selectable marker are packaged into infectious viruses within 48–72 h. Antibiotic selections are used to select cells that stably express the integrated vector. Stable virus-producing cells can be frozen and used in later experiments. Virus produced by both transient and stable transfections can infect target cells and transmit target genes; however, it cannot replicate within target cells because the viral structural genes are absent.

In this study an amphotropic retrovirus packaging cell line (GP+*env*Am12) was used. This amphotropic retrovirus packaging cell line was constructed in which the *gag, pol*, and *env* genes of the helper virus are separated on two different plasmids. A plasmid containing the moloney murine leukemia virus gag and pol genes was transfected into NIH 3T3 cells, and a plasmid containing the 4070A amphotropic env gene was transfected into one of the resulting clones which produced a high level of reverse transcriptase. A clone producing a high level of amphotropic env protein (GP+*env*Am12) was then isolated.[185]

2. Scope of investigation

The purinergic receptor family represents very important targets for the discovery of new drugs for the treatment of various diseases via activation or blockade of those receptors. Therefore the goals of the present study were:

➢ construction of recombinant cell lines expressing purine receptor subtypes

➢ assay development in:

- native tissues and cells

- recombinant cells

In order to develop assays for compound testing such as:

✓ radioligand binding assay at membranes and living cells

✓ functional assays via measurement of:

- cAMP accumulation,

- measurement of intracellular Ca^{2+} levels

- the ERK signaling pathway coupled receptors.

And subsequent

➢ screening of compound libraries

➢ detailed characterization of selected compounds

➢ analysis of their structure-activity relationships

➢ investigation of species differences

➢ and characterization of purinergic receptors in tissues and cells of various species.

In particular, the present study focuses on the newly discovered adenine receptors.

2.1. Adenine receptors (P0 receptors)

2.1.1. Human adenine receptors

Purinergic receptors are divided into two families, P1 receptors activated by nucleosides and P2 receptors activated by nucleotides.[2] The P0 receptors (adenine receptors) have recently been discovered and identified as a third member of the purinergic receptor family.[5] Adenine has been identified as the endogenous agonist for the adenine receptors.[102] Two adenine receptor subtypes were identified, rat Ade1R, its mouse ortholog MrgA10 and mouse Ade2R. Radioligand binding studies at membranes of human astrocytoma 1321N1 cells revealed that a human ortholog of the rAde1R appears to exist.[104] The human adenine receptor was also detected in Jurkat T cells and HEK293 cells.[186]

In HEK293 cells, the adenine receptor is expressed in very high density with a single high-affinity binding site.[186] The affinity of the physiological agonist adenine for human adenine receptors in membrane preparation of HEK293 cells showed a K_i value of 47.1 nM[186] which was in a good agreement with that obtained for adenine receptors in rat cortical membrane preparations (K_i value of 29.2 nM).[104] In the present study, our goal was to characterize the human adenine receptors in intact HEK293 cells using different radioligand binding studies including saturation, competition and kinetic experiments and subsequently compare the obtained results with those obtained with membrane preparations of HEK293 cells. The results will provide information about the behavior of the human adenine receptors in HEK293 cells under more physiological conditions. To investigate whether the human adenine receptors in HEK293 cells are G_i- or G_s-coupled, we plan to functionally characterize the human adenine receptors in the HEK293 cells using cAMP accumulation assays. In addition, adenine-induced ERK signalling will be investigated and a luciferase reporter gene assay is to be established useful for high-throughput screening in native HEK293 cells as well as in recombinant 1321N1 astrocytoma cells.

In order to fully characterize the adenine receptors in different cells or tissues and to understand its physiological role, potent ligands, agonists and antagonists, must be developed. Therefore we aimed to search for potent ligands via screening of compound libraries based on modifications of the physiological agonist adenine, in various positions, either commercially available compounds or newly synthesized compounds, using radioligand binding assays. An important goal was to study their structure-activity relationships at the adenine receptors of human HEK293 cells and rat cortical membrane preparations and to analyze any species differences of the adenine receptor in human and rat. For the most potent compounds, functional assays were to be performed in order to know if they functioned as agonists or antagonists. cAMP assays had to be established using (a) a radioactive cAMP binding assay and (b) a cAMP luciferase gene reporter assay. In addition, we aimed to study the selectivity of the most potent compounds against the adenosine receptors.

2.1.2. Mouse adenine receptors

The mouse adenine receptor sequence found in mouse brain and NG108-15 cells, which is clearly distinct from the mouse ortholog (mMrgA10) of the rat adenine receptor, (mAde2R), was recently cloned.[104] In this study, we aimed at functionally characterizing the cloned mAde2R receptor in order to know whether it is coupled to G_i or G_s proteins. In addition, we

planned to screen the most potent ligands of the purinergic receptors in order to distinguish the properties of the newly cloned adenine receptor from the other members of the purinergic receptor family.

2.1.3. Hamster (CHO cells) and rat (PC12 cells) adenine receptors

The studying of the effect of species differences and expression levels of AdeRs in different mammalian cell lines is very important for the characterization of the adenine receptors. For this reason we aimed at characterizing adenine receptors natively expressed in Chinese hamster ovary cells (CHO K1) and endogenous rat adenine receptors in pheochromocytoma cells (PC12 cells) using cAMP functional studies to determine the coupling of adenine receptors natively expressed in these cell lines. In addition we planned to determine the adenine receptor density in PC12 and CHO cells using radioligand binding studies.

In addition to the main project, which focused on adenine receptors, other goal was to establish cell-based assays for several other members of the purinergic receptor family including adenosine A_{2A} and A_{2B}, $P2Y_1$, $P2Y_{11}$, $P2Y_{12}$, $P2Y_{13}$, $P2X_2$, $P2X_3$ and $P2X_4$ receptors.

3. Results and discussion

3.1. Human adenine receptors

3.1.1. Pharmacology and test systems for the human adenine receptors

Radioligand binding studies at membranes of human astrocytoma 1321N1 cells revealed that a human ortholog of the rAde1R appears to exist.[104] The human adenine receptor was also detected in Jurkat T cells and HEK293 cells, which is in agreement with the expression of adenine receptors in porcine kidneys.[186] In HEK293 cell membranes the adenine receptor was found to be expressed in very high density (B_{max} value of 8.18 pmol/mg protein) with a single high-affinity binding site.[186] In competition studies, the physiological agonist adenine showed a K_i value of 29.2 nM for adenine receptors in rat cortical membrane preparations,[102] and a K_i value of 47.1 nM for human adenine receptors in membrane preparation of HEK293 cells.[186] The K_i value of adenine for human adenine receptors in membrane preparations of HEK293 cells was in good agreement with the determined K_D value obtained in saturation assays (44.1 nM).[186] In the present study we characterized human adenine receptors in more detail.

3.1.1.1. Radioligand binding studies

3.1.1.1.1. [³H]Adenine saturation experiments (saturation experiments for whole cells)

Intact HEK293 cells were used for saturation studies. [³H]Adenine saturation experiments exhibited two binding sites with a K_{D1} value of 92.4 ± 4.7 nM and a B_{max1} value of 1.882 ± 0.075 pmol/mg of protein, and a second site with a K_{D2} value of 4.15 ± 0.5 M and a B_{max2} value of 0.381 ± 0.095 pmol/mg of protein ($n = 2$, Figure 22). We conclude that [³H]adenine labelled two binding sites one with high affinity and a second one with low affinity. The receptor density is quite high with a B_{max} in the picomolar range for the high affinity site.
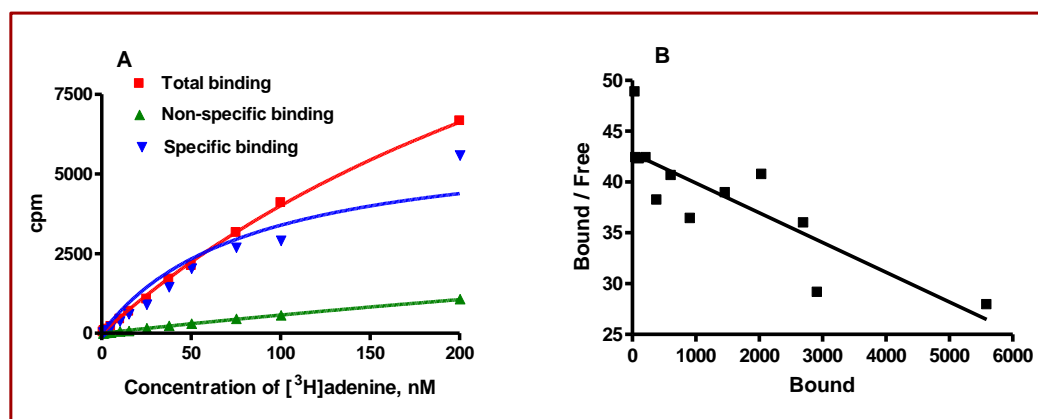
Figure 22. Saturation of [³H]adenine binding to adenine receptors in HEK293 cells. The mean ± S.E.M of two independent experiments, performed in duplicate at room temperature, is shown.

3.1.1.1.2. Kinetic studies at whole HEK293 cells

Association kinetics were performed by measuring the specific binding of [³H]adenine (15 nM) at different time points between 2 and 240 min after addition of [³H]adenine. Nonspecific binding was determined by the addition of 100 µM adenine.

Dissociation studies. Cells were first incubated with [³H]adenine (15 nM) for 60 min. Specific binding was then measured at 2–120 min after the addition of 100 µM adenine.

Results of kinetic studies (Figure 23A) showed that [³H]adenine bound to HEK293 whole cell rapidly, and the steady state appeared to be reached after 15 min and sustained for at least 200 min (K_{obs}= 0.263 ± 0.046 min^{-1}). The binding was slowly reversed by the addition of adenine in a final concentration of 100 µM, with 30% of dissociation being evident after 60 min (Figure 23B). A kinetic K_D value could not be determined and the law of mass action did not apply to the system. An explanation for the observed unusual kinetics could be that the adenine receptor undergoes a conformational change after binding of [³H]adenine; an initial low affinity conformation may be converted to a high-affinity conformation for adenine upon binding. A similar phenomenon had been already observed at rat brain cortical membrane preparations.[186]
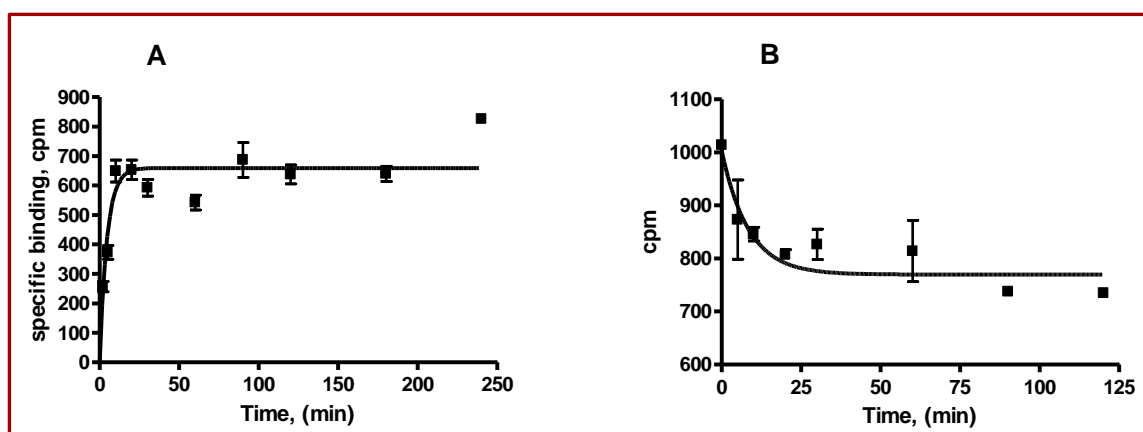
Figure 23. The kinetics of [³H]adenine binding (15 nM) to HEK293 cells at 23°C. (**A**) representative association curve for specific [³H]adenine (15 nM) binding to HEK293. (**B**) Representative dissociation curve obtained by the addition of 100 µM unlabeled adenine to equilibrated specific binding of [³H]adenine (15 nM) to HEK293 cells (*n* = 3).

3.1.1.1.3. [³H]Adenine competition assays

The binding site of adenine receptors in HEK293 cells was further characterized using competition assays. HEK293 cells (3 x 10⁵) were incubated with 15 nM [³H]adenine as a radioligand. Inhibition curves were determined using different concentrations of adenine.

Nonspecific binding was determined with 100 µM adenine. The results showed that adenine exhibits an affinity of 3.44 µM in whole cell binding assays which means a 73-fold lower affinity than in competition assays using adenine and membrane preparations of HEK293 cells (Figure 24). It was also considerable lower than the K_D value determined in saturation assays (see 3.1.1.1.1.).

The difference between the results from whole cell binding studies and binding assays at membrane preparation of HEK293 cells may be due to the fact that the intact cells have a machinery for quickly and efficiently removing physiological receptor agonists, in this case adenine, by degradation or cellular uptake, to limit their actions. However, little is known so far about the extracellular metabolism of adenine. Transporter proteins for adenine have been described, which may contribute to the removal of adenine from the extracellular compartment.[111, 113]
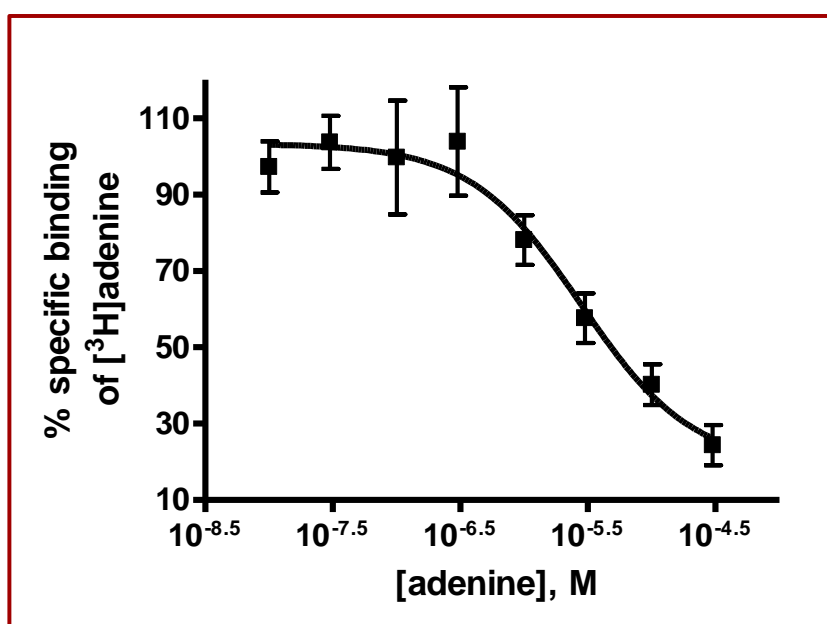
Figure 24. Competition of [³H]adenine binding (15 nM) to adenine receptors in HEK293 cells (intact cells); K_i = 3.44 ± 1.46 µM from three independent experiments performed at room temperature.

The binding sites for [³H]adenine detected in HEK293 cell membranes showed similar properties as in brain cortex. Therefore, this cell line can be used as a model for studying natively expressed adenine receptors.

As a next step the coupling of adenine receptors to adenylate cyclase was to be studied. Therefore functional studies were performed.

3.1.1.2. Functional studies

3.1.1.2.1. cAMP accumulation assays at human adenine receptors in HEK293 cells

It had been shown before that adenine receptors in human HEK293 cells are coupled to G_s protein and therefore adenine leads to an increase in intracellular cAMP in a dose-dependent manner with an IC_{50} value of 4.72 µM.[186] However cAMP assays performed at human adenine receptors in HEK 293 cells in our hands suggested that two distinct subtypes of adenine receptors might exist in this cell line (Figure 25A). Another explanation could be that the adenine receptors in HEK 293 cells might couple to inhibition as well as to activation of adenylate cyclase depending on the test conditions, i.e. the concentration of adenine used for receptor stimulation.
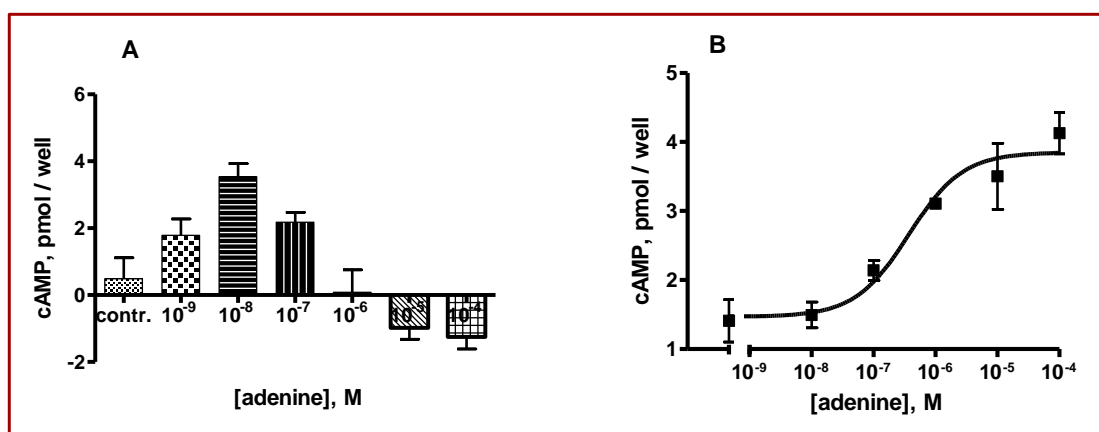
Figure 25. (**A**) The figure shows the amount of intracellular cAMP-accumulation by adenine (0.001–100 µM). (**B**) Stimulation of adenylate cyclase activity by adenine in HEK293 cells after incubation of cells with PTX (100 ng/ml). The figure shows the concentration-dependent stimulation of intracellular cAMP-accumulation by adenine (0.01–1 µM). The EC_{50} value was 0.372 µM ($n = 1$).

To further test this assumption, the effect of pertussis toxin (PTX) on adenine receptors in HEK293 was studied. Cells were pre-treated with PTX (100 ng/ml) over night before the cAMP assay was performed. Pertussis toxin is inhibiting the signal transduction via G_i-coupled GPCRs by catalyzing the ADP ribosylation of the α-subunit of the G protein. Therefore the G_α subunit remains in its GDP-bound inactive state and is not able to inactivate the adenylate cyclase. Pertussis toxin has no effect on the stimulatory G_s proteins. By inactivating the G_i- coupling of the adenine receptor we only see the stimulatory effect of adenine as shown in figure 25B.

We conclude that adenine receptors in HEK293 cells are coupled to stimulation of adenylate cyclase, which is seen at low concentrations, via G_s, and to inhibition of adenylate cyclase (G_i) at high concentrations.

However, the coupling of adenine receptor to the G_s pathway is relatively weak if we compare the produced amount of cAMP/well to that produced in case of adenosine A_{2A} and A_{2B} receptors expressed in CHO cells. Using the same test system both, adenosine A_{2A} and A_{2B} receptors, showed amounts of cAMP not less than 20 pmol/well when stimulated with the agonist NECA at a concentration of 1 μM. In comparison the maximal effect induced by adenine in HEK293 is at least 5-fold weaker.

3.1.1.2.2. Investigation of extracellular signal-regulated kinase (ERK) phosphorylation induced by human adenine receptors in HEK293 cells

The detected coupling of human adenine to adenylate cyclase in HEK293 was not strong using cAMP accumulation assays. Therefore, a further functional study was performed in order to study the pharmacological properties of this receptor in HEK293 cells, using an ERK-phosphorylation assay. To investigate whether adenine has any effects on this downstream target, we performed a luciferase assay using SRE-LUC as a reporter gene for human adenine receptors in HEK293 cells. SRE is located in the promoter region of the c-Fos gene and plays a major role in regulation of c-Fos gene transcription.
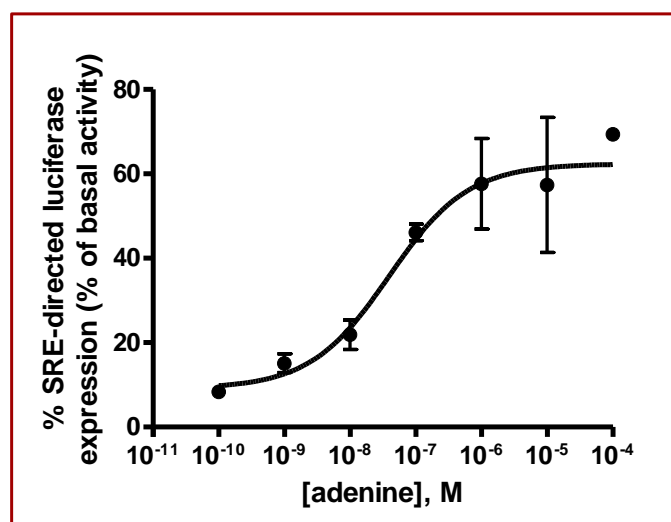
Figure 26. Increases in SRE-dependent luciferase expression upon addition of different concentrations of adenine in HEK293 cells (% of basal activity). The EC_{50} value was 21.5 ± 2.1 nM ($n=3$).

In the luciferase assay, adenine induced the SRE-LUC reporter gene expression in a dose-dependent manner with an EC_{50} value of 21.5 ± 2.1 nM (Figure 26). Because adenine could induce SRE-LUC reporter gene expression, it also influenced the phosphorylation of ERK. Our studies provide new insights into the activation of the ERK signaling pathway via adenine receptors.

Recently, by use of a luciferase gene reporter assay it was shown that the human $P2Y_{12}$ recombinantly expressed in CHO stimulates the ERK-pathway upon receptor activation via SRE-dependent gene expression; this pathway was shown to be pertussis toxin sensitive.[175] The human $P2Y_{12}$ receptor expressed in CHO Flp-In cells showed an increase of ca. 50-60% of basal increases in SRE-dependent luciferase expression activity.[175] Similar results were now obtained with the adenine. At a concentration of 10 μM a $57 \pm 16\%$ increase in SRE-dependent luciferase was observed. From the above data, we conclude that the human adenine receptors in HEK293 cells leads to stimulation of ERK-pathway that is comparable with the reported signal of the human $P2Y_{12}$ receptor inducing $ERK_{1/2}$ phosphorylation. It should be noted that the EC_{50} value of adenine determined in ERK phosphorylation assay (21.5 nM) was much lower than that determined in the cAMP assay (372 nM).

3.1.2. Structure-activity relationships of adenine derivatives at human and rat adenine receptors

It had been shown in studies that even only small modifications at the adenine structure led to a major reduction or loss of affinity for the rAde1R. For example, 1-, 3-, 6-, 7-, or 9-methyl-adenine exhibited K_i values in the micromolar range at the rAde1R compared with nanomolar affinity for adenine.[104]

As already pointed out, there is evidence showing that adenine may play a role in human and pig renal function.[108] Consistent with these observations, we detected a specific binding site for [^{3}H]adenine in HEK293 cell membrane preparations (Figure 27A). Homologous competition experiments with adenine versus [^{3}H]adenine (10 nM) at HEK293 cell membranes yielded a K_i value of 47.1 nM, which is very similar to the K_i value of 29.2 nM obtained for adenine at rat brain cortical membrane preparations (Figure 27B).
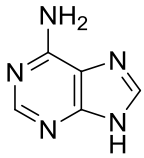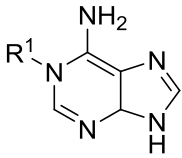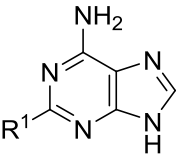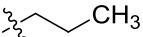
We subsequently performed competition experiments to investigate the structure-activity relationships of selected adenine derivatives at the high-affinity adenine binding site in HEK293 cell membranes. Experimental conditions for the HEK membranes were the same as for the rat receptor preparations. The determined competition curves for the most active adenine derivatives are collected in figure 28 and affinities are compared with those determined for the rAde1R at rat brain cortical membrane preparations using [^{3}H]adenine (10 nM) as a radioligand.[104]
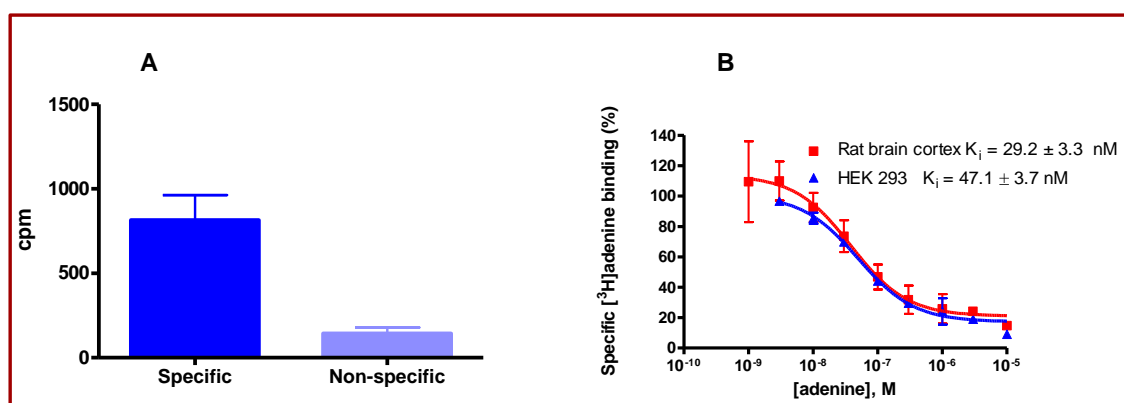
Figure 27. (**A**) Non-specific and specific binding of 10 nM [^{3}H]adenine to HEK293 cell membrane preparations (100 µg protein, n = 3; error bars represent SEM values); (**B**) Homologous competition experiments with adenine vs. [^{3}H]adenine (10 nM) at membrane preparations of rat brain cortical membrane, and HEK293 cell membrane preparations, respectively. Data points are means ± SEM of three experiments performed in triplicates at room temperature.

It has clearly been shown that [³H]adenine is a suitable radioligand for the labelling of AdeR if bacterial contaminations (which can also bind [³H]adenine) in the applied buffer solutions are avoided.[187] A series of compounds was investigated in radioligand binding studies at membrane preparations of human embryonic kidney HEK293 cells in order to assess their affinity for human adenine binding sites.

Table 5. Comparison of affinities of adenine and adenine derivatives for human and rat adenine receptors determined in radioligand binding studies using membrane preparations (modification at position 1 and 2).

Compound		R^1	$K_i \pm$ SEM [µM] vs. [³H]adenine $(n=3)^a$	
			HEK293 cells	Rat brain cortex
1	Adenine	___	**0.0471** $\pm$ 0.037	**0.0292** $\pm$ 0.0034
2	1-Propyladenine	⌇⁓CH₃	>> **100** $(15 \pm 5)^a$	>> **100**[186] $(12 \pm 5)^a$
3	2-Aminoadenine	-§-NH₂	**1.23** $\pm$ 0.49	**4.95** $\pm$ 0.75[186]
4	2-Azidoadenine	-§-N₃	> **100** $(35 \pm 4)^a$	**3.18** $\pm$ 0.67[186]

^{a}Percent inhibition $\pm$ SEM of radioligand binding at 100 µM.
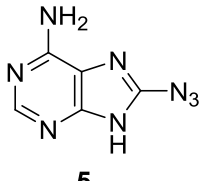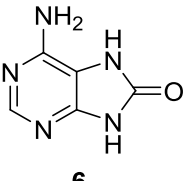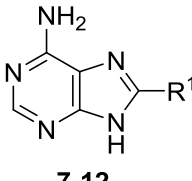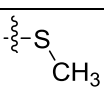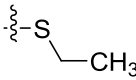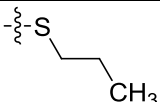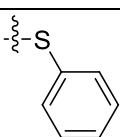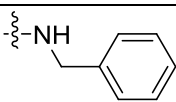
A comparison of the affinities of adenine and three adenine derivatives for the human adenine receptors in membrane preparations of HEK293 cells adenine showed that the affinities and the rank order of potency were similar to those at the adenine receptor expressed in rat brain cortex. (Table 5) The exception was 2-azidoadenine (**4**) which showed affinity for adenine receptors expressed in rat cortical membranes with a K_i value of 3.18 µM, whereas it showed no measurable affinity for the human receptors in membrane preparations of HEK293 cells.

The introduction of an oxo-function in position 8 of adenine (**6**) resulted in increased K_i values (110 µM and 27 µM) in both test systems in comparison with the parent compound adenine. Substituents in the 8-position with alkyl- and arylsulfanyl residues (**8**-**11**) diminished the affinity for the rat adenine receptors in cortical membrane preparation at a concentration of 30 µM when compared to 8-thioadenine (K_i = 2.77 µM).[102] The 8-phenylsulfanyl adenine (**11**) showed affinity in the micromolar range (K_i = 34.8 µM) for the human adenine receptors

in a membrane preparation of HEK293 cells while the 8-alkylsulfanyl residues (**8-10**) abolished affinity in the same test system. 8-Azidodenine (**5**) and 8-benzylaminoadenine (**12**) were able to displace [³H]adenine binding with affinities in the micromolar range in both test systems (Table 6).

Table 6. Comparison of affinities of adenine derivatives with modifications at position 8 for human and rat adenine receptors determined in radioligand binding studies using membrane preparations.
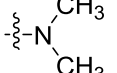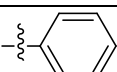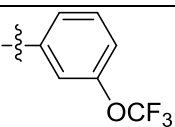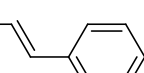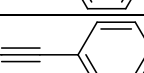
Compound		R¹	$K_i \pm$ SEM [µM] vs. [³H]adenine (n=3)	
			HEK293 cells	Rat brain cortex
5	8-Azidoadenine (HPLL 92)	___	**11.2** ± 2.8	**6.37** ± 0.74[186]
6	8-Oxoadenine (TB 34)	___	**110** ± 4	**27.0** ± 6.5[186]
7	TB 32 (PSB-09032)	$-NH_2$	**0.0341** ± 0.0088	**6.51** ± 1.92[186]
8	TB 37	$-S{-}CH_3$	**>> 100** $(9 \pm 2)^a$	**>> 30** $(10 \pm 6)^b$
9	TB 38	$-S{-}CH_3$	**>> 100** $(24 \pm 1)^a$	**>> 30** $(0 \pm 6)^b$
10	TB 39	$-S{-}CH_3$	**> 100** $(46 \pm 2)^a$	**>> 30** $(0 \pm 4)^b$
11	TB 45	$-S{-}$	**34.8** ± 8.1	**>> 30** $(0 \pm 2)^b$
12	TB 25	$-NH{-}$	**32.9** ± 2.9	**6.67** ± 1.03[186]

^{a}Percent inhibition ± SEM of radioligand binding at 100 µM; ^{b}Percent inhibition ± SEM of radioligand binding at 30 µM.

8-Aminoadenine (**7**) exhibited a K_i value of 0.0341 µM at the human binding site and thus **7** was more potent than adenine itself (K_i = 0.0471 µM). Compound **7** was 190-fold more potent at the human as compared to the rat binding site and therefore shows high species-selectivity. Modifications at position 8 of adenine (Table 7) such as 8-(1-piperidinyl)adenine (**13**), 8-(1-piperazinyl)adenine (**15**), and 8-dimethylaminoadenine (**16**) led to higher AdeR affinities than

bulky, lipophilic residues. However, 8-(1-pyrrolidinyl)adenine (**14**) showed no measurable affinity for the human adenine receptors in membrane preparations of HEK293 cells at a concentration of 100 µM while its K_i value at the rAde1R was 42.5 ± 2.5 µM.

Table 7. Comparison of affinities of adenine derivatives with modifications at position 8 for human and rat adenine receptors determined in radioligand binding studies using membrane preparations.
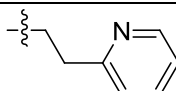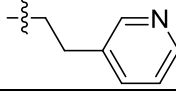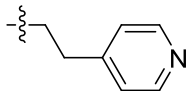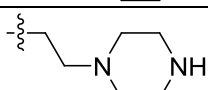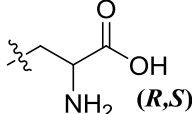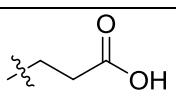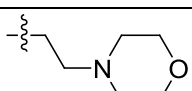
13- 20

| Compound		R^1	$K_i \pm$ SEM [µM] vs. [³H]adenine $(n=3)^a$	
			HEK293 cells	Rat brain cortex
13	ANR 425	–N(piperidinyl)	**31.7** ± 4.8	**3.94** ± 0.87
14	ANR 429	–N(pyrrolidinyl)	> **100** (18 ± 3)^a	**42.5** ± 2.5
15	ANR 426	–N(piperazinyl)NH	**27.4** ± 4.6	**3.27** ± 0.12
16	ANR 430	–N(CH₃)CH₃	**34.1** ± 3.2	**2.30** ± 0.28
17	TB 35	phenyl	>> **100** (22 ± 7)^a	>> **100**[186] (16 ± 11)^a
18	TB 40	phenyl-OCF₃	**7.21** ± 1.37	>> **100**[186] (23 ± 1)
19	TB 41	styryl	**12.2** ± 1.8	**18.2** ± 5.0[186]
20	TB 42	phenylethynyl	≥ **100** (46 ± 1)^a	>> **30** (19 ± 2)^b

^{a}Percent inhibition ± SEM of radioligand binding at 100 µM; ^{b}Percent inhibition ± SEM of radioligand binding at 30 µM.

Phenyl, 3-trifluoromethoxyphenyl, and phenylethynyl substitution (**17**, **18**, and **20**) resulted in a total loss of affinity for rat adenine receptors in rat cortical membrane preparations.

8-Benzylaminoadenine (**12**) and 8-styryladenine (**19**) exhibited an affinity in the low micromolar range. 8-Styryladenine (**19**) showed nearly the same affinity in both species.

Table 8. Comparison of affinities of adenine derivatives with modifications at position 9 for human and rat adenine receptors determined in radioligand binding studies using membrane preparations.
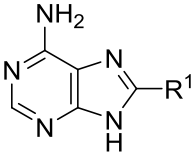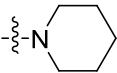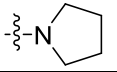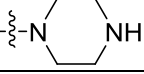

Compound	R^1	$K_i \pm$ SEM [µM] vs. [^{3}H]adenine (n=3)^a	
		HEK293 cells	Rat brain cortex
21 9-Methyladenine	$-CH_3$	ca. **100** $(44 \pm 7)^a$	**17.5** $\pm 2.96^{186}$
22 9-Cyclopentyladenine		ca. **100** $(50 \pm 8)^a$	**43.5** $\pm 7.44^{186}$
23 TB 33		ca. **100** $(57 \pm 2)^a$	**49.1** $\pm 11.7^{186}$
24 TB 68		ca. **100** $(58 \pm 3)^a$	**45.1** $\pm 0.3^c$
25 TB 66		$\geq$ **100** $(41 \pm 2)^a$	**75.1** ± 8.1
26 TB 64		> **100** $(44 \pm 4)^a$	$\geq$ **250** $(46 \pm 3)^b$
27 TB 62		>> **100** $(0 \pm 4)^a$	> **250** $(28 \pm 6)^b$
28 AAla		**6.23** ± 1.81	**10.7** $\pm 1.11^{186}$
29 Apr acid APalpha acid		**18.5** ± 5.6	**20.5** $\pm 0.42^{186}$
30 EA 6203		**5.49** ± 1.42	**2.98** $\pm 0.16^{186}$

^{a}Percent inhibition $\pm$ SEM of radioligand binding at 100 µM; ^{b}Percent inhibition $\pm$ SEM of radioligand binding at 250 µM. ^{c}Data from Dr. Anke Schiedel.
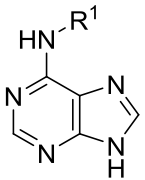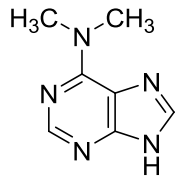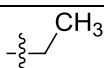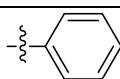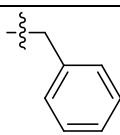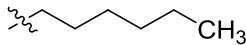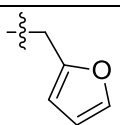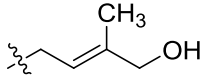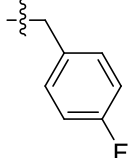
Introduction of the electron-withdrawing trifluromethoxy group in the *m*-position of 8-phenyladenine (**18**) led to increased affinity for human adenine receptors in membrane preparation of HEK293 cells (K_i = 7.21 µM) compared to the unsubstitued rigid phenyl ring, but still had a much lower affinity than the parent compound adenine (K_i = 44.7 nM). The enhanced affinity of the trifluoromethoxyphenyl derivative, compared to the unsubstituted phenyl compound, was probably due to its electron withdrawing property.

9-Methyladenine (**21**) and 9-cyclopentyladenine (**22**) showed no measurable affinity at the human adenine receptors. 9-Phenethyladenine (**23**) exhibited low affinity (K_i = 49.1 µM), whereas the introduction of one or two basic nitrogen atoms to the 9-substituent could result in positive or negative effects on the affinity, depending on the position of the basic function. Both, the piperazine derivative **27** and the 4-pyridyl derivative **26** showed no measurable AdeR affinity. 3-Pyridylethyl-substituted adenine **25** showed a slight increase in affinity (K_i = 75.1 ± 8.1 µM) at rAde1R. Compound **24**, featuring a nitrogen atom in the *ortho*-position, had a quite similar affinity (K_i = 45.1 µM) like the corresponding pyridyl derivatives **25** and **26**. The morpholinyl derivative **30** also showed good AdeR affinity in the low micromolar range (Table 8). The K_i values of **28** and **29** indicated that the introduction of polar functions at position 9 of adenine positively affected the AdeR binding affinity. The 9-substituted adenine derivatives bearing polar substituents (**28**, **29** and **30**) showed almost identical affinities for the human and the rat binding sites. All other 9-substituted compounds were weaker at human binding sites than at the rat adenine receptor.

At position N^6 of adenine, introduction of a methyl group was tolerated by human adenine receptors (**31**, K_i value of 22.6 µM), whereas ethyl (**32**), phenyl (**33**), benzyl (**34**) and hexyl (**35**) residues resulted in a very weak affinity. A small polar substituent as in compounds **36** and **37** led to an increase in affinity for AdeR (K_i values of 0.500 µM and 1.38 µM, respectively). Compounds **36** and **37** exhibited higher affinity (4–19-fold) for the rat AdeR than for the human adenine binding site (Table 9). Dimethylation of the amino group (**38**) abolished affinity in both test systems, indicating that a hydrogen bond donor (N-H) in that position was probably required for binding to the receptor, similarly as in adenosine receptors.[188]

Compounds **39**, **41** and **42** with relatively large ring structures showed higher affinity for the human adenine receptors than N^6-hexyladenine. Thus, this position can probably tolerate bulky substituents with particular ring structures, but not larger, non-polar residues. N^6-(4-fluorobenzyl)adenine (**41**) showed higher affinity with a K_i value of 13.8 µM compared with N^6-benzyladenine (**34**) in both test systems. This improvement in the affinity is a result of the introduction of fluorine atom at the benzyl residue.
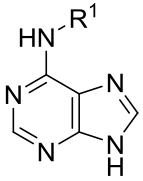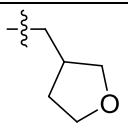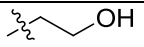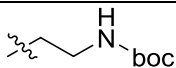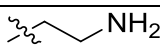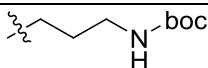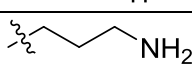
Table 9. Comparison of affinities of adenine derivatives with modifications at N^6 for human and rat adenine receptors determined in radioligand binding studies using membrane preparations (part I).
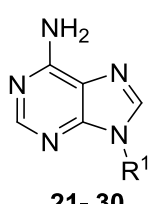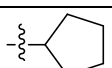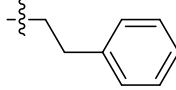

31- 37, 39, 40, 41   **38**

Compound	R^1	$K_i \pm$ SEM [µM] vs. $[^3H]$adenine $(n=3)^a$	
		HEK293 cells	Rat brain cortex
31 N^6-Methyladenine	–§–CH_3	**21.6** $\pm$ 3.2	**3.64** $\pm$ 0.36[186]
32 N^6-Ethyladenine (TB 20)	–§–CH_3	ca. **100** $(60 \pm 2)^a$	**16.4** $\pm$ 2.89[186]
33 6-Anilinopurine	–§–	$\gg$ **100** $(26 \pm 9)^a$	**65.3** $\pm$ 5.98[186]
34 N^6-Benzyladenine	–§–	$\gg$ **100** $(28 \pm 5)^a$	**113** $\pm$ 10.2[186]
35 6-n-Hexyladenine	⌇CH_3	$\gg$ **100** $(22 \pm 8)^a$	**73.3** $\pm$ 4.34[186]
36 N^6-Hydroxyadenine (ANR 427)	–§–OH	**9.53** $\pm$ 1.79	**0.500** $\pm$ 0.104
37 N^6-Aminoadenine (ANR 428)	–§–NH_2	**17.5** $\pm$ 1.7	**1.38** $\pm$ 0.10
38 N^6-Dimethyladenine	___	$\gg$ **100** $(10 \pm 5)^a$	$\gg$ **100**[186] $(11 \pm 2)^a$
39 N^6-Furfuryladenine (Kinetine)	–§–	**8.02** $\pm$ 1.65	**26.7** $\pm$ 5.50[186]
40 *trans*-Zeatin	⌇CH_3 OH	**2.06** $\pm$ 1.12	**22.6** $\pm$ 2.11[186]
41 HPLL047	–§– F	**13.8** $\pm$ 1.1	**14.9** $\pm$ 3.35 [186]

^{a}Percent inhibition $\pm$ SEM of radioligand binding at 100 µM.

The N^6-hydroxypentenyl-substituted adenine derivative trans-zeatin (**40**), acytokinin (phytohormone), was 10-fold more potent at human adenine receptors than at rat adenine receptors (K_i value of 2.06 µM vs. K_i value of 22.6 µM). The N^6-azidoadenine (**43**) showed lower affinity for human adenine receptors with a K_i value of 25.4 µM compared with 8-azidoadenine (**5**) but was still better than 2-azidoadenine (**4**).
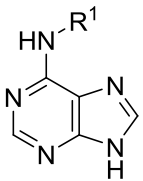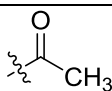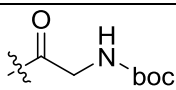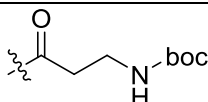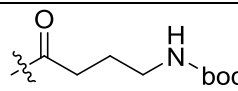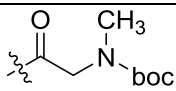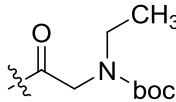
Table 10. Comparison of affinities of adenine derivatives with modifications at N^6 for human and rat adenine receptors determined in radioligand binding studies using membrane preparations (part II).

42- 48

Compound	R^1	$K_i \pm$ SEM [µM] vs. [³H]adenine (n=3)[a]	
		HEK 293 cells	Rat brain cortex
42 HPLL046		**28.2** ± 1.9	**6.73** ± 1.98[186]
43 6-Azidoadenine	$-N_3$	**25.4** ± 1.6	**8.49** ± 0.47[186]
44 TB 21	⌁OH	ca. **100** (58 ± 1)[a]	**23.9** ± 1.80
45 TB 200	⌁N(H)-boc	≥ **100** (40 ± 6)[a]	≥ **100** (21 ± 4)[a]
46 TB 201	⌁NH_2	>> **100** (19 ± 3)[a]	ca. **100** (58 ± 9)[a]
47 TB 202	⌁N(H)-boc	> **100** (26 ± 5)[a]	≥ **100** (46 ± 4)[a]
48 TB 203	⌁NH_2	>> **100** (8 ± 5)[a]	≥ **100** (49 ± 1)[a]

[a]Percent inhibition ± SEM of radioligand binding at 100 µM.

Adenine derivatives (Table 10) bearing aminoalkyl and N-*t*-boc-aminoalkyl substituents at position N^6 (**45**, **46**, **47**, and **48**) exhibited no measurable AdeR affinity, whereas ethyl and hydroxyethyl substitution at that position (**32** and **44**) was still somewhat tolerated (K_i values of 16.4 µM and 23.9 µM, respectively). Interestingly, the corresponding N^6-acetyl-substituted adenine **49** showed a higher affinity (K_i = 2.85 µM) than the corresponding alkyl derivative, consistent with previous observations, that benzoyl substitution at position N^6 was better tolerated than benzyl substitution.[104]

Table 11. Comparison of affinities of adenine derivatives with modifications at N^6 for human and rat adenine receptors determined in radioligand binding studies using membrane preparations (part III).

Compound	R^1	$K_i \pm$ SEM [µM] vs. [^{3}H]adenine (n=3)^a	
		HEK 293 cells	Rat brain cortex
49 TB 23		**0.515** $\pm$ 0.066	**2.85** $\pm$ 0.59[186]
50 TB 93		**0.302** $\pm$ 0.032	**0.403** $\pm$ 0.061
51 TB 74		**0.719** $\pm$ 0.081	**0.334** $\pm$ 0.031
52 TB 96		**2.68** $\pm$ 0.37	**3.39** $\pm$ 0.56
53 TB 155		**12.0** $\pm$ 2.2	**3.85** $\pm$ 0.05
54 TB 158		**14.3** $\pm$ 2.4	**2.21** $\pm$ 0.41
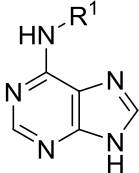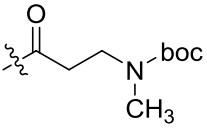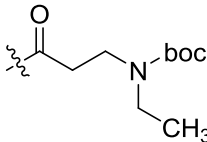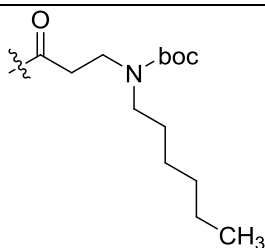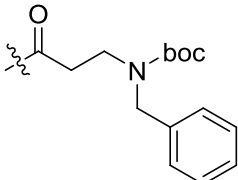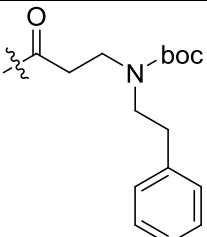
^{a}Percent inhibition $\pm$ SEM of radioligand binding at 100 µM.

Our results indicated that N^6-acylation is more favorable in terms of increased AdeR affinity than N^6-alkylation. Most of the investigated N^6-substituted adenine derivatives, for example compounds **36** and **37**, exhibited higher affinity for the rat AdeR than for the human adenine binding site. Exceptions were compounds **39** and **40**, but the affinity was still in the micromolar range. N^6-Acetyladenine (**49**) was 5.5-fold more potent at adenine receptors in HEK293 cell membranes ($K_i = 0.515$ µM) as compared to the rat receptor ($K_i = 2.85$ µM).

On the basis that N^6-acylation of adenine is tolerated, the synthesized *t*Boc-protected N^6-ω-aminoacyladenine derivatives **50-54** were tested at human and rat adenine receptors. The glycyl- and alanyl-derivatives **50** and **51** showed high affinity for both, human and rat adenine receptors with K_i values in the nanomolar range (Table 11). Increasing the chain length (**52**)

and alkylation of the protected nitrogen atom of the glycyl derivatives (**53** and **54**) resulted in reduced affinity in both test systems.

Table 12. Comparison of affinities of adenine derivatives with modifications at N^6 for human and rat adenine receptors determined in radioligand binding studies using membrane preparations (part IV).
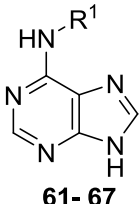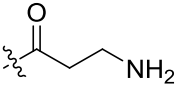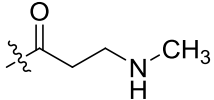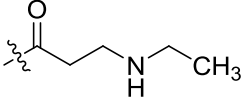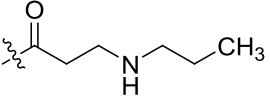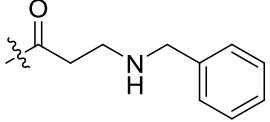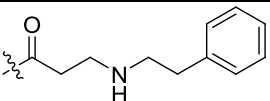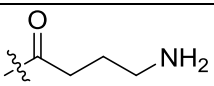
		$K_i \pm$ SEM [μM] vs. [^{3}H]adenine $(n=3)^a$	
Compound	**R^1**	HEK293 cells	Rat brain cortex
55 TB 156		**5.47** ± 1.28	**0.949** ± 0.135
56 TB 159		**7.70** ± 2.40	**2.93** ± 0.40
57 TB 183		ca. **100** $(44 \pm 6)^a$	**11.8** ± 0.8
58 TB 184		**19.7** ± 0.7	**1.56** ± 0.026
59 TB 196		**42.1** ± 1.8	**9.02** ± 0.55
60 TB 197		**17.4** ± 3.2	**9.07** ± 0.80

^{a}Percent inhibition ± SEM of radioligand binding at 100 μM.

The N^6-ω-aminopropionyl-substituted adenine derivatives **55-60** were tested at adenine receptors (Table 12). The introduction of a methyl group at the protected nitrogen atom (**55**) resulted in moderate affinity with a K_i value in the low micromolar range (K_i = 5.47 μM and K_i = 0.949 μM, respectively) for human and rat adenine receptors. Quite similar results were shown by the introduction of an ethyl group at the protected nitrogen atom, while introduction of propyl, hexyl, benzyl and phenethyl substituents (**57**-**60**) somewhat decreased or abolished the affinity for adenine receptors in both species.

Table 13. Comparison of affinities of N^6-substituted adenine derivatives for human and rat adenine receptors determined in radioligand binding studies using membrane preparations (part V).

61- 67

Compound	R^1	$K_i \pm$ SEM [μM] vs. [^{3}H]adenine (n=3)^a	
		HEK293 cells	Rat brain cortex
61 TB 73 (PSB-09073)		**0.0526** ± 0.0034	**0.0215** ± 0.0056
62 TB 162 (PSB-08162)		**1.83** ± 0.09	**0.292** ± 0.056
63 TB 165		**1.34** ± 0.48	**0.508** ± 0.163
64 TB 187		**6.85** ± 2.17	**1.29** ± 0.24
65 TB 198		**3.27** ± 1.23	**0.852** ± 0.131
66 TB 199		**6.93** ± 0.83	**2.12** ± 0.07
67 TB 97 (PSB-09097)		**0.174** ± 0.045	**0.0805** ± 0.0030

^{a}Percent inhibition ± SEM of radioligand binding at 100 μM.

In general, the *N*-boc-protected derivatives bearing relatively bulky and lipophilic substituents still exhibited relatively high affinities with K_i values in the nanomolar or low micromolar range. This fact illustrated that there is obviously much space for voluminous substituents at position 6 offering a high potential for further modifications at the exocyclic amino group of adenine. The binding results for free amines (**61**-**67**) which were obtained by removal of the *t*Boc group of compounds shown previously in table 11 and 12 are collected in table 13. The removal of protecting groups (Table 13) clearly resulted in compounds with higher affinity for adenine receptors in comparison with the protected compounds. Thus, the introduction of a basic amino group at the N^6-acyl substituent yielded adenine derivatives that were well tolerated by adenine binding sites.
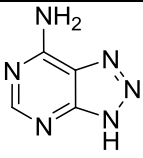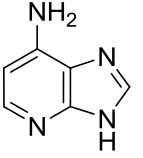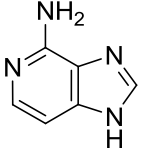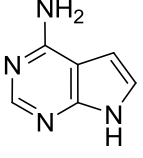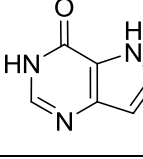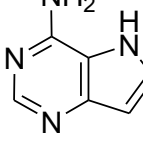
In addition these derivatives showed somewhat higher affinity for the rat than the human adenine receptors. Compounds **64-66**, in which bulky and lipophilic substituent were introduced, were able to displace [^{3}H]adenine from its binding sites at both species with K_i values varying from the nanomolar range or low micromolar range. The most potent adenine receptor ligand of this series was compound **61** exhibiting an even higher affinity for rat adenine receptors (K_i value of 21.5 nM) than the natural ligand adenine itself (K_i value of 29.2 nM). In addition, compound **61** showed similar affinity for human adenine receptors with a K_i value of 52.6 nM compared with the endogenous ligand adenine (K_i = 44.6 nM). Therefore compound **61** represents the most potent adenine receptor ligand that has been described so far. The butyryl analogue of compound **61**, compound **67** also showed high affinity for both, rat and human, adenine receptors (K_i values of 80.5 nM and 174 nM, respectively). In general, substitution in the 8-position (amino, dimethylamino, piperidinyl, piperazinyl), or in the 9-position (2-morpholinoethyl) with basic residues, or introduction of polar substituents at the 6-amino function represented the best modifications, whereas bulky and lipophilic substituents at all positions, or alkyl substitution at N^9 were not well tolerated.

The compounds were additionally investigated in binding studies at human embryonic kidney (HEK293) cells, which also express a high-affinity adenine binding site. Structure-affinity relationships at the human cell line were similar to those at the rat Ade1R, but not identical. The N^6-acetyladenine (**49**, K_i rat: 2.85 μM; K_i human: 0.515 μM) and 8-aminoadenine (**7**, K_i rat: 6.51 μM; K_i human: 0.0341 μM) were much more potent at the human as compared to the rat binding site, while compounds **61** and **67** showed high affinity for both human and rat adenine receptors with K_i values in nanomolar range.
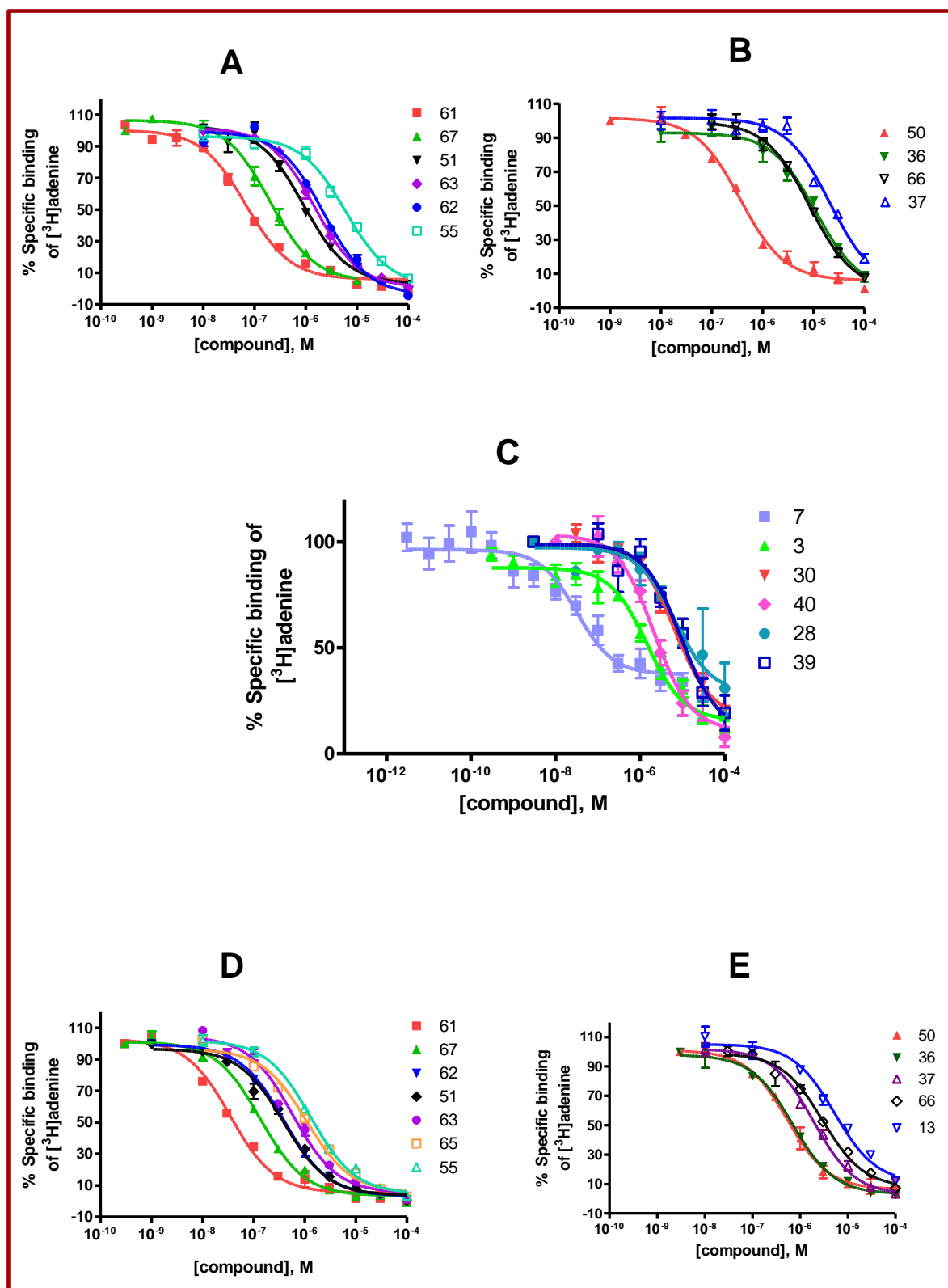
Figure 28. Inhibition of [³H]adenine binding (10 nM) by selected adenine derivatives to (**A-C**) membrane preparations of HEK293 cells, and (**D** and **E**) to rat brain cortical membrane preparations. Data points represent means ± SEM of three separate experiments each performed in triplicate at room temperature.
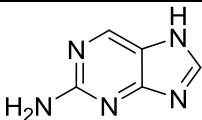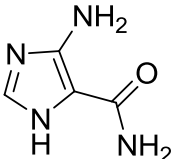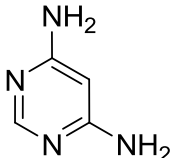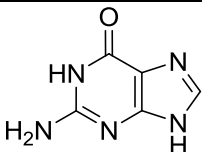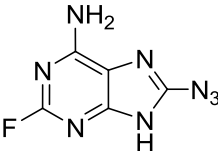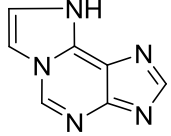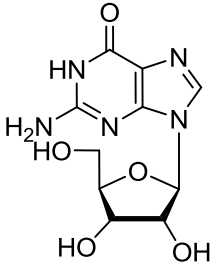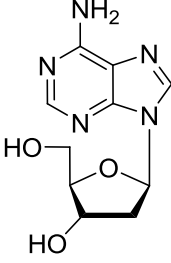
Table 14. Comparison of affinities of aza- and deazapurines for human and rat adenine receptors determined in radioligand binding studies using membrane preparations.

Compound	Structure	$K_i \pm$ SEM [µM] vs. [^{3}H]adenine (n=3)[a]	
		HEK 293cells	Rat brain cortex
68 8-Azaadenine		$\gg$ **100** (7 ± 5)[a]	$\gg$ **100** (21 ± 9) [186]
69 AAG 14		**8.61** ± 2.57	**10.6** ± 2.66[186]
70 AAG 223		**17.1** ± 3.6	**6.81** ± 2.35[186]
71 AAG 225		$>$ **100** (31 ± 3)[a]	$>$ **100** (21 ± 9)[a]
72 AAG 226		$>$ **100** (20 ± 5)[a]	$\gg$ **100** (0 ± 5)[a]
73 AAG 227		$\gg$ **100** (0 ± 3)[a]	$>$ **100** (39 ± 8)[a]

[a]Percent inhibition $\pm$ SEM of radioligand binding at 100 µM.

All tested deazapurines (Table 14) were much less active at the AdeR than the physiological ligand adenine (K_i value of 0.0292 µM). The 7- and 9-deazapurines **71**, **72**, and **73** showed no significant affinity for the AdeR at concentrations up to 100 µM, whereas the 1- and 3-deazapurines **69** and **70** exhibited AdeR affinities in the low micromolar range ($>$ 200-fold decrease in affinity). This result indicated that the presence of a hydrogen bond acceptor at position 7 is essential for AdeR affinity. Interestingly, a similar effect was previously observed for 7-deazaadenosine at adenosine receptors (AdoRs), the 7-deazaadenosine being only weakly active or inactive at A_1, A_{2A}, and A_3 AdoR. 3-Deazaadenosine had exhibited somewhat higher affinity for AdoR in the micromolar range.[189]

Table 15. Comparison of affinities of some adenine-related structures for human and rat adenine receptors determined in radioligand binding studies using membrane preparations.

Compound	Structure	$K_i \pm$ SEM [µM] vs. [^{3}H]adenine (n=3)	
		HEK 293 cells	Rat brain cortex
74 2-Aminopurine		$\gg$ **100** $(5 \pm 1)^a$	$>$ **100** (39 ± 8) [186]
75 5-Amino-4-imidazole carboxamide		$>$ **100** $(32 \pm 8)^a$	**19.0** ± 0.47 [186]
76 4,6-Diaminopyrimidine		$\gg$ **100** $(16 \pm 6)^a$	$\gg$ **100** (22 ± 7) [186]
78 Guanine		$\gg$ **100** $(24 \pm 5)^a$	**3.33** ± 2.14 [186]
79 8-Azido-2-fluoroadenine		$\gg$ **100** $(22 \pm 4)^a$	**17.5** ± 8.34 [186]
80 1,N^6-Ethenoadenine		$\gg$ **100** $(11 \pm 6)^a$	**34.4** ± 8.12 [186]
81 Guanosine		$\gg$ **100** $(20 \pm 4)^a$	$\gg$ **100** (5 ± 3) [190]
82 2´-Deoxyadenosine		$\gg$ **100** $(29 \pm 4)^a$	**11.0** ± 0.55 [186]

^{a}Percent inhibition $\pm$ SEM of radioligand binding at 100 µM.

The best tolerated deazaadenosine derivatives in these studies had been the 1-deaza compounds which was similarly potent as the corresponding adenosine derivatives.[189] In contrast, the N^1, as well as the N^3, are quite important for high AdeR affinity and appear to strongly contribute to receptor binding probably as hydrogen bond acceptors (Table 15). 8-Azaadenosine had been found to possess no affinity for adenosine receptors,[191] likewise 8-azaadenine (**68**) also showed no measurable affinity for the AdeR at concentrations up to 100 μM.

It was described before that 2-fluoroadenine showed affinity for human and rat adenine receptors in the nanomolar range (K_i= 940 nM, and 620 nM, respectively).[186] The introduction of an azido group in position 8 of 2-fluoroadenine resulted in 8-azido-2-fluoroadenine (**79**). Compound **79** showed no measurable affinity for the human adenine receptor at 100 μM and the activity was decreased by 28-f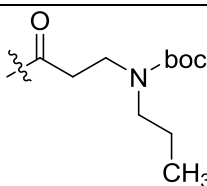old at the rat adenine receptors, whereas 8-azidoadenine (**5**) showed affinity for the human adenine receptors in the micromolar range. 1,N^6-Ethenoadenine (**80**) is a tricyclic adenine derivative in which the nitrogen atoms in position 1 and N^6 are connected by the formation of an imidazole ring. It exhibited no significant binding affinity for the adenine receptor at a high concentration of 100 μM, thus the connection of two nitrogen atoms is not well tolerated for adenine binding sites.

5-Amino-4-imidazole carboxamide (**75**), 4,6-diaminopyrimidine (**76**), guanine (**78**), guanosine (**81**) and 2´-deoxyadenosine (**82**) showed no effects on [^{3}H]adenine binding. In addition, 2-aminopurine (**74**) was not able to inhibit [^{3}H]adenine binding at a concentration of 100 μM. It is concluded that the 6-amino group of adenine is important for adenine binding to the membrane receptors and the 2-amino group impedes adenine binding to the [^{3}H]adenine-binding site.

Based on the results of binding studies of many adenine derivatives at membrane preparations of both, rat and HEK293 cells, we conclude that human embryonic kidney (HEK293) cells and rat brain cortex express binding sites for adenine with similar but not identical structure-activity relationships. Differences in binding affinities may be due to species differences and/or could be explained by the existence of different adenine receptor subtypes. The latter explanation is more likely since no highly homologous gene (> 80% sequence identity) could be identified in the human genome database.

3.1.2.1. Investigation of agonistic properties of adenine and adenine derivatives at the rat adenine receptor

3.1.2.1.1. cAMP accumulation assays

In order to investigate whether the potent rAde1R ligands identified in this study were agonists or antagonists we performed functional studies with selected compounds. Thus, 1321N1 astrocytoma cells were stably transfected with the sequence for the rAde1R using a retroviral expression system.[192] Adenine at 1 µM concentration inhibited isoproterenol-induced cAMP formation in a dose-dependent manner with a maximal inhibition of about 35-40% and an IC_{50} value of 8.29 ± 2.69 nM (Figure 29B). Selected adenine derivatives were tested for their effects to inhibit isoproterenol-induced cAMP accumulation. In order to obtain a full AdeR-activating effect, high concentrations of test compounds (ca. 100 x K_i value; 50 µM, 250 µM or 500 µM) were applied. Compound **13** (8-(1-piperidinyl)adenine) was tested at a lower concentration (30 µM, ca. 8-fold K_i, see Figure 29A) since at 250 µM concentration it had led to a complete inhibition of cAMP production in a preliminary experiment (not shown), likely due to an AdeR-independent effect.

All compounds investigated showed agonistic effects at rAde1R expressed in astrocytoma cells as shown in figure 29A. 8-(1-Piperidinyl)adenine (**13**), 8-aminoadenine (**7**) and 9-(2-morpholinoethyl)adenine (**30**) showed about the same efficacy as adenine. 8-Dimethylaminoadenine (**16**) was even more efficacious than the physiological agonist showing 137% of the maximal effect of adenine. In contrast, N^6-hydroxyadenine (**36**, 51% efficacy), N^6-acetyladenine (**49**, 77% efficacy) and 8-(1-piperazinyl)adenine (**15**, 52% efficacy) were partial agonists in the applied test system.

Compounds **49** and **15** were and in the presence of additionally tested for antagonistic effects. Concentration-response curves for adenine were obtained in the absence 10 µM (ca. 3-fold K_i value) of **49**, or **15**, respectively. Curves for adenine in the presence of **49** in comparison with adenine alone are shown in figure 29B. Both compounds, **49** and **15**, had no statistically significant effects on the IC_{50} value or the efficacy of adenine indicating that they did not behave as antagonists in this test system. Taken together, the results from functional studies showed that minor structural modifications can have a significant impact on functional properties of the adenine derivatives.
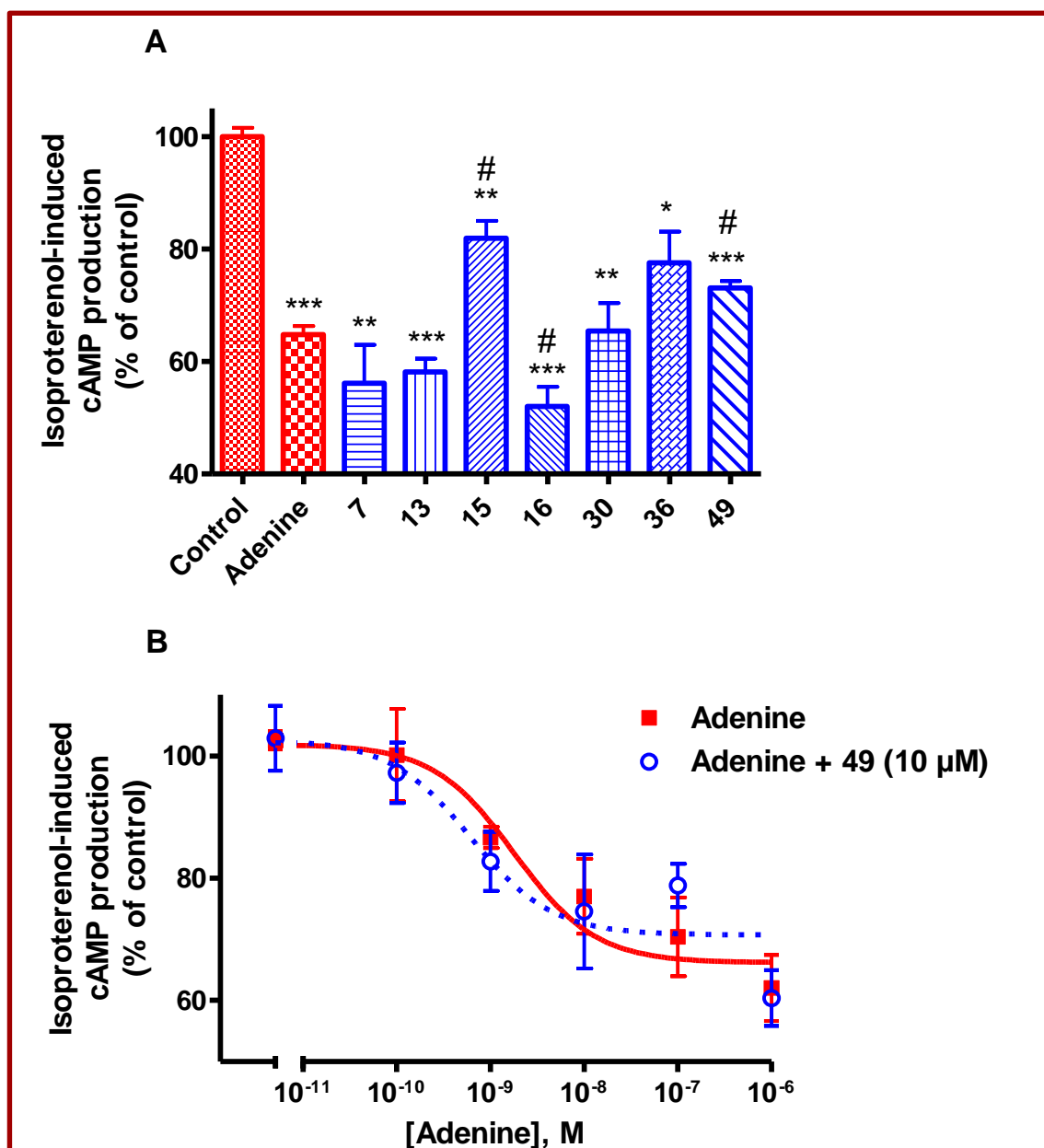
Figure 29. (**A**) Inhibition of isoproterenol-stimulated cAMP accumulation by adenine and selected adenine derivatives in 1321N1 astrocytoma cells stably expressing the rAde1R. Cellular cAMP production was increased by preincubation with 3 nM isoproterenol for 10 min at 37 °C; data are given as percentage of the mean increases in cellular cAMP levels in the presence of isoproterenol alone (% of control, n=3). Adenine and compound **13** were tested at 1 μM and 30 μM, respectively. Compounds **49**, **15**, **16** and **30** were tested at 250 μM (100-fold K_i value). Compounds **36** and **7** were tested at 50 μM and 500 μM, respectively. *p=0.0151; ** p<0.01; *** p<0.0001 indicates statistically significant differences from control (isoprenaline); # p<0.01; ## p=0.0032 indicates statistically significant differences between maximal effect of adenine and effect of test compound at high concentration. (**B**) Concentration-dependent inhibition of isoprenaline-stimulated intracellular cAMP accumulation in the absence and in the presence of compound **49** (10 μM). An IC_{50} value of 8.29 ± 2.69 nM was determined for adenine (n=5). The presence of **49** (10 μM, 3-fold K_i) did not show any significant effect on the IC_{50} value or the efficacy of adenine (n=3).

3.1.2.1.2. cAMP-dependent luciferase assay

In order to examine the functional properties of the most potent adenine receptor ligands identified in radioligand binding studies, we measured the G_i protein-mediated effects of compounds **50**, **55**, **61**, **62**, **63**, **65**, **67**, and adenine (**1**) on isoproterenol-stimulated cAMP production by a luciferase luminescence assay, a gene reporter assay. These experiments were performed with 1321N1 astrocytoma cells stably transfected with the rat adenine receptor. The results are illustrated in figure 30.

This experiment showed that compounds **61**, **63**, **65**, **67**, **55** and **50** represent adenine receptor agonists, whereas compound **62** exhibited no significant effect on isoproterenol-induced cAMP dependent luciferase assay (Figure 30). The agonistic properties of compound **61** were further confirmed by its concentration-dependent inhibition of the isoproterenol-stimulated cAMP dependent signal in a luciferase assay (Figure 31).
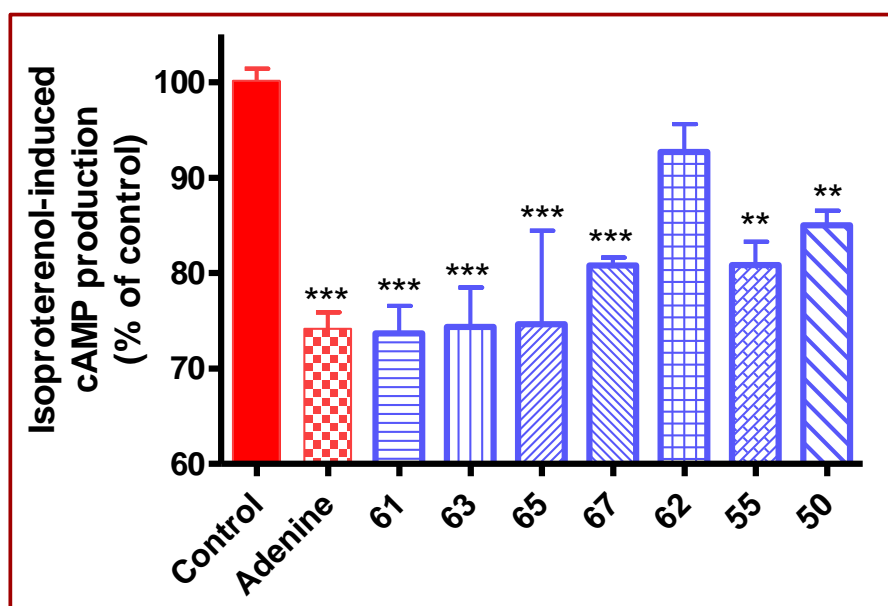
Figure 30. Inhibition of isoproterenol-stimulated cAMP-dependent luciferase assay by adenine and selected adenine derivatives in 1321N1 astrocytoma cells stably expressing the rAde1R. Applied concentrations: adenine and **61**: 1 µM (*n* = 3); **63**, **65**, **67**, **55**, **62**: 10 µM (*n* = 3); $^{***}P < 0.0001$; $^{**}P = 0.004$ (**65**); $^{**}P = 0.0026$ (**55**). Data are given as percentages of the mean increases in cellular cAMP levels in the presence of isoproterenol alone (control).

Adenine (**1**) and **61** both inhibited the maximal cAMP amount produced by 30 - 35 % with IC$_{50}$ values of 3.18 ± 1.51 nM and 28.4 ± 4.3 nM, respectively (Figure 31).
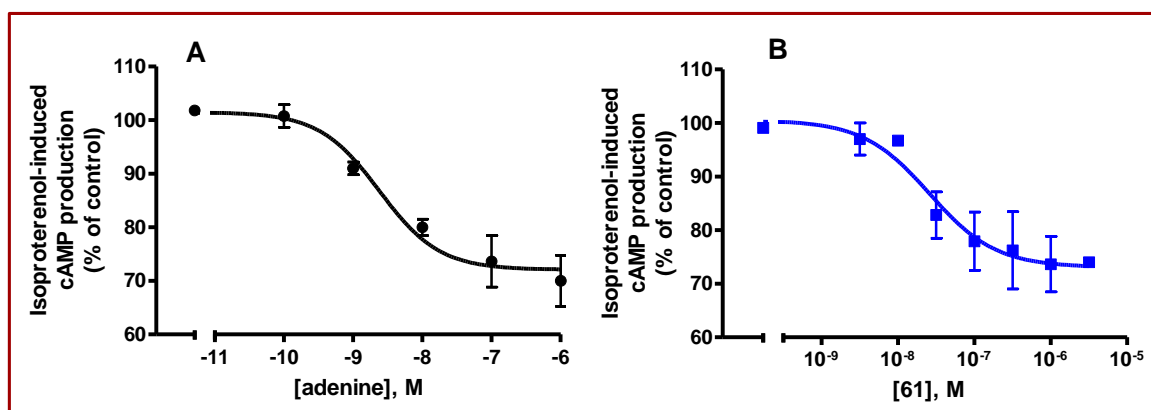
Figure 31. Inhibition of isoproterenol-stimulated cAMP dependent-luciferase assay in 1321N1 astrocytoma cells stably expressing the rAde1R by different concentrations of (**A**) adenine, and (**B**) compound **61**. IC_{50} values: 3.18 ± 1.51 nM (adenine) and 28.4 ± 4.3 nM (**61**). Data points represent means $\pm$ SEM of three separate experiments each performed in triplicate.

The functional studies revealed that compounds **61**, **63**, and **65** exhibited the strongest inhibitory effects on cAMP production with the same maximal effect as adenine (30% inhibition). Therefore, these compounds constitute full agonists (Figure 30).
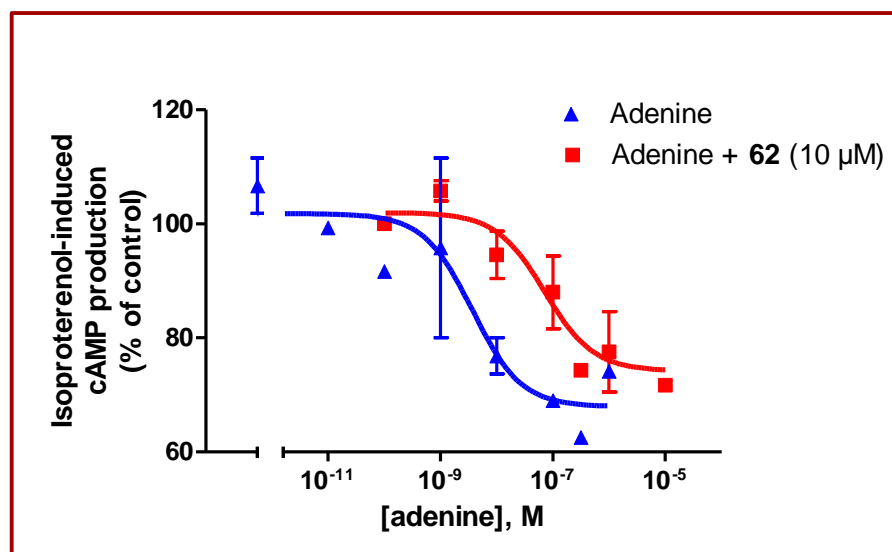
Figure 32. Inhibition of the isoproterenol-stimulated cAMP-dependent signal in a luciferase assay by different concentrations of adenine in the absence (▲) and in the presence (■) of compound **62** (10 μM) in 1321N1 astrocytoma cells stably expressing the rAde1R (*n*=3). Data points represent means $\pm$ SEM of three separate experiments each performed in triplicate. A K_b value of 0.165 μM was calculated.

The adenine derivatives **67**, **55**, and **50** were found to be partial agonists, whereas compound **62** showed only a slight, non-significant decrease in cAMP formation, indicating that N^6-(3-methylaminopropionyl)adenine **62** might be an adenine receptor antagonist. To further investigate the antagonistic properties of **62**, we monitored the inhibitory effect of the natural

agonist adenine on the cAMP formation in the absence (Figure 32, ▲) and in the presence (Figure 32, ■) of **62**. In the absence of **62**, adenine exhibited an EC_{50} value of 3.70 nM, whereas in the presence of **62** the dose-response curve of adenine was shifted to the right (EC_{50} = 71.5 nM). The calculated K_b value was 0.165 μM. This result revealed, that N^6-(3-methylaminopropionyl)adenine (**62**) represents the first adenine receptor antagonist described so far.

3.1.2.2. Extracellular signal-regulated kinase (ERK) phosphorylation assay

The rAde1R expressed in 1321N1 astrocytoma cells was functionally characterized by analyzing the effects of receptor activation on the receptor-mediated inhibition of cellular cAMP production and cAMP response element (CRE)-dependent luciferase expression. Later on the receptor-mediated activation of the serum response element (SRE)-directed luciferase expression was also determined. There is no information available so far about activation of the extracellular signal-regulated protein kinase ERK mediated by the adenine receptors. The dopamine D2-receptor which is a G_i-coupled receptor has been previously shown to couple to the SRE pathway.[171,172] The native $P2Y_{12}$-receptor mediates an activation of the extracellular signal-regulated protein kinase (ERK)[173,174] and recombinant human $P2Y_{12}$ was shown to activate the ERK through coupling to the SRE-pathway.[175] ERK phosphorylation was investigated by a gene reporter assay measuring SRE-dependent luciferase activity in astrocytoma cells stably transfected with the rat adenine receptor (rAde1R).
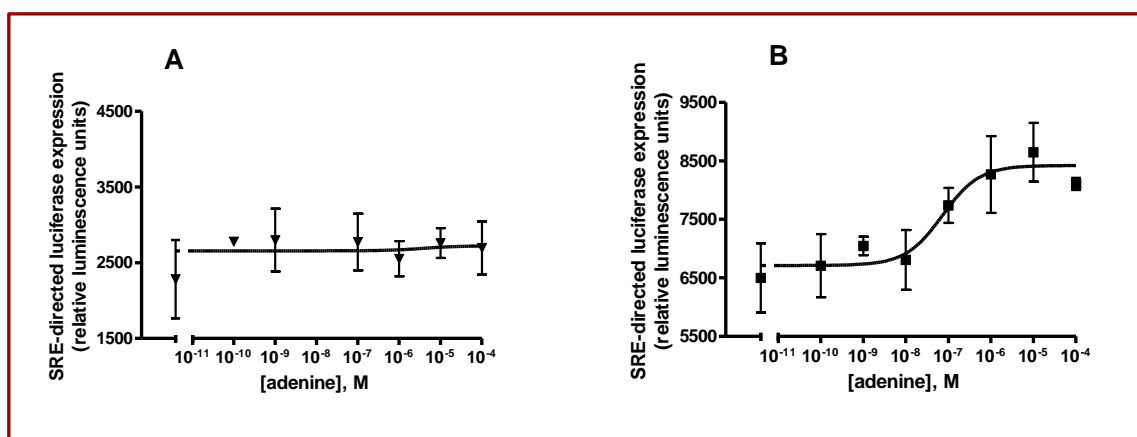
Figure 33. (**A**) The non-transfected 1321-N1 astrocytoma cells showed no change in SRE-dependent luciferase expression in the presence of adenine. (**B**) Increases in SRE-dependent luciferase expression upon addition of different concentrations of adenine to 1321-N1 astrocytoma cells expressing rAde1R.

For this purpose, 1321N1 astrocytoma cells expressing rAde1R were transiently transfected with the pSRE-luc vector. In cells transfected with the pSRE-luc vector alone, adenine (0.1 nM to 0.1 mM) showed no response. In contrast, adenine (0.1 nM to 0.1 mM) increased the SRE-dependent luciferase expression by about 50% with an EC_{50} concentration of 60.6 ± 7.7 nM in cells expressing rAde1R (Figure 33). Similar increases were observed using compound **61**, and an EC_{50} value of 1.87 ± 0.99 nM was determined (Figure 34).

This experiment revealed that adenine receptors are also involved in the regulation of kinase pathways.
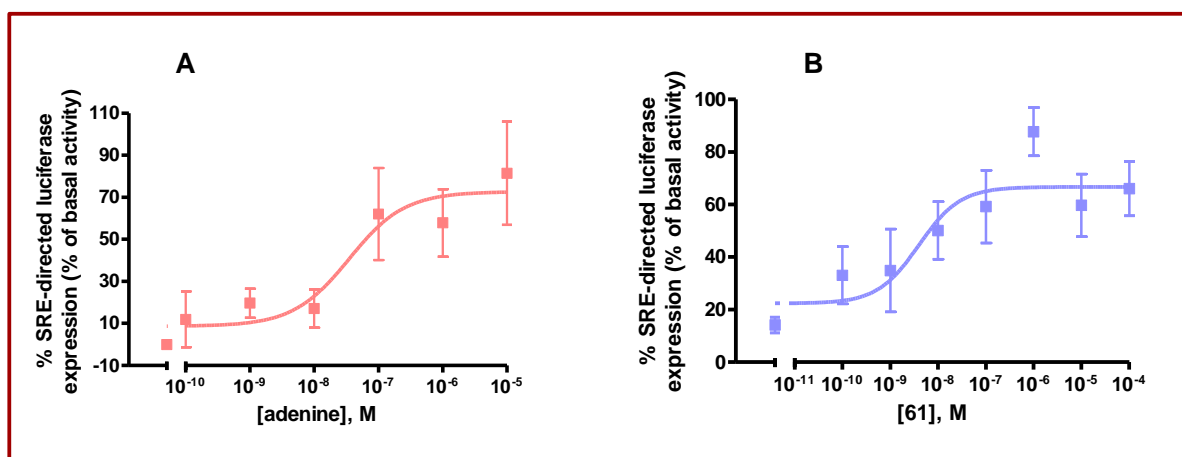
Figure 34. Increases in SRE-dependent luciferase expression upon addition of different concentrations of adenine in 1321-N1 astrocytoma cells expressing rAde1R (% of basal activity) (**A**) adenine, and (**B**) compound **61**. EC_{50} values: 60.6 ± 7.7 nM (adenine) and 1.87 ± 0.99 nM (**61**) (*n*=3).

Therefore, we present here a new lead structure for adenine receptor agonists based on the properties of compound **61**. N^6-acylation of adenine was obviously the best tolerated modification by the rat adenine receptor. A basic terminal amino group further enhanced the potency. A distance of three carbon atoms between the N^6-nitrogen atom and the terminal amino group turned out to be optimal. Moreover, methylation of the amino group led to the first adenine receptor antagonist **62**.

Table 16 showes a comparison of K_i and EC_{50} values determined for adenine and the synthetic agonist **61** obtained in different assays. The compounds appear to be pathway-specific. In contrast to the physiological agonist adenine, compound **61** is more potent and efficacious in activation the ERK pathway than in inhibition of adenylate cyclase.

Table 16. Comparison of affinities of adenine and compound **61** at different test systems.

Compound	Radioligand binding studies	Functional studies using rAde1R expressed in 1321-N1 astrocytoma cells	
	Rat brain cortex $K_i \pm$ SEM [nM] vs. [^{3}H]adenine ($n=3$)	cAMP-assay $IC_{50} \pm$ SEM [nM] ($n=3$)	ERK-pathway $EC_{50} \pm$ SEM [nM] ($n=3$)
Adenine	**29.2** $\pm$ 3.4	**3.18** $\pm$ 1.51	**60.6** $\pm$ 7.7
61	**21.5** $\pm$ 5.6	**28.4** $\pm$ 4.3	**1.87** $\pm$ 0.99

Further evaluation of both compounds (adenine and **61**) in other test systems or other cell lines may provide more information about the functional properties of adenine and compound **61**.

3.1.3. Investigation of the affinity of selected adenine derivatives for rat adenosine A$_1$ and A$_{2A}$ receptors
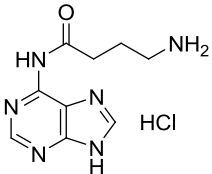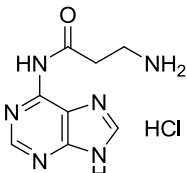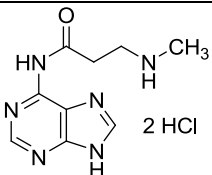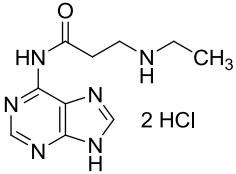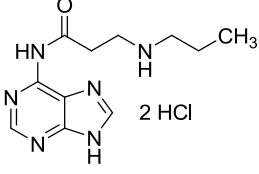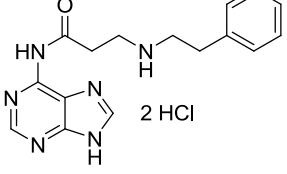
Certain adenine derivatives had previously been described to be antagonists at adenosine receptors. As a next step we therefore wanted to study the affinity of the most potent adenine derivatives at adenosine receptors in order to assess the compounds, selectivity for adenine receptors. The adenine derivatives were investigated in radioligand binding studies at rat brain striatal adenosine A$_{2A}$ receptors using the antagonist radioligand [³H]MSX-2 ([³H]3-(3-hydroxypropyl)-7-methyl-8-(*m*-methoxystyryl)-1-propargylxanthine, 84 Ci/mmol).[193] The affinity for the adenosine A$_1$ receptor subtype was assessed by performing radioligand binding studies at rat brain cortical membranes using [³H]CCPA ([³H]2-chloro-N⁶-cyclopentyladenosine, 48.6 Ci/mmol),[194] as a radioligand.

The result showed that the majority of the tested N⁶-substituted adenine derivatives (Table 17) was not able to displace [³H]MSX-2 (1 nM) from rat brain striatal (adenosine A$_{2A}$ receptor) at a concentration of 100 μM. Similar results were obtained for N⁶-substituted adenine derivatives (table 17) at adenosine A$_1$ receptors in rat brain cortical membranes, at which the compounds mostly showed no measurable affinity at a concentration of 100 μM. Moderate affinity was seen with N⁶-aminoadenine (**37**) (Table 18) which was able to displace [³H]MSX-2 from rat brain striatal membranes by 59 % at 100 μM concentration. Compound **37** showed an inhibition value of 44 % for binding of [³H]CCPA to rat brain cortical membranes. Compounds **62** and **63** showed inhibition values of 48 % for [³H]MSX-2 from rat brain striatal (adenosine A$_{2A}$ receptor). This means that the expected K$_i$ values would be around 100 μM.
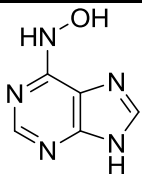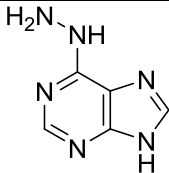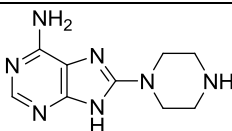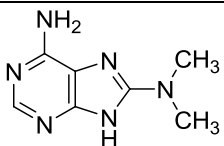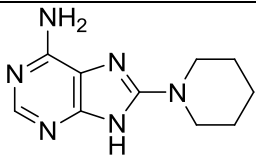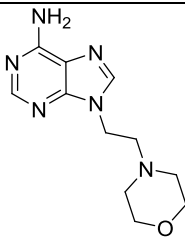
8-(1-Piperazinyl)adenine (**15**) and 8-dimethylaminoadenine (**16**) exhibited similar inhibition values for adenosine A$_{2A}$ receptor in rat brain striatal (46 %). Compounds **15** and **16** showed no measurable affinity at both adenosine A$_1$ and A$_{2A}$ receptor subtypes (see table 18). 8-(1-Piperidinyl)adenine (**13**) showed inhibition values of 46 % and 42 % for adenosine A$_1$ receptors at rat cortical membranes, and adenosine A$_{2A}$ receptors at rat striatal membranes, respectively (Table 18) indicating moderate affinities.

Compounds **13**, **15**, **16**, **37, 62** and **63** exhibited affinities for adenosine A$_1$ receptors at rat cortical membranes and A$_{2A}$ receptor at rat striatal membranes above 100 μM, and therefore the compounds can be considered selective for adenine receptors in comparison with adenosine receptors (table 17 and 18).

Table 17. Comparison of affinities of selected adenine derivatives for adenosine A_1 and adenosine A_{2A} receptors with human and rat adenine receptors determined in radioligand binding studies using membrane preparations.

Compound	Structure	$K_i \pm$ SEM [µM] (or % inhibition at 100 µM) ($n=3$)			
		Adenosine A_1 receptor (rat brain cortical membranes) [³H]CCPA	Adenosine A_{2A} receptor (rat brain striatal membrane) [³H]MSX-2	HEK cells membranes [³H]adenine	Rat brain cortex membranes [³H]adenine
67 TB97 (PSB-09097)		>> 100 (21 ± 9)	>> 100 (33 ± 13)	**0.174 ±** 0.045	**0.0805 ±** 0.0030
61 TB73 (PSB-09073)		>> 100 (15 ± 10)	>> 100 (26 ± 6)	**0.0526 ±** 0.0034	**0.0215 ±** 0.0056
62 TB 162 (PSB-08162)		>> 100 (16 ± 12)	> 100 (48 ± 4)	**1.83 ±** 0.09	**0.292 ±** 0.056
63 TB 165		>> 100 (18 ±10)	> 100 (48 ± 5)	**1.34 ±** 0.48	**0.508 ±** 0.163
64 TB 187		>> 100 (23 ± 9)	>> 100 (29 ± 9)	**6.85 ±** 2.17	**1.29** ± 0.24
66 TB 199		>> 100 (11 ± 9)	>> 100 (10 ± 7)	**6.93 ±** 0.83	**2.12** ± 0.07

Table 18. Comparison of affinities of selected adenine derivatives for adenosine A_1 and adenosine A_{2A} receptors with human and rat adenine receptors determined in radioligand binding studies using membrane preparations.

Compound	Structure	$K_i \pm$ SEM [µM] (or % inhibition at 100 µM) (n=3)			
		Adenosine A_1 receptor (rat brain cortical membrane) [^{3}H]CCPA	Adenosine A_{2A} receptor (rat brain striatal membranes) [^{3}H]MSX-2	HEK cells membranes [^{3}H]adenine	Rat brain cortex membranes [^{3}H]adenine
36 ANR427		**>> 100** (27 ± 8)	**>> 100** (21 ± 3)	**9.53 ±** 1.79	**0.500 ±** 0.104
37 ANR428		**≥ 100** (44 ± 6)	**≥ 100** (59 ± 7)	**17.5 ±** 1.7	**1.38** ± 0.10
15 ANR426		**>> 100** (24 ± 10)	**≥ 100** (46 ± 15)	**27.4 ±** 4.6	**3.27** ± 0.12
16 ANR430		**>> 100** (28 ± 4)	**≥ 100** (46 ± 10)	**34.1 ±** 3.2	**2.30** ± 0.28
13 ANR425		**≥ 100** (46 ± 3)	**≥ 100** (42 ± 8)	**31.7 ±** 4.8	**3.94** ± 0.87
30 EA 6203		n.d	**>> 100** (19 ± 6)	**5.49 ±** 1.42	**2.98** ± 0.16

n.d. = not determined

3.1.4. Characterization of the mouse adenine receptor (mAde2R)

The adenine receptor sequence found in mouse brain and NG108-15 cells, which is clearly distinct from the mouse ortholog (mMrgA10) of the rat adenine receptor, was cloned by Prof. Ivar von kügelgen. Non-transfected human 1321N1 astrocytoma cells possess binding sites for adenine[104] but do not respond upon addition of adenine (0.1 and 1 µM) with a decrease in cAMP formation in the absence and presence of isoproterenol used to stimulate the cellular cAMP accumulation. The lack of any effect of adenine confirms the absence of an endogenous inhibitory receptor for adenine in 1321N1 astrocytoma cells. Therefore, human 1321N1 astrocytoma cells are suitable for a pharmacological characterization of a recombinant inhibitory receptor for adenine.

3.1.4.1. cAMP accumulation assay at the mAde2R

The receptor was expressed in human 1321N1 astrocytoma cells in order to analyze the pharmacological properties of the mouse receptor. In 1321N1 cells stably expressing the mouse receptor adenine (1 nM to 1 µM) inhibited the isoproterenol-induced cAMP formation in a concentration-dependent manner with a half maximal concentration (IC_{50}) of 8 nM (95 % confidence interval: 3-23 nM) and a maximal inhibition by about 40 % (Figure 35A). Similarly, the analogue 2-fluoroadenine caused a concentration-dependent inhibition of cAMP production with an IC_{50} concentration of 15 nM (95 % confidence interval: 7-30 nM) and a maximal inhibition by about 60 % (Figure 35B).
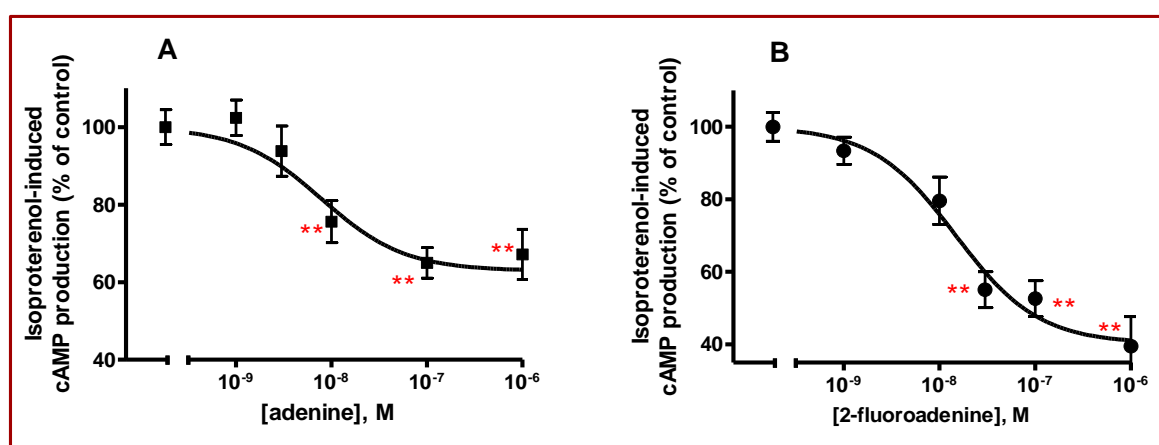
Figure 35. (**A**) Inhibition of isoproterenol-stimulated cAMP accumulation by adenine (IC_{50} = 8 nM, 95 % confidence interval: 3-23 nM) and (**B**) 2-fluoroadenine (IC_{50} = 15 nM, 95 % confidence interval: 7-30 nM) in 1321N1 astrocytoma cells stably expressing the mouse adenine receptor. Cellular cAMP production was increased by addition of isoproterenol 3 nM for 10 min at 36.5 °C; data are given as percentages of the mean increases in cellular cAMP levels in the presence of isoproterenol alone (% of control; average increase in cAMP levels by 15.3 ± 1.3 pmol cAMP per well; n = 17). Means ± SEM from five to 21 experiments.** indicates significant differences from corresponding control.

The recombinant mouse adenine receptor analyzed shows similar pharmacological properties as the adenine receptor endogenously expressed in the mouse neuroblastoma x rat glioma hybrid cell line NG108-15 (which in fact expresses the mouse but not the rat sequence).[104] Both the native and the recombinant receptor couple to inhibition of adenylate cyclase activity via pertussis toxin sensitive G proteins.[104,110] Adenine acted as an agonist at the native [104] and at the recombinant receptor.[110] In addition to adenine, the adenine derivative 2-fluoroadenine was active at the native receptor in NG108-15 cells[104] as well as at the recombinant mouse receptor.[110]

In comparison to the results obtained at the recombinant mouse adenine receptor expressed in astrocytoma cells (IC_{50} = 8 nM) and at membranes from NG108-15 cells (IC_{50} = 21 nM),[104] a higher IC_{50} value of 2.5 µM for the adenine-induced inhibition of forskolin-stimulated cAMP production had been determined in intact NG108-15 cells.[104]

3.1.4.2. Radioligand binding assays

As a next step a suitable system for performing radioligand binding assays at the mAde2R was established. NG108-15 cell membranes natively expressing the mouse adenine receptor had previously been shown to exhibit specific binding of [^{3}H]adenine.[104] However, this cell line may not only express one adenine receptor subtype, but also further adenine receptor subtypes or other specific binding sites that are labelled by [^{3}H]adenine. 1321N1 astrocytoma cells recombinantly expressing the mouse adenine receptor were also not suitable for binding assays since non-transfected 1321N1 astrocytoma cells also express specific binding sites for [^{3}H]adenine.[104] Although a series of cell lines were tested, including CHO and HEK cells, all tested mammalian cell lines natively express specific binding sites for [^{3}H]adenine. In contrast, the non-mammalian cell line Sf21 insect cells did not show any specific binding of [^{3}H]adenine.[110]

The novel mouse adenine receptor was subsequently expressed in Sf21 insect cells using the baculovirus expression system by Bernt Alsdorf and Dr. Anke Schiedel (group of Prof. Müller).[110] Saturation experiments with [^{3}H]adenine (0.75 - 150 nM) and membrane preparations of infected Sf21 cells showed a single high affinity binding site with a K_D value of 113 ± 17 nM, and a B_{max} value of 1.98 ± 0.39 pmol/mg protein was determined (n=3) (Figure 36). The K_D value was slightly higher to that previously determined for the rat adenine receptor in brain cortical membranes.

A comparison of the affinities of adenine and other adenine derivatives for the recombinant mouse adenine receptor showed that the affinities and the rank order of potency were similar to the mouse adenine receptor natively expressed in NG108-15 cells and the adenine receptor expressed in rat brain cortex (Table 19).
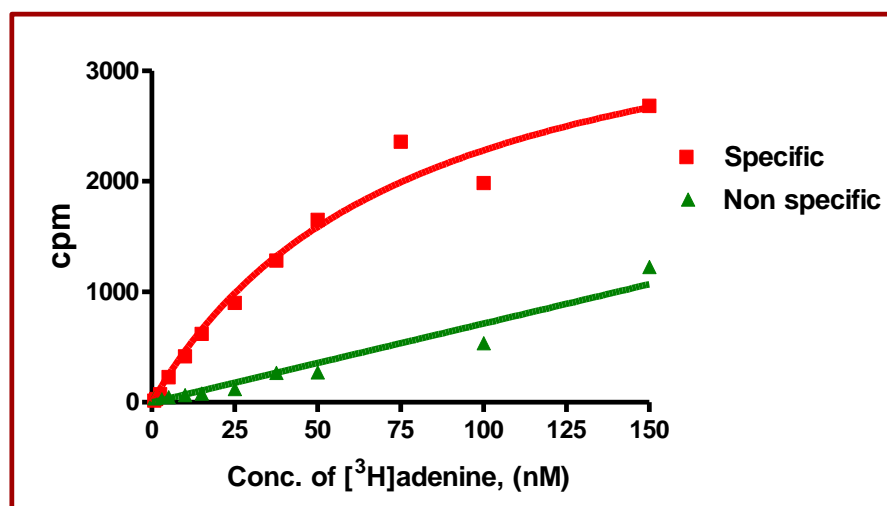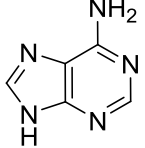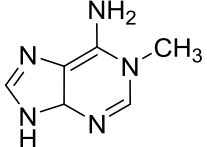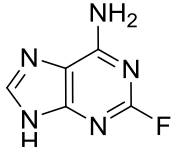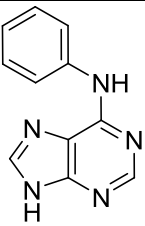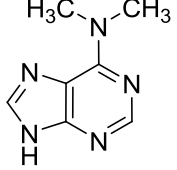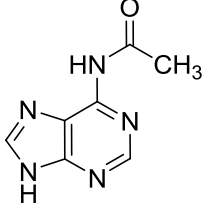
Figure 36. Saturation curve of [^{3}H]adenine binding to membranes prepared from S21 insect cells expressing the mouse adenine receptor. K_D and B_{max} values were 113 ± 17 nM and 1.98 ± 0.39 pmol/mg protein (*n*=3). The result shown represents one of three independent experiments, each performed in duplicates.
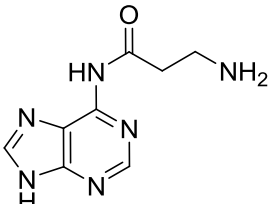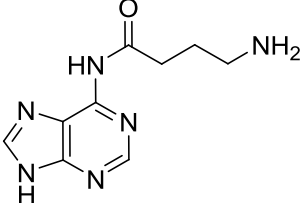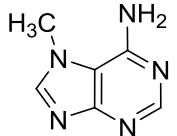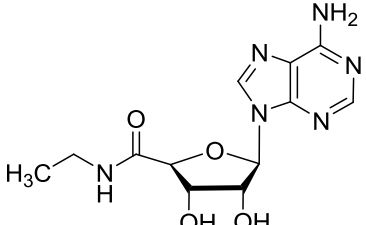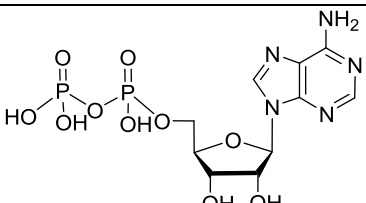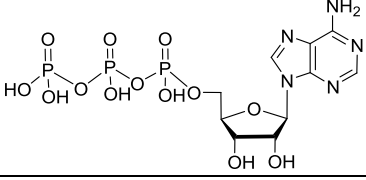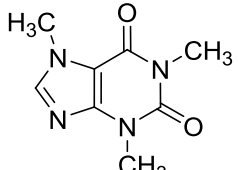
The rank order of potency was: adenine (**1**) > 2-fluoroadenine (**84**) > 7-methyladenine (**85**) > 1-methyladenine (**83**) >> N^6-benzyladenine (**34**) > N^6-dimethyladenine (**38**). The latter two compounds did not show any affinity at the mouse receptor and only negligible affinity at a concentration of 100 μM for the rat receptor. The synthesized compounds **49**, **61** and **67** showed affinity in the low micromolar range for native mouse adenine receptors at membrane preparation of NG108-15 cells. Similar results were obtained with the mouse adenine receptor expressed in Sf21 insect cell membranes. IC$_{50}$ values determined in radioligand binding studies were generally several-fold higher than IC$_{50}$ values obtained in functional cAMP assays due to the amplification of the signal mediated by a GPCR by the intracellular signalling transduction pathway. The same differences between IC$_{50}$ values determined in radioligand binding and functional studies has previously been observed for the recombinant rat adenine receptor expressed in CHO cells.[102]

Affinities of adenine, selected adenine derivatives, as well as other substances known to activate GPCRs, at the mouse adenine receptor expressed in Sf21 insect cell membranes were determined and compared with those for the adenine receptor expressed in NG108-15 mouse

neuroblastoma x rat glioma cell membranes and the affinities determined in rat brain cortical membrane preparations (Figure 37, Table 19). The unsubstituted adenine showed the highest affinity in all three test systems exhibiting K_i values in the nanomolar range (IC_{50} = 63.7 nM for the mouse receptor in Sf21 cells, 54.9 nM in NG108-15 cells, K_i = 29.2 nM in rat brain cortex).

Table 19. Comparison of affinities of adenine and selected compounds for mouse and rat adenine receptors determined in radioligand binding studies using membrane preparations.

	Compound	Structure	IC_{50} or K_i value ± SEM [µM] (or % inhibition at 100 µM)		
			Mouse recombinant receptor expressed in Sf21 cells	NG108-15 cells	Rat brain cortex
1	Adenine		**0.0737** ± 0.0129[110]	**0.0549** ± 0.0422	**0.0292** ± 0.0033
83	1-Methyladenine		≥ **100** (62 ± 7)	≥ **100** (60 ± 4)	**29.3** ± 9.3[186]
84	2-Fluoroadenine		**1.279** ± 0.139	**0.304** ± 0.097	**0.622** ± 0.144[104]
34	N^6-Benzyladenine		>> **100** (12 ± 12)	>> **100** (8 ± 12)	> **100** (30 ± 3)[186]
38	N^6-Dimethyladenine		>> **100** (0 ± 8)	>> **100** (0 ± 6)	>> **100** (11 ± 2)[186]
49	TB 23		**7.51**	**7.69** ± 2.99	**2.85** ± 0.59[186]

61	TB 73 (PSB-09073)		**3.51 ±** 1.39[190]	**3.53 ±** 0.55	**0.025 ±** 0.006
67	TB 97 (PSB-09097)		**0.375 ±** 0.128[190]	**0.273 ±** 0.035	**0.094 ±** 0.003
85	7-Methyladenine		**5.76 ±**1.02	**1.447 ±** 0.440	**4.13 ±** 1.08[186]
86	NECA		**>> 100** (28 ± 1)	**>> 100** (7 ± 1)	**>> 100** (10 ± 2)[186]
87	ADP		**>> 100** (28 ± 3)	**≥ 100** (50 ± 5)	**≥ 100** (51 ± 3)[186]
88	ATP		**>> 100** (14 ± 1)	**≥ 100** (61 ± 4)	**> 100** (39 ± 7)[186]
89	Caffeine		**>> 100** (0 ± 1)	**>> 100** (0.4 ± 1)	**>> 100** (2 ± 1)[186]

The rank order of potency for the mouse receptor expressed in Sf21 cells was: adenine (**1**) > N^6-(4-aminobutyryl)adenine (**67**) > 2-fluoroadenine (**83**) > N^6-(3-aminopropionyl)adenine (**61**) > 7-methyladenine (**85**) > N^6-acetyladenine (**49**) > 1-methyladenine (**83**) >> N^6-benzyladenine (**34**) > N^6-dimethyladenine (**38**). The same rank orders of potency were observed for NG108-15 cellular membranes and rat brain cortical membranes. All other tested substances (NECA, ADP, ATP and caffeine) were inactive (Table 19).

In conclusion, a novel receptor for the purine nucleobase adenine from mouse brain was pharmacologically characterized. The low sequence identity with the previously described rat adenine receptor (76 %) suggests that the new receptor is not a species homologue but rather a distinct receptor subtype. Since human cells also posses specific binding sites for adenine[104] the existence of a receptor for adenine in human tissues seems to be very likely. However, a human sequence encoding for an adenine receptor has yet to be identified. The rat adenine receptor discovered[102] and the mouse adenine receptor characterized in the present study appear to be members of a new, possibly larger family of receptors for purine nucleobases.
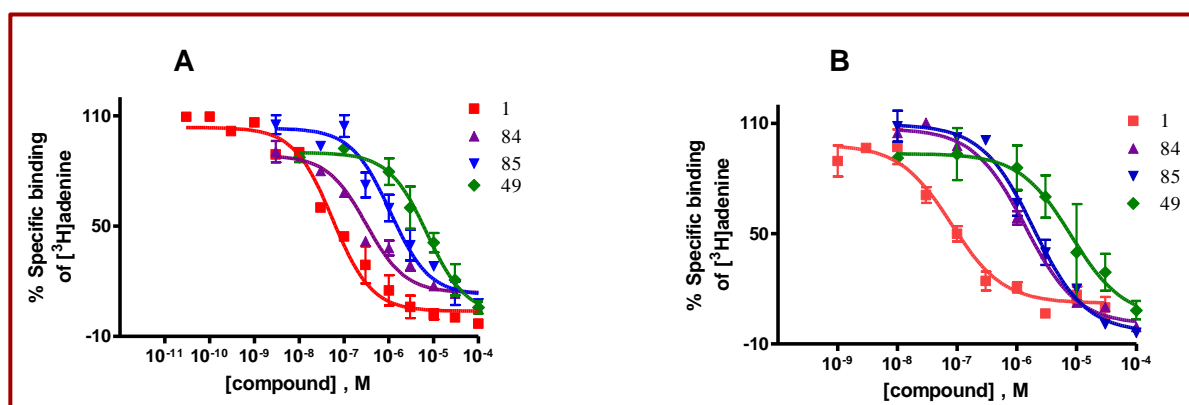
Figure 37. Competition curves for adenine and adenine derivatives at membranes from NG108-15 cells, natively expressing the mouse adenine receptor (**A**) and Sf21 cells recombinantly expressing the mouse adenine receptor (**B**).

3.1.5. Investigation of adenine receptors natively expressed in Chinese hamster ovary cells (CHO K1)

It had previously been reported by our group that adenine receptors were natively expressed in CHO cells. Adenine in a concentration-dependent manner stimulated d intracellular cAMP accumulation with an IC_{50} value of 0.43 ± 0.24 µM in native CHO cells indicating the presence of a hamster adenine receptors.[186] Here we aimed to furthers study adenine receptors natively expressed in CHO-K1 cells and to compare results of the coupling of adenine receptors in CHO-K1 with those present in CHO flp-in cells.

3.1.5.1. Accumulation cAMP assay for CHO K1 and CHO flp-in cells

The function of adenine receptors in CHO K1 and CHO flp-in cells was assessed by analyzing the activity of cellular adenylate cyclase activity. Cellular cAMP production was stimulated by the addition of 5 µM forskolin.
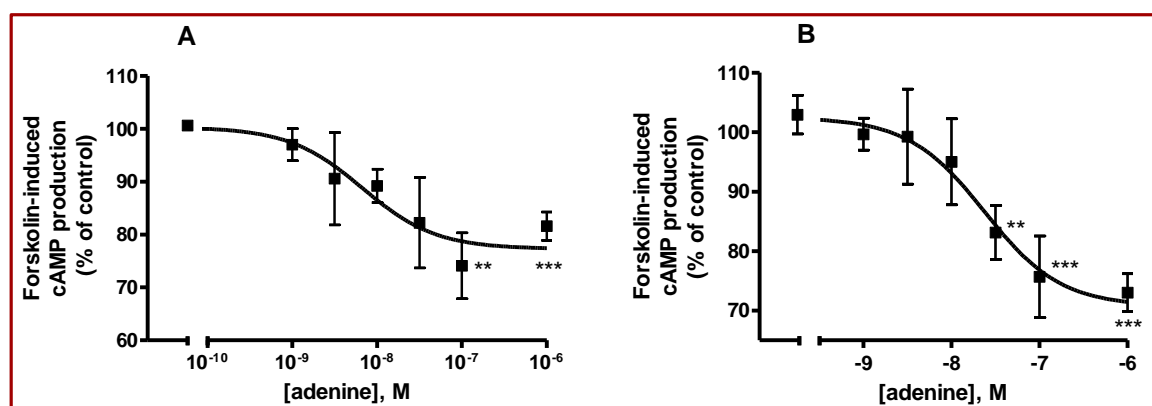
Figure 38. Inhibition of adenylate cyclase activity of adenine receptor in intact (**A**) CHO K1 cells and (**B**) CHO flp-in cells. Cellular cAMP production was stimulated by 5 µM of forskolin. The figure shows the concentration-dependent inhibition of intracellular cAMP accumulation by adenine (1 nM − 1000 nM). The IC_{50} value was 4.04 ± 2.7 nM for adenine receptors in CHO K1 cells and 23.8 ± 2.1 nM for adenine receptor in CHO flipIn cells (n = 3). *** indicates significant differences from corresponding control ($p < 0.001$) or ** ($p < 0.01$).

The forskolin-induced cAMP production in the presence of agonists was expressed as percentage of the forskolin-induced cAMP production in the absence of agonists (% of control) ($n = 3$, Figure 38). The results showed that adenine receptors in CHO K1 and CHO-flp-in cells are coupled to inhibition of adenylate cyclase with IC_{50} values of 4.04 ± 2.7 nM and 23.8 ± 2.1 nM, respectively. An explanation of the 6-fold lower IC_{50} value of adenine in CHO K1 cells as compared to CHO-flp-in cells could be a lower receptors expression in the latter cell line.

3.1.5.2. [³H]Adenine saturation experiments

For further characterization of the adenine receptors in CHO K1 cells saturation binding studies were performed using membrane preparations of CHO K1 cells and [³H]adenine (0.75-150 nM).
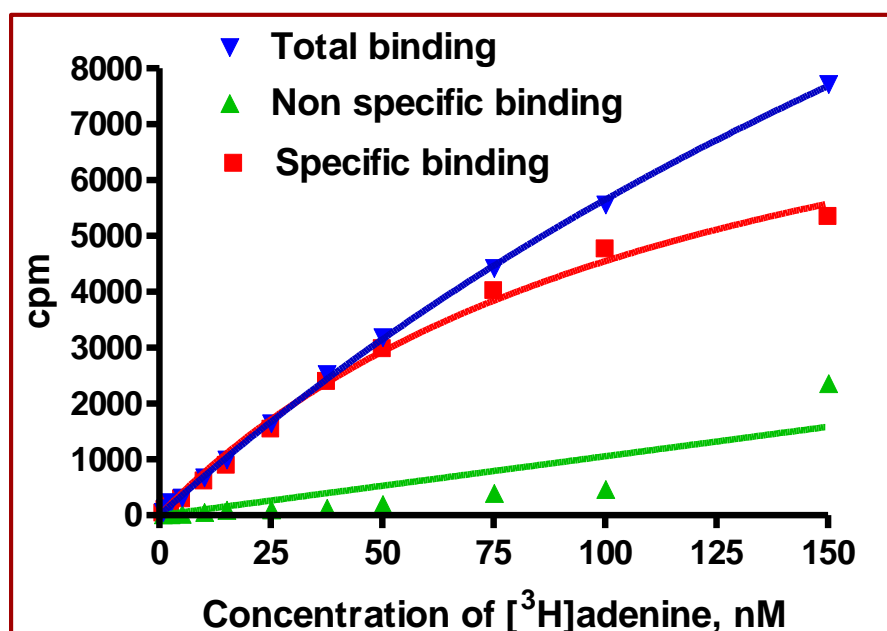
Figure 39. Saturation of [³H]adenine binding to adenine receptors in membrane preparations of CHO K1 cells.

The results showed that CHO cells exhibited a single binding site for [³H]adenine with a K_D value of 121 nM and a B_{max} value of 1.536 pmol/mg of protein ($n = 1$, Figure 39). The determined K_D value was quite similar to that determined at the mAde2R expressed in Sf21 cells ($K_D = 113$ nM).

Thus, the hamster also appears to express at least one adenine receptor coupled to inhibition of adenylate cyclase and the expression level in CHO K1 cells was found to be high.

3.1.6. Homologous competition assays

3.1.6.1. Principle of assay

A competitive binding experiment is termed *homologous* when the same compound is used as the hot and cold ligand. Homologous competitive binding experiments have the same goals as saturation binding experiments which can be used to determine the affinity of a ligand for the receptor as well as the receptor number. In order to analyze a homologous competition binding curve, one needs to make the following assumptions:[120]

- The receptor has identical affinity for the labeled and the unlabeled ligand.
- There is no cooperativity.
- There is no ligand depletion. The methods in this section assume that only a small
- fraction of ligand binds. In other words the method assumes that the free concentration equals the concentration added.
- There is only one class of binding sites. It is difficult to detect a second class of binding sites unless the number of lower affinity sites vastly exceeds the number of higher affinity receptors (because the single low concentration of radioligand used in the experiment will bind to only a small fraction of low affinity receptors).

The Cheng and Prussoff equation is used to analyze a homologous competition binding curve in which K_i is calculated from the IC_{50}. In this case the hot ligand has identical affinity with the cold ligand so that K_D is the same as K_i (equation 6).[120]

$$K_D = K_i = IC_{50} - [\text{Radioligand}]$$

Equation 6. Cheng and Prussoff equation

The difference between the top and bottom plateaus of the curve represents the specific binding of the radioligand at the concentration used. Depending on how much radioligand is used, this value may be close to the B_{max} or far from it. To determine the B_{max}, specific binding is divided by the fractional occupancy (equation 7), calculated from the K_D and the concentration of radioligand.

$$B_{max} = \frac{\text{Top - Bottom}}{\text{Fractional occupancy}} = \frac{\text{Top - Bottom}}{[\text{Radioligand}] \big/ (K_D + [\text{Radioligand}])}$$

Equation 7. Calculation of receptor density (B_{max})

3.1.6.2. Homologous competition binding curves for characterization of endogenous rat adenine receptors in pheochromocytoma cells and human melanoma 1539 cells

Radioligand binding studies were performed of membrane preparations of various cell lines. High affinity binding of [^{3}H]adenine was found in membrane preparations of various cell lines, including rat pheochromocytoma (PC12) cells, human astrocytoma cells, human embryonic kidney cells and human melanoma 1539 cells (Figure 40).
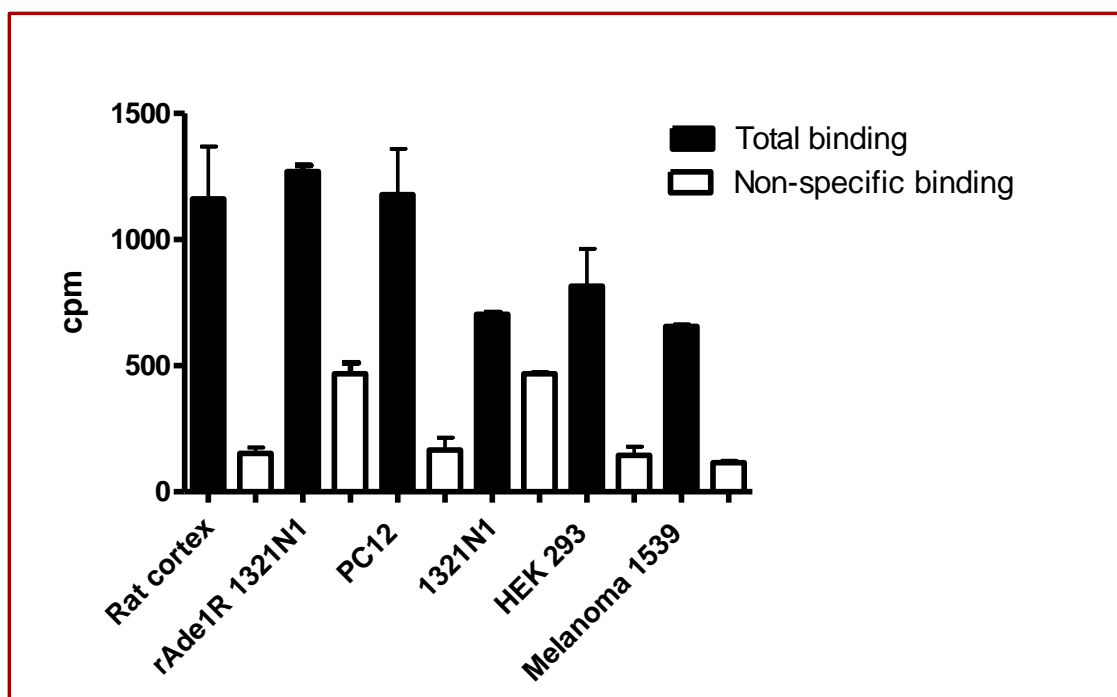
Figure 40. [^{3}H]Adenine binding (10 nM) to membrane preparations of rat cortex, 1321N1 astrocytoma cells heterologously expressing rAde1R, PC12 cells, astrocytoma 1321N1 cells, human embryonic kideny cell (HEK293) and human melanoma 1539 cell (100 µg of protein) (*n*=3).

Competition binding assays were performed as described at adenine receptors of human melanoma 1539 cells and rat pheochromocytoma cell membranes using different concentrations of adenine as shown in figure 41. Adenine showed relatively low affinity for adenine receptors in human melanoma 1539 cells with an IC$_{50}$ value of 341 ± 119 nM compared to the adenine receptors in human embryonic kidney cells (HEK293) ($K_i = 44.3$ nM). The calculated K_D value from the homologous competition experiments was 315 ± 104 nM, which is much higher than the K_D value calculated for the human adenine receptor in membrane preparation of HEK293 cells ($K_D = 44.7$ nM).[186] The adenine receptors density at membrane preparations of melanoma cells was very low with a B_{max} value of 6.96 ± 1.99 fmol/mg protein. Quite similar results were obtained for adenine receptors in membrane

preparations of rat PC12 cells: adenine showed lower affinity (IC_{50} = 489 ± 206 nM) in comparison with the adenine receptor in rat cortical membrane preparations (K_i = 29.2 nM).
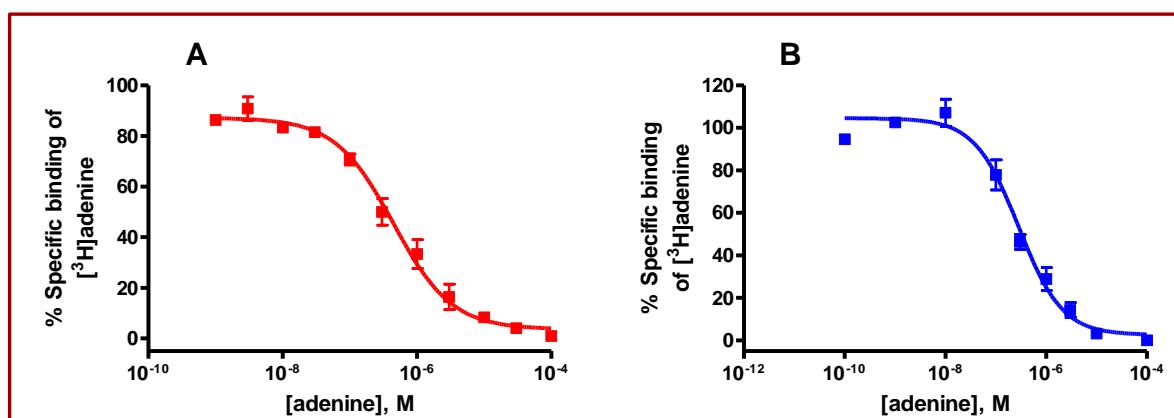
Figure 41. Competition curves for adenine derivatives versus 10 nM [^{3}H]adenine obtained (**A**) at membrane preparations of PC12 cells (**B**) at membrane preparations of melanoma cells (n=3). The apparent K_D and B_{max} values were 479 ±106 nM and 21.3 ± 5.6 pmol/mg protein and, IC_{50} 489 ± 206 nM for endogenous rat adenine receptors in pheochromocytoma cells, and the apparent K_D = 315 ± 104 nM, B_{max} 6.96 ± 1.99 fmol/mg protein and IC_{50} value of 341 ± 119 nM at human melanoma 1539 cells (n = 3).

The apparent K_D value calculated from homologous competition experiments was 479 ± 106 nM, while the determined K_D value for adenine receptors at rat brain cortical membrane preparation was 27.2 nM. A high receptor density with a B_{max} value of 21.3 ± 5.6 pmol/mg was detected in membrane preparations of PC12 cells (n = 3).

Despite the low affinity for adenine, the amount of specific binding determined in radioligand binding studies using 10 nM [^{3}H]adenine at membrane preparations from rat PC12 cells was higher than at human embryonic kidney cells (HEK293), human melanoma 1539 cells and rat brain cortical membranes (Figure 41). This can be explained by the very high expression level of [^{3}H]adenine binding sites in PC12 cells.

3.1.6.2.1. Functional studies at PC12 cells

In order to study functional properties of rat adenine receptors in PC12 cells we measured the activity of adenylate cyclase in PC12 cells. cAMP reporter gene assays were performed. For this purpose, the pCER-luc (the cAMP responsive reporter plasmid) was transiently transfected into PC-12 cells using Lipofectamine 2000 as a transfection reagent. The results showed that adenine in a dose dependent manner affects forskolin-stimulated cAMP production in the luciferase luminescence assay (Figure 42). Adenine at a concentration of

100 µM inhibited forskolin-stimulated cAMP levels by up to 60% with an IC_{50} value of 12.8 ± 2.1 µM. The determined IC_{50} value is in the micromolar range while the rAde1R receptor expressed in 1321N1 astrocytoma cells had shown an IC_{50} value in the nanomolar range.
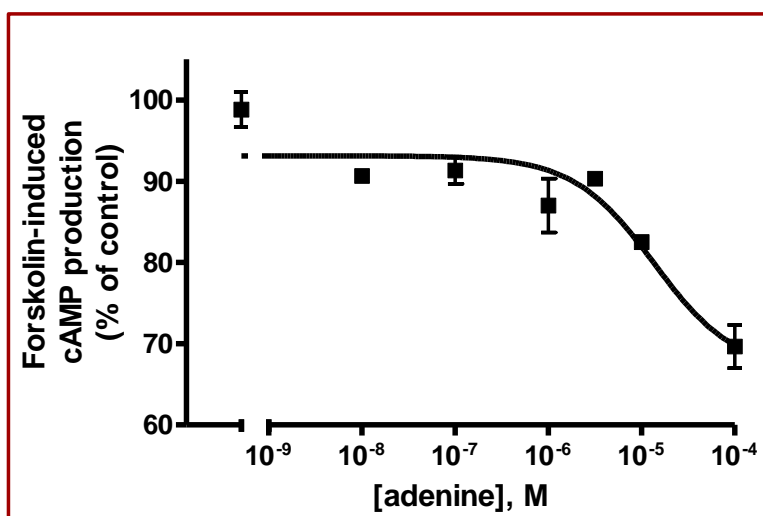
Figure 42: Inhibition of forskolin-stimulated cAMP-dependent luciferase activity by adenine activating endogenous rat adenine in PC12 cells. Data are given as percentages of the mean increases in cellular cAMP levels in the presence of forskolin alone. Adenine induced a dose-dependent inhibition of forskolin-stimulated intracellular cAMP, reducing stimulated cAMP levels by up to 60%. The IC_{50} value was 12.8 ± 2.1 µM (mean ± SEM determined in 2 independent experiments).

One explanation for this discrepancy could be that PC12 cells express an adenine receptor subtype which is different from the rAde1R. An alternative explanation could be that the adenine receptor in PC12 cells forms heteromers with other receptor or interact with other proteins which modulate receptor activation.

3.1.6.2.2. mRNA localization studies for endogenous rat adenine receptors in PC12 cells

In order to investigate whether PC12 cells express mRNA for the rAde1R, mRNA was extracted from PC12 cells. Primers were designed as shown in table 20.
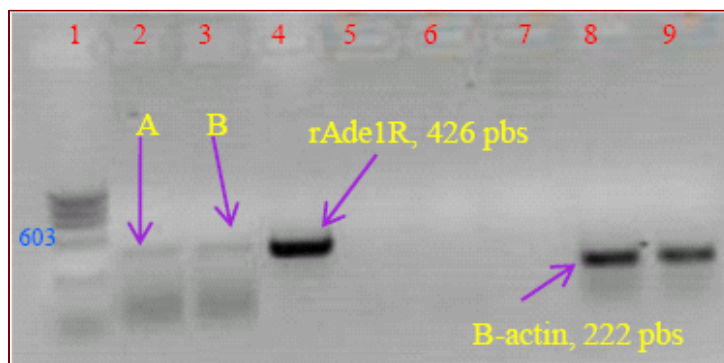
Figure 43. PCR product experiment. *Lane* 2 and 3, 426 bps, are PCR product with cDNA from PC12 cells. *Lane* 4 is PCR product with rAde1R plasmid (426 bps). Control samples without primers (5) or primers without plasmid (7) revealed no products. *Lane* 8 and 9 are PCR product using β-actin cDNA from PC12 cells with specific primers as control.

Analysis of PCR products showed that bands 426 bps (A and B, Figure 43) were obtained which have the expected size of the rAde1R plasmid using the same primers 426 pbs (Figure 43).

Table 20. Information about primers used in PCR.

		Sequence (5'->3')	Start	Stop	T_m	Product length
Primer Set 1	Forward primer rAde1R	GGCATCGAACTTCTTTACTGC	573	593	62	426
	Reverse primer rAde1R	CATCACGGCTCCACCTTGC	998	980	62	
Primer Set 2	Forward -b-actin rat	CCCTAAGGCCAACCGTGAAAAGAT	414	437	72	222
	Reverse b-actin rat	AGGTCCCGGCCAGCCAGGTC	635	616	70	

From the functional studies and primary mRNA localization studies for endogenous rat adenine receptors in PC12 cells, we can conclude that PC12 cells express rat adenine receptors. Further studies must be performed in order to determine the exact sequence for endogenous rat adenine receptors in PC12 cells and to compare it with the rAde1R sequence.

3.2. Adenosine receptors

3.2.1. Evaluation of adenosine A$_{2B}$ receptors expressed in CHO cells

3.2.1.1. Adenosine A$_{2B}$ receptors

Adenosine A$_{2B}$ receptors have been generally defined as the "low affinity adenosine receptors" due to their lower affinity for the endogenous ligand adenosine and for some typical agonists, such as 5′-N-ethylcarboxamidoadenosine (NECA, **86**, Table 19) by contrast with other AR subtypes.[195,197]Activation of adenosine A$_{2B}$ receptors leads to stimulation of adenylate cyclase and activation of phospholipase C through the coupling to G$_s$ and G$_{q/11}$ proteins, respectively. From a pharmacological point of view, adenosine A$_{2B}$ receptors are known as the most poorly characterized of the adenosine P1 receptors. Only very recently some reports about important advancement in identifying adenosine A$_{2B}$ receptor agonists with improved *in vitro* pharmacological profile have been published.[197] BAY-60–6583 (**90**, Figure 44) had been characterized in CHO cells expressing recombinant human adenosine A$_1$, A$_{2A}$ or A$_{2B}$ receptors.[197]The compound (**90**) showed EC$_{50}$ values for receptor activation >10,000 nM for both human adenosine A$_1$ and A$_{2A}$ receptors and 3 nM for the human adenosine A$_{2B}$ receptor subtype. Moreover, it showed no agonistic activity in the adenosine A$_3$-G$_{\alpha16}$ assay up to a concentration of 10 μM.[198] BAY-60–6583 (**90**) has been examined as adenosine A$_{2B}$ receptor agonist for its potential in treating disorders of the coronary arteries and atherosclerosis,[199] and for prophylaxis and/or treatment of ischemia-reperfusion injury[200] and angina pectoris. In our work we aimed at developing a recombinant stable CHO cell line expressing the human adenosine A$_{2B}$ receptors. Furthermore the newly prepared cell line was to be used for characterizing the non-selective agonist NECA (**86**) and the selective agonist BAY-60–6583 (**90**).
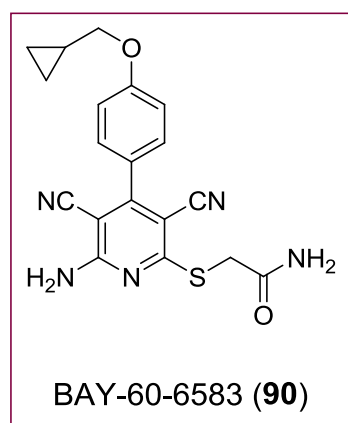
BAY-60-6583 (**90**)

Figure 44. Chemical structures of the adenosine A$_{2B}$ agonist (nonadenosine-like, non-nucleosidic ligand) BAY 60-6583 (**90**).

3.2.1.2. cAMP accumulation assay for CHO cells stably expressing the human adenosine A$_{2B}$ receptor

The function of the human adenosine A$_{2B}$ receptor was assessed by analyzing the activity of cellular adenylate cyclase activity in CHO cells stably expressing the human adenosine A$_{2B}$ receptor. Experiments were carried out with increasing concentrations (0.001–10 μM) of the agonist NECA (**86**) and increasing concentrations (0.001–1 μM) of BAY 60-6583 (**90**).
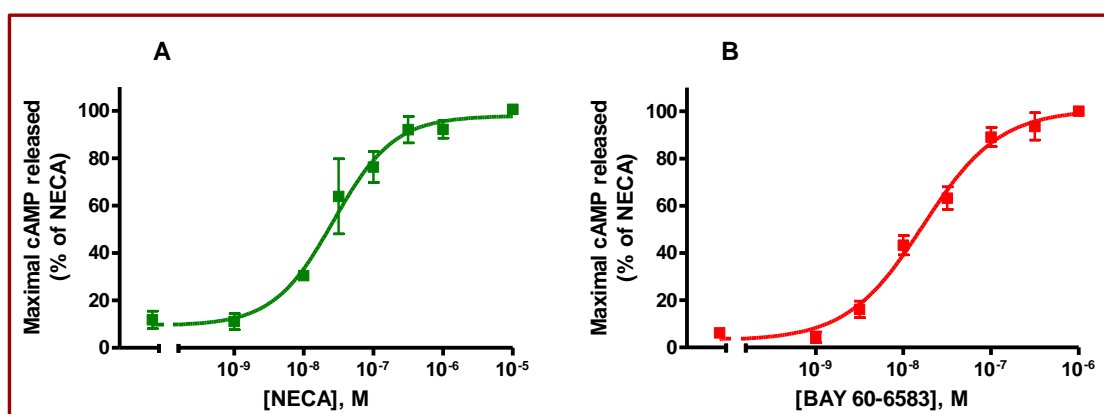
Figure 45. (**A**) Stimulation of adenylate cyclase activity by the human A$_{2B}$ receptor expressed in CHO K1 cells. The figure shows the concentration-dependent stimulation of intracellular cAMP-accumulation by NECA (0.001–10 μM). The EC$_{50}$ value was 0.035 ± 0.014 μM (*n* = 3). (**B**) Stimulation of adenylate cyclase activity by the human adenosine A$_{2B}$ receptor expressed in CHO K1 cells. The figure shows the concentration-dependent stimulation of intracellular cAMP-accumulation by BAY 60-6583 (0.001–1 μM). The EC$_{50}$ value was 0.016 ± 0.004 μM (*n* = 3).
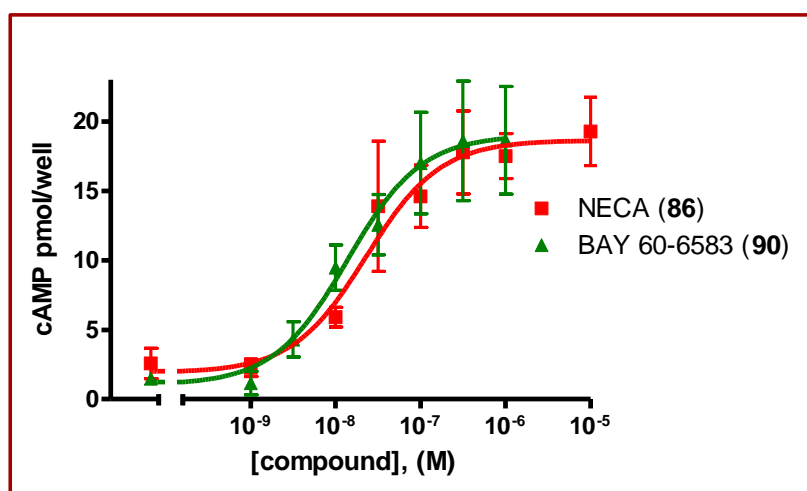
Figure 46. Dose response curves of NECA (**86**) and BAY 60-6583 (**90**) obtained in cAMP assays with CHO cells expressing the human adenosine A$_{2B}$ receptor (*n*=3).

Figure 45, A and B shows the dose-response curves for NECA and BAY 60-6583 at the human adenosine A$_{2B}$ receptor expressed in CHO cells. NECA and BAY 60-6583 exhibited

agonistic properties at human adenosine A_{2B} receptors expressed in CHO cells with EC_{50} values of 0.035 ± 0.014 µM and 0.016 ± 0.004 µM, respectively. From our results it can be concluded that both ligands acted as full agonists in this system since the maximal effect was very similar (see figure 46). It should be noted that the low EC_{50} values for both ligands indicate a very high A_{2B} receptor expression level. In such systems partial agonism may not be detectable.

3.2.2. Modification of a protein-binding method for rapid quantification of cAMP in cell-culture supernatants

Competitive binding assays are widely used methods for cAMP quantification in which the cAMP-binding properties of antibodies raised against chemically modified cAMP[201] or binding of cAMP to the regulatory subunit of cAMP-dependent protein kinase[202,203] is determined. When measuring cAMP with competition techniques, protein-bound tracer must be separated from free tracer. Separation of protein-bound cAMP from free cAMP can be achieved with albumin-saturated charcoal,[202] ammonium sulfate,[204] or by filtration over cellulose filters.[203] The major disadvantages of the separation methods as presently described are that they are time-consuming and labor-intensive and therefore not suitable for analysis of large numbers of samples. Therefore we tried to apply a rapid, semiautomatic modification of the protein-binding method described before,[202, 205] in which cAMP-dependent protein kinase from bovine adrenal cortices is used as a binding protein, and [³H]cAMP with a very high specific activity is used as a radioligand.

3.2.2.1. Modified protocol

In order to test the binding protein prepared from calf adrenal glands a cAMP assay was performed as mentioned above using A_{2B} receptor-expressing CHO cells. cAMP levels in the supernatant were then quantified by incubation of an aliquot with cAMP binding protein prepared from calf adrenal glands (40 µg) and [³H]cAMP (3 nM). The samples were harvested by filtration through Whatman GF/B filters using a cell harvester. A parallel assay was performed using the cAMP binding protein from the assay kit TRK 432 from Amersham Biosciences, Freiburg, Germany. The results are shown in figure 47. There was good agreement between cAMP values obtained with the protein-binding method prepared from calf adrenal cortex and the commercially available kit that was used as a reference method. More than 500 samples could be assayed in duplicate or triplicate in less than 6 h.
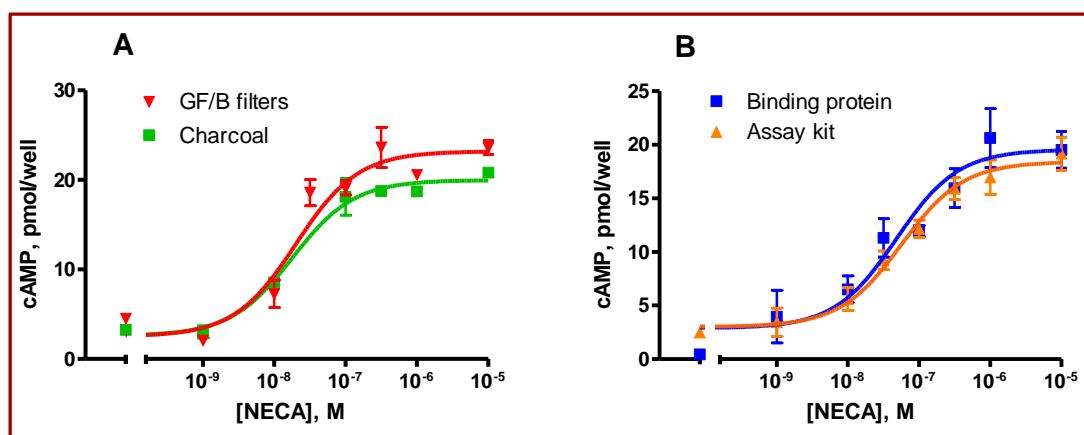
Figure 47. Comparison of dose response curves for NECA in cAMP assays using CHO cells expressing the human adenosine A_{2B} receptor: (**A**) filtration through Whatman GF/B filters using a harvester or adsorption to charcoal for separation of bound from free [^{3}H]cAMP; (**B**) binding protein prepared from calf adrenals gland and binding protein from assay kit TRK 432.

In conclusion, the data presented here show that cAMP in cell-culture supernatants can be measured accurately with the presented modification of the protein-binding assay. The sensitivity of the method compared favorably with other protein-binding methods described[205] with a sensitivity limit in the femtomole range. The major advantages of the method are:

(i)   the low cost (small volumes of tracer and reagents),

(ii)   the ease of setting up large assays with commercially available equipment designed for microtiter plates,

(iii)   the rapidity of the separation of bound from free tracer. It is not difficult to assay 400-500 samples in duplicate or triplicate during a period of 6 h.

The developed protocol which is similar to a protocol previously described by Fredholm and coworker[205] has now become the standard procedure in our laboratory to measure cAMP accumulation.

3.2.3. Adenosine A_{2A} receptor agonists

3.2.3.1. cAMP accumulation assay for CHO cells stably expressing the human adenosine A_{2A} receptor

A newly synthesized adenosine receptor agonist PBS-0777 had showen high affinity for adenosine A_{2A} receptors at rat cortical membranes with a K_i value of 44.2 ± 2.4 nM and selectivity over the other adenosine receptors subtypes. Further evaluation of the agonistic properties of PBS-0777 at adenosine A_{2A} receptors and comparison with the non-selective adenosine receptor agonist NECA was done under the same conditions.

The function of the adenosine A_{2A} receptor was assessed by analyzing the activity of cellular adenylate cyclase activity in CHO cells stably expressing the human adenosine A_{2A} receptor. Experiments were carried out with increasing concentrations of the agonist NECA (0.001–10 µM) and increasing concentrations of the newly synthesized adenosine A_{2A} receptor agonist PSB-0777 (0.001–1 µM) as shown in figure 48.
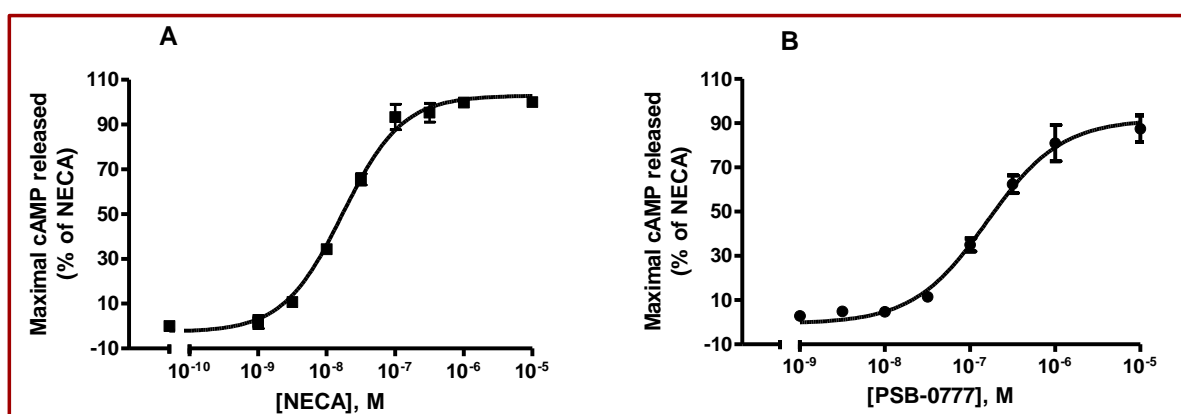
Figure 48. Stimulation of adenylate cyclase activity via the human adenosine A_{2A} receptor expressed in CHO K1 cells. (**A**) Concentration-dependent stimulation of intracellular cAMP-accumulation by NECA (0.001–10 µM). The EC_{50} value was 17.6 ± 14 nM (n=4). (**B**) Concentration-dependent stimulation of intracellular cAMP-accumulation by PSB-0777 [0.001–10 µM]. The EC_{50} value was 117 ± 10 nM (n = 3).

Figure 48 shows the dose-response curves of NECA and PSB-0777 at the human adenosine A_{2A} receptor expressed in CHO cells (EC_{50} values 17.6 ± 14 nM, and 117 ± 10 nM, respectively). The amount of cAMP produced by compound PSB-0777 at 10 µM showed no significant difference compared with the amount of cAMP produced at the same high concentration of NECA (Figure 49 and 50). From these results it can be concluded that PSB-0777 acts as a full agonist and has high affinity for human adenosine A_{2A} receptors expressed

in CHO K1 cells. The compound showed six fold lower affinity compared with the parent compound NECA for human adenosine A_{2A} receptors expressed in CHO cells.
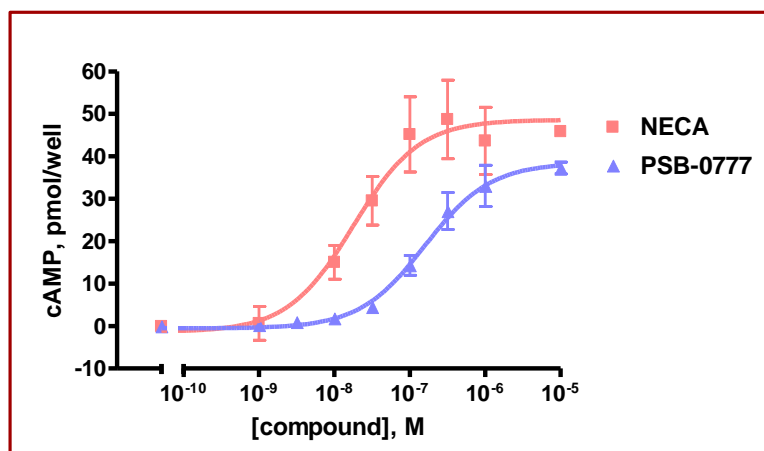
Figure 49. Dose response curves of NECA (**86**) and PSB-0777 in cAMP assays using CHO K1 cells expressing the human adenosine A_{2A} receptor ($n = 3$). EC_{50}: 17.6 ± 14 nM (NECA) and 117 ± 10 nM (PSB-0777).
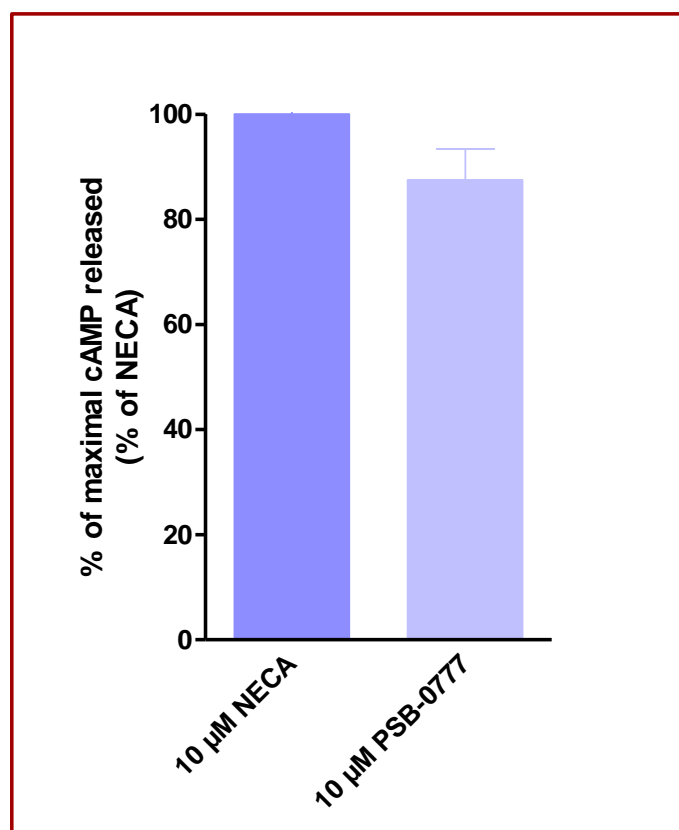
Figure 50. Maximal amount of cAMP produced by stimulation with 10 µM of NECA and PSB-0777; the result showed no significant different and therefore PSB-0777 is a full agonist at human adenosine A_{2A} receptors in this test system.

3.2.4. Adenosine A$_{2A}$ receptor antagonists

3.2.4.1. cAMP accumulation assay at CHO cells stably expressing the human adenosine A$_{2A}$ receptor for investigation of the new adenosine A$_{2A}$ receptor antagonist AA-01

The new antagonist AA-01 was to be functionally characterized in order to investigate whether it has an allosteric or a competitive mechanism of action. Standard A$_{2A}$ antagonists were investigated under the same conditions for comparison.

CHO cells transfected with the human adenosine A$_{2A}$ receptor were used for this purpose. For experiments with antagonists, cells were incubated with different concentrations of adenosine A$_{2A}$ antagonists for 10 min before addition of the agonist NECA (1 nM - 100000 nM). Then the cells were incubated for 10 more minutes. Alternatively both, agonist and antagonist were added at the same time. As antagonists AA-01, KW6002 (istradefylline) (**91**) and SCH420814 (preladenant) (**92**) were investigated (Figure 51). AA-01 (10 nM, 100 nM, 1 µM) showed a concentration-dependent shift of the concentration-response curve of NECA to the right. The maximal effect of NECA was significantly reduced in a concentration-dependent manner (Figure 52).
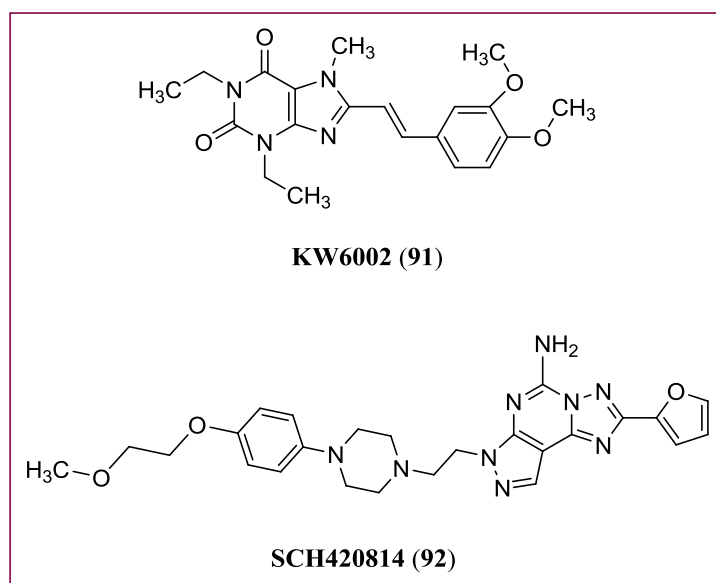
Figure 51. Chemical structures of the adenosine A$_{2A}$ antagonists KW6002 (**91**) and SCH420814 (**92**).

KW6002 (**91**) (1 µM) and SCH420814 (**92**) (100 nM) also shifted the concentration-response curve of NECA (**86**) to the right. The maximal effect was also decreased, although to a smaller extent than seen with AA-01 (Figure 52 and 53). Figure 53 shows the effect on the maximal NECA-induced cAMP response in the presence of antagonists.
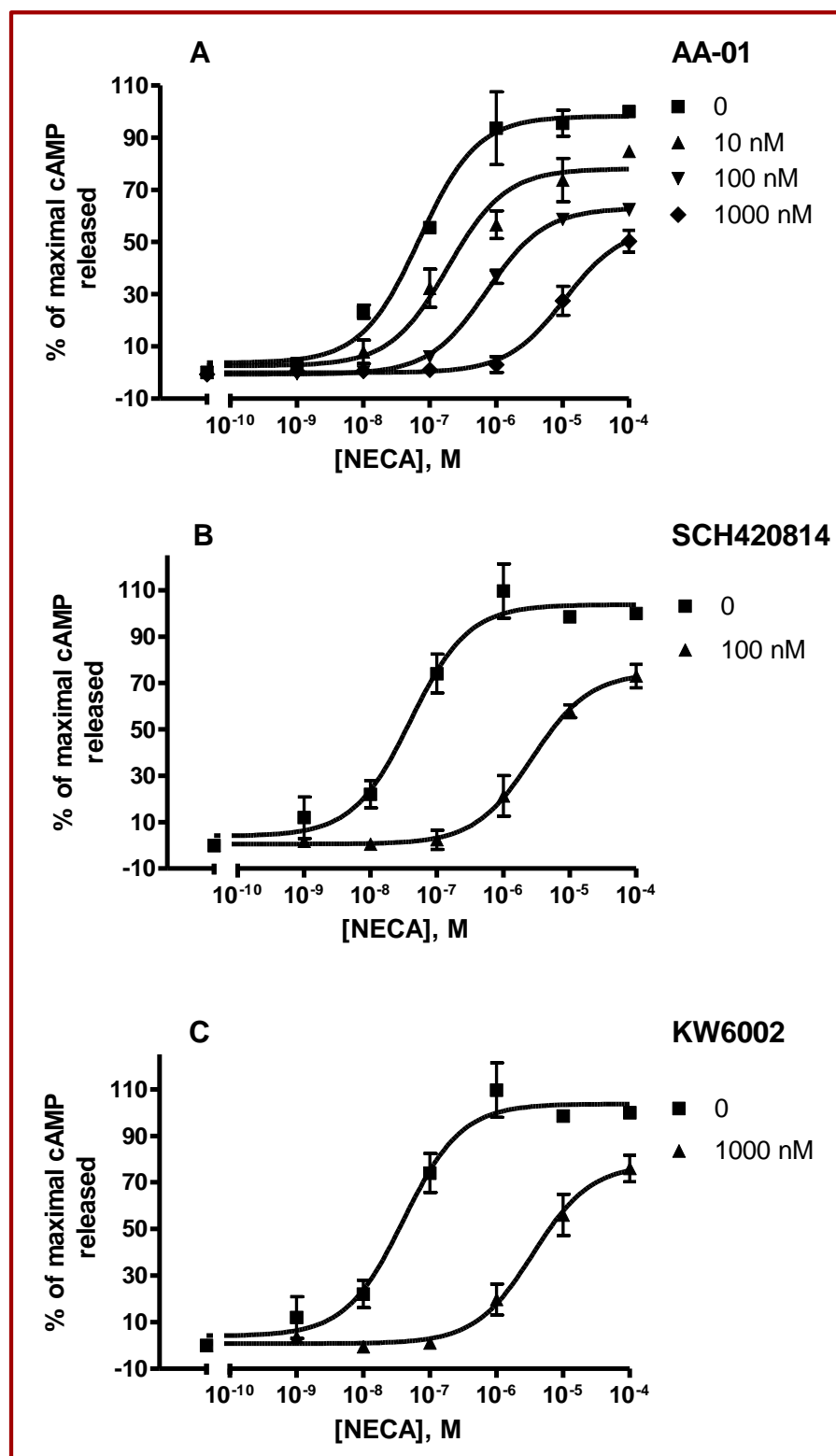
Figure 52. Measurement of stimulation of adenylate cyclase activity by human adenosine A_{2A} receptors expressed in CHO cells. The figure shows the stimulation of intracellular cAMP-accumulation by NECA alone (**A-C**), and (**A**) by NECA after preincubation with different concentrations of AA-01 (10 nM, 100 nM and 1000 nM), (**B**) by NECA after preincubation with 100 nM SCH420814, and (**C**) by NECA after preincubation with 1 μM KW6002. The cells were incubated with antagonist for ten minutes before addition of agonist (*n*=3).

The reduction in the maximal effect by AA-01 was statistically highly significant. Table 21 shows the EC_{50} values obtained for NECA (**86**) in the absence and in the presence of antagonist.
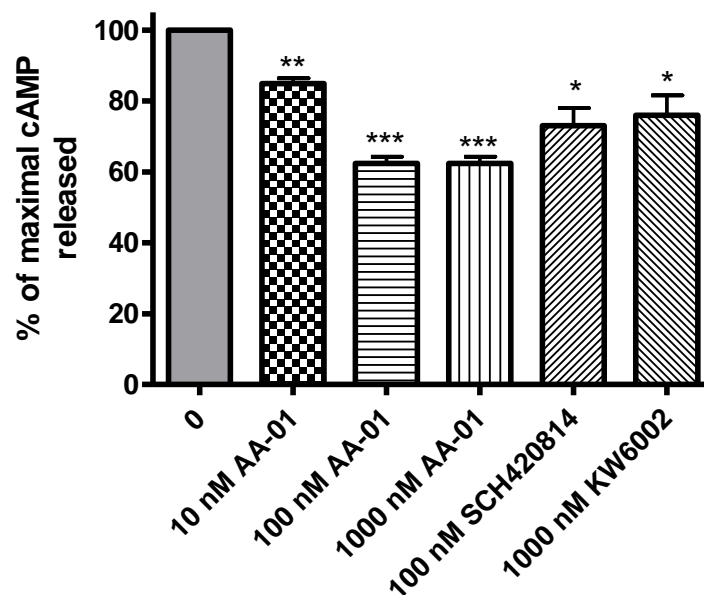
Figure 53. Maximal amount of cAMP released at 100 µM of NECA without and after preincubation with antagonists. *P values for SCH420814 (**92**) and KW6002 (**91**) are 0.0254 and 0.0458, respectively; **P value for 10 nM of AA-01 is 0.0046 while the ***P vor 100 and 1000 nM AA-01 value is < 0.0001.

Table 21. EC_{50} values for NECA-induced cAMP accumulation without and after preincubation with antagonist.

Compounds	$EC_{50} \pm$ SEM (µM) ($n = 3$)
NECA (**86**)	**0.0714** $\pm$ 0.0046
NECA +10 nM AA-01	**0.202** $\pm$ 0.065
NECA + 100 nM AA-01	**0.737** $\pm$ 0.093
NECA + 1000 nM AA-01	**16.7** $\pm$ 2.5
NECA + 100 nM SCH420814 (**92**)	**3.11** $\pm$ 0.87
NECA + 1000 nM KW6002 (**91**)	**4.54** $\pm$ 1.32

Simultaneous addition of agonist and antagonist

In the following experiments the antagonist was added at the same time as the agonist. AA-01 again showed a concentration-dependent shift of the NECA (**86**) curve (Figure 54). The maximal effect of NECA (**86**) was not significantly reduced by the antagonist. A K_B value

was calculated for AA-01: it was 4.14 nM (Table 22). Thus AA-01 is similarly potent as SCH420814 (**92**) (K_B value 2.61 nM), which could also be characterized as a competitive antagonist. Co-administration of NECA (**86**) and KW6002 (**91**) led to a shift of the concentration-response curve for NECA (**86**) (Figure 56). The maximal effect of NECA (**86**) was reduced (Figure 57). The level of statistical significance, however, was low. The K_B value for KW6002 (**91**) could be calculated as 22.9 ± 9.9 nM.
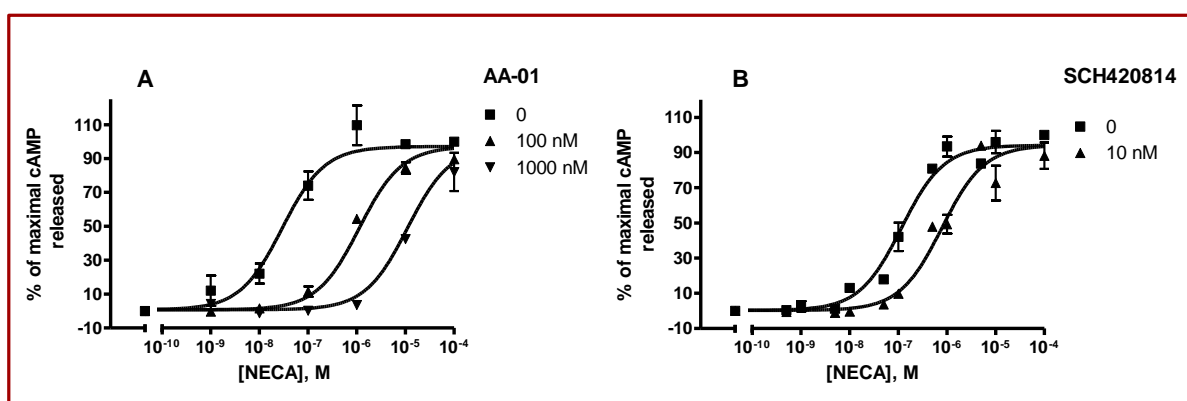
Figure 54. NECA-induced stimulation of adenylate cyclase activity via the human adenosine A_{2A} receptor expressed in CHO cells in the absence and in the presence of (**A**) two different concentrations of AA-01 (100 nM and 1000 nM) and (**B**) 10 nM SCH420814. Agonist and antagonists were added at the same time (*n*=3).
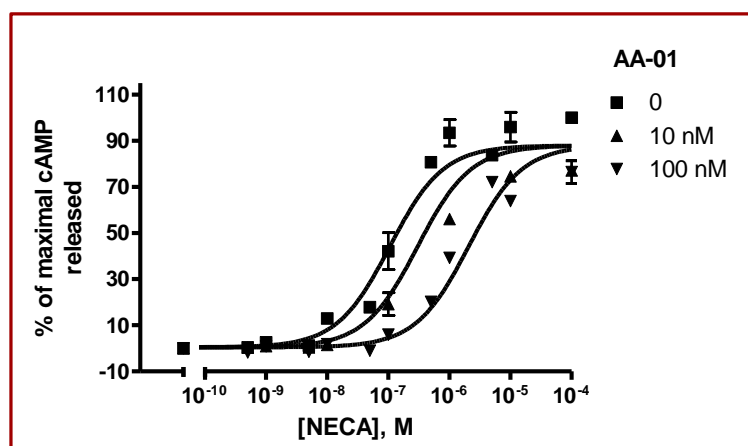
Figure 55. NECA-induced stimulation of adenylate cyclase activity via the human adenosine A_{2A} receptor expressed in CHO cells in the absence and in the presence of two different concentrations of AA-01 (100 nM and 1000 nM). Agonist and antagonists were added at the same time (*n*=3).

Table 22. Potency of selected adenosine receptor antagonists in CHO cells transfected with the human adenosine A_{2A} receptor

Antagonist	$K_B \pm$ SEM (nM), *n*=3	Hill slop
SCH420814 (**92**)	**2.61** $\pm$ 1.27	**1.06** $\pm$ 0.27
AA-01	**4.14** $\pm$ 3.08	**0.94** $\pm$ 0.14
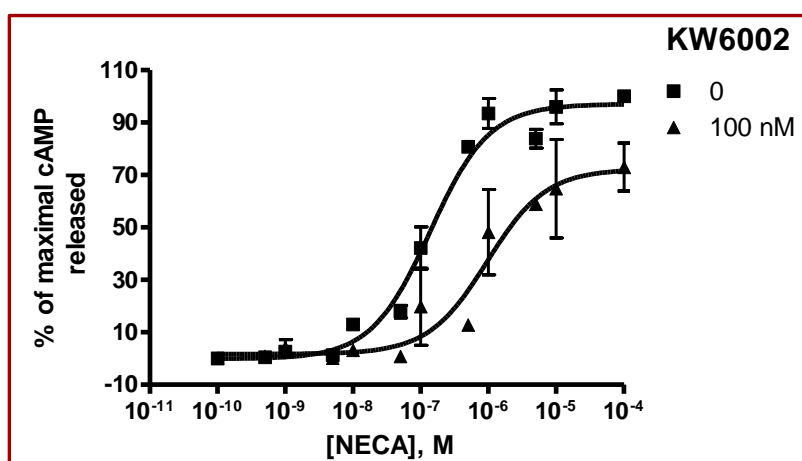
Figure 56. NECA-induced stimulation of adenylate cyclase activity via the human adenosine A_{2A} receptor expressed in CHO cells in the absence and in the presence of 100 nM KW6002. Agonist and antagonist were added in the same time (*n*=3).
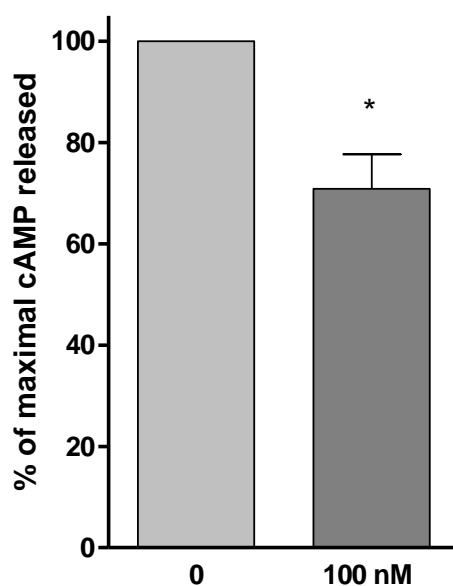
Figure 57. Maximal amount of cAMP produced by stimulation with 100 μM of NECA in the absence and in the presence of 100 nM KW6002 (coadministration) (*P* values is 0.0464).

In conclusions, AA-01 appears to be a competitive antagonist at human adenosine A_{2A} receptors, like KW 6002 (**91**) and SCH420814 (**92**). The compound shows a large decrease in the maximal effect induced with NECA (**86**) when applied prior to the agonist (10 min preincubation). This might be due to slow dissociation from the receptor. But this would require further investigation, e.g. by performing kinetic studies with radiolabelled AA-01. Slow receptor dissociation may be pharmacologically relevant.

3.2.5. Interactions of Magnolia extract with adenosine A_1 receptors

The bark of Magnolia officinalis has a history of use in traditional Asian medicine for mild anxiety, nervousness and sleep-related problems. A proprietary combination containing Magnolia extract, Seditol®, has demonstrated effectiveness in alleviating sleep difficulties in an open-label clinical assessment.[206]

In order to better understand the pharmacological targets for Seditol®(S), the product and its component extracts (Magnolia = **M** and Ziziphus = **Z**) were tested for binding affinity to a number of central nervous system receptors associated with relaxation and sleep.

For this purpose, a series of different plant extracts was investigated for their affinity and function at adenosine receptors in radioligand binding studies (the extracts were provided by Dr. Koetter Consulting Services, Uttwil, Switzerland). An extract concentration of 100 µg/ml was used to determine the inhibition of the radioligand binding at all four adenosine receptor subtypes. Only extract **M** at A_1 adenosine receptor and extracts **M** and **S** at A_3 adenosine receptor could inhibit the respective radioligand binding by ≥ 50 % and showed therefore significant affinity. The radioligand binding studies showed that extract **S** exhibited an affinity for human adenosine A_3 receptors (K_i= 3.65 µg/ml), while extract **M** showed affinities to both, rat adenosine A_1 receptor with a K_i-value of 9.20 µg/ml and to human adenosine A_3 receptors (K_i-value of 32.0 µg/ml).[206] This indicates that there are interactions between Seditol®, and/or one of its constituent extract of Magnolia, with the adenosine A_1 receptor. These interactions are consistent with the reported anxiolytic and sleep-inducing activities of extracts of Magnolia, Ziziphus and their combination. The results provide further indications of the mode of action of these plant extracts.

Extracts of **M**. officinalis bark and **Z**. spinosa seed are combined in a proprietary product called Seditol® that is produced by Next Pharmaceuticals. Seditol is characterized as containing a minimum of 2.7% honokiol and 0.1% spinosin. Seditol is a dietary supplement, marketed for the improvement of sleep difficulties associated with restlessness, stress or anxiety.

In order to fully understand the nature of interaction of Mongolia extract with adenosine A_1 receptors further testing were performed.

3.2.5.1. Luciferase cAMP assay

The CHO K1 cells stably transfected with human adenosine A_1 receptors were transiently transfected with pCRE-luc (cAMP response element). The reporter cells were stimulated for cAMP production with forskolin (4 µM) and N^6-cyclopentyladenosine (CPA) was used as an adenosine A_1 receptor agonist to inhibit the forskolin-stimulated cAMP production. CPA at a concentration of 1 µM showed about 60% inhibition of maximal cAMP produced. The Magnolia extract **M** was tested at a concentration of 10 µg/ml and 100 µg/ml completely inhibited forskolin-stimulated cAMP accumulation in CHO cells expressing the adenosine A_1 receptor (Figure 58).
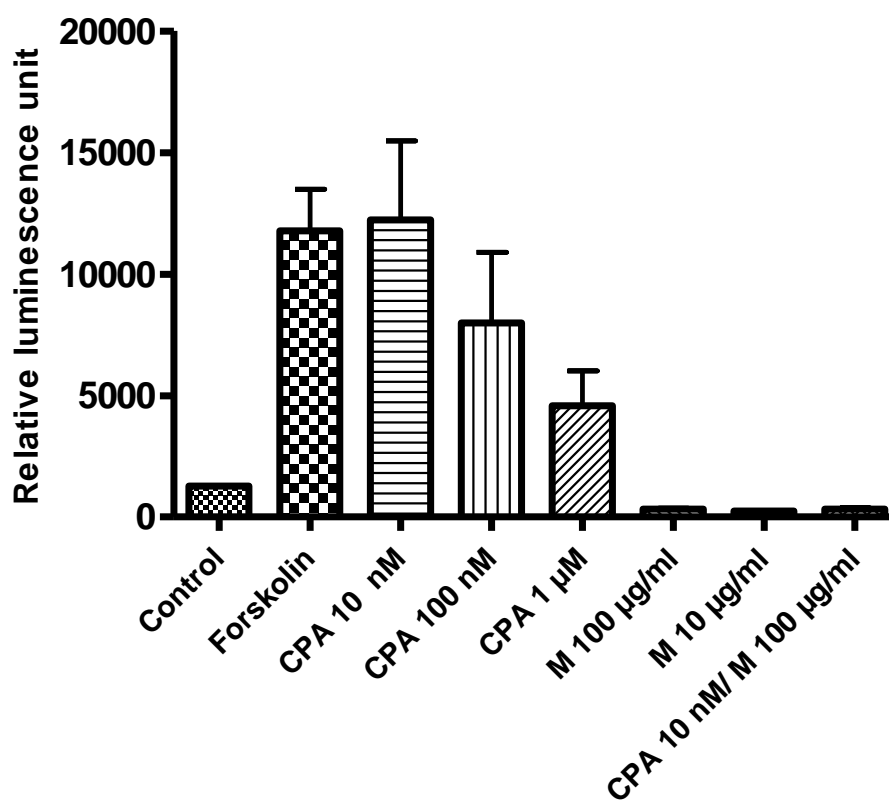
Figure 58. Inhibition of forskolin-stimulated cAMP accumulation by CPA and plant extract **M** at different concentrations in CHO cells stably expressing the human adenosine A_1 receptor (*n*=2).

The extract seemed to disturb the assay system by an unknown mechanism. In the presence of the extract, the cells were not able to produce any cAMP after stimulation of the adenylate cyclase with forskolin (4 µM).

3.2.5.2. GTP-shift experiments

As the cAMP luciferase result was considered likely to be an artifact, the functional properties (agonist, antagonist) of the magnolia extract **M** were investigated in GTP-shift experiments using a rat cortical membrane preparation containing adenosine A_1 receptors. The magnolia extract showed no GTP-shift in this experiment. Results are shown in table 23 and figure 59.
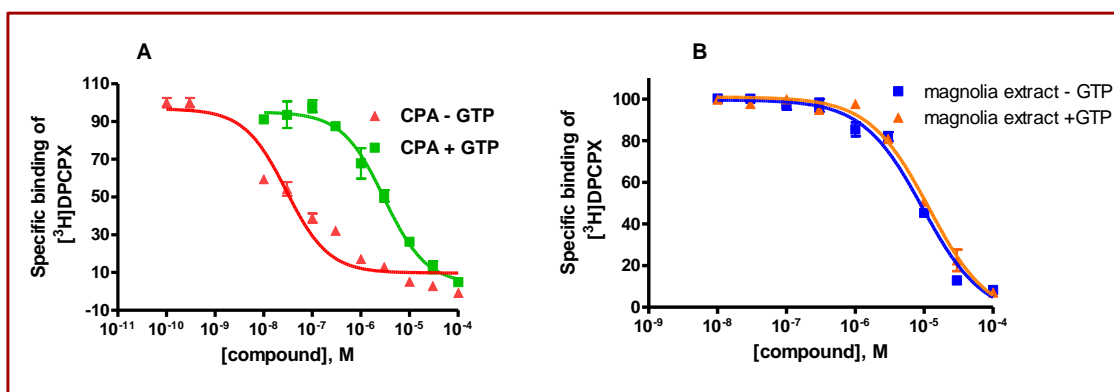
Figure 59. GTP-shift curves (**A**) for the full A_1 agonist CPA and (**B**) for the plant extract **M** to determine shifts in IC_{50} values in order to estimate the functional properties. Data points represent means of 1 or 3 independent experiments $\pm$ SEM.

The full A_1-adenosine receptor agonist N^6-cyclopentyladenosine (CPA) led to 101-fold (see also Table 23) right word shift of IC_{50}-value in the presence of 100 μM GTP indicating the maximum level for agonists. By contrast, plant extract **M** showed no significant shift of the K_i-value in the presence of GTP (P-value 0.347 in a two-tailed student´s t-test, not significant), indicating that plant extract **M** is an antagonist at adenosine A_1 receptors.

Table 23. GTP-shift experiment for the magnolia extract **M** and CPA at adenosine A_1 receptor in rat cortical membrane preparations.

	IC_{50} $\pm$ SEM A_1 vs. [³H]DPCPX at rat cortex		**Shift**
	Control	**+ GTP (100 μM)**	
Plant extract M	9.49 ± 0.47 μg/ml	12.1 ± 1.7 μg/ml	1.2 ± 0.1 (ns)
CPA (*n* = 1)	29.3 nM	2985 nM	101

In conclusion, the GTP-shift and cAMP experiments with the Magnolia extract indicate that it may be either a week partial agonist or an antagonist.

Seditol® showed an interaction with the adenosine A_1 receptor that appears to be due to the constituent Magnolia extract. Adenosine A_1 is known to play an important role in the initiation of sleep. During the day, adenosine accumulates in neurons and in the evening it is released into the nerve synapses where it prepares the body to enter into a relaxed state.[207] The Magnolia extract was tested for adenosine A_1 agonist activity. The rationale for this is that it was hypothesized that the Magnolia extract might act in a similar was as an extract of Valerian root (Valeriana officinalis L). Previously it has been reported that a valerian extract counteracted functional central arousal caused by the oral administration of caffeine, a adenosine receptor antagonist.[208] Results with the Valerian extract indicated that it is a partial agonist of adenosine A_1.[209,210] The GTP-shift experiments with the Magnolia extract indicate that it may be either a weak partial agonist in analogy with the Valerian extract, or more likely, an antagonist.

3.3. Characterization of [³H]PSB-0413, the first selective radioligand for P2Y₁₂ receptors

ADP plays a key role in arterial thrombosis.[211] ADP is released at sites of vascular injury and interacts with two G protein-coupled receptor subtypes of the P2 receptor family on platelets, the P2Y₁ and P2Y₁₂ receptors. The P2Y₁₂ receptor is the target of the antithrombotic thienotetrahydropyridine derivatives clopidogrel and prasugrel.[212] The platelet P2Y₁₂ receptor has been extensively characterized in functional assays. However, characterization on the protein level has been hampered by the lacking of a selective radioligand.
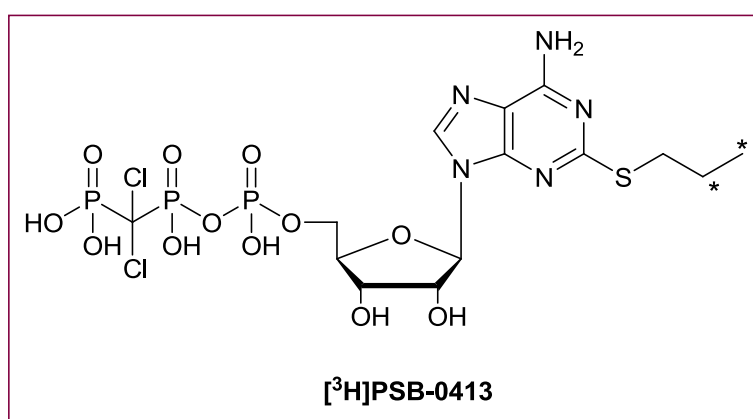
[³H]PSB-0413

Figure 60. Chemical structure of [³H]PSB-0413, the first selective radioligand for P2Y₁₂ receptors.

In a preliminary communication we reported on the development of [³H]PSB-0413 (Figure 60) as a high affinity, subtype selective antagonist radioligand for the characterization of P2Y₁₂ receptors on the protein level.[213]

Here we want to complete the full characterization of [³H]PSB-0413 by using human P2Y₁₂ receptors transfected in 1321N1 astrocytoma cells. Saturation and competition experiments were performed at astrocytoma 1321N1 cells recombinantly expressing the human P2Y₁₂, P2Y₁, or P2Y₁₃ receptor, respectively. Cell lines were prepared by retroviral transfection.

3.3.1. cAMP accumulation assay for astrocytoma cells stably expressing the human P2Y₁₂ receptor

In 1321 N1 astrocytoma cells stably expressing the human P2Y₁₂ receptors, 2-MeSADP or ADP induced a dose-dependent inhibition of forskolin stimulated intracellular cAMP accumulation, reducing stimulated cAMP levels by up to 60–80% (Figure 61). Data are given as percentages of mean increases in cellular cAMP levels in the presence of forskolin alone (4 μM). cAMP levels increased to 23 pmoles/well and were reduced to about 6–8 pmoles / well

in the presence of each diphosphate nucleotide. IC_{50} values were determined for ADP and 2-MeSADP and found to be 1.68 ± 0.73 µM and 0.00129 ± 0.00109 µM, respectively (means ± SEM in 3–6 independent experiments). The rank order of potency was 2-MeSADP >> ADP.
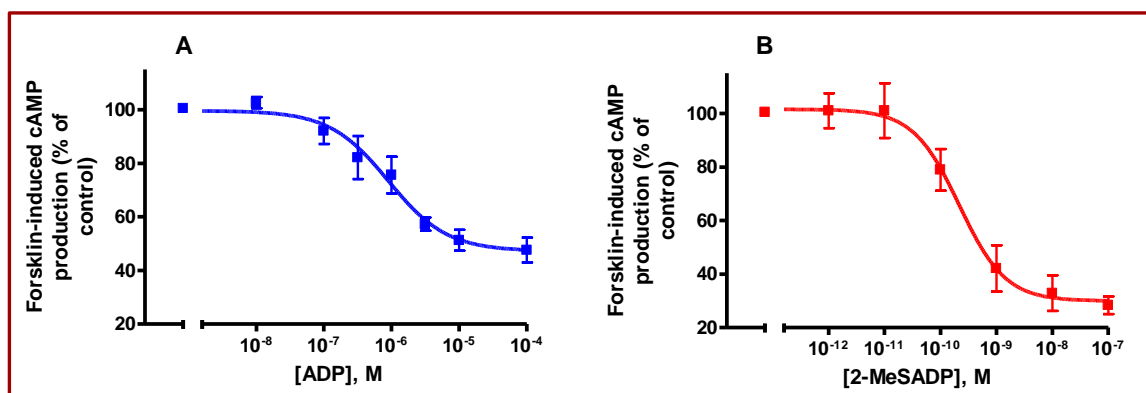
Figure 61. Inhibition of forskolin-stimulated cAMP accumulation by ADP and 2-MeSADP in 1321N1 astrocytoma cells stably expressing human $P2Y_{12}$ receptor. cAMP production was stimulated with forskolin (4 µM) in the presence of IBMX (100 µM) and caffeine (10 µM). (**A**) ADP induced a dose-dependent inhibition of forskolin-stimulated intracellular cAMP accumulation, reducing stimulated cAMP levels by up to 60 %. The IC_{50} value was 1.68 ± 0.73 µM (mean ± SEM in 3 independent experiments). (**B**) 2-MeSADP reduced the production of cAMP induced by forskolin (4 µM) up to 80%. The IC_{50} value was 0.00129 ± 0.00109 µM (*n*= 3).

3.3.2. Radioligand binding studies

3.3.2.1. Saturation experiments

As shown in figure 62, binding of [^{3}H]PSB-0413 to 1321N1 cells expressing human $P2Y_{12}$ receptors was concentration-dependent, and the nonspecific binding measured in the presence of ADP (10 mM) was low and depended on the [^{3}H]PSB-0413 concentration. The results showed two classes of binding sites one exhibiting high affinity with a K_D value of 13.1 ± 1.1 nM. The total number of binding sites (B_{max}) corresponds to $61,925 \pm 10,153$ receptors per cell. The second binding site has a low affinity with a K_D value of 0.229 ± 0.041 M and with a B_{max} value of $30,737 \pm 8,228$ receptors per cell.

The K_D value for [^{3}H]PSB-0413 obtained from saturation studies to intact astrocytoma cells was in close agreement with the K_D value calculated from kinetic experiments and saturation studies at human platelet membranes (ca. 5 nM).[214]
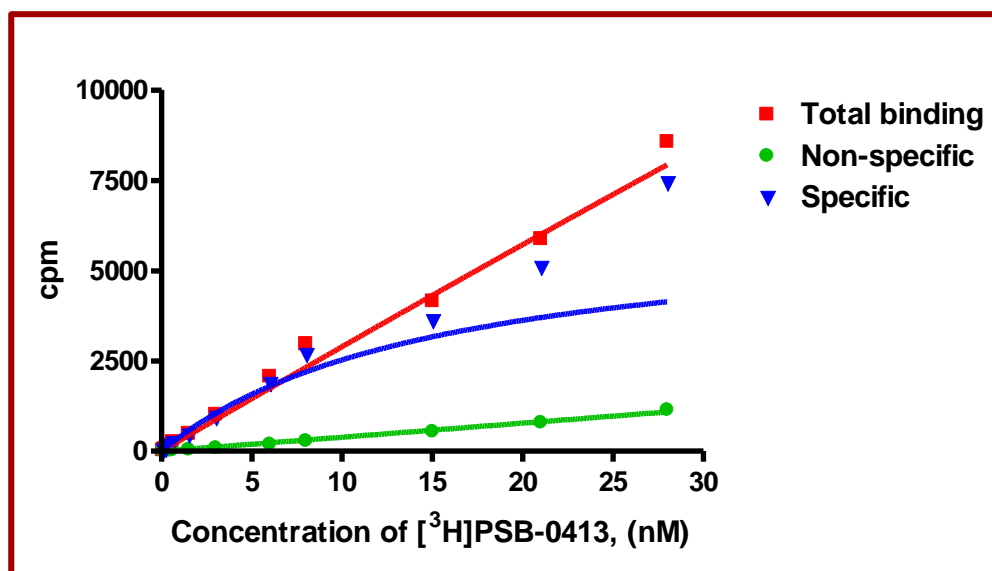
Figure 62. Saturation binding studies of [³H]PSB-0413 to intact astrocytoma cells expressing the human P2Y$_{12}$ receptors**.**

3.2.2. Competition experiments

The competition assays were carried out using [³H]PSB-0413 in a concentration of 5 nM using intact 1321N1 cells stably expressing human P2Y$_{12}$ receptors or membrane preparations of the same cell line. The non-specific binding was determined using 10 mM ADP. Serial dilutions of test compounds were used. As shown in table 24, 2-MeSADP showed high affinity for human P2Y$_{12}$ receptors expressed in 1321N1 cells with a K$_i$ value of 0.00521 ± 0.00036 µM. ADP itself showed a K$_i$ value of 2.32 ± 0.58 µM (Figure 63). Quite similar results were obtained with membrane preparations of astrocytoma 1321N1 cells expressing human P2Y$_{12}$ receptors (Figure 63 and Table 24). IC$_{50}$ values determined in radioligand binding studies for the human P2Y$_{12}$ receptor expressed in 1321N1 astrocytoma cells were similar to IC$_{50}$ values obtained in functional cAMP assays. The rank order of potency in competition assays at P2Y$_{12}$ receptors natively expressed in human platelets was 2-MeSADP (4.88 nM) >> ADPβS (4.11 µM) > ADP (17.6 µM). Similar affinities were observed at human P2Y$_{12}$ receptors expressed in astrocytoma 1321N1 cells. ADP showed an affinity of 2.32 µM in whole cell binding assays with a 23-fold lower affinity than in competition assays using membrane preparations of 1321N1-astrocytoma cells expressing the human P2Y$_{12}$ receptors (K$_i$ 0.00979 µM) (Figure 63 and Table 24).

Table 24. P2Y$_{12}$ receptors affinities, expressed as K$_i$ values, of selected P2Y$_{12}$ receptor ligands determined at membrane preparations of blood platelets natively expressing the human P2Y$_{12}$ receptors and whole 1321N1 cells expressing the human P2Y$_{12}$ receptors.

	K$_i$ (or IC$_{50}$) ± SEM [µM] vs. [^{3}H]PSB-0413 (*n*=3)		
Compound	Membrane preparation of 1321N1-astrocytoma cells expressing the human P2Y$_{12}$ receptors	Whole 1321N1 cells expressing the human P2Y$_{12}$ receptors	Membrane preparation of blood platelets natively expressing the human P2Y$_{12}$ receptors[214]
ADP	0.0979 ± 0.0049	2.32 ± 0.58	17.6 ± 0.7
ADPβS	1.120	2.33 ± 0.83	4.11 ± 1.17
2-MeSADP	0.00340 ± 0.00156	0.00521 ± 0.00036	0.00506 ± 0.00010
ATPγS	4.54 ± 0.29	n.d.	13.2 ± 0.2
AR-C67085	0.00579 ± 0.00331	n.d.	0.00241 ± 0.00025

n.d. (not determined)

The reason for this difference may be due to degradation or cellular uptake of ADP in the intact cells and accordingly the available amount for receptor activation is reduced. ADP is metabolically unstable and metabolized by ectonucleotidases (ENTPDases) which leads to a decrease in the extracellular concentrations of ADP.[11]
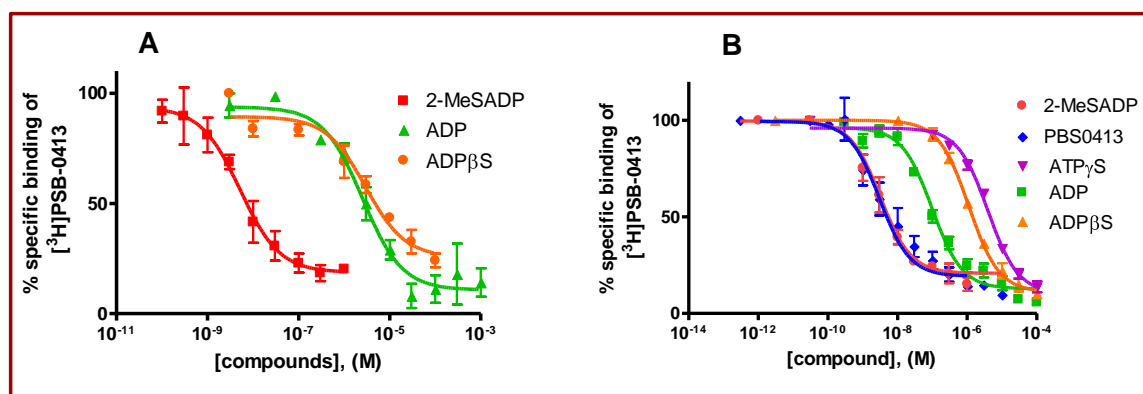
Figure 63. Competition curves for ADP and ADP derivatives vs. 5 nM [^{3}H]PSB-0413 obtained at: (**A**) intact astrocytoma 1321N1 cells recombinantly expressing the human P2Y$_{12}$ receptors. (**B**) Membranes preparation of astrocytoma 1321N1 cells recombinantly expressing the human P2Y$_{12}$ receptors.

Besides the P2Y$_{12}$ receptor, there are 2 more subtypes of P2 receptors that are stimulated by ADP, P2Y$_1$, and P2Y$_{13}$. AR-C67085 was developed as an antagonist at P2Y$_{12}$ receptors in nanomolar concentrations and it was suggested that it may also act as an antagonist at P2Y$_{13}$ receptors in micromolar concentrations.[88] Therefore, the binding affinity of the newly

synthesized structurally similar [3H]PSB-0413 as a radioligand for $P2Y_{12}$ receptors was studied at human $P2Y_{13}$ receptors expressed in 1321 N1 astrocytoma cells, human $P2Y_1$ receptors expressed in astocytoma cells and at non-transfected astrocytoma cells. The results are shown in figure 64.
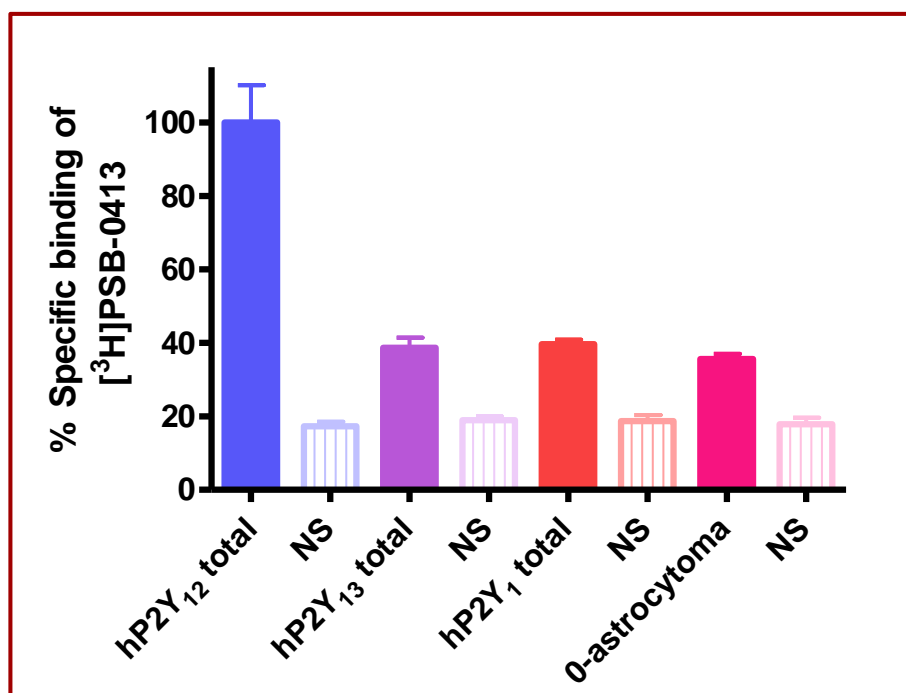
Figure 64. Specific binding of 3 nM of [3H]PSB-0413 at human $P2Y_{12}$, human $P2Y_{13}$ and human $P2Y_1$ receptors expressed in 1321N1 cells and non-transfected astrocytoma cells (*n*=3).

As shown in figure 65, astrocytma cells expressing the human $P2Y_{12}$ receptors showed the highest binding affinity for [3H]PSB-0413. Human $P2Y_{13}$ receptors, human $P2Y_1$ receptors and non-transfected astrocytoma cells showed very low specific binding of the radioligand.

In summary, the human $P2Y_{12}$ receptors were stably expressed in astrocytoma 1321N1 cells using a retroviral vector (pLXSN) and characterized in radiolgand binding and functional studies. [3H]PSB-0413 is the first selective high affinity radioligand for $P2Y_{12}$ receptors. The new radioligand will allow the setting up of a high-throughput screening assay to identify new receptor agonists and antagonists.

3.4. Characterization of 1321N1 astrocytoma cells stably expressing the human P2Y$_{13}$ receptor

Human P2Y$_{13}$ receptors were expressed in 1321N1 astrocytoma cells in order to be used in measurement of the [^{3}H]PSB-0413 radioligand subtype selectivity. To proof the expression, functional characterization of the produced cell lines were performed.

3.4.1. cAMP accumulation assay in 1321N1 astrocytoma cells stably expressing the human P2Y$_{13}$ receptor

As shown in figure 65, ADP produced an inhibition of forskolin (4 μM)-induced accumulation of cAMP in 1321N1 astrocytoma cells stably expressing the human P2Y$_{13}$ receptor. The IC$_{50}$ value of ADP was 0.00747 ± 0.00291 nM (mean $\pm$ S.E.M. of two independent experiments), whereas the published data for human P2Y$_{13}$ receptor transfected into CHO K1 cells showed for ADP an IC$_{50}$ value of 0.07 ± 0.14 nM. This means that in our case the human P2Y$_{13}$ receptor is highly expressed in 1321N1 astrocytoma cells. The inhibition of forskolin-stimulated cAMP production was 47 ± 5 % at a maximal concentration of 10 nM of ADP.

In the literature, the reversal of that inhibition at higher concentrations, as well as an enhancement of cAMP accumulation after pertussis toxin pretreatment, and a greater potency of 2-MeSADP have been reported. These effects are explained by a promiscuous coupling to G$_s$, which has been observed with several other G$_i$-coupled receptors as well.[88,89]
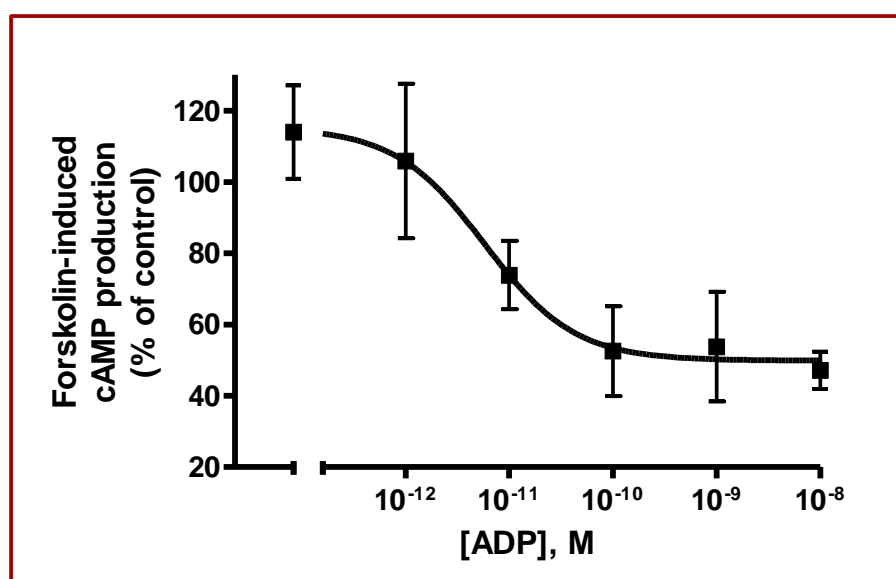
Figure 65. 1321N1 astrocytoma transfected cells were incubated with ADP for 10 min in the presence of 4 μM forskolin. The data represent the mean $\pm$ S.E.M of triplicate experimental points obtained from one experiment that was representative of two separated experiments.

Our results at the human P2Y$_{13}$ receptor recombinantly expressed in1321N1 astrocytoma cells are in agreement with the reported data. Inhibition of adenylyl cyclase mediated by the P2Y$_{13}$ receptor was confirmed in recombinant 1321N1 cells. We conclude that the human P2Y$_{13}$ receptor was successfully expressed in 1321N1 astrocytoma cells and was used to study the selectivity of [^{3}H]PSB0413.

3.5. Principle of measurement of intracellular Ca^{2+} levels

Ester derivatives of fluorescent indicators and chelators bearing carboxylic acid residues are uncharged molecules that can permeate cell membranes (Figure 66). Once inside the cell, the esters are cleaved by nonspecific esterases, resulting in a charged form that leaks out of cells far more slowly than its parent compound. Frequently, hydrolysis of the esterified groups is essential for binding of calcium ions resulting in fluorescence. A dispersing agent like Pluronic$^®$ F-127 may be used because of the relatively insolubility of esters in aqueous solutions.

After addition of agonists G$_q$-coupled receptors or ion channels can be activated leading to an increase in the intracellular calcium concentration which can be detected by the formation of a complex with such fluorescent dye.
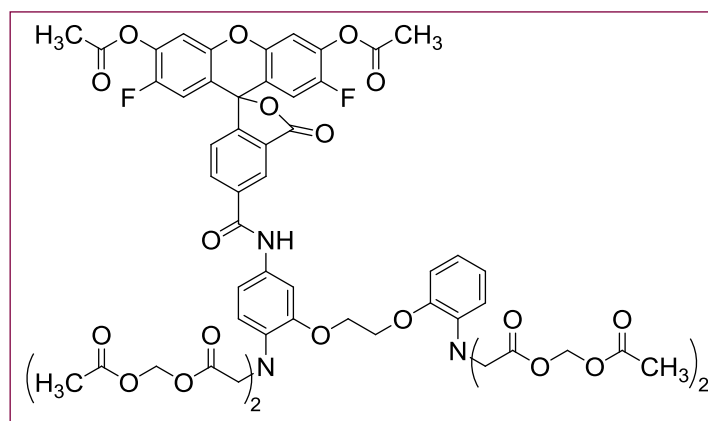
Figure 66. Structure of estreified Oregon Green (Oregon Green acetoxymethylester = Orgen Green AM).

Activation of P2X and P2Y receptors subtypes results in an increase in [Ca^{2+}]$_i$ either caused by an influx of Ca^{2+} through ligand gated ion channels (P2X$_{1-7}$) or by a release of Ca^{2+} from intracellular stores initiated by G$_q$-protein-coupled receptors (P2Y$_{1,2,4,6,11}$). Thus, the measurement of intracellular Ca^{2+} levels is used for studying the functional properties of different purinergic receptor subtypes.

3.5.1. Investigation of nicotinamide adenine dinucleotide (NAD) as a ligand of the P2Y$_1$ receptor by measurement of intracellular calcium release

Extracellular nicotinamide adenine dinucleotide (NAD, **93**) (Figure 67) is known to increase the intracellular calcium concentration $[Ca^{2+}]_i$ in different cell types and by various mechanisms. It was shown that NAD triggers a transient rise in $[Ca^{2+}]_i$ in human monocytes activated with lipopolysaccharide (LPS), which is caused by a release of Ca^{2+} from IP$_3$-responsive intracellular stores and an influx of extracellular Ca^{2+}. P2 receptors play a role in the NAD-induced calcium response in activated monocytes. Recently it has been shown that high amounts of NAD (**93**) are set free during inflammation.[215] The dinucleotide NAD (**93**) shares structural characteristics with adenosine triphosphate (ATP). Similar to ATP, it contains an adenine based purine moiety. The action of ATP is far better understood than that of NAD and it is already known to function as an extracellular messenger. Like NAD (the intracellular concentration is about 1 mM), ATP is present in high concentrations (5–10 mM) in mammalian cells.

Whereas ATP has been shown to function through the specific activation of P2 receptors, there is hardly any information about surface receptors triggering intracellular events induced by intact NAD. Only recently it was shown, that NAD is an agonist of the human P2Y$_{11}$ receptor in human granulocytes mediating an increase in $[Ca^{2+}]_i$ responsible for the functional activation of these cells.[216] Thus, NAD not only bears structural similarities with ATP but also shares its potential to modulate intracellular Ca^{2+} concentrations.

Nicotinamide adenine dinucleotide (NAD) (93)
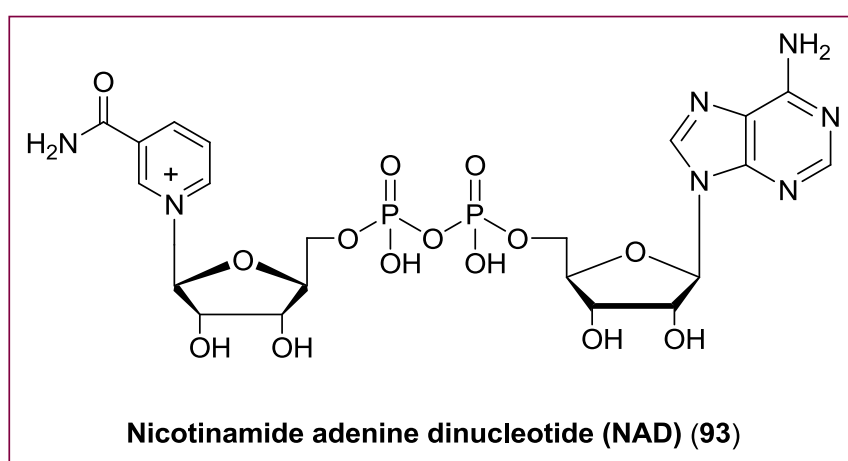
Figure 67. Chemical structure of NAD (**93**).

It was shown that NAD (**93**) acts as an agonist at the human P2Y$_{11}$ receptor, which is coupled to G$_q$- and G$_s$-proteins. By using human granulocytes and 1321N1 astrocytoma cells stably

expressing the human $P2Y_{11}$ receptor, an increase in intracellular Ca^{2+} and cAMP levels in response to extracellular NAD was found.[216]
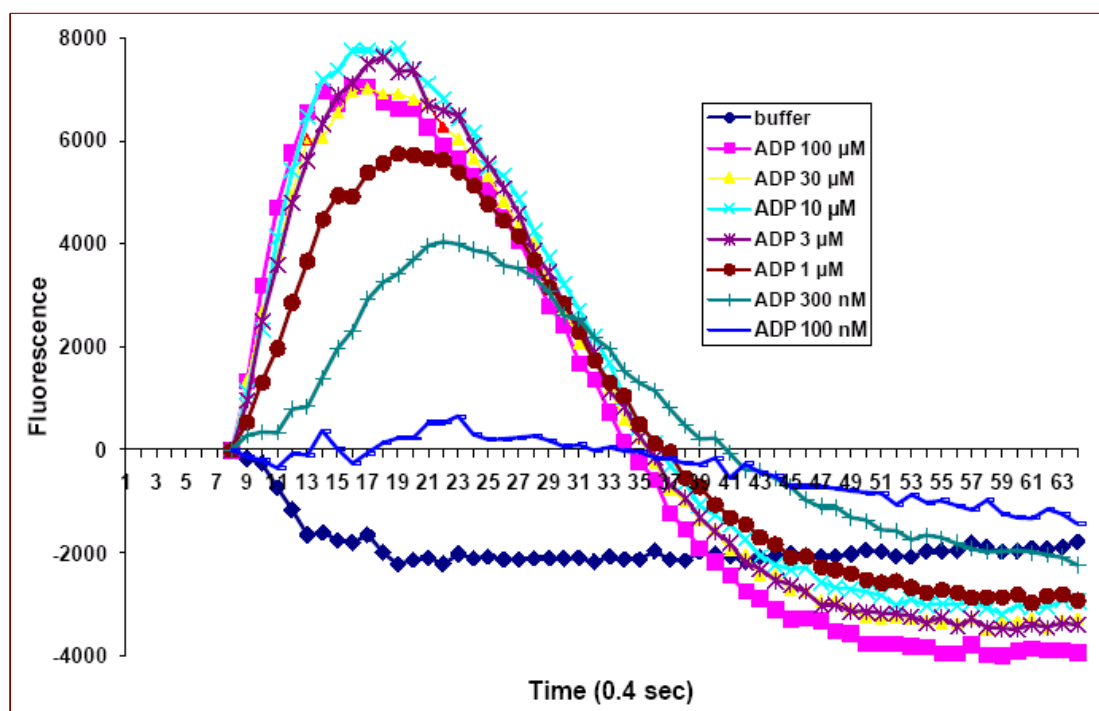
Figure 68. Fluorescence intensity: measured at 520 nm for 30 seconds at 0.4 second intervals for human $P2Y_1$ receptors stably expressed in 1321N1 astrocytoma cells and stimulated with dilutions of ADP.
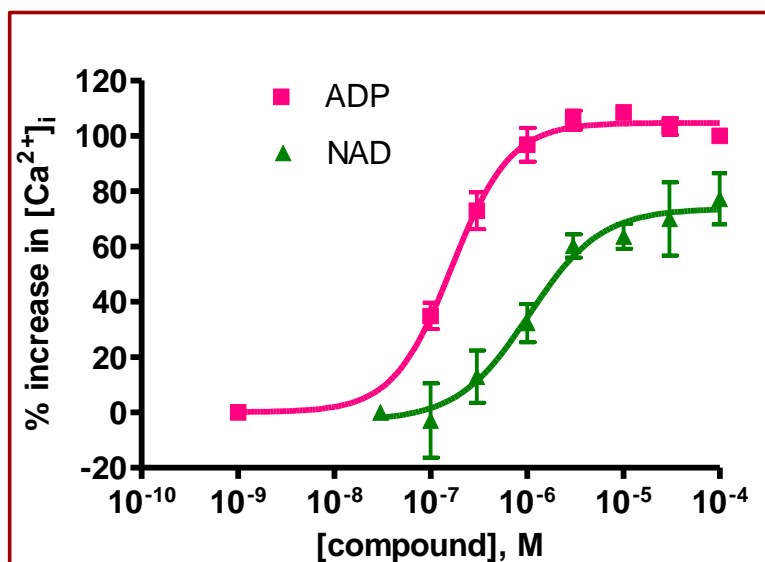
Figure 69. Concentration-dependent increase in intracellular calcium release by ADP and NAD (**93**) in 1321N1 astrocytoma cells stably transfected with the human $P2Y_1$ receptor. The EC_{50} value of ADP was 113 ± 26 nM ($n = 4$). The EC_{50} value of NAD (**93**) was 743 ± 274 nM ($n = 3$). NAD (**93**) showed an efficacy of 77 ± 10 % compared to the physiological agonist ADP (set at 100 % efficacy).

To determine whether $P2Y_1$ receptors are also activated by NAD (**93**), we measured the effect of the dinucleotide on $[Ca^{2+}]_i$ in human 1321N1 astrocytoma cell lines stably expressing either the $P2Y_1$ receptor subtype.

Non-transfected control cells did not show any calcium response after the addition of NAD (**93**) (100 µM, data not shown).[217] 1321N1 cells expressing the human $P2Y_1$ receptor showed a concentration-dependent calcium mobilization (Figure 69) with an EC_{50} value of 743 ± 274 nM (*n*=3) (Figure 69). In comparison the physiological $P2Y_1$ receptor agonist ADP was about 7-fold more potent exhibiting an EC_{50} value of 113 ± 26 nM (*n*=4). Compared to ADP, NAD (**93**) was somewhat less efficacious (77 ± 10 % of the maximal effect of ADP).

Previous studies performed on 1321N1 astrocytoma cells transfected with the $P2Y_{11}$ receptor had demonstrated that NAD activated the $P2Y_{11}$ receptor.[216] Here the effect of NAD^+ was examined at human $P2Y_1$ receptor transfected in 1321N1 astrocytoma cells. Extracellular NAD^+ showed an increase in $[Ca^{2+}]_i$ at the 1321N1 astrocytoma cells stably transfected with the $P2Y_1$ receptor, whereas the native 1321N1 cells, which lack the expression of any known P2 receptor subtype showed no response. $P2Y_1$ and $P2Y_{11}$ receptors were found to be expressed on human monocytes and they were shown to be responsible for the NAD-induced calcium signal in activated monocytes. Thus extracellular NAD had similar effects as ATP on calcium levels in lipopolysaccharide (LPS) activated human monocytes by inducing transient rises in $[Ca^{2+}]_i$ mediated in part by Ca^{2+} influx and in part by the release of Ca^{2+} from IP_3-sensitive intracellular Ca^{2+} stores.[217] These cytoplasmic calcium signals have an important role in regulating biological activities of monocytes/macrophages.[218]

3.6. Molecular biology

3.6.1. Cloning of the human P2X$_2$ and P2X$_3$ receptor DNAs into the vectors pQCXIP-pQCXIN

The P2X$_3$ receptors are rapidly desensitizing receptors[21,36, 39-43] and therefore it is difficult to functionally characterize them. The P2X$_3$ exists as a homomer or a heterodimer with P2X$_2$ receptors to form P2X$_{2/3}$. Both P2X$_3$ and P2X$_{2/3}$ channels have similar pharmacological response but differ in their desensitization kinetics, the P2X$_{2/3}$ receptor being slowly desensitizing.[39,41] The retoviral transfection is fast and efficient to produce stable cell lines. Thus, we aimed to clone the P2X$_2$ and P2X$_3$ receptor DNA into the same retrovial vector using different selection antibiotics in order to select the cells which specifically express both receptor subtypes (P2X$_2$ and P2X$_3$) after the transfection.

3.6.1.1. Polymerase chain reaction (PCR)

Human P2X$_2$ and P2X$_3$ were obtained using suitable primers from the P2X$_2$-plXSN or P2X$_3$-pLXSN, respectively. The PCR amplification was carried out with the denaturation procedure of the template, the annealing of primers, and the elongation of the primers with DNA-polymerase.

The resulting PCR products are shown in figure 70. The human P2X$_2$ product (1,443-pbs) and the human P2X$_3$ receptor (1,221-bps) were obtained, by gel extraction of the DNA.
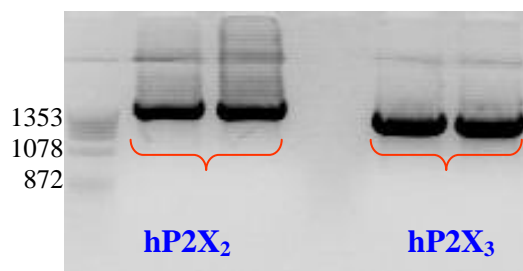
Figure 70. PCR products: hP2X$_2$ DNA pieces (1443 bps), and hP2X$_3$ receptor DNA (1221 bps).

3.6.1.2. Restriction of the PCR product

The PCR products were restricted using NotI and EcoRI restriction enzymes in order to prepare them for ligation. In addition, the vectors (pQCXIP or pQCXIN) were restricted with the same enzymes. The results of the restrictions are shown in figure 72. The restriction of the PCR products of the P2X$_2$ DNA piece with NotI and EcoRI showed 1,423 bps length while that of the restriction of the P2X$_3$ DNA piece had a length of 1,201 bps. The restriction of the

pQCXIP and the pQCXIN vectors showed lengths of 7,120 bps and 7,339 bps, respectively (Figure 71).

3.6.1.3. Extraction of DNA from an agarose gel

After the DNA samples were run on an agarose gel, the gel was placed on a UV transilluminator to make the ethidium bromide-stained DNA visible. The desired bands were identified, cut out and transferred to Eppendorf tubes. The extraction of the DNA was performed as described in the QIAquik® Gel Extraction Kit protocol.

3.6.1.4. Ligation of DNA fragments

Ligation of double-stranded DNA fragments (after restrictive digest) was performed with T4-DNA-Ligase. DNA fragments were added in a molar ratio of vector to insert 1:3.
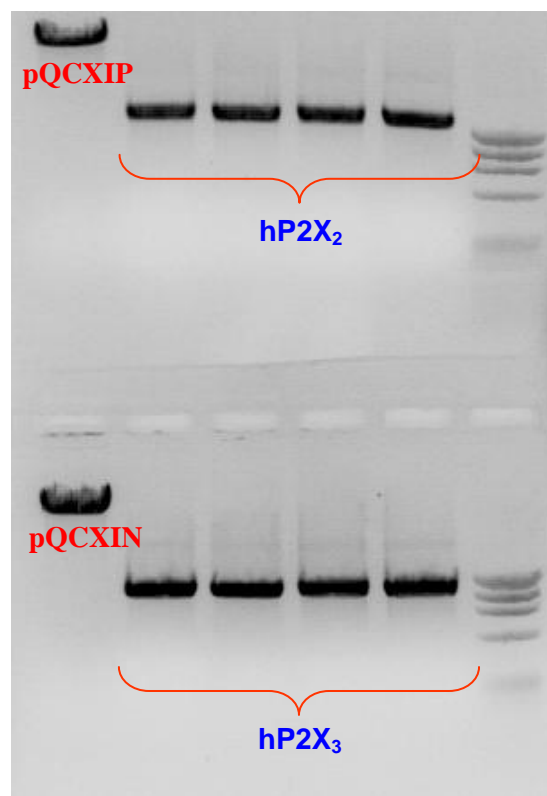
Figure 71. Restriction products of $hP2X_2$, $hP2X_3$, pQCXIP and pQCXIN

Ligation resulted in $P2X_2$ cloned into pQCXIP (8,543 pbs) and $P2X_3$ was cloned into pQCXIN (8,540 pbs) (Figure 72).
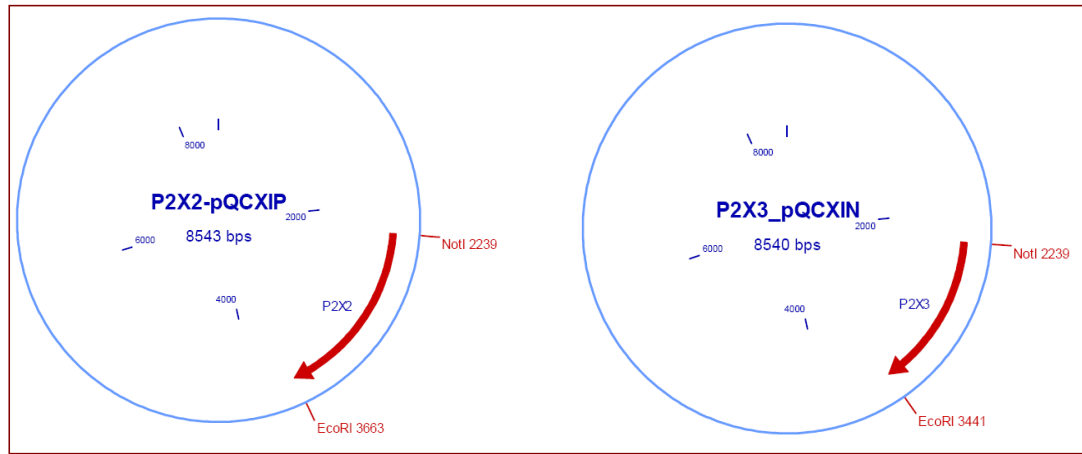
Figure 72. Cloning of the human P2X$_2$ and P2X$_3$ receptor DNAs into the vectors pQCXIP, or pQCXIN respectively.

3.6.1.5. Transforming chemically competent cells

The ligation products were transformed into the chemically competent Top 10 *(Escherichia coli)* cells. Then, single bacterial colonies from each transformation were incubated in individual sterile culture LB medium. After that, the DNAs were isolated: up to 40 µg of plasmid DNA was obtained from 4 ml of liquid culture. Resulting DNAs were analyzed by digestion with restriction enzymes to identify those carrying the desired DNA sequence. Restriction was done as described before using NotI and EcoRI as restriction enzymes (Figure 73). DNA sequencing was done by GATC Biotech.
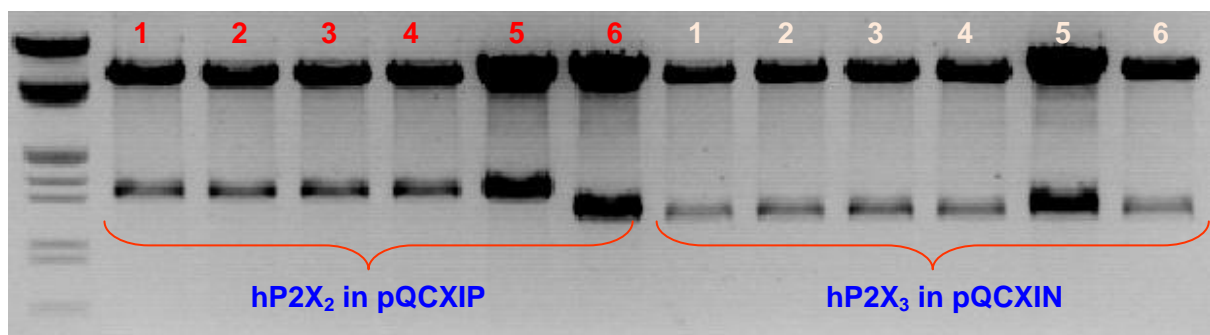
Figure 73. Restriction of Miniprep of hP2X$_2$ cloned in pQCXIP and hP2X$_3$ cloned in pQCXIN using EcoRI and NotI to select the positive colonies (containing insert for desired receptors gene).

Clone two of P2X$_2$ DNA in pQCXIP and clone three of P2X$_3$ DNA in pQCXIN showed the desired DNA sequences.

In conclusion, we successfully cloned the human P2X$_2$ and P2X$_3$ receptor DNAs into the vectors pQCXIP-pQCXIN. Subsequently these DNAs were used to produce a stable 1321N1 astrocytoma cell line expressing the human P2X$_{2/3}$ receptor.

3.6.2. Cloning of the human P2Y$_{11}$ receptor DNA into the pLXSN vector

The human P2Y$_{11}$ receptor cloned into the pLXSN vector was obtained from the group of Dr. T. Kendall Harden (Medical School, University of North Carolina, Chapel Hill). This DNA was used in retroviral transfection several times in order to produce a stable cell line expressing human P2Y$_{11}$ receptors. During the selection all the cells died without understanding the reason for it; therefore, we decided to clone the receptor again in our laboratory in order to find out the problem.

3.6.2.1. PCR cloning primers

The cloning of human P2Y$_{11}$ receptor DNA into pLXSN was performed as described before. In brief, PCR was performed using the forward, the reverse primers and the template for hP2Y$_{11}$ DNA (see the experimental part). Then, the PCR product and the pLXSN vector were prepared for ligation by restriction using **EcoRI** and **XhoI** followed by ligation using T4-DNA-Ligase. After that, the ligation product was transformed into *E. coli* and the DNA was isolated from individual clones. Sequencing was performed by GATC Biotech (Konstanz, Germany).

3.6.2.2. Results

The sequence of clone two and three showed unexpected results which include two pieces from different DNAs, one is a guanine deaminase and the other one is the P2Y$_1$ receptor as shown below:

```
>for
CCATCTCCTTTATCCAGCCCTCACTCCTTCTCTAGGCGCCGGAATTCTAAGTCGAGGAGGAGAGAATGTACCCCTA
CGACGTGCCCGACTACGCGTCCGATCGAGGTGCCAAGTCCTGCCCTGCCAACTTCTTGGCAGCTGCCGACGACAAA
CTCAGTGGGGTTCCAGGGGGACTTCCTGTGGCCCATACTGGTGGTTGAGTTCCTGGTGGCCGTGGCCAGCAATGGCC
TGGCCCTGTACCGCTTCAGCATCCGGAAGCAGCGCCCATGGCACCCCGCCGTGGTCTTCTCTGTCCAGCTGGCAGT
CAGCGACCTGCTCTGCGCCCTGACGCTGCCCCCGCTGGCCGCCTACCTCTATCCCCCCAAGCACTGGCGCTATGGG
GAGGCCGCGTGCCGCCTGGAGCGCTTCCTCTTCACCTGCAACCTGCTGGGCAGCGTCATCTTCATCACCTGCATCA
GCCTCAACCGCTACCTGGGCATCGTGCACCCCTTCTTCGCCCGAAGCCACCTGCGACCCAAGCACGCCTGGGCCGT
GAGCGCTGCCGGCTGGGTCCTGGCCGCCCTGCTGGCCATGCCCACACTCAGCTTCTCCCACCTGAAGAGGCCGCAG
CAGGGGGCGGGCAACTGCAGCGTGGCCAGGCCCGAGGCCTGCATCAAGTGTCTGGGGACAGCAGACCACGGGCTGG
CGGCCTACAGAGCGTATAGCCTGGTGCTGGCGGGGTTGGGCTGCGGCCTGCCGCTGCTGCTCACGCTGGCAGCCTA
CGGCGCCCTCGGGCGGGCCGTGCTACGCAGCCCAGGCATGACTGTGGCCGAGAAGCTGCGTGTGGCAGCGTTGGTG
GCCAGTGGTGTGGCCCTCTACGCCAGCTCCTATGTGCCCTACCACATCATGCGGGTGCTCAACGTGGATGCTCGGC
GGCGCTGGAGCACCCGCTGCCCGAGCTTTGCAGACATAGCCCAGGCCACAGCAGCCCTGGAGCTGGGGCCCTACGT
GGGCTACCAGGTGATGCGGGGCCTCATGCCCCTGGCCTTCTGTGTCCACCCTCTACTCTACATGGCCGCAGTGCCC
AGCCTGGGCTGCTGCTGCCGAAACTGCCCCGGCTACAGGGACAGCTGGAACCCAAAAGACGCCAAAAACACTGGCC
AAACCTCTGCCCCTCAATGCCAAAGCCGCCCCTAAACCGTCAAAACCCCAGTCTCGTAGACGTTGACCAATGACTT
CGAGAAACCCGGCTTGGGAAATGTTGTCTACTTAAGGGGTTGGAAAAGTCCCCAAGG
```

Leishmania donovani guanine deaminase (GDA) gene, complete cdsLength=1392

Score = 54.7 bits (29), Expect = 3e-05, Identities = 29/29 (100%), Gaps = 0/29 (0%)
Strand=Plus/Plus

```
Query  19   ATGTACCCCTACGACGTGCCCGACTACGC   47
            |||||||||||||||||||||||||||||
Sbjct  1    ATGTACCCCTACGACGTGCCCGACTACGC   29
```

Homo sapiens cDNA, FLJ94559, highly similar to Homo sapiens purinergic receptor P2Y, G-protein coupled, 1 (P2RY$_1$), mRNALength=1397

Score = 36.2 bits (18), Expect = 0.68
Identities = 18/18 (100%), Gaps = 0/18 (0%)
Strand=Plus/Plus

```
Query  1     TAAGTCGAGGAGGAGAGA   18
             ||||||||||||||||||
Sbjct  258   TAAGTCGAGGAGGAGAGA   275
```

Similar problems occurred to other colleagues due to a general DNA contamination problem in the labaratory, which has been solved by now. In order to overcome this problem a new primer was designed to attach the missing DNA sequence in the hP2Y$_{11}$ sequence and then the cloning procedure was repeated.

The first PCR was performed using the following primers:

f-hP2Y$_{11}$-ATG: 5'-atggcagccaacgtctcgggtgccaagtcctgccctg-3' (64°C)
r-hP2Y$_{11}$-XhoI: 5'- cttactactcgagtcattggctcagctcacggg (62°C)

The PCR steps were done as mentioned before using 62°C as annealing temperature.
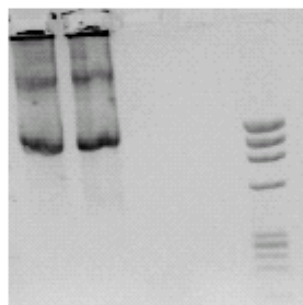
Figure 74. The first PCR product (1139 pbs): hP2Y$_{11}$ receptor.

The PCR product (1139 pbs) from the first PCR (Figure 74) was used as a template for the second PCR. The second PCR for the hP2Y$_{11}$ was carried out using the primers f-hP2Y$_{11}$-EcoRI and r-hP2Y$_{11}$-XhoI and the results (1152 pbs) are shown in figure 75.
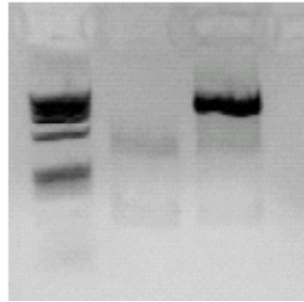
Figure 75. The second PCR product (1152 pbs): hP2Y$_{11}$ receptor.

3.6.2.3. Restriction of the second PCR product

The PCR-product of the hP2Y$_{11}$ DNA (1152 pbs) and the pLXSN vector were prepared for ligation by digestion with the restriction enzymes EcoRI and NotI. The restriction of the pLXSN vector showed a length of 5,863 bps and the hP2Y$_{11}$ DNA showed a length of 1132 bps (Figure 76).
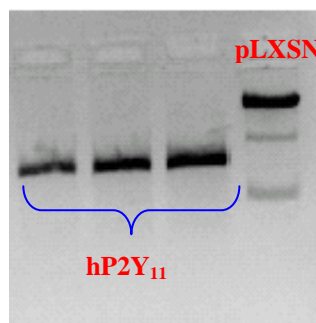
Figure 76. Restriction products of the human P2Y$_{11}$ and pLXSN
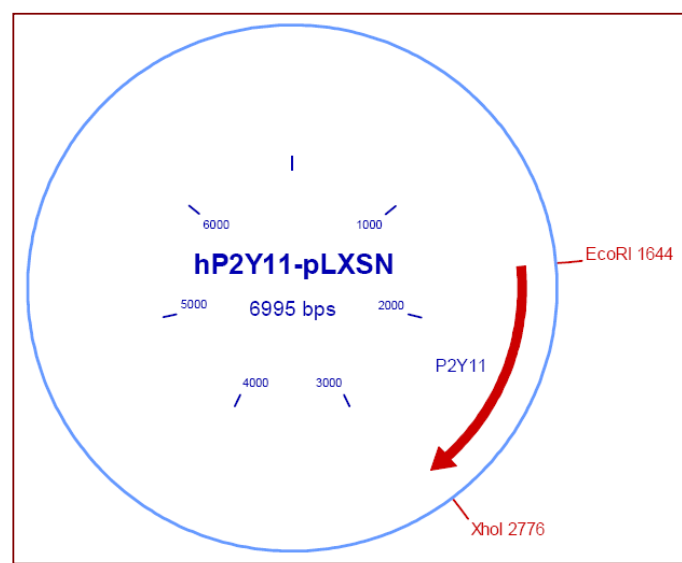
Figure 77. Cloning of the human P2Y$_{11}$ receptor into the pLXSN vector. The insert contained the sequence of the human P2Y$_{11}$ receptor and was ligated into the pLXSN vector.

The ligation product of the human $P2Y_{11}$ receptor cloned into the pLXSN vector (Figure 77), with a DNA length of 6,995 bps, was transformed into *E. coli* and the DNA was isolated from individual clones using the PureLink™ HiPure Plasmid DNA Miniprep Kit as described in the manufacturer's protocol.

Resulting DNAs were analyzed by digestion with restriction enzymes to identify those carrying the desired DNA sequence. Restriction was done as mentioned above using **EcoRI** and **XhoI** as restriction enzymes (Figure 78). DNA sequencing was done by GATC Biotech.
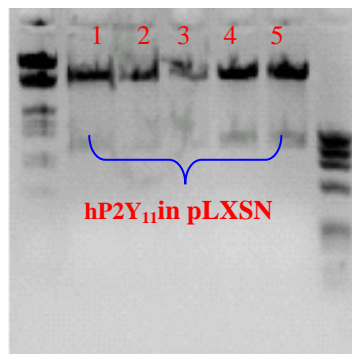
Figure 78. Restriction of Miniprep DNA of the $hP2Y_{11}$ receptor cloned into the pLXSN vector using EcoRI and XhoI to select the positive colonies (containing the insert for the desired receptor gene).

Clone five was carrying the desired DNA sequence of the $hP2Y_{11}$ which could be used to produce a stable cell line, expressing the $hP2Y_{11}$ receptor.

In conclusion, the human $P2Y_{11}$ DNA was successfully cloned into the pLXSN vector using PCR technique. After recombination in E. coli DNA was purified and the plasmids were digested using restriction enzymes. The sequence analysis showed the desired DNA sequence of the human $P2Y_{11}$ which was subsequently used to produce a stable 1321N1 astrocytoma expressing human $P2Y_{11}$ receptor.

3.7. Retroviral transfection of 1321N1-astrocytoma cells for the stable expression of hP2X$_2$ and hP2X$_{2/3}$ receptors

The human P2X$_2$ and P2X$_3$ DNAs were inserted into the retroviral vector pQCXIP and pQCXIN, respectively, as described above. The DNA was transfected into 1321N1 astrocytoma cells using a retroviral system[192] with minor modification. GP+envAM12 packaging cells were first transiently cotransfected with a retroviral vector and a viral expression vector (pVSV-G) to generate two retroviruses. The retroviral vector containing the hP2X$_2$ as insert was initially used to create a stable astrocytoma cell line, expressing P2X$_2$, which was then infected with a P2X$_3$ containing virus carrying a neomycin resistance gene for selection. In a second approach, astrocytoma cells were co-infected with the two retroviruses carrying the P2X$_2$ and P2X$_3$ DNAs, respectively, and simultaneously selected with G418 (800 µg/ml) and puromycin (6 µg/ml) to produce the desired stable cell line, expressing both receptors.

3.8. Functional characterization of selected P2X receptors

3.8.1. Functional characterization of the P2X$_2$ receptor

The human P2X$_2$ receptor cloned in pLXSN or pQCXIP vectors and stably transfected in astrocytoma cells was functionally characterized on the basis of agonist-mediated increase in $[Ca^{2+}]_i$ caused by an influx of Ca^{2+} through ligand-gated ion channels. The same was performed for double transfected astrocytoma cells expressing the human P2X$_{2/3}$ receptors. The fluorescent Ca^{2+} chelating dye Fura-2 AM was used as an indicator of the relative levels of intracellular Ca^{2+} in a 96-well format using a Novostar® fluorimeter. Agonists and antagonists were used in order to characterize the P2X receptors.

P2X$_2$ receptor activation leads to large and non-desensitizing transmembrane current and Ca^{2+} influx. The human P2X$_2$ receptor expressed in 1321N1 astrocytoma cells was maximally activated by ATP. ATP showed an EC$_{50}$ value of 3.09 ± 0.96 µM at the human P2X$_2$ receptor cloned in pLXSN vector and stably expressed into the 1321N1 cells (Figure 79A and 80). These results are similar to those obtained with human P2X$_2$ receptors cloned into pQCXIP and transfected in 1321N1 astrocytoma cells, where ATP showed an EC$_{50}$ value of 2.45 ± 0.97 µM (Figure 79B and 81). This means that both cell lines are suitable for characterization of human P2X$_2$ receptor ligands.
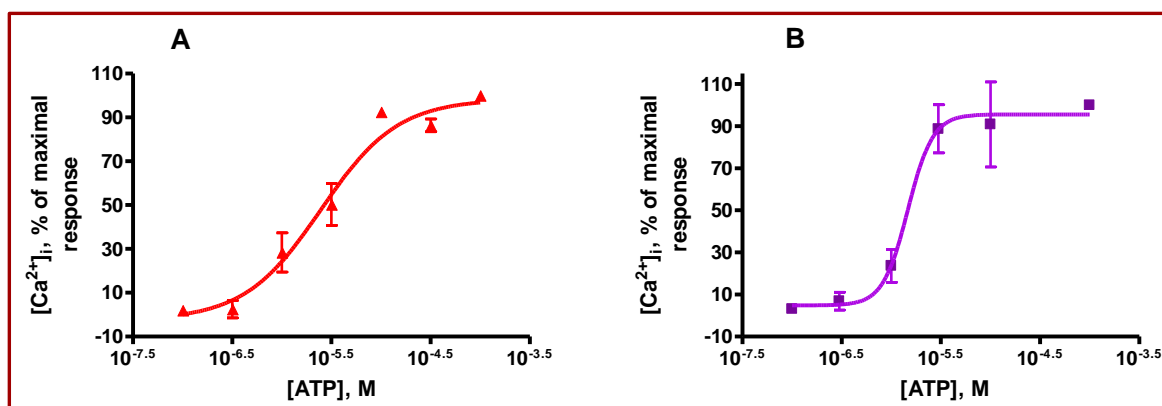
Figure 79. (**A**) Functional characterization of human P2X$_2$ receptors cloned in pQCXIP. (**B**) Functional characterization of human P2X$_2$ receptors cloned in pLXSN. Human P2X$_2$ receptor function was measured using Fura-2AM Ca^{2+} influx assay. The cell line shown was treated with increasing concentrations of ATP. EC$_{50}$s: 2.45 ± 0.97 (**A**) and 3.09 ± 0.96 µM (**B**). Data are shown as the mean percentage of the maximum signal mediated by ATP (*n=3*).
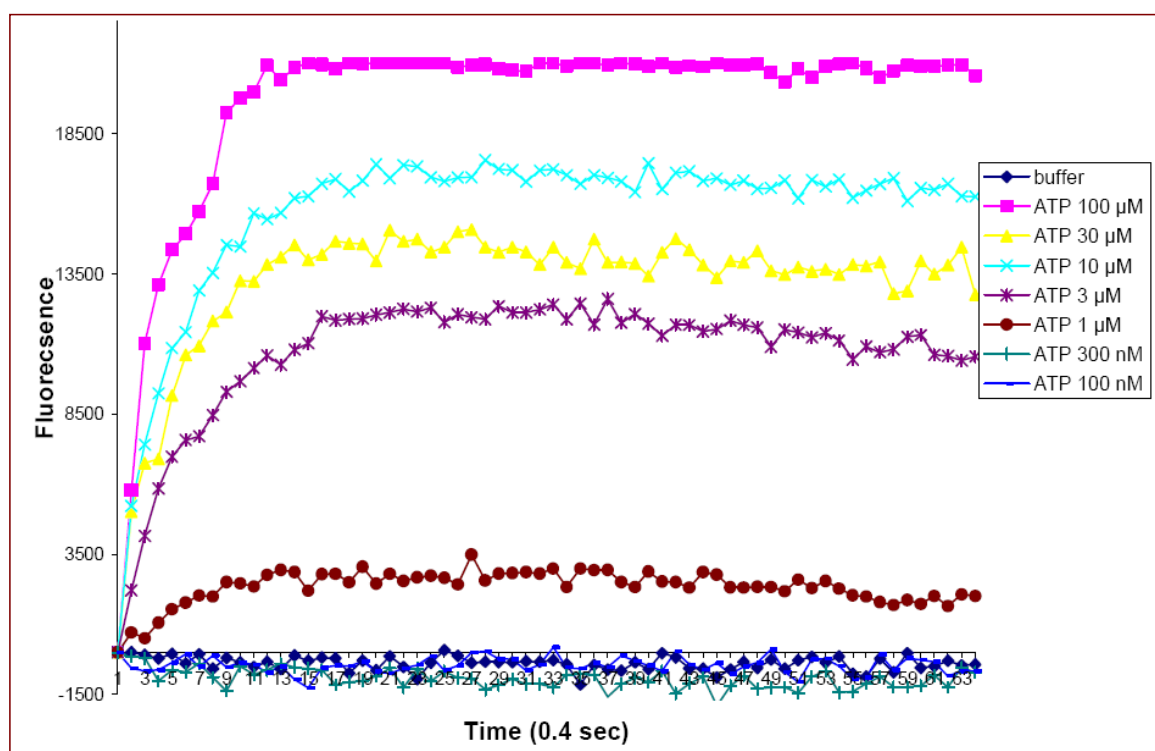
Figure 80. Concentration-dependent effects of ATP on 1321N1 astrocytoma cells expressing the hP2X$_2$ receptor cloned in pLXSN. Cells were loaded with the fluorescent, calcium sensitive dye Fura-AM. Fluorescence intensity was measured at 380 nm for 30 seconds at 0.4 second intervals.
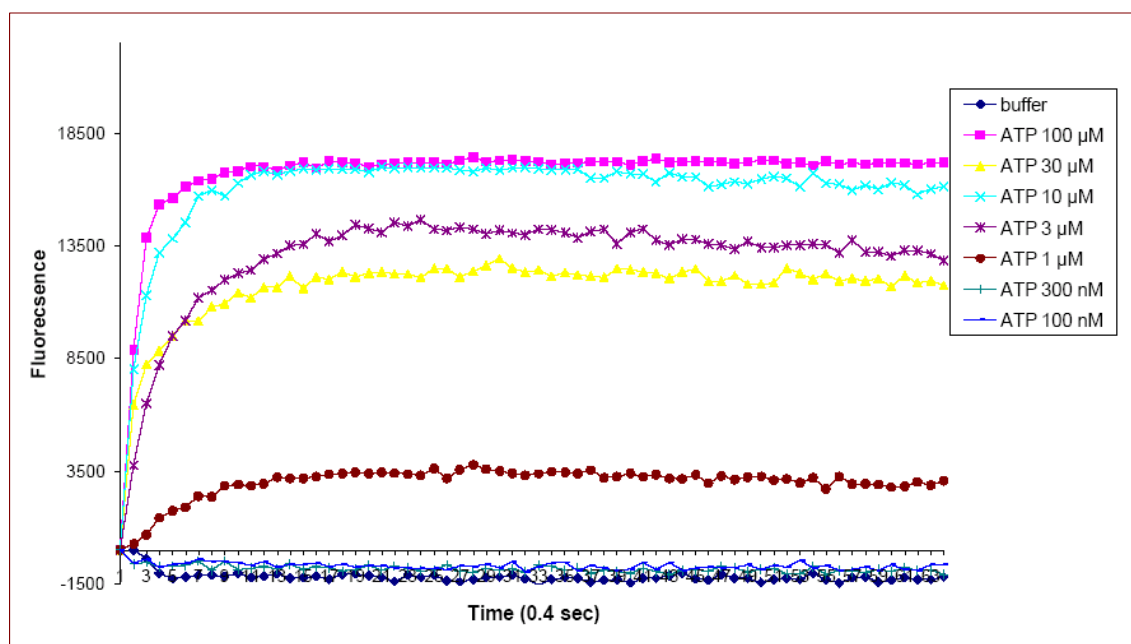
Figure 81. Concentration-dependent effects of ATP on 1321N1 astrocytoma cells expressing the $hP2X_2$ receptor cloned in pQCXIP.

3.8.1.1 Functional characterization of $P2X_2$ receptor antagonists

1321N1 astrocytoma cells, expressing the human $P2X_2$ receptor were pre-incubated with suramin or reactive blue-2 for 15-20 min before activation with agonist (4 µM ATP).
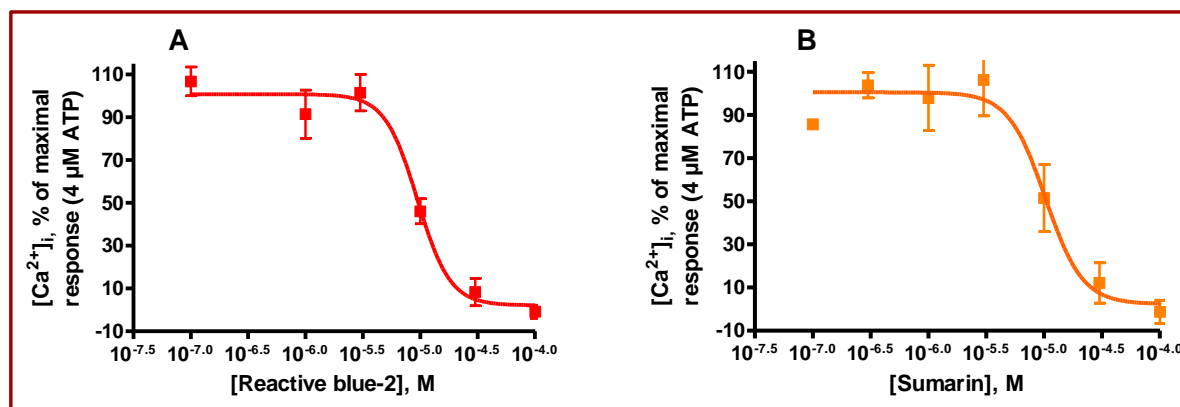
Figure 82. Functional characterization of $P2X_2$ receptor antagonists, measured by a Fura-AM Ca^{2+} influx assay. The cells were treated with increasing concentrations of antagonist and 4 µM of ATP. Data are shown as the mean percentages of the maximum signal mediated by ATP (4 µM) in the absence of antagonist (*n*=3). (**A**) Reactive blue-2 showed an IC_{50} value of 12.6 ± 1.81 µM and (**B**) sumarin an IC_{50} value of 19.4 ± 3.7 µM, respectively.

Reactive blue-2 and sumarin showed antagonistic properties with a quite similar potency at human $P2X_2$ receptors (Figure 82A and B) with IC_{50} values of 12.6 ± 1.81 µM and 19.4 ± 3.7 µM, respectively.

3.8.2. Functional characterization of human P2X$_{2/3}$ receptors

The activation of P2X$_3$ receptors produces a rapidly desensitizing transmembrane and Ca^{2+} current influx which rapidly returns to base line in the continued presence of agonist. [21,36, 39-43] Consistent with pervious reports[39,41] the heteromeric receptor consisting of P2X$_2$ and P2X$_3$ subunits (P2X$_{2/3}$) shared the pharmacological properties of P2X$_3$ with respect to activation by nucleotides. Studies using whole cell recording techniques have shown that endogenous P2X receptors expressed in sensory neurons exhibit functional properties and pharmacological profiles unlike either the P2X$_2$ or the P2X$_3$ receptor subtype.[41,219] The receptors were sensitive to activation by α,ß-methylene ATP but did not desensitize in continued presence of agonist.

The human P2X$_{2/3}$ receptor expressed in 1321N1 human astrocytoma cells using serial transfection, showed an increase in intracellular calcium with an EC$_{50}$ value of 0.566 ± 0.006 µM after stimulation with ATP (Figure 83 and 84A). α,ß-Methylene-ATP which is a selective agonist at P2X$_3$ and P2X$_{2/3}$ receptors activation versus P2X$_2$ receptor activation mediated a submaximal response when compared to ATP (Figure 84B and 85). The α,ß-methylene ATP showed an EC$_{50}$ value of 3.71 ± 1.52 µM ($n = 4$).
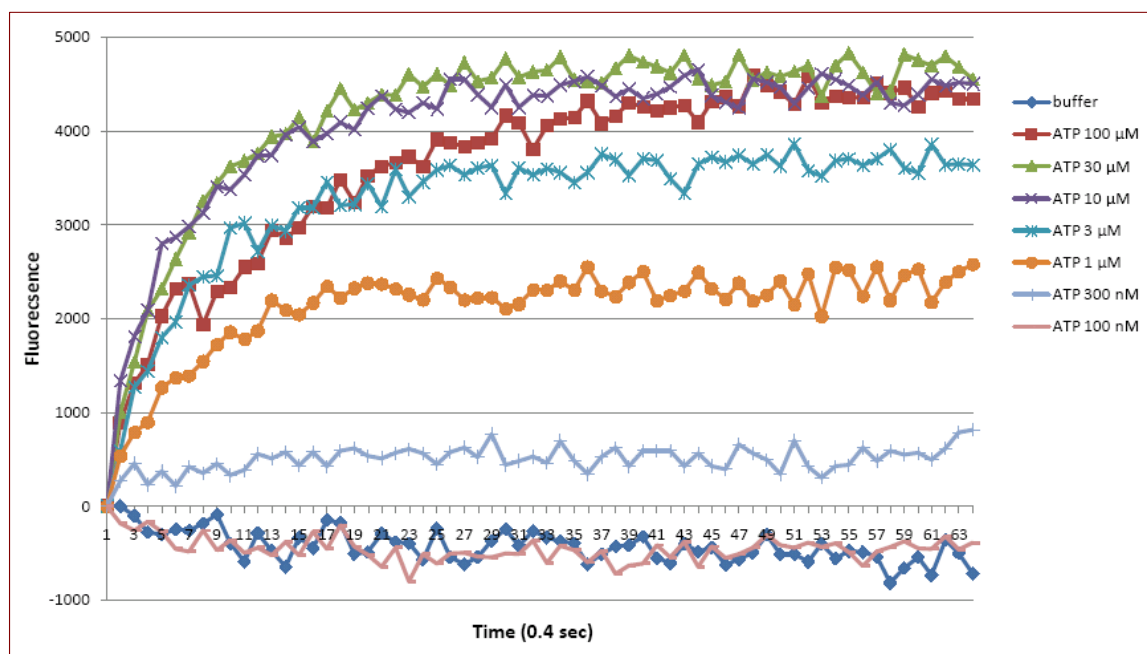
Figure 83. Concentration-dependent effects of ATP on 1321N1 astrocytoma cells expressing the human P2X$_{2/3}$ receptor (serial transfection). Cells were loaded with the fluorescent, calcium-sensitive dye Fura-AM. Fluorescence intensity was measured at 380 nm for 30 seconds at 0.4 second intervals.

The 1321N1-hP2X$_{2/3}$ cell line which expressed both the human P2X$_2$ and P2X$_3$ receptor subtypes, exhibit α,β-meATP sensitivity and slow desensitization kinetics. α,β-MeATP mediated a sub-maximal response (84%) when compared to ATP in these cells. Since α,β-meATP selectively activates human P2X$_3$ and human P2X$_{2/3}$ receptors, the greater response to ATP relative to α,β-meATP is assumed to the additional presence of homomeric ATP-sensitive human P2X$_2$ receptors in 1321hX$_{2/3}$ cells (Figure 85). These results were consistent with the reported ones for rat P2X$_{2/3}$ stably expressed in 1321N1 astrocytoma cells, where α,β-meATP showed sub-maximal effects compared with ATP (71%) with an EC$_{50}$ value of 3.39 μM.[21]
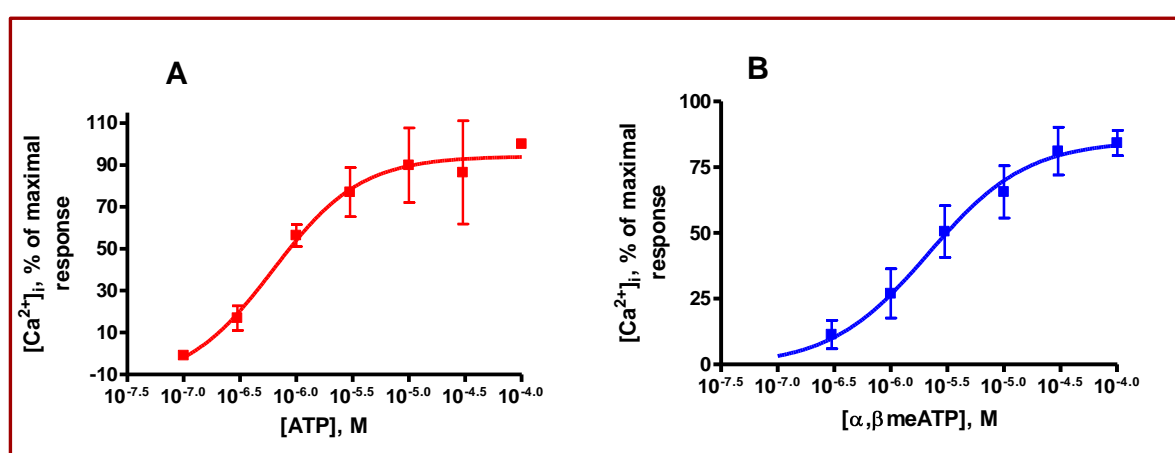
Figure 84. Functional characterization of human P2X$_{2/3}$ receptor, measured by Fura-AM Ca^{2+} influx assay. The cell line shown was treated with (**A**) increasing concentrations of ATP or (**B**) increasing concentrations of α,β-meATP. An EC$_{50}$ values of 0.566 ± 0.006 μM and 3.71 ± 1.52 μM were determined for ATP and α,β-meATP, respectively.
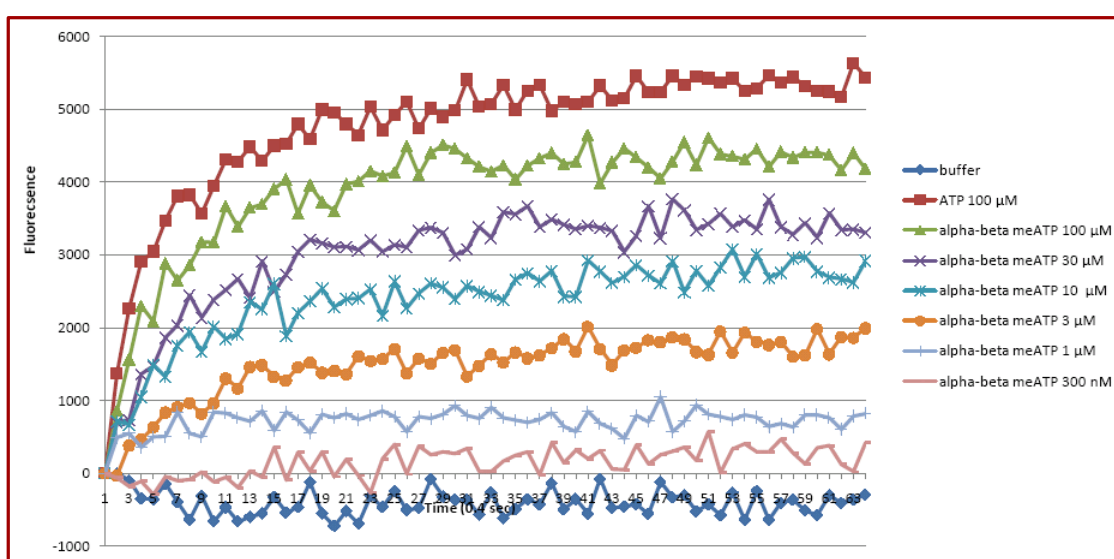
Figure 85. Concentration-dependent effects of α,ß-meATP on 1321N1 astrocytoma cells expressing the human P2X$_{2/3}$ receptor (serial transfection) compared with the maximal effect of ATP.

3.8.3. Functional characterization of the human $P2X_4$ receptor

The human $P2X_4$ receptors cloned into the pLXSN vector and stably transfected in 1321N1 astrocytoma cells using a retroviral transfection system was also functionally characterized on the basis of agonist-mediated increases in $[Ca^{2+}]_i$ caused by an influx of Ca^{2+} through the ligand-gated ion channels.
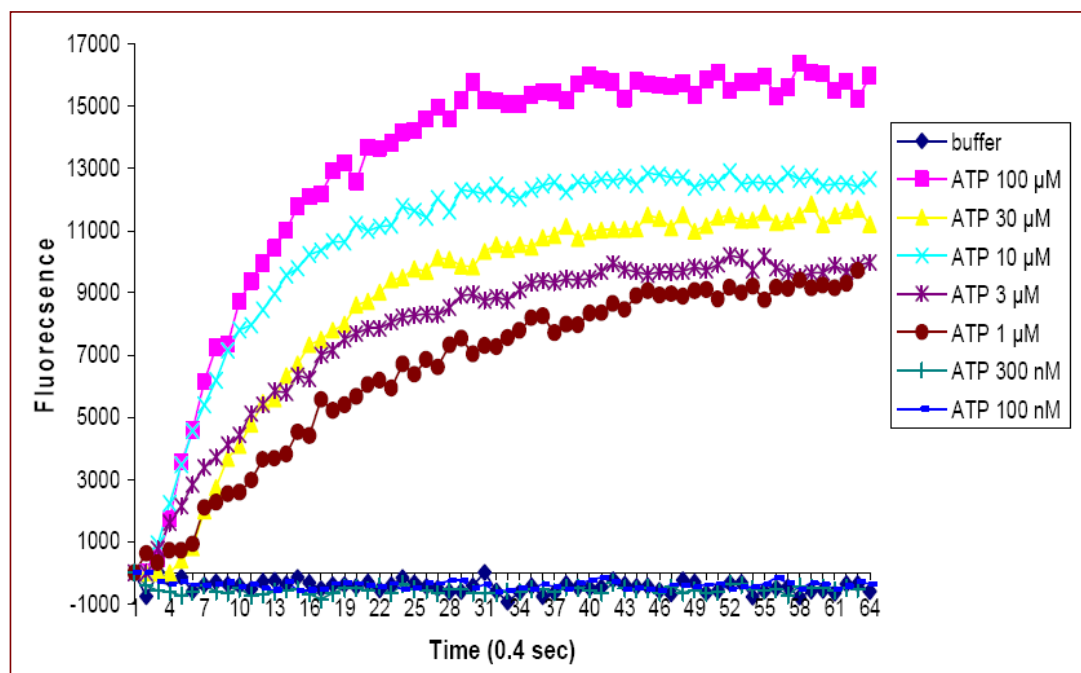
Figure 86. Concentration-dependent effects of ATP on 1321N1 astrocytoma cells expressing the human $P2X_4$ receptor. Cells were loaded with a lipophilic ester derivative of the fluorescent, calcium-sensitive dye Fura (Fura-AM). Fluorescence intensity: measured at 380 nm for 30 seconds at 0.4 second intervals.
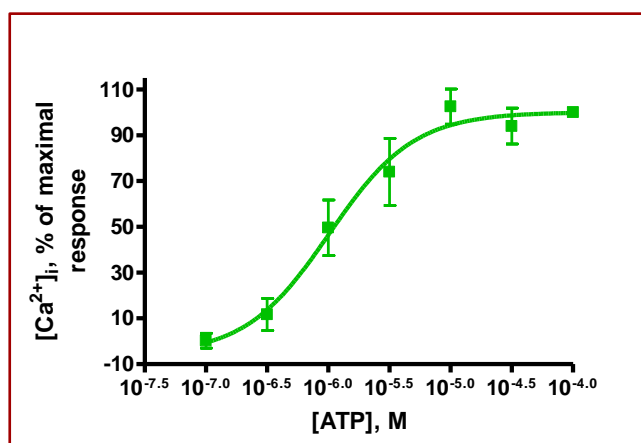
Figure 87. Functional characterization of human $P2X_4$ receptors. Concentration-response curve for the agonist ATP. Data represent the mean percentage of the signal mediated by ATP $\pm$ SEM (n=3, maximal effect of ATP = 100 %). An EC_{50} value of 1.07 ± 0.46 µM was determined for ATP.

The activation of the human $P2X_4$ receptor expressed in 1321 N1 astrocytoma cells leads to an increase in $[Ca^{2+}]_i$ by calcium influx. ATP showed an EC_{50} value of 1.07 ± 0.46 µM (Figure 86 and 87). Reactive blue 2 and sumarin were inactive as antagonists in concentrations up to 100 µM at the human $P2X_4$ receptor expressed in 1321N1 astrocytoma cells (Figure 88 and 89).
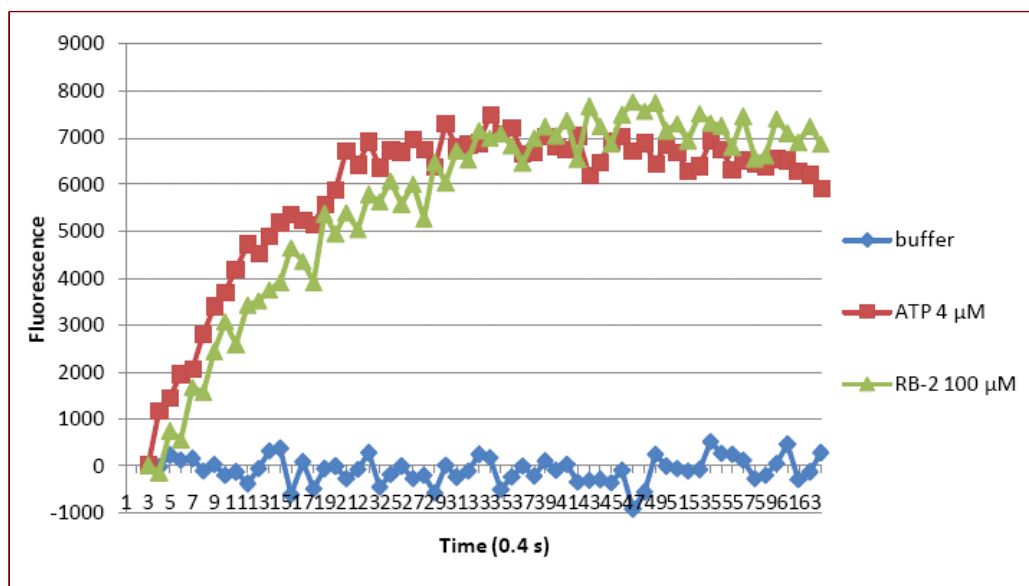
Figure 88. Increase in fluorescence caused by an increase of intracellular Ca^{2+} due to stimulation of the human $P2X_4$ receptor recombinantly expressed in 1321N1 astrocytoma, by ATP (4 µM). Reactive blue-2 in a concentration of 100 µM did not block the effect of ATP 4 µM.
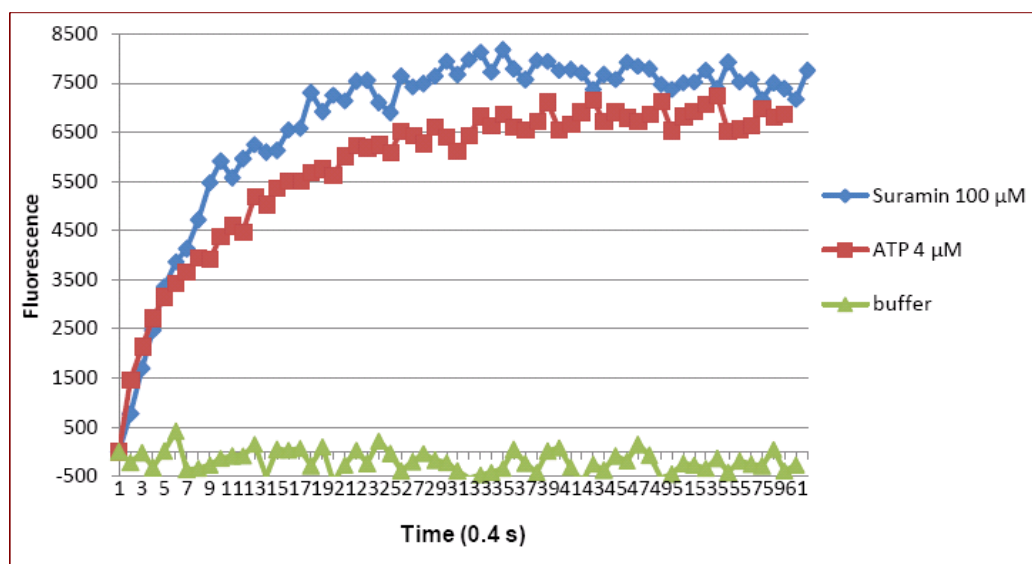
Figure 89. Increase in fluorescence caused by an increase of intracellular Ca^{2+} due to stimulation of the human $P2X_4$ receptor recombinantly expressed in 1321N1 astrocytoma. Suramin in a concentration of 100 µM did not block the effect of ATP 4 µM.

In conclusion, the human $P2X_2$, $P2X_{2/3}$ and $P2X_4$ receptors recombinantly expressed in 1321N1 astrocytoma cells were functionally characterized on the basis of agonist-mediated

increases in $[Ca^{2+}]_i$ caused by an influx of Ca^{2+} through the ligand-gated ion channels. The function was determined by measuring a Fura-AM Ca^{2+} influx assay. The produced stable cell lines may be used for screening of different chemical compounds in order to search for selective ligands, agonists and antagonists, for these receptor subtypes.

4. Summary

The thesis deals with the development of different cell-based assay techniques in order to characterize the receptors under investigation at the protein level, mapping of the distribution of the receptors of interest in different cells and tissues, studying receptor-ligand interactions and investigating signaling pathways inside the cells subsequent to activation or blocking of these receptors. Such information is important for assessing the receptors' potential as drug targets.

The following assays have been employed:

- Radioligand binding assays including saturation, competition and kinetic experiments in order to characterize the receptors at the protein level and for characterizing novel ligands.

- Functional assays have been established via measurement of cAMP accumulation, measurement of intracellular Ca^{2+} levels and quantification of ERK signalling.

The assays were performed in native cells using intact cell lines or membrane preparations from the receptors under investigation, or at receptors that we have successfully expressed in different cell lines using molecular biology techniques.

The most important results are summarized below.

4.1. Adenine receptors (P0 receptors)

We have successfully characterized the human adenine receptors in intact HEK293 cells using different assays including saturation, competition and kinetic experiments, and subsequently compared the obtained results with those obtained with membrane preparations of HEK293 cells.

➤ The saturation experiments in intact HEK293 cells showed that [^{3}H]adenine exhibited two binding sites with a K_{D1} value of 92.4 ± 4.7 nM and a B_{max1} value of 1.882 ± 0.075 pmol/mg of protein, and a second one with a K_{D2} value of 4.15 ± 0.5 M and a B_{max2} value of 0.381 ± 0.095 pmol/mg of protein. The receptor density was quite high with a B_{max} in picomolar range for the high affinity site. The obtained result was in a agreement with that obtained from a membrane preparation with the exception that in whole HEK293 cells [^{3}H]adenine labelled two binding sites, one with high affinity and a second one with low affinity.

➢ We have performed, for the first time, kinetic studies at HEK293 cell. The results showed that [^{3}H]adenine bound to intact HEK293 cells rapidly, and the steady state appeared to be reached after 15 min and sustained for at least 200 min (K_{obs}). The binding was slowly reversed with only 30% of dissociation being evident after 60 min. A kinetic K_D value could not be determined and the law of mass action did not apply to the system.

➢ For better understanding of the binding properties of adenine to adenine receptors in intact HEK293 cells, the binding site of adenine receptors in HEK293 cells was further characterized using competition assays. Adenine showed an affinity of 3.44 µM in whole cell binding assays which means a 73-fold lower affinity than in competition assays using adenine and a membrane preparation of HEK293 cells. This may be explained by a fast degradation or uptake of the physiological agonist adenine by the cells.

The coupling of adenine receptors in HEK293 cells to adenylate cyclase, either G_i or G_s, and the possible coupling to other pathways namely the ERK-pathway were examined and the obtained results were as follows:

➢ Functional studies at human adenine receptors in HEK293 cells using cAMP accumulation assays showed that two distinct subtypes of adenine receptors might exist in HEK293 cells, one was found to inhibit adenylate cyclase via G_i protein and the second one to stimulate it via G_s protein. The other suggested explanation could be that the adenine receptors in HEK293 cells might couple to inhibition as well as to activation of adenylate cyclase. To further test this assumption, the effect of PTX on adenine receptor in HEK293 was studied. Cells were pre-treated with PTX over night before the cAMP assay was performed. By inactivating the G_i- coupling of the adenine receptor we only see the stimulatory effect of adenine with an EC_{50} value of 372 nM.

Furthermore, the ERK-pathway was studied at the human adenine receptors in HEK293 cells. We succeeded to establish a luciferase reporter gene assay using SRE-LUC as a reporter gene for human adenine receptors in HEK293 cells. Adenine induced the SRE-LUC reporter gene expression in a dose-dependent manner, reflected by the elevated levels of SRE-LUC expression and phosphorylated ERK with an EC_{50} value of 21.5 ± 2.1 nM.

We have screened more than 80 compounds based on modifications of the physiological agonist adenine. Adenine derivatives bearing substituents at the 2-, N^6-, 8- or 9-position, a

series of deazapurines and some adenine-related structures were investigated in [^{3}H]adenine binding studies at adenine receptors in rat brain cortical membrane preparations (rAde1R) and membrane preparations of HEK293 (human) cells to test species differences. The obtained results and the structure activity relationships were as following:

- The 2-substituted adenine derivatives tested showed no measurable affinity for the AdeR or possessed micromolar affinity. The rank order of potency was similar at human adenine receptors in membrane preparations of HEK293 cells and at the adenine receptor expressed in rat brain cortex.

- At position 8, basic substituents e.g. 8-aminoadenine (**7**) led to higher AdeR affinities than bulky, lipophilic residues. The introduction of 8-alkyl- and 8-arylsulfanyl residues diminished the AdeR affinity. Compound **7** exhibited a K_i value of 0.0341 μM at the human binding site and thus it was more potent than adenine itself (K_i = 0.0471 μM).

- 9-Phenethyladenine (**23**) exhibited low affinity, whereas the 9-substituted adenine derivatives bearing polar substituents (**28**, **29** and **30**) showed affinity in the low micromolar range indicating that the introduction of polar functions at position 9 positively affected the AdeR affinity.

- At position N^6 small polar substituents led to higher AdeR affinities than alkyl residues indicating that N^6-acylation is more favorable in terms of increased AdeR affinity than N^6-alkylation.

- At position N^6 a basic terminal amino group further enhanced the potency. The most potent adenine receptor ligand in this series was N^6-(3-aminopropionyl)adenine (**61**) exhibiting an even higher affinity for rat adenine receptors (K_i value of 21.5 nM) than the natural ligand adenine itself (K_i value of 29.2 nM). In addition, compound **61** showed similar affinity for human adenine receptors with a K_i value of 52.6 nM compared with the endogenous ligand adenine (K_i = 44.6 nM).

Based on the results of binding studies of more than 80 adenine derivatives at membrane preparations of both rat and HEK293 cells, we concluded that HEK293 cells and rat brain cortex express binding sites for adenine with similar but not identical structure-activity relationships. Differences in binding affinities may be due to species differences and/or could be explained by the existence of different adenine receptor subtypes. The latter explanation is more likely since no highly homologous gene (> 80% sequence identity) could be identified in the human genome database.

In order to investigate whether the potent AdeR ligands identified in this study were agonists or antagonists we have established and performed functional studies for selected compounds. Thus, 1321N1 astrocytoma cells were stably transfected with the sequence for the rAde1R using a retroviral expression system. Selected adenine derivatives were tested for their effects to inhibit isoproterenol-induced cAMP accumulation. Investigated compounds showed agonistic effects at rAde1R expressed in astrocytoma cells.

For Further characterization, a luciferase luminescence reporter gene assay was also established for the most potent adenine receptor ligands identified in radioligand binding studies. Compounds **61**, **63**, **65**, **67**, **55** and **50** represent adenine receptor agonists. The agonistic properties of compound **61** were further confirmed by its concentration-dependent inhibition of isoproterenol-stimulated cAMP-dependent luciferase assay. Adenine (**1**) and **61** both inhibited the maximal cAMP produced with IC_{50} value of 3.18 ± 1.51 nM and 28.4 ± 4.3 nM, respectively. N^6-(3-methyl-amino-propionyl)adenine (**62**) exhibited no significant effect on isoproterenol-induced cAMP dependent luciferase assay. To further investigate the antagonistic properties of **62**, we monitored the inhibitory effect of the natural agonist adenine on the cAMP formation in the absence and in the presence of **62**. In the presence of **62** the dose-response curve of adenine was shifted to the right. The calculated K_b value was 0.165 µM. This result revealed compound **62** represents the first adenine receptor antagonist described so far.

We also investigated ERK phosphorylation by a gene reporter assay measuring SRE-dependent luciferase activity in astrocytoma cells stably transfected with rAde1R. This experiment revealed that rat adenine receptors are involved in the regulation of kinase pathways. In contrast to the physiological agonist adenine, compound **61** is more potent and efficacious in activation the ERK pathway than in inhibition of adenylate cyclase.

As a next step we studied the affinity of 12 of the most potent adenine derivatives at adenosine A_1 and A_{2A} receptors subtypes in order to assess the compounds` selectivity for adenine receptors. None of screened compounds showed measurable affinity for adenosine receptors at a concentration of 100 µM.

We also functionally characterized the cloned mouse adenine 2 receptor (mAde2R) using cAMP accumulation assays. Adenine inhibited isoproterenol-induced cAMP accumulation in a concentration-dependent manner with an IC_{50} of 8 nM and a maximal of inhibition about

40 %. 2-Fluoroadenine caused an inhibition of cAMP production with an IC_{50} of 15 nM and a maximal inhibition of about 60 %.

➢ Saturation experiments at membrane preparations of Sf21 cells expressing the mAde2R with [^{3}H]adenine revealed a single-high affinity binding site with a K_D value of 113 ± 17 nM, and a B_{max} value of 1.98 ± 0.39 pmol/mg protein. Competition binding experiment using membrane preparations of infected Sf21 cells and selected adenine derivatives showed the following rank order of potency: adenine (**1**) > N^6-(4-aminobutyryl)adenine (**67**) > 2-fluoroadenine (**83**) > N^6-(3-aminopropionyl)adenine (**61**) > 7-methyladenine (**85**) > N^6-acetyladenine (**49**) > 1-methyladenine (**83**) >> N^6-benzyladenine (**34**) > N^6-dimethyladenine (**38**).

➢ Chinese hamster ovary cells (CHO K1) cells showed inhibition of forskolin stimulated adenylate cyclase activity in a concentration dependent manner with an IC_{50} value for adenine of 4.04 ± 2.7 nM. Saturation binding studies performed with membrane preparations of the CHO-K1 cells exhibited a single binding site with a K_D value of 121 nM and a B_{max} value of 1.536 pmol/mg of protein. Thus, the hamster also appears to express at least one adenine receptor coupled to inhibition of adenylate cyclase and high expression level was found in CHO K1 cells.

➢ Homologous competition experiments were performed for characterization of the endogenous rat adenine receptors in PC12 cells. Adenine showed relatively low affinity at native adenine receptors in membrane preparations of PC12 cells with an IC_{50} value of 489 ± 206 nM. The apparent K_D value calculated from homologous competition experiments was 479 ±106 nM and a high receptor density with a B_{max} value of 21.3 ± 5.6 pmol/mg was detected in membrane preparations of PC12 cells.

➢ The functional properties of the rAdeR in PC12 cells were investigated by measuring the activity of adenylate cyclase in a cAMP-dependent luciferase assay. Adenine inhibited forskolin-stimulated cAMP levels with an IC_{50} value of 12.8 ± 2.1 µM. The explanation for this high IC_{50} value could be that PC12 cells express an adenine receptor subtype which is different from the rAde1R. It might also be possible that the adenine receptor in PC12 cells forms heteromers with other receptors or interacts with other proteins which modulate receptor activation.

➢ In order to investigate whether PC12 cells express mRNA for the rAde1R, mRNA was extracted from PC12 cells. From the functional studies and preliminary mRNA localization studies for endogenous rat adenine receptors in PC12 cells. We can conclude that PC12 cells very likely express the rAde1R. Further studies must be performed in

order to determine the exact sequence of endogenous rat adenine receptors in PC12 cells and to compare it with the rAde1R sequence.

4.2. Adenosine receptors (P1 receptors)

Beside the new adenine receptors, the well-established families of adenosine receptors has been studied.

➤ Characterization of CHO cells stably expressing the human A_{2B} receptor was performed using the non-selective agonist NECA (**86**) and the selective agonist BAY-60–6583 (**90**) in cAMP accumulation assay. The compounds were found to exhibit agonistic properties with EC_{50} values of 0.035 ± 0.014 μM and 0.016 ± 0.004 μM, respectively.

➤ cAMP accumulation assays at CHO cells stably expressing the human adenosine A_{2A} receptor were performed and the agonistic properties of a newly synthesized selective adenosine A_{2A} receptor agonist PBS-0777 in comparison with the non-selective adenosine receptor agonist NECA was evaluated. They showed EC_{50} values of 17.6 ± 14 nM and 117 ± 10 nM, respectively. PSB-0777 acts as a full agonist at human adenosine A_{2A} receptors expressed in CHO K1 cells.

➤ cAMP accumulation assays at CHO cells stably expressing the human adenosine A_{2A} receptor were used for investigation of the new adenosine A_{2A} receptor antagonist AA-01. AA-01 appears to be a competitive antagonist at human adenosine A_{2A} receptors with K_B value of 4.14 nM.

➤ Luciferase cAMP assays were performed for Mongolia extract using CHO K1 cells stably transfected with human adenosine A_1 receptors and transiently transfected with pCRE-luc. The Magnolia extract **M** completely inhibited forskolin-stimulated cAMP accumulation in CHO cells expressing the adenosine A_1 receptor. The extract seemed to disturb the assay system by an unknown mechanism.

➤ The functional properties of the magnolia extract **M** were investigated in GTP-shift experiments using a rat cortical membrane preparation containing adenosine A_1 receptors. The GTP-shift and cAMP experiments with the Magnolia extract **M** indicate that it may be either a week partial agonist or an antagonist.

4.3. P2 receptors

Several studies were performed to investigate P2 receptors.

Characterization of the high-affinity, subtype-selective $P2Y_{12}$ antagonist radioligand [^{3}H]PBS-0413 was performed:

- ➢ We expressed the human $P2Y_{12}$ receptor in 1321N1 astrocytoma using a retroviral expression system. The produced cells were functionally characterized in cAMP accumulation assay using ADP and 2-MeSADP as agonists.

- ➢ The saturation radioligand binding studies showed two classes of binding sites one exhibiting high affinity with a K_D value of 13.1 ± 1.1 nM and a total number of binding sites (B_{max}) of $61,925 \pm 10,153$ receptors per cell. The second binding site had a low affinity with a K_D value of 0.229 ± 0.041 M and a B_{max} value of $30,737 \pm 8,228$ receptors per cell.

- ➢ The IC_{50} values obtained from competition assays at the human $P2Y_{12}$ receptor expressed in 1321N1 astrocytoma cells were similar to IC_{50} values obtained in functional cAMP assays and comparable with the rank order of potency in competition assays at $P2Y_{12}$ receptors natively expressed in human platelets.

- ➢ The selectivity of [^{3}H]PSB-0413 as a radioligand for $P2Y_{12}$ receptors was determined *vs* human $P2Y_{13}$ receptors, human $P2Y_1$ receptors and at non-transfected astrocytoma cells. The results showed that the astrocytoma cells expressing the human $P2Y_{12}$ receptors showed the highest binding affinity for [^{3}H]PSB-0413. Human $P2Y_{13}$ receptors, human $P2Y_1$ receptors and non-transfected cells showed very low specific binding.

The effect of NAD^+ on $[Ca^{2+}]_i$ in human 1321N1 astrocytoma cell lines stably expressing $P2Y_1$ receptors was measured and the results showed a concentration-dependent calcium mobilization with an EC_{50} value of 743 ± 274 nM. Compared to ADP, NAD was somewhat less efficacious (77 ± 10 % of the maximal effect of ADP).

The human $P2X_2$ receptor cloned in the pLXSN or the pQCXIP vector and expressed in 1321N1 astrocytoma cells. It was activated by ATP and found to exhibit similar EC_{50} values, 3.09 ± 0.96 µM and 2.45 ± 0.97 µM, respectively indicating that both cell lines can be used for characterization of human $P2X_2$ receptors.

The human $P2X_{2/3}$ receptor expressed in 1321N1 human astrocytoma cells using serial transfection, showed an increase in intracellular calcium with an EC_{50} value of 0.566 ± 0.006 µM after stimulation with ATP. α,ß-Methylene ATP showed an EC_{50} value of 3.71 ± 1.52 µM.

Human $P2X_4$ receptors cloned into the pLXSN vector and stably transfected in 1321N1 astrocytoma cells using a retroviral transfection system was also functionally characterized and ATP showed EC_{50} value of 1.07 ± 0.46 µM.

We have been successful in recombinantly expressing the human $P2X_2$, $P2X_{2/3}$ and $P2X_4$ receptors in 1321N1 astrocytoma cells and we functionally characterized the transfected receptors on the basis of agonist-mediated increase in $[Ca^{2+}]_i$ caused by an influx of Ca^{2+} through the ligand-gated ion channels. The produced stable cell lines will be used for screening of different agonist or antagonists.

5. Experimental section

5.1. Instruments

Analytical balance	Sartorius CP225D
Autoclave	Varioklav® Dampfsterilisator, H+P
Bacteria shaker	Innova 4200 Incubator Shaker, New Brunswick Scientific
Centrifuge	Allegra™ 21 R, Beckman Coulter
	Avanti™ J-201, Beckman
	BIOFUGE pico, Heraeus
	Rotofix 32, Hettich
Filter	Whatman GF 51, Schleicher & Schuell Microscince, Germany
	Whatman GF/B Glass fibre cuts, 10428183, Germany.
	Machery & Aager GF-2, 071102, Germany
Hamilton syringe	Syringes 705 (10 μl, 50 μl), Roth
Harvester	Brandell M24, 48, Gaithersburg, MD, U.S.A.
Heater	Thermomixer comfort, Eppendorf
	Heidolph MR 3001
Homogenizer	RW 16 basic, IKA Labortechnik, Germany
Incubators	Jouan IG 650, Heraeus HERAcell® 240
Laminar airflow workbenches	NUNC® Safe flow 1.2
	NUNC® BIOFLOW
LSC-counter	Tricarb® 2900 TR, Canberra Packard/Perkin Elmer
Magnetic stirrer and hot plate	RCT Basic, IKA Labortechnik
Microscope	Axiovert 25, Zeiss
	Hund Wetzlar (Seiler)
Microplates	655095, white 96-well plate, clear bottom, Greiner Bio-One
	655096, black 96-well plate, clear bottom, Greiner Bio-One
	EW-01929-60 white 96-well plate, Nunc™ Nunclon™

	21313241, imaging plate 96 FC, Zell Kontakt
Multipette	Eppendorf Multipette Plus
Microwave	Microwave 800, Severin
Pipettes	Eppendorf research (0,5-10 µl, 10-100 µl, 20-200 µl, 100-1000 µl, 1000-5000 µl)
pH Meter	WTW pH Electrode SenTix 41
	WTW pH 197
Photometer	Beckman DU ®, 530 Life Science
Plates	6, 24 Loch Sarstedt
Photo documentation system	Geldoc, BioRad
Safe-lock tubes	Eppendorf
Water bath	GFL® 1083
	Memmert WNB 14
Shaker	Mini rocker MR-1
Software	Chromas 1.45, Conor McCarthy
	ChemDraw Ultra 9.0
	ClustalW2, European Bioinformatics Institute
	DNAtrans 2.0, Dr. A. Schiedel / J. Bosmann
	Isis™/Draw 2.5, MDL Information Systems
	Prism® 4.0, GraphPad
Sterile filters	Filtropur 0.22 µm, Sarstedt, 831826001
Voltage equipment (electrophoresis)	Power Pac® 3000, BioRad
Thermocycler	Biometra® TPersonal
Thermomixer	HeizThermoMixer MHR 23
	Eppendorf thermomixer confert
Ultrasonic bath	Bandelin SONOREX RK 52H
Vortexer	IKA Labortechnik MS1, Minishaker $2x^3$, UniEquip
Ultraturrax	T25 basic, IKA Labortechnik, Germany.

5.2. Materials

5.2.1. Chemical substances

ADP	Applichem, 16178-48-6
ADPβS	Sigma, A8016
Adenine	Sigma, A8626
ATP	Roth, 987-65-5
Agarose	Roth, 2267.2
Ampicillin sodium salt	AppliChem, A0839
BSA / albumin fraction V	AppliChem, A1391
Bromphenol blue	AppliChem, 3640
Calcium chloride dihydrate	Fluka, 21097
[^{3}H] cAMP Biotrak assay system	Amersham Bioscience, TRK 432
Caffeine	University of Bonn
CADO	Fluka, 22997
Copper sulphate pentahydrate	AppliChem, A1034
CPA	RBI, A-17
Di-sodium carbonate	AppliChem, A 1881
Di-sodium hydrogen phosphate	AppliChem, A 1646
DMSO	AppliChem, A3608
DMSO for cell culture	AppliChem, A3672
DPCPX	Sigma, C-101
EDTA	Roth, 8040.3
Ethanol p.a.	ZVE Universität Bonn, 123974
Ethidium bromide, 1%	AppliChem, A1152
Folin's reagent	Sigma, F-9252
Forskolin	Applichem, 66575-29-9
Fura-2 AM	Molecular probes, F1221
Glacial acetic acid	Merck, 1.00063.1011
GTP dilithium salt	Applichem, 95648-84-3
D-(+)-Glucose	Sigma, G-7021
Glycerine	AppliChem, A1123,1000
HEPES	Sigma, H-3375
Hydrochloric acid, 37 %	AppliChem, A 0659

IBMX	Fluka, 58620
Isoprenaline hydrochloride	Fluka, 59650
Isopropanol	ZVE Universität Bonn, 123903
Luciferase assay kit	Bright-Glo^{TM} luciferase assay buffer, luciferase assay substrat, Promega, 608-274-4330
LB-Agar	Invitrogen, 22700-041
LB-powder medium	AppliChem, A0954,901
Lipofectamine	Invitrogen, 11668019
Magnesium chloride	Sigma, M-8266
Magnesium sulphate	Sigma, M-2643
2-Mercaptoethanol	AppliChem, A4338
2-MeS-ADP trisodium salt	Tocris, 1624
α,β-Methylen-ATP	Sigma, M6517
Monopotassium phosphate	Sigma, P-9791
Mycophenolic acid	Tocris, 1505
NAD	Applichem, 53-84-9
NECA	Sigma, E-2387
Oregon Green$^®$ 488 BAPTA-1, AM	Molecular probes, O6807
Paraformaldehyde	AppliChem, 3813,025
Pluronic F-127	Sigma, P2443
PMSF	AppliChem, A0999
Polybrene	Aldrich, 10,768-9
Poly(ethyleneimine) in 50% (W/V) water	Sigma Aldrich, P 3143-1L
Potassium chloride	Fluka, 60128
Reactive blue 2	Alexis biochemicals, 550-293-G005
Ro20-1724	Hoffmann La Roche
Scintillation cocktail	Ready safe scintillation cocktail, Beckmann,141349 Luma safe scintillation cocktail, Perkin Elmer, 3087
Sodium acetate	AppliChem, 4555,025
Sodium butyrate	Fluka, 19364

Sodium chloride   Sigma, P-9541

Sodium hydrogen carbonate   Sigma, S-5761

Sodium hydroxide   Fluka, 71689

Suramin   Sigma, S2671

Di-sodium tetrate dihydrate   AppliChem, A 2662

TRIS   Roth, AE15.3

Triton X-100   Sigma, X-100

Xanthine   AppliChem, 6665,001

Yeast extract   AppliChem, A3732,01

5.2.2. Compounds for cell culture

Dulbecco's Modified Eagle Medium (DMEM)   Gibco, 41966-029

Dulbecco's Modified Eagle Medium: Gibco, 31330

Nutrient Mixture F-12 (DMEM-F12)

Cell culture flasks, sterile   Sarstedt

Counting chamber Neubauer improved   Marienfeld

Cryovials, sterile   Sarstedt, 72380

Falcon tubes   Sarstedt, 62547254

Fetal calf serum (FCS)   Sigma, F-0804

G418   Calbiochem, 345810

L-Glutamine   Cambrex Bioscience

Horse serum (HS)   Sigma, H1138

Pipette for single use only   Sarstedt, 62547254

Pen-Strep   Gibco, 15140

Phenol red 0.5%, liquid, sterile-filtered   Sigma-Aldrich, P0290

RPMI 1640   Gibco, 31870-025

Trypsin   Lonza, 17-160

5.3. Cell lines

- 1321N1 human astrocytoma cells from human brain.

- CHO cells from Chinese hamster ovary.

- NG108-15 cells are hybrid cells of mouse neuroblastoma and rat glioma.

- PC12 cells are obtained from a rat adrenal pheochromocytoma.

- HEK-293 human embryonic kidney cells.

- Melanoma 1539 cells were provided by A. Horstmeyer (Pharmaceutical Institute, University of Bonn).

- GP+envAM12 cells obtained from mouse embryo fibroblasts.

- Human adenosine A_{2A} expressed in CHO cells obtained from AK Prof. Dr. Karl-Norbert Klotz, Pharmazeutisches Institut, Würzburg.

- Adenosine A_{2B} receptors expressed in FlpIn-CHO-cells obtained AK Prof. Dr. Christa E. Müller.

- mAde2R expressed in 1321N1 human astrocytoma cells obtained from AK Prof. Dr. Ivar von Kügelgen.

Cell culture media

Media for Different CHO cell lines.

	CHO-K1	FlpIn-CHO	Transfected CHO cells*
DMEM/ F12	+	+	+
10% FCS	+	+	+
100 U/ml penicillin G	+	+	+
100 µg/ml streptomycin	+	+	+
1 % GlutaMAX	+	+	+
200 µg/ml G 418	–	–	+
100 µg/ml zeocin	–	+	–

Receptors expressed in CHO cells cloned in vectors which contain neomycin as a resistance gene.

Media for different 1321N1 human astrocytoma cell lines

	1321N1 astrocytoma	Transfected 1321N1 astrocytoma*	Double transfected 1321N1 astrocytoma[#]
DMEM	+	+	+
10% FCS	+	+	+
100 U/ml penicillin G	+	+	+
100 µg/ml streptomycin	+	+	+
1 % GlutaMAX	+	+	+
800-400 µg/ml G 418	_	+	+
8 µg/ml prumycin	_	_	+

Receptors expressed in 1321N1 human astrocytoma cells cloned in vectors which contain neomycin as a resistance gene [#]Receptor expressed in 1321N1 human astrocytoma cells cloned in vectors which contains neomycin and second receptor cloned in vector which contain puromycin as a resistance gene.

Media for various cells

	PC12	HEK293	Melanoma	NG108-15
RPMI 1640	+	_	_	_
DMEM	_	+	+	+
10% FCS	+	+	+	+
100 U/ml penicillin G	+	+	+	+
100 µg/ml streptomycin	+	+	+	+
1 % GlutaMAX	+	+	+	+
5% HS	+	_	_	_
2% HAT*	_	_	_	+

* Containing 5 mM hypoxanthine, 20 µM and aminopterin and 0.8 mM thymidine

5.4. Tissues

- Frozen Sprague-Dawley rat brains were purchased from Pel-Freez Biologicals (Rogers, AR, U.S.A.).
- Calf adrenals were obtained from a local slaughterhouse (Cologne, Germany).

5.5. Radioligands

- [³H]Adenine (S.A.: 28 Ci/mmol, S.A.: 26 Ci/mmol, S.A.: 27 Ci/mmol) obtained from Amersham Bioscience,

- [³H]DPCPX (S.A.: 129 Ci/mmol) obtained from Amersham Life Science,

- [³H]MSX-2 (S.A.: 84 Ci/mmol) obtained from Amersham Life Science, UK Amersham Biosciences, UK,

- [³H]PSB-0413 (S.A.: 85 Ci/mmol) labelled by Amersham Int.l, UK, the precursor PSB-0412 was synthesized in our group by Dr. Ali El-Tayeb Ak Prof. Müller,[213]

- [³H]cAMP (S. A.: 23 Ci/mmol) obtained from Amersham Bioscience,

- [³H]cAMP (S. A.: 13 Ci/mmol) obtained from Hartmann Analytic,

- [³H]CCPA (S.A.: 42.6 Ci/mmol) obtained from Perkin Elmer Life Sciences.

5.6. Buffer and solutions

▪ *50 mM Tris/HCl buffer, pH 7.4*

Tris (6.05 g) was dissolved in 1000 ml; pH was adjusted to 7.4 using concentrated HCl (37 %). For adenine assay the washing or incubation buffer was autoclaved before use.

▪ *Incubation buffer for [³H]PSB-0413 binding assay*

Tris (6.05 g, 50 mM), of NaCl (5.84 g, 100 mM) and of $MgCl_2$ (0.476 g, 4.99 mM) were dissolved in 1000 ml of water. The pH was adjusted with HCl to 7.4.

▪ *Sucrose (0.32 M) solution*

Sucrose (109.5 g) was dissolved in 1000 ml of water.

▪ *Krebs-Hepes buffer (KHP), pH 7.4 (buffer for calcium assay)*

NaCl (16.8 g, 118.6 mM), KCl (0.875 g, 4.7 mM), KH_2PO_4 (0.4 g, 1.2 mM), $NaHCO_3$ (0.875 g, 4.2 mM), D-glucose (5.25 g, 11.7 mM), HEPES (5.95 g, 10 mM), $CaCl_2$ (0.14 g, 1.3 mM) and of $MgSO_4$ (0.07 g, 1.2 mM) were dissolved in 1000 ml of water and a kept at 4 °C, then the pH value was adjusted to 7.4.

▪ *Hanks buffer salt solution (HBSS), pH 7.3 (buffer for cAMP assay)*

Hepes (4.77 g, 20 mM), NaCl (7.59 g, 130 mM), glucose (0.99 mg, 5.5 mM), $MgSO_4$ (0.99 g, 0.83 mM), $MgCl_2$.6 H_2O (0.1 g, 0.5 mM), $CaCl_2$.$2H_2O$ (0.205 g, 1.4 mM), $NaHCO_3$ (0.35 g,

4.17 mM), KCl (0.399 g, 5.36 mM), KH_2PO_4 (0.054 g, 0.4 mM) and Na_2HPO_4 (0.043 g, 0.3 mM) were dissolved in autoclaved water and the pH was adjusted to 7.3 using 1 N NaOH.

- *Lysis buffer pH 7.3 (buffer for cAMP assay)*

Na_2EDTA (1.49 g, 4 mM) were dissolved in 1000 ml of water and the pH was adjusted to 7.3 using HCl (37 %). Then 100 µl of triton X-100 (0.01%) was added.

- *Phosphate buffered saline (PBS), pH 7.3 (washing buffer for cells)*

NaCl (8 g, 137 mM), KCl (0.2 g, 2.7 mM), Na_2HPO_4 (0.609 g, 4.3 mM) and KH_2PO_4 (0.2 g, 1.47 mM) were dissolved in 1000 ml of water. HCl (37 %) was used to adjust the pH to 7.3.

- *Buffer for cAMP binding protein from bovine adrenals*

Tris (12.1 g, 100 mM) were dissolved in 1000 ml of water and the pH was adjusted to 7.4 using HCl (37 %). Then NaCl (14.6 g, 250 mM), Na_2EDTA (3.7 g, 10 mM), 0.1% 2-mercaptoethanol, and of sucrose (85 g, 0.25 M) were added.

- *Buffer for membrane preparation of PC12 cells, melanoma cells, HEK293 cells, 1321N1 human astrocytoma cells and rAde1 or human $P2Y_{12}$ receptor expressed in 1321N1 human astrocytoma cells*

Tris (0.605 g, 5 mM) were dissolved in 1000 ml of water and then the pH was adjusted to the pH 7.4 using HCl (37 %). Finally, of Na_2EDTA (0.744 g, 2 mM) was added.

- *Buffer for membrane preparation of Sf21 cells expressing mAde2R*

TRIS (6.05 g, 50 mM) with of PMSF (0.137 g, 1 mM) were dissolved in 1000 ml of water. The pH was adjustd using 37% HCl to 7.4.

- *Tris-acetate-EDTA buffer (TAE), pH 8 (buffer for agarose gel electrophoresis)*

TRIS (4.84 g, 40 mM) was dissolved in 1000 ml of water. The pH was adjusted to 8 using glacial acetic acid, then Na_2EDTA (0.744 g, 2 mM) was added.

- *Hypoxanthine or Xanthine*

About 80% of the required volume of water was added to suspend hypoxanthine (10 mg/ml) or xanthine (10 mg/ml). To the suspension sterile few drops of 1 N aq. NaOH solution the rest of the water was added. Then the solution was sterile-filtered and kept at -20°C till further use.

  ▪ *Mycophenolic acid*

Mycophenolic acid (10 mg/ml) was suspended in water and dissolved by addition of some drops of 1 N aq. NaOH solution. Then the solution was sterile filtered and frozen at -20 °C protected from light

  ▪ *Hygromycin B*

Hygromycin B (50 mg/ml) was dissolved in water, sterile-filtered and kept at-20°C.

  ▪ *HXM Medium*

DMEM (500 ml) medium containing 10% FCS, 100 U/ml penicillin G, 100 µg/ml streptomycin, 1% Ultraglutamin, hypoxanthine (0.75 ml, 10 mg / ml), xanthine (12.5 ml, 10 mg / ml), mycophenolic acid (1.25 ml, 10 mg/ml) and hygromycin B (2 ml, 50 mg/ml).

  ▪ *SOC-Medium (medium for molecular biology)*

Tryptone (20.0 g), extract of yeast (5.0 g), NaCl (0.5 g, 8.5 mM), KCl (18.9 g, 0.25 M), $MgCl_2$ (2 M) and glucose (1 M) all were dissolved in water (1000 ml). The pH was adjusted with 1 N NaOH aq. to 7.0. Then the medium was autoclaved.

  ▪ *LB-Medium (medium for molecular biology)*

LB-powder medium (25 g) was dissolved in 900 ml water, and the pH was adjusted with 1 N aq. NaOH at 7.5. After the volume was completed to 1000 ml, the medium was autoclaved.

  ▪ *Oregon Green stock solution*

The fluorescent dye Oregon Green 488 BAPTA-1/AM (Mr = 1258.07 g/mol; 50 µg was dissolved in 39.7 µl DMSO in order to get a 1 mM concentration. The stock solutions were aliquoted into Eppendorf vials and kept in 20°C until used at calcium assays.

  ▪ *Fura-2 stock solution*

Calcium-sensitive dye Fura-2/AM (Mr =1001.86 g/mol; 50 µg) were dissolved in 49.9 µl DMSO to get a stock solution of 1 mM. Then it was aliquoted into Eppendorf vials and kept at -20 ° C.

  ▪ *Pluronic® -F-127 stock solution*

Pluronic F-127 (200 mg) was dissolved in 800 µl of DMSO to give a 20% (w/v) stock solution. This requires heating at ~30° for about 20 minutes. The solution is stored at room

temperature. The Pluronic F-127 comes out of solution if it is refrigerated or frozen. If the solution does crystallize, it can be reheated until it goes back into solution.

5.7. Preparation of stable cell lines
5.7.1. Molecular biology
5.7.1.1. Gel electrophoresis

For preparing agarose gels, 1% agarose solution was made in 100 ml Tris acetate EDTA (TAE). A solution of up to 4% can be used if small DNA molecules are analyzed, and for large molecules, a solution as low as 0.8% is preferable. The solution was boiled to dissolve the agarose in a microwave oven and was cooled down to about 60 °C at room temperature. Ethidium bromide (5 μl, 0.01%) was added for 50 ml gel solution. The solution was poured into the gel rack. A comb was inserted at one side of the gel, about 5-10 mm from the end of the gel. After the gel has cooled down and become solid, the comb was removed and the gel was placed into a tank with TAE buffer. The gel was completely covered with TAE. DNA samples, stained with loading dye were pipetted into the slits. The lid of the electrophoresis chamber was closed and a current was applied (100 V for about 30 minutes). The DNA was detected by UV using a gel-Doc system.

5.7.1.2. Extraction of DNA from an agarose gel

After the DNA samples were run on an agarose gel, the gel was placed on a UV transilluminator to make the ethidium bromide-stained DNA visible. The desired bands were identified, cut out and transferred into Eppendorf tubes. The extraction of DNA was preformed as described in the QIAquik® Gel Extraction Kit protocol.

5.7.1.3. Agar plates

LB-agar (32 g) was added to 800 ml of deionized water. The agar was melted in the microwave oven and the volume was adjusted to 1L with deionized water. The solution was sterilized by autoclaving. The solution was cooled down to about 50 °C at room temperature. Ampicillin was added to the sterilized solution in a final concentration of 100 μg/ml. About 15-20 ml of agar solution was poured into 10 cm Petri dishes. The plates were kept in a plastic back in 4 °C.

5.7.1.4. Vectors

PQCXIN	**PQCXIP**	**PLXSN**

<div align="center">

5'-acgccatccacgctgttttgacct-3'
5'-aagcggcttcggccagtaacgtta-3'

5'-acgccatccacgctgttttgacct-3'
5'-aagcggcttcggccagtaacgtta-3'

5'-cccttgaacctcctcgttcgacc–3'
5'-gagcctggggactttccacaccc–3'

</div>
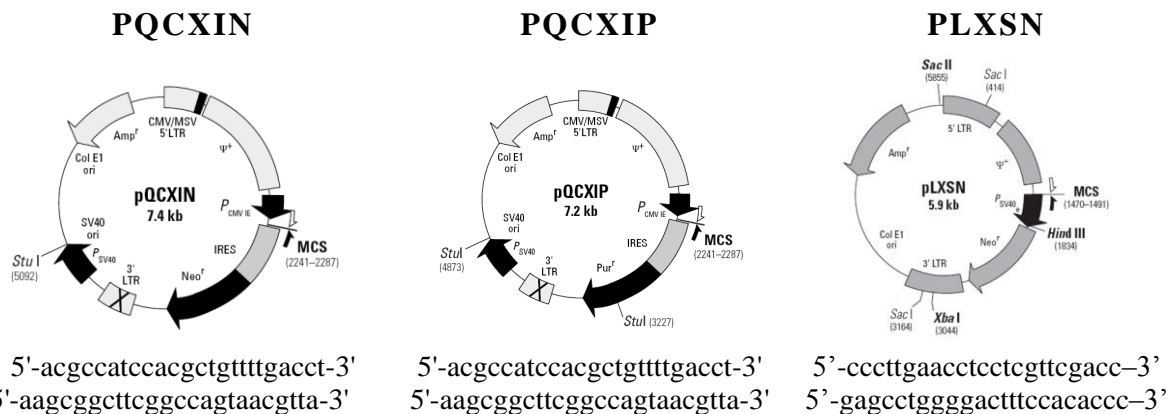
5.7.1.5. PCR primer design

PCR primers define the target region to be amplified and generally range in length from 15–30 bases. Ideally primers have a GC-content of 40–60%. Avoid three G or C residues in a row near the 3′-end of the primer to minimize nonspecific primer annealing. Also, avoid primers with intra- or intermolecular complementary sequences to minimize the production of primer-dimers. Intermolecular regions of the secondary structure can interfere with primer annealing to the template and should be avoided. Ideally, the melting temperature (Tm), the temperature at which 50% of the primer molecules are annealed to the complementary sequence, of the two will be within 5°C, so the primers anneal efficiently at the same temperature. Primers can be designed to include sequences that can be useful for downstream applications.

5.7.2. Cloning of the human P2X$_2$ and P2X$_3$ receptor DNAs into pQCXIP or pQCXIN vectors, respectively

4.7.2.1. PCR primer design

○ *The sequence of the cloning primers used for P2X$_2$:*

f-hP2X$_2$-NotI: 5'-*cgagacg*gcggccgc**atg**gccgccgcccagcc (62°C)

r-hP2X$_2$-EcoRI: 5'-cttactgaattctcagagttgagccaaacctttg (64°C)

○ *The sequence of the cloning primers used for P2X$_3$:*

f-hP2X$_3$-NotI: 5'-gtgacagcggccgc**atg**aactgcatatccgacttc (60°C)

r-hP2X$_3$-EcoRI: 5'-cttactagaattcctagtggcctatggagaagg (62°C)

5.7.2.2. The polymerase chain reaction (PCR)

The PCR amplification was carried out with the following denaturation procedure of template, annealing of primers, and elongation of primers with DNA polymerase.

This was preformed under the following conditions: 94°C initial denaturation for 4 min, followed by 1 min denaturation at 94°C and 1 min at 60°C annealing, 2 min elongation at 72 °C for 35 cycles. A final elongation was preformed for 10 min at 72°C and then maintained indefinitely at 4°C. KOD Hot Start Polymerase was used as a thermostable DNA-polymerase.

10x Buffer	2.5 µl	2.5 µl
25 mM $MgSO_4$	1.5 µl	1.5 µl
2 mM dNTPs	2.5 µl	2.5 µl
Forward primer	1 µl	1 µl
Reverse primer	1 µl	1 µl
DNA template	1 µl	0.5 µl
KOD Hot Start Polymerase	1 µl	1 µl
H_2O	14.5µl	15 µl

All samples were prepared in a 25 µl reaction volume. The total primer concentration was 0.2 pmol/µl.

5.7.2.3. Restriction

o *Restriction of the PCR product*

The PCR-products and vectors were prepared for ligation by digestion with the restriction enzymes EcoRI and NotI as follow:

BSA (10x)	5 µl
Buffer 4 (10x)	3.5 µl
EcoRI	2.5 µl
NotI	2.5 µl
H_2O	5 µl
$P2X_2$ or $P2X_3$ DNA	30 µl

All samples were prepared in a 50 µl total volume.

o *Restriction of the vectors*

BSA (10x)	1 µl
Buffer 3 (10x)	1 µl
EcoRI	0.5 µl
NotI	0.5 µl
H_2O	6 µl
pQCXIP or pQCXIN vector	30 µl

The samples were incubated for one hour at 37 °C.

5.7.2.4. Extraction of DNA from an agarose gel

After the DNA samples were run on an agarose gel, the gel was placed on a UV transilluminator to make the ethidium bromide-stained DNA visible. The desired bands were

identified, cut out and transfered to Eppendorf tubes. The extraction of the DNA was performed as described in the QIAquik® Gel Extraction Kit protocol.

5.7.2.5. Ligation of DNA fragments

Ligation of double-stranded DNA fragments (after restrictive digest) was performed with T4-DNA-Ligase. This enzyme forms ATP-dependent phosphodiester bond catalysis between 3'-hydroxyl and 5'-phosphate ends. DNA fragments were added in a molar ratio of vector to insert of 1:3. The ligation reaction was incubated at 25°C for two hours.

pQCXIP or pQCXIN vector	12.5 µl
hP2X$_2$ or hP2X$_3$	25 µl
T4-Ligase buffer (10x)	6 µl
ATP (10 mM)	6 µl
T4-DNA-Ligase	3.5 µl
H$_2$O	7 µl

5.7.2.6. Transforming chemically competent cells

The chemically competent Top 10 or DH5α™ *(Escherichia coli)* cells were thawed on ice. The ligation product of each ligation reaction was directly added to the competent cells (100 µl) and was gently mixed. The vial was incubated on ice for 30 minutes followed by a heat-shock for about 1-2 minutes at 37°C in the water bath. Afterwards the vial was transferred to ice for 2 minutes and 300 µl of SOC medium was added. The bacteria were incubated at 37°C for 1 hour while shaking at ~300 rpm. Each transformation sample was spread on separate, labelled LB agar plates containing 100 µg/ml ampicillin. The plates were inverted and incubated at 37°C overnight. On the next day, single bacterial colonies from each transformation were incubated in individual sterile culture tubes containing 5 mL of LB with 100 ug/mL ampicillin. The incubation was performed at 37 ℃ overnight with constant shaking.

5.7.2.7. DNA preparation

- *Miniprep method*

DNA minipreparation is a method for the isolation of up to 40 µg plasmid DNA from 4 mL liquid culture. The PureLink™ HiPure Plasmid DNA Miniprep Kit was used as described in the manufacturer's protocol. Resulting DNAs were analysed by digestion with restriction enzymes to identify those carrying the desired DNA sequence. Restriction was done as mentioned above using **EcoRI** and **NotI** as restriction enzymes.

- *Midiprep method*

Midiprep isolation of DNA is used for producing up to 500 µg of plasmid DNA from 100 mL of liquid culture: 5 mL of a pre-culture were added to 95 mL of LB-amp and were grown overnight at 37°C with shaking. The DNA was isolated from the liquid culture using PureLink™ HiPure Plasmid DNA Midiprep Kit according to the manufacturer's protocol. The concentration of each DNA sample was determined, and DNA was stored at -20°C.

5.7.2.8. Determination of DNA stock concentration

DNA stock (2 µl) was mixed with 998 µl of water. The concentration was determined using a photometer. Water was used as zero value and the absorption was determined at 260 nM.

5.7.2.9. DNA sequencing

DNA sequencing was done by GATC Biotech.

5.7.2.10. Creating a glycerol stock

An overnight culture (800 µl) containing the bacteria with the desired plasmid with the insert was mixed with 200 µl of sterile glycerol, and gently resuspended. Once the solution was homogenous, the glycerol stock was stored at -80°C. This stock can be used for the next several years to inoculate a fresh liquid culture in order to amplify more DNA. Simply a small portion of the frozen glycerol stock is removed (thawing the tube is not required) from the tube by scraping the surface with a pipette tip, and deposited in a sterile culture tube containing LB-amp. The culture should be incubated overnight at 37°C with agitation before proceeding to step 1.

5.7.3. Cloning of the human P2Y$_{11}$ receptor DNA into the pLXSN vector

5.7.3.1. PCR cloning primers

f-hP2Y$_{11}$-EcoRI: 5'-gtgacag<u>aatcg</u>**atg**gcagccaacgtctcgg (62°C)

r-hP2Y$_{11}$-XhoI: 5'- cttacta<u>ctcgag</u>tcattggctcagctcacggg (62°C)

The cloning of human P2Y$_{11}$ receptor DNA into pLXSN was preformed as mentioned above. In brief, PCR was performed using the forward, the reverse primers and the template for hP2Y$_{11}$ DNA as follows:

Initial denaturation	94°C	4 min
Denaturation	94°C	1 min
Annealing	62°C	1 min
Elongation	72°C	1 min
A final elongation	72°C	10 min
Cooling	4°C	

(Denaturation, Annealing, Elongation: 25 cycles)

The PCR product and the pLXSN vector were prepared for ligation by restriction using EcoRI and XhoI followed by ligation using T4-DNA-Ligase. The ligation product was transformed into Top 10 *E. coli* and the DNA was isolated from individual clones. Sequencing was performed by GATC Biotech (Konstanz, Germany).

A problem appeared in which a DNA sequence in the hP2Y$_{11}$ sequence was missing. In order to overcome this problem a new primer was designed to attach the missing DNA sequence and then the cloning procedure was repeated.

The first PCR was performed using the following primers:

f-hP2Y$_{11}$-ATG: 5'-atggcagccaacgtctcgggtgccaagtcctgccctg-3'(64°C)
r-hP2Y$_{11}$-XhoI: 5'- cttacta<u>ctcgag</u>tcattggctcagctcacggg (62°C)

The PCR steps were done as mentioned before using 62°C as annelling temperature. The PCR product from the first PCR was used as a template for the second PCR. The second PCR for hP2Y$_{11}$ was carried out using the primers f-hP2Y$_{11}$-EcoRI and r-hP2Y$_{11}$-XhoI at 62°C for 30 cycles.

5.7.3.2. Restriction

- ***Restriction of the second PCR product***

The PCR products and vectors were prepared for ligation by digestion with the restriction enzymes EcoRI and NotI as follows:

BSA (10x)   5 µl
10x buffer 4   3.5 µl
EcoRI   2.5 µl
XhoI   2.5 µl
H$_2$O   5 µl
Second PCR product   30 µl

 ▪ *Restriction of the vectors*

BSA (10x)   1 µl
10x buffer 4   1 µl
EcoRI   0.5 µl
XhoI   0.5 µl
H$_2$O   6 µl
pLXSN vector   1 µl

The sample was prepared in a total volume of 10 µl. The incubation was performed as mentioned before at 37 °C for one hour, followed by ligation using T4-DNA-Ligase which was performed over night at 16 °C.

The ligation prodct was transformed into *E. coli* and the DNA was isolated from individual clones using the PureLink™ HiPure Plasmid DNA Miniprep Kit as described in the manufacturer's protocol. Resulting DNAs were analysed by digestion with restriction enzymes to identify those carrying the desired DNA sequence. Restriction was done as mentioned above using **EcoRI** and **XhoI** as restriction enzymes.

5.7.4. Stable transfection

The packing cell line (GP+envAM12260) was split one day before transfection (1.5×10^6 in 25 cm^2 flask) in normal culturing medium (*HXM-medium)* without xanthine, hypoxanthine and mycophenolic acid. Cells were transfected by using lipofectamine 2000. Briefly, 10 µg of DNA (6.25 µg of plasmid and 3.75 µg of VSV-G protein DNA) was incubated in a final volume of 625 µl of DMEM (without FCS or antibiotics); then, 25 µl of lipofectamine 2000 was incubated in 600 µl DMEM (without FCS or antibiotics) for 5 minutes. The lipofectamine in the medium was mixed with the DNA-medium mixture and incubated for 20 minutes. The DNA-lipid mixture was added to the GP+envAM12260 cells (80% confluent; 25 cm^{2}flask) and incubated for 12-15 hour. Then the medium was changed with 3 ml medium (DMEM, 10% FCS, 100 U/ml penicillin G, 100 µg/ml streptomycin and 1% ultraglutamine) and 30 µl of sodium butyrate was added. The cells were cultured at 32°C for 2 days. Finally, 3 ml of

virus supernatant were collected and filtered though 45 µm filters. The sterile virus supernatant with 6 µl of polybrene solution was infected into 1321N1 human astrocytoma cells (80% confluent 25 cm^2 flask) for 2 hour, and then the medium was exchanged for new one. 48 hours after transfection, cells were subcultured in growth medium containing 800 mg ml^{-1} G 418 (human P2X$_2$ HAtag, human P2X$_3$ HAtag, human P2X$_{2-3}$, human P2Y$_{12}$ and human P2Y$_{13}$, P2Y$_{14}$ and rAde1). Cells expressing P2X$_2$, P2X$_3$ and P2Y$_{12}$ and P2Y$_{13}$ receptors were maintained at 37°C in DMEM with 4 mM L-glutamine, 10% fetal bovine serum, 100 U/ml penicillin G, 100 µg/ml streptomycin and 400 µg ml^{-1} G 418.

> **Retroviral transfection of 1321N1 human astrocytoma cells for the stable expression of hP2X$_2$ and P2X$_{2/3}$ receptors**

The human P2X$_2$ and P2X$_3$ DNAs were inserted into the retroviral vector pQCXIP and pQCXIN, respectively, as mentioned above.
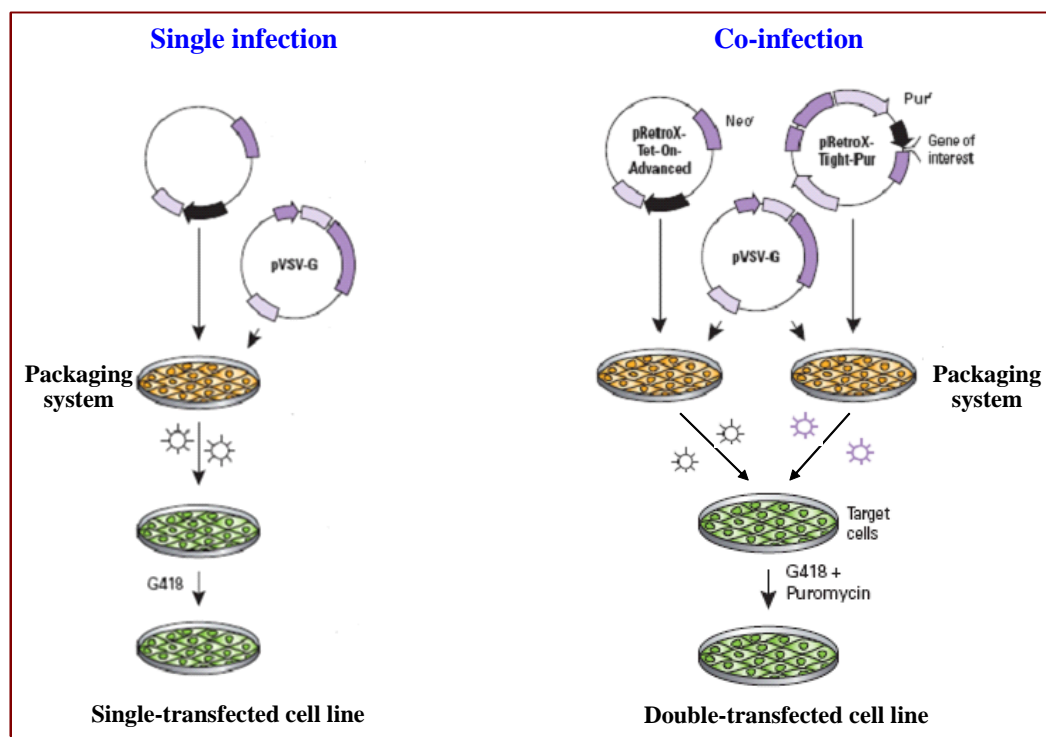
Figure 90. Packaging cells are first transiently cotransfected with a retroviral vector and a viral expression vector containing pVSV-G for pseudotyping to generate retroviruses. Those viruses are initially used to generate a stable cell line, expressing one receptor only. This cell line can then be used for the infection with viruses containing a second gene of interest. This produces a cell line that expresses two receptors or proteins of interest in the presence of doxycycline (**left**). Target cells may also be coinfected with the two retroviruses carrying two genes of interest and selected simultaneously with G418 and puromycin to produce the desired cell line, expressing two different proteins (**right**).

The DNA was transfected in 1321N1 human astrocytomacells using a retroviral system as described[192] with some modifications. GP+envAM12 packaging cells were first transiently cotransfected with a retroviral vector and a viral expression vector (pVSV-G) to generate two retroviruses

The retroviral vector containing the $hP2X_2$ insert was initially used to create a stable 1321N1 human astrocytoma cell line, expressing $P2X_2$, which was then infected with a $P2X_3$ containing virus carrying a neomycin resistance gene for selection. In a second approach, 1321N1 human astrocytoma cells were co-infected with the two retroviruses carrying the $P2X_2$ and $P2X_3$ DNAs, respectively, and selected simultaneously with G418 (800 µg/ml) and puromycin (6 µg/ml) to produce the desired stable cell line, expressing both receptors (Figure 90).

5.8. Cell culture

5.8.1. Thawing of cells

The backups of the cell lines were thawed as quickly as possible and transferred to a cell culture bottle under laminar air flow. Then the cells were cultured in the incubator at 95% humidity, 5% CO_2 and 37 °C. After about 5 hours in the incubator, the medium is exchanged with fresh one. The medium is exchanged in order to remove the dead cells which are toxic.

5.8.2. Cells splitting

After the cell line is approximately 80-90% confluent, the cells are washed with about 10 ml of medium PBS buffer. This washing step is in order to remove the remaining FCS or HS-serum which negatively influences the enzymatic action of trypsin / EDTA. For the separation of the adherent by growing cells, depending on the enzymatic activity of trypsin, approximately 3-4 ml of trypsin / EDTA are added to the cells. The sterile bottle was incubated for 5 min in the incubator to increase the enzymatic activity of trypsin. Afterward, the still adherent cells were detached by gentle tapping of the cell culture bottle. Sufficient volume of medium was rapidly added to the cell suspension. The volume of medium added is depending on the ratio of splitting. In turn the ratio of the splitting will affect the speed of growth of cells obtained from different cell lines. The resulting cell suspension is pipetted several times, allowing the cells to be isolated and increase the homogeneity of the suspension.

5.8.3. Freezing of cells producing backups

To create backups cell medium is removed from the culture flask. After the cells have been detached from the flask using trypsin / EDTA solution the contents was transferred into a 50

ml Falcon tube. The cell suspension was centrifuged at 200 g, 4 °C for 5 min. The pellet was resuspended in a 10% solution of sterile DMSO, 40 % medium and 50 % FCS. The solution is aliquoted into cryovials (2 ml). The cryovails remained for 2 days at -20 °C, then 6 days at 80 °C and at the end they were transferred into the liquid nitrogen tank.

5.8.4. Cell membrane preparation

For the adherent by growing cell lines, the cells are grown in dishes until 80-90% confluent. The medium are removed and the cells are washed with sterile PBS buffer. After removing the PBS buffer the dishes were frozen at -80 ° C until further preparation.

The cells were thawed and resuspended in 5 mM Tris and 2 mM EDTA, pH 7.4 (Tris/EDTA buffer). The cells were homogenized by using a glass-teflon homogenizer. The resulting suspension is centrifuged at 1000 *g* for 10 min to remove unbroken cells and nuclei. The supernatant is homogenized with an Ultraturrax and subsequently centrifuged at 48,400 *g* for 60 min. The resulting pellets are resuspended in 50 mM Tris-HCl buffer, pH 7.4. Protein concentration was determined, and the membranes were stored at −80°C until required.

For the membrane preparation of a non-adherent by growing cell line, the cell culture was also grown in tissue culture dishes. The contents of the cell culture plates were transferred into a falcon tube, and it was followed by a first centrifugation at 200 g and 4 ° C for 5 min. The supernatant was discarded and the cell pellet was resuspended in 5 mM Tris-HCl buffer pH 7.4 with 2 mM EDTA. All cell suspensions are combined and centrifuged under the same conditions, and subsequently stored on ice. After finishing the first centrifugation step, the preparation is continued as mentioned above.

5.8.5. Membrane preparations from Sf21 cells expressing the mAde2 receptor

After infection of cells with recombinant baculoviruses, cells were homogenized with 20 strokes in a tight by fitting Dounce homogenizer in 50 mM Tris-HCl buffer, pH 7.4, containing 1 mM PMSF. The cell suspension was centrifuged for 10 min at 200 g, 4°C. The supernatant was then centrifuged at 48,000 g, 60 min, 4°C and the resulting pellet was resuspended in 50 mM Tris-HCl buffer, pH 7.4. The protein concentration was determined. Membranes were kept frozen at -80°C until use.

5.9. Membrane preparation of organs tissue

5.9.1. Rat cortex

Frozen brains were removed from the -80 °C freezer and immediately placed in ice-cold saline before dissection of the cortex. Tissues were homogenized in sucrose using a glass-teflon homogenizer, the homogenate was centrifuged at $1000 \times g$ for 10 min, and the resulting supernatant was centrifuged at $37,000 \times g$ for 1 hour. The synaptosomal - mitochondrial P_2 pellet was homogenised with Ultraturrax for 10 s, then centrifuged at $37,000 \times g$ for 60 min. The membrane pellet was resuspended in 50 mM Tris-HCl buffer (pH 7.4), and stored at $-80°C$. The protein concentration of the suspension was determined.

5.9.2. Rat striatum

After the cerebral cortex of rat brain had been scraped off, the left and right striatum was dissected and placed in ice cold 50 mM Tris-HCl buffer pH 7.4. The tissue was homogenized with an Ultraturrax (stage 3-4, about 2-3 s). The resulting suspension is centrifuged at 48,400 g for 15 min. The supernatant is discarded, the pellet was resuspended in 50 mM Tris-HCl buffer pH 7.4, homogenized and again centrifuged under the above conditions. After this second washing step, the supernatant was discarded and the pellet was resuspended in 50 mM Tris-HCl buffer pH 7.4. After homogenization, the preserved tissue suspension was aliquoted in 1 ml Eppendorf tubes. The tubes were frozen in -80 °C after protein determination.

5.9.3. Preparation of cAMP binding protein

The bovine adrenals from four animals were dissected free of subcapsular fat and medullar tissue. They were then homogenized in 10 volumes of buffer consisting of 100 mM Tris/HCl, pH 7.4, 250 mM NaCl, 10 mM EDTA, 0.1% 2-mercaptoethanol, and 0.25 M sucrose with an Ultra-Turrax. The homogenate was filtered through cheesecloth and then cleared by centrifugation (30,000 g, 4°C for 60 min). The supernatant with the soluble proteins was used without further processing, as binding protein. The protein was frozen in l-ml aliquots at -20 °C. Under these circumstances, the activity of the protein was retained for at least 2 years.

5.10. Protein determination

5.10.1. Bradford protein determination

The Bradford protein assay is a dye-binding assay based on the observation that the absorbance maximum for an acidic solution of Coomassie Brillant Blue G 250 shifts from λ= 465 nm to λ= 595 nm when binding with protein occurs. To determine the concentration of the protein following the Bradford procedure, a master solution was prepared, made of 100 mg Coomassie brilliant Blue G diluted in 50 ml ethanol (v/v), with 100 ml phosphoric acid and diluted with water to 1000 ml when the dye has completely dissolved. The Bradford reagent should be of a light brown in color. Bovine serum albumin was used as a standard protein. The Coomassie protein assay was calibrated within a protein concentration range from 10 to 250 μg (λ = 595 nm). The samples are diluted with water so that their concentrations amount to approximately 10-100 μg proteins. A volume of 0.1 ml of these dilutions was mixed with 2.0 ml Bradford reagent. The sample-dye mixtures were assayed within 1 hour of mixing, due to the progressive reduction of the optical density. The basic amino acids, arginine, lysine and histidine play a role in the formation of dye-protein complexes color. Small proteins less than 3 kDa and amino acids generally do not produce color changes.

5.10.2. Lowry protein determination

This procedure is one of the most used for quantification of soluble proteins. Protein concentrations are determined and reported with reference to standards of a common protein bovine serum albumin (1 mg/ml). A series of dilutions of the protein standard is prepared in appropriately labelled test tubes (Table 25).

Reagents

A	Na_2CO_3	2 %	10 g
	NaOH 0.1 N		500 ml
B	$Cu_2SO_4 . 5H_2O$	0.5 %	0.25 g
	Na- Tartrat	1 %	0.5 g
	Deionised water		50 ml

C   Frishly prepared by mixing: 50 parts of reagent A with 1 part of reagent

D   Folin & Ciocalteaus phenol reagent working solution:

Add 90 ml of deionised water to 18 ml Folin Reagent (**F-9252**) and store in dark at room temperature.

In this method, protein is pretreated with copper (II) in a modified biuret reagent (alkaline copper solution stabilized with sodium potassium tartrate; **C**). Addition of Folin & Ciocalteus

phenol reagent (**D**), which contains sodium molybdate and sodium tungstate in phosphoric acid, generates a change of reagent colour from yellow to blue colour. That is due to the reduction of Folin & Ciocalteus phenol reagent by the copper – protein complex that gives an increasing in absorbance between 550–750 nm. Normally, absorbance at the peak (750 nm) or shoulder (660 nm) is used to quantitate protein concentrations between 1–100 μg/ml while absorbance at 550 nm is used to quantitate higher protein concentrations.

A volume of 1 ml of Lowry reagent is added to 0.2 ml of protein sample (appropriately diluted) and incubated exactly 20 minutes at room temperature. The last step is to add the Folin-Ciocalteau reagent and incubate it for 30 minutes at room temperature. The concentration of each unknown protein sample is determined based on the standard curve.

Table 25. Dilutions of the bovine serum albumin (BSA)

Protein standard solution (µl)	*Deionised water (µl)*	*Protein conc. (µg/ml)*
10	190	50
20	180	100
40	160	200
60	140	300
80	120	400

5.11. Radioligand binding studies

5.11.1. Saturation buinding studies

5.11.1.1. Saturation experiments using intact cells

5.11.1.1.1. Saturation experiments for human adenine receptors using intact cells

HEK293 cells were grown to confluence, washed and resuspended in HBSS buffer solution. Cells (3 x10^5) were incubated with increasing amounts (0.5 - 200 nM) of [^{3}H]adenine as radioligand in a total volume of 200 μl for 60 min at room temperature. Nonspecific binding was determined with 100 μM adenine. Incubation was terminated using vacuum filtration through Whatman GF/B glass fibre filters, using a Brandel 24 or 48-channel cell harvester. The vials were rinsed three times with 3 ml of Tris-HCl buffer (50 mM, pH 7.4) and consequently both bound and free radioligand were separated. The filters were punched out and transferred to 4 ml scintillation vials. 2.5 ml Ultima Gold® scintillation cocktail was added and samples were counted after 6 hours for 1 min each, using a liquid scintillation counter (LSC).

Scheme for pipetting

50 µl	Tris 90 % / DMSO 10 % total binding; containing adenine (100 µM) for nonspecific binding
50 µl	[^{3}H]adenine (final concentration 0.5 - 200 nM) in HBSS buffer; pH 7.3
100 µl	Cell suspension in HBSS buffer; pH 7.3
200 µl	Total volume

5.11.1.1.2. Saturation experiment of [^{3}H]PSB-0413 at intact 1321N1 human astrocytoma cells expressing human P2Y$_{12}$ receptor

1321N1 human astrocytoma cells expressing the human P2Y$_{12}$ receptor were harvested with 0.05 % trypsin / 0.02 % EDTA and rinsed with culture medium. The cell suspension was centrifuged at 200 x g and resuspended (5 x 10^5 cells/ml) in DMEM medium, supplemented with 100 U/ml penicillin G, 100 µg/ml streptomycin, 1 % GlutaMAX and 400 µg/ml G418. Increasing concentrations of [^{3}H]PSB-0413 (0.05-30 nM) were incubated with cell suspension. The nonspecific binding measured in the presence of ADP (10 mM). Samples were incubated for 60 min at 37 ºC in 500 µl total volume. The incubation was stopped by vacuum filtration through Whatman GF/B glass fiber filters, using a Brandel 24- or 48-channel cell harvester. The vials were rinsed three times with 1 ml aliquots of PBS buffer.

Scheme for pipetting

50 µl	HBSS buffer; pH 7.3, ADP 10 mM
50 µl	[^{3}H]PSB-0413 (0.05-30 nM) in HBSS buffer; pH 7.3
400 µl	Cell suspension in DMEM medium
500 µl	Total volume

5.11.1.2. Saturation experiments using membrane preparations

5.11.1.2.1. Membrane preparation of mAde2 receptor expressed in Sf21 cells or CHO cells

For the saturation assay increasing amounts (0.75-150 nM) of [^{3}H]adenine in 50 mM Tris-HCl, pH 7.4 in a total volume of 200 µl were used. Nonspecific binding was determined with 100 µM adenine. The binding was terminated as mentioned before. In brief, vacuum filtration through Whatman GF/B glass fibre filters was used to separate binding radioligand from free radioligand, using a Brandel 24- or 48-channel cell harvester. The vials were rinsed three times with 3 ml of ice-cold Tris-HCl buffer (50 mM, pH 7.4).

Schematic for pipetting

50 µl	Tris 90 % / DMSO 10 %, adenine (100 µM)
50 µl	[^{3}H]adenine (final concentration 0. nM) in 50 mM Tris-HCl buffer pH 7.4
100 µl	Protein membrane preparation (100 µg/vial) in 50 mM Tris-HCl buffer, pH 7.4
200 µl	Total volume

5.11.2. Competition experiments

5.11.2.1. Competition experiments at intact cells

5.11.2.1.1. Competition experiment using whole cells of HEK 293

HEK293 cells were grown to 85% confluence, washed and collected in HBSS buffer (containing 20 mM HEPES, pH 7.3). The incubation was started by addition of [^{3}H]adenine (15 nM) to the cell (3 x10^5) suspension. About 6-9 dilutions of adenine were made in HBSS buffer. The incuabtion was preformed at room temprature for 60 minutes in a total volume of 200 µl. Nonspecific binding was determined with 100 µM adenine. The binding was terminated as described before.

Scheme for pipetting:

50 µl	HBSS buffer; pH 7.4, adenine (100 µM) or tested compound
50 µl	[^{3}H]adenine (final concentration 15 nM) in HBSS buffer, pH 7.4
100 µl	Cell suspension in HBSS buffer, pH 7.4
200 µl	Total volume

5.11.2.1.2. Competition experiment with [^{3}H]PSB-0413 cell at whole human P2Y$_{12}$

1321N1 human astrocytoma cells expressing the human P2Y$_{12}$ receptor, were harvested with 0.05 % trypsin / 0.02 % EDTA and rinsed with culture medium. The cell suspension was centrifuged at 200 x g and resuspended (5 x 10^5 cells/ml) in DMEM medium, supplemented with 100 U/ml penicillin G, 100 µg/ml streptomycin, 1 % GlutaMAX and 400 µg/ml G 418. The nonspecific binding measured in the presence of ADP (10 mM). Samples were incubated for 60 min at 37 ℃ in a total volume of 500 µl. The incubation was stopped using vacuum filtration through Whatman GF/B glass fiber filters using a Brandel 24- or 48-channel cell harvester. The vials were rinsed three times with 1 ml aliquots of PBS buffer.

Scheme for pipetting

50 µl	HBSS buffer, pH 7.3, ADP 10 mM or test compound
50 µl	[^{3}H]PSB-0413 (5 nM) in HBSS buffer, pH 7.3
400 µl	Cell suspension in DMEM medium
500 µl	Total volume

5.11.2.2. Competition experiments using membrane preparations

5.11.2.2.1. [^{3}H]Adenine competition experiments using membrane preparations

The competition assays were carried out using [^{3}H]adenine in a concentration of 10 nM and were done in triplicates. For the non-specific binding, adenine (100 µM) was dissolved in Tris-HCl / DMSO mixture buffer (9:1). 6-9 Dilutions of test compounds previously dissolved in DMSO were prepared using Tris-HCl / DMSO mixture buffer. The mixture was added to the incubation tubes. After the addition of [^{3}H]adenine and protein (rat cortical membranes, HEK293 membranes, PC12 cell membranes, melanoma cell membranes, the membrane preparations of recombinant mAde2R expressed in Sf21 insect cells, or NG108-15 membrane preparations), the samples were incubated for 60 min at room temperature. The incubation was stopped using vacuum filtration through Whatman GF/B glass fibre filters, using a Brandel 24 or 48-channel cell harvester. The vials were rinsed three times with 3 ml of Tris-HCl buffer (50 mM, pH 7.4) and consequently both bound and free radioligand were separated. The filters were punched out and transferred to 4 ml scintillation vials. 2.5 ml Ultima Gold® scintillation cocktail was added and samples were counted after 6 hours for 1 min each, using a liquid scintillation counter (LSC).

Scheme for pipetting

50 µl	Tris 90 % / DMSO 10%, adenine (100 µM) or tested compound
50 µl	[^{3}H]adenine (final concentration 10 nM) in 50 mM Tris-HCl buffer pH 7.4
100 µl	Protein membrane preparation (100 µg/vial) in 50 mM Tris-HCl buffer, pH 7.4
200 µl	Total volume

5.11.2.2.2. [^{3}H]PSB-0413 competition experiments at membranes of human P2Y$_{12}$ receptors expressed in 1321N1 astrocytoma cells

The competition assays were carried out using [^{3}H]PSB-0413 in a concentration of 5 nM. The non-specific binding was determined using 10 mM ADP. 6-9 dilutions of test compound were prepared using assay buffer. The assays were performed in triplicate in a final volume of 500

µl in test tubes containing 50 mM Tris-HCl, pH 7.4. Samples were incubated for 60 min at room temperature. The incubation was stopped using vacuum filtration through Whatman GF/B glass fiber filters, using a Brandel 24 or 48-channel cell harvester. The vials were rinsed three times with 1 ml aliquots of Tris-HCl buffer 50 mM pH 7.4.

Scheme for pipetting

50 µl	50 mM Tris-HCl, 100 mM NaCl, 5 mM MgCl$_2$; pH 7.4, ADP 10 mM or test compound
50 µl	[^{3}H]PSB-0413 (5 nM) in 50 mM Tris-HCl, 100 mM NaCl, 5 mM MgCl$_2$, pH 7.4
100 µl	Membrane preparation of cells (100-150 µg/ml)
300 µl	50 mM Tris-HCl, 100 mM NaCl, 5 mM MgCl$_2$, pH 7.4
500 µl	Total volume

5.11.2.2.3. Adenosine A$_{2A}$ receptor competition assays

The competition assays were carried out using [^{3}H]MSX-2 (3-(3-hydroxypropyl)-8-(*m*-methoxystyryl)-7-methyl-1-propargylxanthine, antagonist)[193] in a concentration of 1 nM and were done in triplicates. Non-specific binding was determined using NECA (50 µM). After the addition of [^{3}H]MSX-2 and test compound, the incubation was started by the addition of protein (rat striatum with 2 IU ADA/ml) for 30 min at RT in Tris-HCl, 50 mM, pH 7.4. The incubation was performed in a total volume of 400 µl. The binding was terminated as described before using vacuum filtration with a minor modification: the GF/B filter was preincubated in 0.3 % PEI solution for 30 min to minimize non-specific binding to the filter prior to harvesting.

Scheme for pipetting

10 µl	DMSO, total binding, NECA (50 µM) or test compound diluted in DMSO
100 µl	[^{3}H]MSX-2 (1 nM) in 50 mM Tris-HCl buffer pH 7.4; K_D = 8 nM[193]
100 µl	Protein membrane preparation in 50 mM Tris-HCl buffer, pH 7.4
190 µl	50 mM Tris-HCl buffer, pH 7.4
400 µl	Total volume

5.11.2.2.4. Adenosine A$_1$ receptor competition experiments

The competition assays was performed using [^{3}H]CCPA (2-Chlor-N^6-cyclopentyladenosine 42.6 Ci/mmol)[194] in a concentration of 1 nM and were done in triplicates. CADO (2-chloroadenosin, agonist) 10 µM was used for non-specific binding. The incubation started

with addition of protein (rat cortex with 2 IU ADA/ml) and lasted for 90 min at room temperature in Tris-HCl buffer, 50 mM, pH 7.4, in a total volume of 400 µl. The incubation was terminated as described before.

Scheme for pipetting

10 µl	DMSO, total binding, NECA (50 µM) or test compound diluted in DMSO
100 µl	[³H]CCPA (1 nM in 50 mM Tris-HCl buffer pH 7.4); $K_D = 0.2$ nM[194]
100 µl	Protein membrane preparation in 50 mM Tris-HCl buffer, pH 7.4
190 µl	50 mM Tris-HCl buffer, pH 7.4
400 µl	Total volume

5.11.3. Kinetic experiments

5.11.3.1. Association kinetics for human adenine receptors in HEK293 cells

The association was initiated by the addition of HEK293 whole cells in HBSS, pH 7.3, with [³H]adenine (15 nM) in a total volume of 200 µl and at different time interval from 2 to 240 minute. Nonspecific binding was determined by addition of 100 µM adenine. The incubation process was performed at room temperature for 1 hour. The experiments were carried out in triplicate. The incubation was terminated by rapid vacuum filtration through Whatman GF/B glass fibre filters. The vials were rinsed three times with 3 ml ice-cold tris buffer (50 mM), to allow the separation of the bound from the free radioligand. The filters were punched out, transferred into 4 ml scintillations vials and 2.5 ml Ultima Gold Cocktail was added. The incubation of samples with scintillation fluid was allowed to take place for sufficient time (6 hours). The radioactivity was measured, 1 minute per sample, using a liquid scintillation counter (LSC).

5.11.3.2. Dissociation experiments for human adenine receptors in HEK293 cells

Binding was initiated by addition of re-suspended HEK293 whole cells to incubation tubes with HBSS buffer, pH 7.3, and 15 nM [³H]adenine, for 1 hour. The dissociation was initiated by addition of adenine (100 µM) and specific binding was then measured at different time interval (2–120 minutes). The incubation process was performed at room temperature. The experiments were carried out in triplicates. The incubation was terminated as described above.

5.12. Functional studies

5.12.1. cAMP assays

General procedure

Receptor function was assessed by analyzing the activity of cellular adenylate cyclase. For this purpose, cells stably expressing the recombinant receptor were cultured on 24-well plates (150,000-200,000 cell/well). After removal of the culture medium, cells were washed with HBSS (containing 20 mM HEPES, pH 7.3) buffer and then incubated with the same buffer for 2 h at 37 °C. Additives were added to the cells at 36.5 °C. After incubation with additives the reaction was stopped by removal of the reaction buffer followed by the addition of a hot lysis solution (500 µl; 90 °C; Na_2EDTA 4 mM; Triton X 100, 0.1 ‰).

Cyclic AMP levels were quantified by incubation of an aliquot with cAMP binding protein and [³H]cAMP. The assay is based on competition between unlabelled cAMP and a fixed amount of [³H]cAMP for binding to a protein which has high affinity for cAMP. The amount of labelled protein-cAMP complex formed is inversely related to the amount of unlabelled cAMP present in the assay sample (Figure 91). Measurement of the protein–bound radioactivity enables the amount of unlabelled cAMP in the sample to be calculated. Separation of the labelled protein from unlabeled one is achieved by one of the following methods:

- ✓ Adsorption of the free nucleotide on coated charcoal, in which 50 µl of charcoal was added to each tube. The samples were incubated on ice for 5 min at 4 ºC, then centrifuged at the same temperature at 14000 rpm for 5 min. An aliquot of the supernatant was transferred to scintillation vials, mixed with scintillation cocktail and incubated for two hours. Then each sample was measured for 10 min using a liquid scintillation counter.

- ✓ Filtration through GF/B filters using a Brandel 24- or 48-channel cell harvester. The filters were punched out and transferred to 4 ml scintillation vials. 2.5 ml Ultima Gold® scintillation cocktail was added and samples were counted after 6 hours for 1 min.

Figure 91. cAMP determination.

Cyclic AMP protocol (separation by adsorption)

Tube	Lysis buffer	Standard	Unknown	[³H]cAMP (3 nM)	Binding protein
Zero dose	25 µl	_	_	30 µl	40 µl
Charcoal blank	65 µl	_	_	30 µl	40 µl
Standard	_	25 µl	_	30 µl	40 µl
unknown	_	_	25 µl	30 µl	40 µl

Cyclic AMP protocol (separation by filtration)

Tube	Lysis buffer	Standard	Unknown	[³H]cAMP (3 nM)	Binding protein (50 µg/ml)
Zero dose	50 µl	_	_	30 µl	40 µl
Standard	_	50 µl	_	30 µl	40 µl
unknown	_	_	50 µl	30 µl	40 µl

Analysis of Data

➢ Average of the cpm for samples in the absence of unlabeled cAMP was calculated (C_0).

➢ C_0/C_x was also determined for each concentration of cAMP and unknowns in the assay.

➢ 3. C_0/C_x was plotted against pmoles of standard cAMP; a straight line should be obtained with an intercept of 1.

Calibration curve
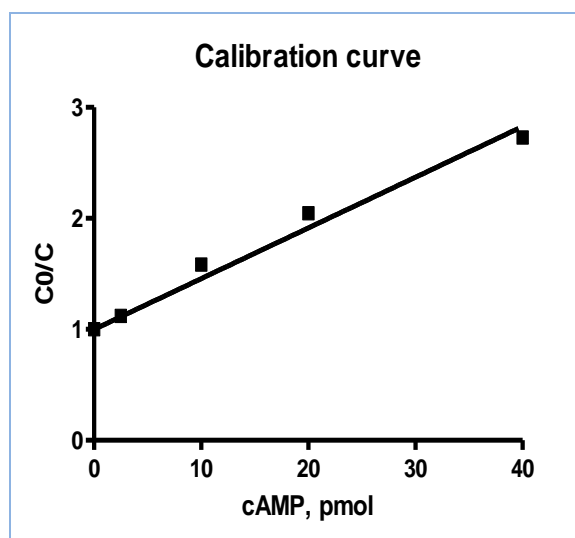
5.12.1.1. *cAMP assay for G_i protein-coupled receptors (G_i signaling pathway)*

5.12.1.1.1. rAde1 receptor or mAde2 receptor expressed in 1321N1 human astrocytoma cells

Cellular cAMP production was stimulated by the addition of 3 nM isoproterenol at 37 °C. Solvent (control), adenine or adenine derivatives were added together with isoproterenol.

5.12.1.1.2. Adenine receptor natively expressed in CHO K1 or CHO flp-in cells

Cells were stimulated for cAMP production by the addition of 5 µM forskolin at 37 °C. Solvent (control) and adenine was added.

5.12.1.1.3. Human P2Y$_{12}$ receptor or human P2Y$_{13}$ receptor expressed in 1321N1 human astrocytoma cells

The cells were preincubated with phosphodiesterase inhibitor 3-isobutyl-1-methylxanthine (IBMX), 100 µM, and caffeine (250 µM), a mixed adenosine receptor antagonist, to block the effects of adenosine generated by degradation of nucleotides for 10 min at 37 °C.[R] Nucleotides were then added to a final volume of 500 µL, 30 s before forskolin (4 µM).

5.12.1.2. *cAMP assays for G$_s$ protein-coupled receptors (G$_s$ signaling pathway)*

5.12.1.2.1. Human adenosine A$_{2A}$ receptors or human adenosine A$_{2B}$ receptors expressed in CHO cells

The cells were incubated with HBSS buffer containing adenosine deaminase (1 IU/ml) for 120 min at 37 °C. Then the cells were then preincubated with the phosphodiesterase inhibitor 4-(3-butoxy-4-methoxybenzyl)-2-imidazolidone (Ro 20-1724), 40 µM, for 10 min. Drugs were added in 0.1 ml HBSS buffer and incubations were continued for 10 minutes at 37 °C.

For experiments with antagonists, cells were incubated with different concentrations of adenosine A$_{2A}$ antagonists for 10 min before addition of the agonist NECA (1 nM - 100000 nM). Then the cells were incubated for 10 more minutes. Alternatively both, agonist and antagonist were added at the same time.

5.12.1.2.2. cAMP assays for adenine receptors in HEK293 cells

The function of adenine receptor in HEK293 cells was assessed by analyzing the activity of cellular adenylate cyclase activity. A 24-well plate was coated with poly-L-lysine, 0.001 % solution was applied. Coating of the 24-well plate was carried out for 30-60 min at room temperature. The 24-well plate was then washed with PBS twice and with culture medium for once. After that, cells were cultured on the 24-well plates for one day in the culture medium at 37 °C, 5% CO_2. The assay was continued with the modified procedure as described before.

Furthermore another experiment was performed with these cells in which the effect of PTX on adenine receptors in HEK293 was studied. Cells were pre-treated with PTX 100 ng/ml over night before the cAMP assay was performed.

5.13. Reporter gene assay

General remarks

Reporter constructs incorporating the coding sequence of luciferase (Luc) are convenient tools with which to perform high-throughput screens of multiple cellular function.[134] These reporter genes are introduced into mammalian cell lines by transfection so that the level of Luc activity may be determined in whole-cell lysates or living cells in which Luc-catalyzed oxidation of luciferin generates photons detected by a photomultiplier tube or an imaging photon detector. When the expression of Luc is placed under the control of a minimal promoter incorporating a cyclic adenosine monophosphate (cAMP) response element (CRE), cAMP-elevating agents act via protein kinase A (PKA) and the CRE-binding protein transcription factor (cAMP response element binding protein, CREB) to activate the gene expression of Luc. This technology is particularly applicable to the screening of cell lines expressing recombinant G protein–coupled receptors (GPCRs) positively linked to cAMP production. For example, small molecules with GPCR agonist activity or orphan GPCRs with constitutive activity can be identified on the basis of their ability to stimulate Luc expression via the cAMP pathway.[139]

Cell culture and DNA transfection

rAde1 receptor stably expressed in 1321N1 human astrocytoma cells, human adenosine A_1 receptors expressed in CHO cells or PC12 cells were cultured in 75 cm^2 flasks (3.2 x 10^5) for 24 h without antibiotics so that they were 90-95% confluent before transfection. The cAMP responsive reporter plasmid (pCER-luc), 5 μg, was transfected into the cells using Lipofectamine 2000 as a transfection reagent.

5.13.1. Luciferase assay as an alternative measurment for cyclic adenosine monophosphate (cAMP)

5.13.1.1. rAde1R expressed in 1321N1 human astrocytoma cells

Reporter cells were seeded at a density of 200,000 – 150,000 cells/well in a 24-well plate 18-20 h prior to assay. After removal of the culture medium, cells were washed twice with Hanks' balanced salt solution. Adenine and selected adenine derivatives were diluted in Hanks' balanced salt solution containing 3 nM isoproterenol and then incubated with reporter cells in the same buffer for 3 h at 37 °C. The reaction was stopped by removal of the reaction buffer and the luciferase expression was determined using the Bright-Glo™ Luciferase assay system (Promega) as described in the kit protocol. Plates were shaken for 2 min to ensure complete lysis of cells. Then the total volume from each well was transferred to a white 96-

well plate (Greiner bio-one). Luminescence was determined using a NOVOstar microplate reader (BMG labtech); each well was counted for 2 s at 20 °C.

5.13.1.2. Endogenous rat adenine receptors in PC12 cells

After 48 hours of transienent transfection, culture medium was removed from reporter cells by centrifugation at 200 x g for 5 min. Cells were washed twice with Hanks' balanced salt solution (containing 20 mM HEPES, pH 7.3) and resuspended in the same buffer. The cells were plated in a white opaque 96-well plate. Adenine was diluted in Hanks' balanced salt solution and then added to a final volume of 100 μl, 30 s before forskolin (4 μM). The reporter cells with additives were incubated at 37 °C for 3 hrs. The reaction was stopped according to the Bright-Glo^{TM} Luciferase assay system (Promega) and the luminescence measurement was continued using a NOVOstar microplate reader (BMG labtech).

5.13.1.3. Human adenosine A$_1$ receptor expressed in CHO cells

Reporter cells were stimulated for cAMP production using 4 μM forskolin and the reaction was continued as described above.

5.13.2. Reporter gene assay for ERK signaling pathway

▪ *Cell culture and DNA transfection*

1321N1 cells stably expressing rAde1R were cultured in DMEM supplemented with 10% (v/v) FCS, L-glutamine (2 mM), penicillin (100 U/ml), streptomycin (100 U/ml) and 800 μg/ml G418, at 37 °C under a humidified atmosphere containing 5% CO$_2$. Cells were cultured in 75 cm^2 flasks (3.2 x 10^5) for 24 h without antibiotics so that they were 90-95% confluent before transfection. The ERK responsive reporter plasmid (SRE-luc) was transfected into 1321N1 cells expressing rat adenine receptors using Lipofectamine 2000 as a transfection reagent.

▪ *Luciferase assay*

Reporter cells were seeded at a density of 200,000 – 150,000 cells/well in a 24-well plate 18-20 hr prior to the assay. After the cells were attached and started growing the medium was exchanged for medium without FCS. After removal of the culture medium, cells were washed twice with Hanks' balanced salt solution with out HEPES, pH 7.3. Adenine was diluted in the same buffer and then added to the cells, which were incubated for 6 h at 37 °C. The reaction was stopped by removal of the reaction buffer, and the luciferase expression was determined

using Bright-Glo^{TM} Luciferase assay system (Promega) as described in the kit protocol. Plates were shaken for 2 min to ensure complete lysis of cells. Then the total volume from each well was transferred to a white 96-well plate (Greiner bio-one). Luminescence was determined using a NOVOstar microplate reader (BMG labtech); each well was counted for 2 s at 20 °C.

5.13.3. GTP-shift experiment

The competition assays were carried out using adenosine A_1 receptor selective antagonist radioligand [^{3}H]DPCPX in a concentration of 0.4 nM and were performed in triplicate. The assays were performed with or without 100 µM GTP. For the non-specific binding, DPCPX (10 µM) was used. 6-9 dilutions of test compound or plant extract previously dissolved in DMSO were prepared. The samples were added to incubation tubes. After the addition of [^{3}H]DPCPX and protein (preincubated with 2 U/ml ADA) the samples were incubated for 90 min at room temperature. The incubation was stopped using vacuum filtration and Tris-HCl buffer (50 mM, pH 7.4) as a washing buffer.

Scheme for pipetting

25 µl	DMSO, total binding, 10 µM DPCPX (10 µM) or test compound diluted in DMSO
50 µl	100 µM GTP in 50 mM Tris-Puffer, pH 7.4
100 µl	[^{3}H] DPCPX (0.4 nM in 50 mM Tris-HCl buffer pH 7.4); $K_D = 0.28$ nM
100 µl	Protein membrane preparation (70 µg/ml) in 50 mM Tris-HCl buffer, pH 7.4
725 µl	50 mM Tris-HCl buffer, pH 7.4
1000 µl	Total volume

5.13.4. Calcium assay
5.13.4.1. Measurement of intracellular calcium mobilisation (G_q signaling pathway)

Measurements were performed using a Novostar® microplate reader. Calcium assays were performed according to published procedures.[192] 1321N1 human astrocytomacells expressing the human P2Y were harvested with 0.05 % trypsin / 0.02 % EDTA and rinsed with culture medium. The cells were kept under 5 % CO_2 at 37°C for 45 min and then centrifuged at 200 x g and 4°C for 5 min. After that the cells were incubated for 1 h at 25°C in Krebs-Ringer-HEPES buffer, pH 7.4 containing 3 µM Oregon Green BAPTA-1/AM and 1 % Pluronic® F127.

Setting off the Novostar®

Measurement parameters	Oregon Green BAPTA-1	Fura-2
Excitation wavelength	485, bandwidth 25 nM	320, bandwidth 25 nM
Emission wavelength	520, bandwidth 25 nM	520, bandwidth 25 nM
Number of flashes per well interval	10 (20)	10 (20)
Gain	Variable	Variable
Measurement start time 1 (2)	0 s (11.6 s)	0 s (11.6 s)
End time of kinetic windows	4 s (35.6 s)	4 s (35.6 s)
Interval time	0.4	0.4
No. of interval	60	60
Injection start time	11.6	11.6
Pump speed	65 µl/s	65 µl/s

The cells were rinsed 3 times with KRH buffer, diluted and plated into 96-well plates with clear bottoms at a density of approximately 16,000 cells/well and left for 20 min. Fluorescence intensity was measured at 520 nm for 30 s at 0.4 s intervals. Buffer or test compounds were injected sequentially into separate wells using the automatic pipetting device. At least three independent experiments were performed in quadruplicates.

5.13.4.2. Calcium assay at P2X receptors (Ligand – gated ion channel receptor)

The human $P2X_2$ receptor cloned in pQCXIP and pLXSN and stably transfected in 1321N1 human astrocytoma cells were functionally characterized on the basis of agonist-mediated an increase in $[Ca^{2+}]_i$ caused by an influx of Ca^{2+} through ligand gated ion channels. The same was performed for double-transfected 1321N1 human astrocytoma containing the human $P2X_{2/3}$ receptors.

The fluorescent Ca^{2+} chelating dye Fura-2 AM was used as an indicator of the relative levels of intracellular Ca^{2+} in a 96-well format using a Novostar®. The cells (60,000) were grown to confluence in 96-well black-walled tissue culture plates and loaded with 2.4 µM Fura-2 AM and Pluronic® F127 in KRH buffer, pH 7.4 for 2 hr at 23 ℃. Prior to the assay, each plate was washed three times with 100 µl KRH buffer, to remove extracellular dye. Dilutions of ATP were prepared in KRH buffer. 35 µl of tested compound was added into a second 96-well-microtiter plate-with V-base. The middle injector takes 20 µl from the reagent plate wells and injects it into the wells of the measurement plate. For testing antagonists, the receptor-

expressing cell lines were pre-incubated with antagonists for 15-20 min prior to activation with agonists (4 μM ATP). Finally, the fluorescence in each well was measured at 0.4 second intervals.

5.14. mRNA localization studies for endogenous rat adenine receptors in PC12 cells

In order to check whether PC12 cells express mRNA for rAde1R, mRNA was extracted from PC12 cells using Trizol® reagent (Invitrogen), In brief, a 1 ml of Trizol® was mixed with 0.2 ml chloroform and PC12 cells pallet before centrifugation. Two different samples of PC12 cells were used at the same time. The aqueous phase was collected for mRNA extraction. mRNA was detected after treatment with Omniscript reverse transcriptase (Qiagen), according to the manufacturers' instructions, and polymerase chain reaction (PCR) assay with primers was performed (table 20; primer set 1). β-actin was used as a positive control for mRNA detection by another set of primers (table 20; primer set 2). Aliquots of 3 μl cDNA were used for each PCR reaction, which was carried out using Taq DNA polymerase supplied in BioMix™ (Bioline) amplification kit, the plamid of rAde1R used as a control in PCR reaction. The PCR parameters were as follows: an initial denaturation at 94 °C for 10 minutes, followed by 25 cycles of 94 °C for 75 seconds, 60 °C for 90 seconds, and 72 °C for 90 seconds, with a final extension step of 72°C for 10 minutes. PCR products were separated by electrophoresis using a 1.5 % agarose gel and visualised by GelRed™ staining.

6. References

1. Burnstock, G. Purinergic receptors. *J. Theor. Biol.* **1976**, *62*, 491–503.

2. Burnstock, G. A basis for distinguishing two types of purinergic receptor. In: cell membrane receptors for drugs and hormones: a multidisciplinary approach (*Straub R. W. and Bolis L.* eds.), pp. 107–118, Raven, New York, **1978**.

3. Ralevic, V.; Burnstock, G. Receptors for purines and pyrimidines. *Pharmacol. Rev.* **1998**, *50*, 413–492.

4. Khakh, B. S.; Burnstock, G.; Kennedy , C.; King, B. F.; North, R. A.; Séguéla, P.; Voigt, M.; Humphrey, P. P. International union of pharmacology. XXIV. Current status of the nomenclature and properties of P2X receptors and their subunits. *Pharmacol. Rev.* **2001**, *53*, 107-118.

5. Brunschweiger, A.; Müller, C. E. P2 receptors activated by uracil nucleotides – an update. *Curr. Med. Chem.* **2006**, *13*, 289–312.

6. Abbracchio, M. P.; Burnstock, G.; Boeynaems, J. M.; Barnard, E. A.; Boyer, J. L.; Kennedy, C.; Knight, G. E.; Fumagalli, M.; Gachet, C.; Jacobson, K. A.; Weisman, G. A. International union of pharmacology LVIII: update on the P2Y G protein-coupled nucleotide receptors: from molecular mechanisms and pathophysiology to therapy. *Pharmacol. Rev.* **2006**, *58*, 281–341.

7. Fischer, W.; Krügel, U. P2Y receptors: focus on structural, pharmacological and functional aspects in the brain. *Curr. Med. Chem.* **2007**, *14*, 2429–2455.

8. Köles, L.; Fürst, S.; Illes, P. Purine ionotropic (P2X) receptors. *Curr. Pharm. Des.* **2007**, *13*, 2368–2384.

9. Young, M. T. P2X receptors: dawn of the post-structure era. *Trends Biochem. Sci.* **2010**, *35*, 83-90.

10. Nakata, H.; Yoshioka, K.; Kamiya, T. Purinergicreceptor oligomerization: implications for neural functions in the central nervous system. *Neurotox. Res.* **2004**, *6*, 291–297.

11. Volonté, C.; D'Ambrosi, N. Membrane compartments and purinergic signalling: the purinome, a complex interplay among ligands, degrading enzymes, receptors and transporters. *FEBS. J.* **2009**, *276*, 318-329.

12. Kawate, T.; Michel, J. C.; Birdsong, W. T.; Gouaux, E. Crystal structure of the ATP-gated $P2X_4$ ion channel in the closed state. *Nature* **2009**, 460, 592-608.

13. Garcia-Guzman, M.; Soto, F.; Gomez-Hernandez, J. M.; Lund, P. E.; Stuhmer, W. Characterization of recombinant human $P2X_4$ receptor reveals pharmacological differences to the rat homologue. *Mol. Pharmacol.* **1997**, *51*, 109–118.

14. Garcia-Guzman, M.; Stühmer, W.; Soto, F. Molecular characterization and pharmacological properties of the human P2X$_3$ purinoceptor. *Brain Res. Mol*. **1997**, *47*, 59–66.

15. Le, K. T.; Paquet, M.; Nouel, D.; Babinski, K.; Seguela, P. Primary structure and expression of a naturally truncated human P2X ATP receptor subunit from brain and immune system. *FEBS Lett.* **1997**, *418*, 195–199.

16. North, R. A. Molecular physiology of P2X receptors. *Physiol. Rev.* **2002**, *82*, 1013-1067.

17. Rassendren, F.; Buell, G. N.; Virginio, C.; Collo, G.; North, R. A.; Surprenant, A. The permeabilizing ATP receptor, P2X$_7$. Cloning and expression of a human cDNA. *J. Biol. Chem.* **1997**, *272*, 5482–5786.

18. Urano, T.; Nishimori, H.; Han, H.; Furuhata, T.; Kimura, Y.; Nakamura, Y.; Tokino, T.; Cloning of P2XM, a novel human P2X receptor gene regulated by p53. *Cancer Res*. **1997**, *57*, 3281–3287.

19. Valera, S.; Hussy, N.; Evans, R. J.; Adami, N.; North, R. A.; Surprenant, A.; Buell, G. A new class of ligand-gated ion channel defined by P2X receptor for extracellular ATP. *Nature* **1994**, *371*, 516–519.

20. Burnstock, G. Physiology and pathophysiology of purinergic neurotransmission. *Physiol. Rev.* **2007**, *87*, 659-797.

21. Bianchi, B. R.; Lynch, K. J.; Touma, E.; Niforatos, W.; Burgard, E. C.; Alexander, K. M.; Park, H. S.; Yu, H.; Metzger, R.; Kowaluk, E.; Jarvis, M. F.; van Biesen, T. Pharmacological characterization of recombinant human and rat P2X receptor subtypes. *Eur. J. Pharmacol.* **1999**, *376*, 127–138.

22. Donnelly-Roberts, D. L.; Jarvis, M. F. Discovery of P2X$_7$ receptor-selective antagonists offers new insights into P2X$_7$ receptor function and indicates a role in chronic pain states. *Br. J. Pharmacol.* **2007**, *151*, 571–579.

23. Gerver, J. R.; Cackayne, D. A.; Dillon, M. P.; Burnstock, G.; Ford, A. P. Pharmacology of P2X channels. *Pflugers Arch.* **2006**, *452*, 513–537.

24. Jacobson, K. A.; Jarvis, M. F.; Williams, M. Purine and pyrimidine (P2) receptors as drug targets. *J. Med. Chem.* **2002**, *45*, 4057–4093.

25. Jarvis, M. F. Contributions of P2X$_3$ homomeric and heteromeric channels to acute and chronic pain. *Expert Opin. Ther. Targets* **2003**, *7*, 513–522.

26. McGaraughty, S.; Chu, K. L.; Namovic, M. T.; Donnelly-Roberts, D. L.; Harris, R. R.; Zhang, X. F.; Shieh, C. C.; Wismer, C. T.; Zhu, C. Z.; Gauvin, D. M.; Fabiyi, A. C.; Honore, P.; Nelson, D. W.; Gregg, R. J.; Carroll, W. A.; Faltynek, C. R.; Jarvis, M. F.

P2X$_7$-related modulation of pathological nociception in rats. *Neuroscience* **2007**, *146*, 1817–1828.

27. Nelson, D. W.; Gregg, R. J.; Kort, M. E.; Perez-Medrano, A.; Voight, E. A.; Wang, Y.; Grayson, G.; Namovic, M. T.; Donnelly-Roberts, D. L.; Niforatos, W.; Honore, P.; Jarvis, M. F.; Faltynek, C. R.; Carroll, W. A. Structure-activity relationship studies on a series of novel, substituted 1-benzyl-5-phenyltetrazole P2X$_7$ antagonists. *J. Med. Chem.* **2006**, *49*, 3659–3666.

28. Romagnoli, R.; Baraldi, P. G.; Cruz-Lopez, O.; Lopez-Cara, C.; Preti, D.; Borea, P.; Gessi, S. The P2X$_7$ receptor as a therapeutic target. *Expert Opin. Ther. Targets* **2008**, *12*, 647–661.

29. Donnelly-Roberts, D.; McGaraughty, S.; Shieh, C. C.; Honore, P.; Jarvis, M. F. Painful purinergic receptors. *J. Pharmacol. Exp. Ther.* **2008**, *324*, 409-415.

30. Köles, L.; Gerevich, Z.; Oliveira, J. F.; Zadori, Z. S.; Wirkner, K.; Illes, P. Interaction of P2 purinergic receptors with cellular macromolecules. *Naunyn-Schmiedebergs. Arch. Pharmacol.* **2008**, *377*, 1-33.

31. Khakh, B. S.; North. R. A. P2X receptors as cell-surface ATP sensors in health and disease. *Nature* **2006***, 442*, 527-532.

32. Jarvis, M. F.; Khakh, B. S. ATP-gated P2X cation-channels. *Neuropharmacology* **2009**, *56*, 208-215.

33. Evans, R. J.; Lewis, C.; Buell, G.; Valera, S.; North, R. A.; Surprenant, A. Pharmacological characterization of heterologously expressed ATP-gated cation channels (P2x purinoceptors). *Mol. Pharmacol.* **1995**, *48*, 178-183.

34. King, B. F.; Ziganshina, L. E.; Pintor, J.; Burnstock, G. Full sensitivity of P2X$_2$ purinoceptor to ATP revealed by changing extracellular pH. *Br. J. Pharmacol.* **1996**, *117*, 1371-1371.

35. Lynch, K. J.; Touma, E.; Niforatos, W.; Kage, K. L.; Burgard, E. C.; van Biesen, T.; Kowaluk, E. A.; Jarvis, M. F. Molecular and functional characterization of human P2X$_2$ receptors. *Mol. Pharmacol.* **1999**, *56*, 1171–1181.

36. Neelands, T. R.; Burgard, E. C.; Uchic, M. E.; McDonald, H. A.; Niforatos, W.; Faltynek, C. R.; Lynch, K. J.; Jarvis, M. F. 2′,3′-O-(2,4,6,trinitrophenyl)-ATP and A-317491 are competitive antagonists at a slowly desensitizing chimeric human P2X$_3$ receptor. *Br. J. Pharmacol.* **2003**, *140*, 202–210.

37. Pintor, J.; King, B. F.; Miras-Portugal, M. T.; Burnstock, G. Selectivity and activity of adenine dinucleotides at recombinant P2X$_2$ and P2Y$_1$ purinoceptors. *Br. J. Pharmacol.* **1996**, *119*, 1006–1012.

38. Wildman, S. S.; Brown, S. G.; King. B. F.; Burnstock, G. Selectivity of diadenosine polyphosphates for rat P2X receptor subunits. *Eur. J. Pharmacol*. **1999**, *367*, 119–123.

39. Burgard, E. C.; Niforatos, W.; van Biesen, T.; Lynch, K. J.; Touma, E.; Metzger, R. E.; Kowaluk, E. A.; Jarvis, M. F. P2X receptor mediated ionic currents in dorsal root ganglion neurons. *J. Neurophysiol.* **1999**, *82*, 1590–1598.

40. Grubb, B. D.; Evans, R. J. Characterization of cultured dorsal root ganglion neuron P2X receptors. *Eur. J. Neurosci.* **1999**, *11*,149–154.

41. Lewis, C.; Neidhart, S.; Holy, C.; North, R. A.; Buell, G.; Surprenant, A. Coexpression of P2X$_2$ and P2X$_3$ receptor subunits can account for ATP-gated currents in sensory neurons. *Nature* **1995**, *377,* 432–435.

42. Robertson, S. J.; Rae, M. G.; Rowan, E. G.; Kennedy, C. Characterization of a P2X-purinoceptor in cultured neurones of the rat dorsal root ganglia. *Br. J. Pharmacol.* **1996**, *118*, 951–956.

43. Virginio, C.; North, R. A., Surprenant, A. Calcium permeability and block at homomeric and heteromeric P2X$_2$ and P2X$_3$ receptors, and P2X receptors in rat nodose neurones. *J. Physiol.* **1998**, *510*, 27–35.

44. Volpini, R.; Mishra, R. C.; Kachare, D. D.; Dal Ben, D.; Lambertucci, C.; Antonini, I.; Vittori, S.; Marucci, G.; Sokolova, E., Nistri, A.; Cristalli, G. Adenine-based acyclic nucleotides as novel P2X$_3$ receptor ligands. *J. Med. Chem.* **2009**, *52*, 4596-4603.

45. Ford, K. K.; Matchett, M.; Krause, J. E.; Yu, W. The P2X$_3$ antagonist P1, P5-di[inosine-5'] pentaphosphate binds to the desensitized state of the receptor in rat dorsal root ganglion neurons. *J. Pharmacol. Exp. Ther. 2005, 315*, 405-413.

46. Liu, M.; King, B. F.; Dunn, P. M.; Rong, W.; Townsend-Nicholson, A.; Burnstock, G. Coexpression of P2X$_3$ and P2X$_2$ receptor subunits in varying amounts generates heterogeneous populations of P2X receptors that evoke a spectrum of agonist responses comparable to that seen in sensory neurons. *J. Pharmacol. Exp. Ther.* **2001**, *296*, 1043–1050.

47. Burgard, E. C.; Niforatos, W.; Van, Biesen, T.; Lynch, K. J.; Kage, K. L.; Touma, E.; Kowaluk, E. A.; Jarvis, M. F. Competitive antagonism of recombinant P2X$_{2/3}$ receptors by 2′, 3′-O-(2,4,6-trinitrophenyl)adenosine-5′-triphosphate (TNP-ATP). *Mol. Pharmacol.* **2000**, *58*, 1502–1510.

48. Virginio, C.; Robertson, G.; Surprenant, A.; North, R. A. Trinitrophenyl-substituted nucleotides are potent antagonists selective for P2X$_1$, P2X$_3$, and heteromeric P2X$_{2/3}$ receptors. *Mol. Pharmacol.* **1998**, *53*, 969–973.

49. Dunn, P. M.; Liu, M.; Zhong, Y.; King, B. F.; Burnstock, G. Diinosine pentaphosphate: an antagonist which discriminates between recombinant P2X$_3$ and P2X$_{2/3}$ receptors and between two P2X receptors in rat sensory neurones. *Br. J. Pharmacol.* **2000**, *130*, 1378–1384.

50. Carter, D. S.; Alam, M., Cai, H.; Dillon, M. P.; Ford, A. P.; Gever, J. R.; Jahangir, A.; Lin, C.; Moore, A. G.;Wagner, P. J.; Zhai, Y. Identification and SAR of novel diaminopyrimidines. Part 1: The discovery of RO-4, a dual P2X$_3$/P2X$_{2/3}$ antagonist for the treatment of pain. *Bioorg. Med. Chem. Lett.* **2009**, *19*, 1628-1631.

51. Buell, G.; Lewis, C.; Collo, G.; North, R. A.; Surprenant, A. An antagonist-insensitive P2X receptor expressed in epithelia and brain. *EMBO. J.* **1996**, *15*, 55–62.

52. Jones, C. A.; Chessell, I. P.; Simon, J.; Barnard, E. A.; Miller, K. J.; Michel, A. D.; Humphrey, P. P. A. Functional characterization of the P2X$_4$ receptor orthologues. *Br. J. Pharmacol.* **2000**, *129*, 388–394.

53. Seguela, P.; Haghighi, A.; Soghomonian, J. J.; Cooper, E. A novel neuronal P2X ATP receptor ion channel with widespread distribution in the brain. *J. Neurosci.* **1996**, *16*, 448–455.

54. Bo, X.; Zhang, Y.; Nassar, M.; Burnstock, G.; Schoepfer, R. A P2X purinoceptor cDNA conferring a novel pharmacological profile. *FEBS. Lett.* **1995**, *375*, 129–133.

55. Miller, K. J.; Michel, A. D.; Chessell, I. P.; Humphrey, P. P. A. Cibacron blue allosterically modulates the rat P2X$_4$ receptor. *Neuropharmacology* **1998**, *37*, 1579–1586.

56. Soto, F.; Garcia-Guzman, M.; Gomez-Hernandez, J. M.; Hollmann, M.; Karschin, C.; Stuhmer, W. P2X$_4$: an ATP-activated ionotropic receptor cloned from rat brain. *Proc. Natl. Acad. Sci. USA* **1996**, *93*, 3684–3688.

57. Nagata, K.; Imai, T.; Yamashita, T.; Tsuda, M.; Tozaki-Saitoh, H.; Inoue, K. Antidepressants inhibit P2X$_4$ receptor function: a possible involvement in neuropathic pain relief. *Mol. Pain.* **2009**, *23*, 5-20.

58. Jacobson, K. A.; Ivanov, A. A.; de Castro, S.; Harden, T. K.; Ko, H. Development of selective agonists and antagonists of P2Y receptors. *Purinergic Signal.* **2009**, *5*, 75-89.

59. Yoshioka, K.; Nakata, H. ATP- and adenosine-mediated signaling in the central nervous system: purinergic receptor complex: generating adenine nucleotide-sensitive adenosine receptors. *J. Pharmacol. Sci.* **2004**, *94,* 88–94.

60. Prinster, S. C.; Hague, C.; Hall, R. A. Heterodimerization of G protein-coupled receptors: specificity and functional significance. *Pharmacol. Rev.* **2005**, *57*, 289–298.

61. Tonazzini, I.; Trincavelli, M. L.; Montali, M.; Martini, C. Regulation of A_1 adenosine receptor functioning induced by $P2Y_1$ purinergic receptor activation in human astroglial cells. *Neurosci. Res.* **2008**, *86*, 2857-2866.

62. Gine´s, S.; Hillion, J.; Torvinen, M.; Le, Crom, S.; Casado, V.; Canela, E. I.; Rondin, S.; Lew, J. Y.; Watson, S.; Zoli, M.; Agnati, L. F.; Verniera, P.; Lluis, C.; Ferre, S.; Fuxe, K.; Franco, R. Dopamine D_1 and adenosine A_1 receptors form functionally interacting heteromeric complexes. *Proc. Natl. Acad. Sci. USA* **2000**, *97*, 8606–8611.

63. Ecke, D.; Hanck, T.; Tulapurkar, M. E.; Schäfer, R.; Kassack, M.; Stricker, R.; Reiser, G. Hetero-oligomerization of the $P2Y_{11}$ receptor with the $P2Y_1$ receptor controls the internalization and ligand selectivity of the $P2Y_{11}$ receptor. *Biochem. J.* **2008**, *409*, 107-116.

64. Burnstock, G. Purinergic signalling and disorders of the central nervous system. *Nat. Rev. Drug Discov.* **2008**, *7*, 575-590.

65. Waldo, G. L.; Corbitt, J.; Boyer, J. L.; Ravi, G.; Kim, H. S.; Ji, X. D.; Lacy, J.; Jacobson, K. A.; Harden, T. K. Quantitation of the $P2Y_1$ receptor with a high affinity radiolabeled antagonist. *Mol. Pharmacol.* **2002**, *62*, 1249-1257.

66. Waldo, G. L.; Harden, T. K. Agonist binding and Gq-stimulating activities of the purified human $P2Y_1$ receptor. *Mol. Pharmacol.* **2004**, *65,* 426-436.

67. Chhatriwala, M.; Ravi, R. G.; Patel, R. I.; Boyer, J. L.; Jacobson, K. A.; Harden, T. K. Induction of novel agonist selectivity for the ADP-activated $P2Y_1$ receptor versus the ADP-activated $P2Y_{12}$ and $P2Y_{13}$ receptors by conformational constraint of an ADP analog. *J. Pharmacol. Exp. Ther.* **2004**, *311*, 1038-1043.

68. Palmer, R. K.; Boyer, J. L.; Schachter, J. B.; Nicholas, R. A.; Harden, T. K. Agonist action of adenosine triphosphates at the human $P2Y_1$ receptor. *Mol. Pharmacol.* **1998**, *54*, 1118-1123.

69. Leon, C.; Hechler, B.; Vial, C.; Leray, C.; Cazenave, J. P.; Gachet, C. The $P2Y_1$ receptor is an ADP receptor antagonized by ATP and expressed in platelets and megakariyoblastic cells. *FEBS. Lett.* **1997**, *403*, 26–30.

70. Hechler, B.; Vigne, P.; Leon, C.; Breittmayer, J. P.; Gachet, C.; Frelin, C. ATP derivatives are antagonists of the $P2Y_1$ receptor: similarities to the platelet ADP receptor. *Mol. Pharmacol.* **1998**, *53*, 727–733.

71. Boyer, J. L.; Mohanram, A.; Camaioni, E.; Jacobson, K. A.; Harden, T. K. Competitive and selective antagonism of P2Y$_1$ receptors by N^6-methyl 2'-deoxyadenosine 3',5'-bisphosphate. *Br. J. Pharmacol.* **1998**, *124*, 1-3.

72. Camaioni, E.; Boyer, J. L.; Mohanram, A.; Harden, T. K.; Jacobson, K. A. Deoxyadenosine-bisphosphate derivatives as potent antagonists at P2Y$_1$ receptors. *J. Med.Chem.* **1998**, *41*,183–190.

73. Boyer, J.; Adams, M.; Ravi, R. G.; Jacobson, K. A.; Harden, T. K. 2-Chloro N^6- methyl-(N)-methanocarba-2`-deoxyadenosine-3`,5`-bisphosphate is a selective high affinity P2Y$_1$ receptor antagonist. *Br. J. Pharmacol.* **2002***, 135*, 2004–2010.

74. Communi, D.; Govaerts, C.; Parmentier, M.; Boeynaems, J. M. Cloning of a human purinergic P2Y receptor coupled to phospholipase C and adenylyl cyclase. *J. Biol. Chem.* **1997**, *272*, 31969–31973.

75. Communi, D.; Robaye, B.; Boeynaems, J. M. Pharmacological characterization of the human P2Y$_{11}$ receptor. *Br. J. Pharmacol.* **1999**, *128*, 1199-1206.

76. Qi, A. D.; Kennedy, C.; Harden, T. K.; Nicholas, R. A. Differential coupling of the human P2Y$_{11}$ receptor to phospholipase C and adenylyl cyclase. *Br. J. Pharmacol.* **2001**, *132*, 318-326.

77. Suh, B. C.; Kim, T. D.; Lee, I. S.; Kim, K. T. Differential regulation of P2Y$_{11}$ receptor-mediated signalling to phospholipase C and adenylyl cyclase by protein kinase C in HL-60 promyelocytes. *Br. J. Pharmacol.* **2000**, *131*, 489–497.

78. White, P. J., Webb, T. E.; Boarder, M. R. Characterization of a Ca^{2+} response to both UTP and ATP at human P2Y$_{11}$ receptors: evidence for agonist-specific signaling. *Mol. Pharmacol.* **2003**, *63*, 1356–1363.

79. Gachet, C. ADP receptors of platelets and their inhibition. *J. Thromb. Haemost.* **2001**, *86*, 222–232.

80. Kauffenstein, G.; Hechler, B.; Cazenave, J. P.; Gachet, C. Adenine triphosphate nucleotides are antagonists at the P2Y$_{12}$ receptor. *J. Thromb. Haemost.* **2004**, *2*, 1980–1988.

81. Savi, P.; Herbert, J. M. Clopidogrel and ticlopidine: P2Y$_{12}$ adenosine diphosphate-receptor antagonists for the prevention of atherothrombosis. *Semin. Thromb. Hemost.* **2005**, *31*, 174-183.

82. Niitsu, Y.; Jakubowski, J. A.; Sugidachi, A.; Asai, F. Pharmacology of CS-747 (prasugrel, LY640315), a novel, potent antiplatelet agent with in vivo P2Y$_{12}$ receptor antagonist activity. *Semin. Thromb. Hemost.* **2005**, *31*, 184–194.

83. Gachet, C. The platelet P2 receptors as molecular targets for old and new antiplatelet drugs. *Pharmacol. Ther.* **2005**, *108*,180–192.

84. Ingall, A. H.; Dixon, J.; Bailey, A.; Coombs, M. E.; Cox, D.; McInally, J. I.; Hunt, S. F.; Kindon, N. D.; Teobald, B. J.; Willis, P. A.; Humphries, R. G.; Leff. P.; Clegg, J. A.; Smith, J. A.; Tomlinson, W. Antagonists of the platelet P2T receptor: a novel approach to antithrombotic therapy. *J. Med. Chem.* **1999**, *42*, 213–220.

85. Storey, R. F.; Wilcox, R. G.; Heptinstall, S. Comparison of the pharmacodynamic effects of the platelet ADP receptor antagonists clopidogrel and AR-C69931MX in patients with ischaemic heart disease. *Platelets* **2002**, *13*, 407– 413.

86. van Giezen, J. J.; Humphries, R. G. Preclinical and clinical studies with selective reversible direct P2Y$_{12}$ antagonists. *Semin. Thromb. Hemost.* **2005**, *31*, 195–120.

87. Andre, P.; Delaney, S. M.; LaRocca, T.; Vincent, D.; De Guzman, F.; Jurek, M.; Koller, B.; Phillips, D. R.; Conley, P. B. P2Y$_{12}$ regulates platelet adhesion/activation, thrombus growth, and thrombus stability in injured arteries. *J. Clin. Investig.* **2003**, *112*, 398–406.

88. Marteau, F.; Le, Poul, E.; Communi, D.; Labouret, C.; Savi, P.; Boeynaems, J. M.; Gonzalez, N. S. Pharmacological characterization of the human P2Y$_{13}$ receptor. *Mol. Pharmacol.* **2003**, *64*,104–112.

89. Fumagalli, M., Trincavelli, L.; Lecca, D.; Martini, C.; Ciana, P.; Abbracchio, M. P. Cloning, pharmacological characterisation and distribution of the rat G-protein coupled P2Y$_{13}$ receptor. *Biochem. Pharmacol.* **2004**, *68*,113–124.

90. Savi, P.; Labouret, C.; Delesque, N.; Guette, F.; Lupker, J.; Herbert, J. M. P2Y$_{12}$ a new platelet ADP receptor, target of clopidogrel. *Biochem. Biophys. Res. Commun.* **2001**, *283*, 379–383.

91. Communi, D.; Gonzalez, N. S.; Detheux, M.; Brezillon, S.; Lannoy, V.; Parmentier, M.; Boeynaems, J. M. Identification of a novel human ADP receptor coupled to G$_i$. *J. Biol. Chem.* **2001**, *276*, 41479–41485.

92. Zhang, F. L., Luo, L.; Gustafson, E.; Palmer, K.; Qiao, X.; Fan, X.; Yang, S.; Laz, T. M.; Bayne, M.; Monsma, F. Jr. P2Y$_{13}$: identification and characterization of a novel Gαi-coupled ADP receptor from human and mouse. *J. Pharmacol. Exp. Ther.* **2002**, *301*, 705–713.

93. Nicholas, R. A.; Watt, W. C.; Lazarowski, E. R.; Li, Q.; Harden, K. Uridine nucleotide selectivity of three phospholipase C-activating P2 receptors: identification of a UDP-selective, a UTP-selective, and an ATP- and UTP-specific receptor. *Mol. Pharmacol.* **1996**, *50*, 224-229.

94. Stoop, R.; Surprenant, A.; North, R. A. Different sensitivities to pH of ATP-induced currents at four cloned P2X receptors. *J. Neurophysiol.* **1997**, *78*, 1837-1840.

95. Cantiello, H. F. Electrodiffusional ATP movement through CFTR and other ABC transporters. *Pflugers. Arch.* **2001**, *443*, Suppl 1, 22.

96. Müller, C. E. Medicinal chemistry of adenosine A_3 receptor ligands. *Curr. Top. Med. Chem.* **2003**, *3*, 445-462.

97. Cobb, B. R.; Clancy, J. P. Molecular and cell biology of adenosine receptors. *Curr. Top. Membr.* **2003**, *54*, 151–181.

98. Olah, M. E.; Stiles, G. L. The role of receptor structure in determining adenosine receptor activity. *Pharmacol. Ther.* **2000**, *85*, 55–75.

99. Cristalli, G.; Müller, C. E.; Volpini, R. Recent developments in adenosine A_{2A} receptor ligands. *Handb. Exp. Pharmacol.* **2009**, *193*, 59-98.

100. Yan, L.; Burbiel, J. C.; Maass, A.; Müller, C. E. Adenosine receptor agonists: from basic medicinal chemistry to clinical development. *Expert Opin. Emerg. Drugs* **2003**, *8*, 537-576.

101. Moro, S.; Gao, Z. G.; Jacobson, K. A.; Spalluto, G. Progress in the pursuit of therapeutic adenosine receptor antagonists. *Med. Res. Rev.* **2006**, *26,* 131-159.

102. Bender, E.; Buist, A.; Jurzak, M.; Langlois, X.; Baggerman, G.; Verhasselt, P.; Ercken, M.; Guo, HQ.; Wintmolders, C.; Van den Wyngaert, I.; Van Oers, I.; Schoofs, L.; Luyten, W. Characterization of an orphan G protein-coupled receptor localized in the dorsal root ganglia reveals adenine as a signaling molecule. *Proc. Natl. Acad. Sci.* **2002**, *99*, 8573-8578.

103. Matthews, E. A.; Dickenson, A. H. Effects of spinally administered adenine on dorsal horn neuronal responses in a rat model of inflammation. *Neurosci. Lett*. **2004**, *19*, 211-214.

104. Gorzalka, S.; Vittori, S.; Volpini, R.; Cristalli, G.; von Kügelgen, I.; Müller, C. E. Evidence for the functional expression and pharmacological characterization of adenine receptors in native cells and tissues. *Mol. Pharmacol.* **2005**, *67*, 955-964.

105. Watanabe, S.; Ikekita, M.; Nakata, H. Identification of specific [^{3}H]adenine-binding sites in rat brain membranes. *J. Biochem.* **2005**, *137*, 323-329.

106. Yoshimi, Y.; Watanabe, S.; Shinomiya, T.; Makino, A.; Toyoda, M.; Ikekita, M. Nucleobase adenine as trophic factor acting on Purkinje cells. *Brain Res.* **2003**, *991*, 113-122.

107. Watanabe, S.; Yoshimi, Y.; Ikekita, M. Neuroprotective effect of adenine on purkinje cell survival in rat cerebellar primary cultures. *J. Neurosci. Res.* **2003**, *74*, 754-759.

108. Wengert, M.; Adão-Novaes, J.; Assaife-Lopes, N.; Leão-Ferreira, L. R.; Caruso-Neves, C. Adenine-induced inhibition of Na^+-ATPase activity: Evidence for involvement of the G_i protein-coupled receptor in the cAMP signaling pathway. *Arch. Biochem. Biophys.* **2007**, *467*, 261-267.

109. Slominska, E. M.; Szolkiewicz, M.; Smolenski, R. T.; Rutkowski, B.; Swierczynski, J. High plasma adenine concentration in chronic renal failure and its relation to erythrocyte ATP. *Nephron* **2002**, *91*, 286-291.

110. von Kügelgen, I.; Schiedel, A. C.; Hoffmann, K.; Alsdorf, B. B.; Abdelrahman, A.; Müller, C. E. Cloning and functional expression of a novel G_i protein-coupled receptor for adenine from mouse brain. *Mol. Pharmacol.* **2008**, *73*, 469-477.

111. De Koning, H.; Diallinas, G. Nucleobase transporters. *Mol. Membr. Biol.* **2000**, *17*, 75-94.

112. Köse, M.; Schiedel, A. C. Nucleoside/nucleobase transporters-drug targets of the future? *Future Med. Chem.* **2009**, *1*, 303-326.

113. Redzic, Z. B.; Segal, M. B.; Gasic, J. M.; Markovic, I. D.; Vojvodic, V. P.; Isakovic, A.; Thomas, S. A.; Rakic, L. M. The characteristics of nucleobase transport and metabolism by the perfused sheep choroid plexus. *Brain Res.* **2001**, *888*, 66-74.

114. Nagai, K.; Nagasawa, K.; Matsunaga, R.; Yamaji, M.; Fujimoto, S. Novel Na^+-independent and adenine-specific transport system for adenine in primary cultured rat cortical neurons. *Neurosci. Lett.* **2006**, *407*, 244-248.

115. Yamamura, H. I.; Hulme, E. C. Receptor-ligand interactions: a practical approach. ISBN: 0199630917, Oxford University Press: New York , **1992**.

116. Deupree, J. D.; Bylund, D. B. Basic principles and techniques for receptor binding. Published and distributed by Tocris Cookson, Bristol, UK 1-8, **2002**.

117. Bylund, D. B.; Toews, M. L. Radioligand binding methods: practical guide and tips. *Am. J. Physiol.* **1993**, *265*, L421-429.

118. Bylund D. B. Graphic Presentation and Analysis of Inhibition Data from Ligand-Binding Experiments. *Anal. Biochem.* **1986**, *159*, 50-57.

119. Cheng, Y.; Prusoff, W. H. Relationship between the inhibition constant (K1) and the concentration of inhibitor which causes 50% (IC_{50}) of an enzymatic reaction. *Biochem. Pharmacol.* **1973**, *22*, 3099-4108.

120. Motulsky, H. The graphpad guide to analyzing radioligand binding data, Graphpad software, Inc. (**1995-96**).

121. Gether, U. Uncovering molecular mechanisms involved in activation of G protein-coupled receptors. *Endocr. Rev.* **2000**, *21*, 90-113.

122. Marinissen, M. J.; Gutkind, J. S. G-protein-coupled receptors and signaling networks: emerging paradigms. *Trends. Pharmacol. Sci.* **2001**, *22*, 368-376.

123. Cabrera-Vera, T. M.; Vanhauwe, J.; Thomas, T. O.; Medkova, M.; Preininger, A.; Mazzoni, M. R.; Hamm, H. E. Insights into G protein structure, function, and regulation. *Endocr. Rev.* **2003**, *24*, 765-781.

124. Hamm, H. E. The many faces of G protein signaling. *J. Biol. Chem.* **1998**, *273*, 699-672.

125. Hur, E. M.; Kim, K.T. G protein-coupled receptor signalling and cross-talk: achieving rapidity and specificity. *Cell. Signal.* **2002**, *14*, 397–405.

126. Greasley P. J.; Jansen, F. P. G-protein-coupled receptor screening technologies. *Drug Dis. Today Technology* **2005**, *2*, 163-170.

127. Christopoulos, A. Allosteric binding sites on cell-surface receptors: novel targets for drug discovery. *Nat. Rev. Drug Discov.* **2002**, *1*, 198-210.

128. Williams, C. cAMP detection methods in HTS: selecting the best from the rest. *Nat. Rev. Drug Discov.* **2004**, *3*, 125-135.

129. Hanoune, J.; Defer, N. Regulation and role of adenylyl cyclase isoforms. *Annu. Rev. Pharmacol. Toxicol.* **2001**, *41*, 145-174.

130. Patel, T. B.; Du, Z.; Pierre, S., Cartin, L.; Scholich, K. Molecular biological approaches to unravel adenylyl cyclase signaling and function. *Gene* 2001, *269*, 13-25.

131. Thompson, W. J. Cyclic nucleotide phosphodiesterases: pharmacology, biochemistry and function. *Pharmacol. Ther.* **1991**, *51*, 13-33.

132. Prystay, L.; Gagné, A.; Kasila, P.; Yeh, L. A.; Banks, P. Homogeneous cell-based fluorescence polarization assay for the direct detection of cAMP. *J. Biomol. Screen* **2001**, *6*, 75-82.

133. Golla, R.; Seethala, R. A homogeneous enzyme fragment complementation cyclic AMP screen for GPCR agonists. *J. Biomol. Screen* **2002**, *6*, 515-525.

134. Hill, S. J.; Baker, J. G.; Rees, S. Reporter-gene systems for the study of G-protein-coupled receptors. *Curr. Opin. Pharmacol.* **2001**, *5*, 526-532.

135. Southward, C. M., Surette, M. G. The dynamic microbe: green fluorescent protein brings bacteria to light. *Mol. Microbiol*. **2002**, *45*, 1191-1196.

136. Wood, K. V. Marker proteins for gene expression. *Curr. Opin. Biotechnol*. **1995**, *6*, 50–58.

137. Greer, L. F.; Szalay, A. A. Imaging of light emission from the expression of luciferases in living cells and organisms. *Luminescence* **2002**, *17*, 43–74.

138. Johnston, P. A.; Johnston, P. A. Cellular platforms for HTS: three case studies. *Drug Discov. Today* 2002, *7*, 353–363.

139. Stables, J.; Scott, S.; Brown, S.; Roelant, C., Burns, D., Lee, M. G.; Rees, S. Development of a dual glow-signal firefly and Renilla luciferase assay reagent for the analysis of G-protein coupled receptor signalling. *J. Recept. Signal. Transduct. Res.* **1999**, *19*, 395-410.

140. Viviani, V. R. The origin, diversity and structure function relationships of luciferases. *Cell. Mol. Life Sci*. **2002**, *59*, 1833–1850.

141. Baker, J. G.; Hall, I. P., Hill, S. J. Influence of agonist efficacy and receptor phosphorylation on antagonist affinity measurements: differences between second messenger and reporter gene responses. *Mol. Pharmacol*. **2003**, *64*, 679–688.

142. Allen, M.; Hall, D.; Collins, B.; Moore K. A homogeneous high throughput nonradioactive method for measurement of functional activity of G_s-coupled receptors in membranes. *J. Biomol. Screen* 2002, *7*, 35-44.

143. Nagmani, R. Evaluation of beta-adrenergic receptor subtypes in the human prostate cancer cell line-LNCaP. *Biochem. Pharmacol.* **2003**, *65*, 1489–1494.

144. Goetz, A. S.; Andrews, J. L., Littleton, T. R.; Ignar, D. M. Development of a facile method for high throughput screening with reporter gene assays. *J. Biomol. Screen* **2000**, *5*, 377–384.

145. George, S. E. Evaluation of a CRE-directed luciferase reporter gene assay as an alternative to measuring cAMP accumulation. *J. Biomol. Screen* **1997**, *2*, 235–240.

146. Sullivan, E.; Tucker, E. M.; Dale, I. L. Measurement of $[Ca^{2+}]$ using the fluorometric imaging plate reader (FLIPR). *Methods Mol. Biol.* **1999**, *114*, 125–133.

147. An, W. F.; Tolliday, N. J. Introduction: cell-based assays for high-throughput screening. *Methods Mol. Biol.* **2009**, *486*, 1-12.

148. Miret, J. J.; Zhang, J.; Min, H.; Lewis, K.; Roth, M.; Charlton, M.; Bauer, P. H. Multiplexed G-protein-coupled receptor Ca^{2+} flux assays for high-throughput screening. *J. Biomol. Screen* **2005**, *10*, 780-787.

149. Offermans, S.; Simon, M. I. $G_{\alpha15}$ and $G_{\alpha16}$ couple a wide variety of receptors to phospholipase C. *J. Biol. Chem.* **1995**, *270*, 15175–15180.

150. Conklin, B. R.; Herzmark, P.; Ishida, S.; Voyno-Yasenetskaya, T. A.; Sun, Y.; Farfel, Z.; Bourne, H. R. Carboxy-terminal mutations of $G_{q\alpha}$ and $G_{s\alpha}$ that alter the fidelity of receptor activation. *Mol. Pharmacol.* **1996**, *50*, 885–890.

151. Milligan, G.; Rees, S. Chimeric G_α proteins: their potential use in drug discovery. *Trends Pharmacol. Sci.* **1999**, *20*, 118–124.

152. Kostenis, E. Is $G_{\alpha16}$ the optimal tool for fishing ligands of orphan G-protein-coupled receptors? *Trends Pharmacol. Sci.* **2001**, *22*, 560–564.

153. Shimomura, O.; Johnson, F. H.; Saiga, Y. Extraction, purification and properties of aequorin, a bioluminescent protein from the luminous hydromedusan, Aequorea. *J. Cell Comp. Physiol.* **1962**, *59*, 223–239.

154. Shimomura, O. Luminescence of aequorin is triggered by the binding of two calcium ions. *Biochem. Biophys. Res. Commun.* **1995**, *211*, 359-363.

155. Stables, J.; Green, A.; Marshall, F.; Fraser, N.; Knight, E.; Sautel, M.; Milligan, G.; Lee, M.; Rees, S. A bioluminescent assay for agonist activity at potentially any G-protein-coupled receptor. *Anal. Biochem.* **1997**, *252*, 115-126.

156. FluoForte™ Calcium assay kit.

157. Osmond, R. I.; Sheehan, A.; Borowicz, R.; Barnett, E.; Harvey, G.; Turner, C.; Brown, A.; Crouch, M. F.; Dyer, A. R. GPCR screening via *ERK*$_{1/2}$: a novel platform for screening G protein-coupled receptors. *J. Biomol. Screen* **2005**, *10*, 730-737.

158. Faure, M.; Voyno-Yasenetskaya, T. A.; Bourne, H. R. cAMP and βγ subunits of hererotrimeric G proteins stimulate the mitogen activated protein kinase pathway in COS-7 cells. *J. Biol. Chem.* **1994**, *269*, 7851-7854.

159. Hawes, B. E.; Luttrell, L. M.; van Biesen, T.; Lefkowitz, R. J. Distinct pathways of G_i- and G_q-mediated mitogen activated protein kinase activation. *J. Biol. Chem.* **1995**, *270*, 17148-17153.

160. Luttrell, L. M. 'Location, location, location': activation and targeting of MAP kinases by G protein-coupled receptors. *J. Mol. Endocrinol.* **2003**, *30*, 117-126.

161. Wong, S. K. F. A 384-well cell-based phosphor-ERK assay for dopamine D2 and D3 receptors. *Anal. Biochem.* **2004**, *333*, 265-272.

162. Hill, C. S.; Treisman, R. Differential activation of c-fos promoter elements by serum, lysophosphatidic acid, G-proteins and polypeptide growth factors. *EMBO J.* **1995**, *14*, 5037-5047.

163. Price, M. A.; Hill, C. S.; Treisman, R. Integration of growth factor signals at the c-fos serum response element. Philos. *Trans. R. Soc. Lond. Biol.* **1996**, *351*, 551-559.

164. May, L. T.; Hill, S. J. ERK phosphorylation: spatial and temporal regulation by G protein-coupled receptors. *Int. J. Biochem. Cell Biol.* **2008**, *40*, 2013-2017.

165. van Biesen, T.; Hawes, B. E.; Raymond, J. R.; Luttrell, L. M.; Koch, W. J.; Lefkowitz, R. J. G_o-protein alpha-subunits activate mitogen-activated protein kinase via a novel protein kinase C-dependent mechanism. *J. Biol. Chem.* **1996**, *271*, 1266-1269.

166. Megson, A. C.; Walker, E. M.; Hill, S. J. Role of protein kinase Cα in signalling from the histamine H1-receptor to the nucleus. *Mol. Pharmacol.* **2001**, *59*, 1012-1021.

167. Shi, C. S.; Sinnarajah, S.; Cho, H.; Kozasa, T.; Kehrl, J. H. $G_{13\alpha}$-mediated PYK2 activation. PYK2 is a mediator of $G_{13\alpha}$-induced serum response element-dependent transcription. *J. Biol. Chem.* **2000**, *275*, 24470-24476.

168. An, S.; Zheng, Y.; Bleu, T. Sphingosine 1-phosphate-induced cell proliferation, survival, and related signalling events mediated by G-protein-coupled receptors Edg3 and Edg5. *J. Biol. Chem.* **2000**, *275*, 288-296.

169. Guardiola-Diaz, H. M.; Boswell, C.; Seasholtz, A. F. The cAMP-responsive element in the corticotrophin-releasing hormone gene mediates transcriptional regulation by depolarization. *J. Biol. Chem.* **1994**, *269*, 14784-14791.

170. Minneman K. P.; Lee, D.; Zhong, H.; Berts, A.; Abbott, K. L.; Murphy, T. J. Trancriptional responses to growth factor and G-protein-coupled receptors in PC12 cells: comparison of α1-adrenergic receptor subtypes. *J. Neurochem.* **2000**, *74*, 2392-2400.

171. Takeuchi, Y.; Fukunaga, K. Dopamine D2 receptor activates extracellular signal-regulated kinase through the specific region in the third cytoplasmic loop. *J. Neurochem.* **2004**, *89*, 1498–1507.

172. Wang, Y.; Ho, G.; Zhang, J. J.; Nieuwenhuijsen, B.; Edris, W.; Chanda, P. K.; Young, K. H. Regulator of G protein signaling Z1 (RGSZ1) interacts with G alpha i subunits and regulates Galpha i-mediated cell signaling. *J. Biol. Chem.* **2002**, *277*, 48325–48332.

173. Shankar, H.; Garcia, A.; Prabhakar, J.; Kim, S.; Kunapuli, S. P. $P2Y_{12}$ receptor-mediated potentiation of thrombin induced thromboxane A2 generation in platelets occurs through regulation of $Erk_{1/2}$ activation. *J. Thromb. Haemost.* **2006**, *4*, 638–647.

174. Garcia, A.; Shankar, H.; Murugappan, S.; Kim, S.; Kunapuli, S. P. Regulation and functional consequences of ADP receptormediated ERK_2 activation in platelets. *Biochem. J.* **2007**, *404*, 299–308.

175. Hoffmann, K.; Sixel, U.; Di Pasquale, F.; von Kügelgen, I. Involvement of basic amino acid residues in transmembrane regions 6 and 7 in agonist and antagonist recognition of the human platelet $P2Y_{12}$-receptor. *Biochem. Pharmacol.* **2008**, *76*, 1201-1300.

176. Schwarz, M. A.; Owaribe, K.; Kartenbeck, J.; Franke, W. W. Desmosomes and hemidesmosomes: constitutive molecular components. *Annu. Rev. Cell Biol.* **1990**, *6*, 461-491.

177. De Wet, J. R.; Wood, K. V.; De-Luca, M.; Helinski, D. R.; Subramani, S. Firefly luciferase gene: structure and expression in mammalian cells. *Mol. Cell Biol.* **1987**, *7*, 725-737.

178. Yan, Y. X.; Boldt-Houle, D. M.; Tillotson, B. P.; Gee, M. A.; D'Eon, B. J.; Chang, X. J.; Olesen, C. E.; Palmer, M. A. Cell-based high-throughput screening assay system for monitoring G protein-coupled receptor activation using beta-galactosidase enzyme complementation technology. *J. Biomol. Screen.* **2002**, *7*, 451-459.

179. Yin, H.; Chu, A.; Li, W.; Wang, B.; Shelton, F.; Otero, F.; Nguyen, D. G.; Caldwell, J. S.; Chen, Y. A. Lipid G protein-coupled receptor ligand identification using beta-arrestin PathHunter assay. *J. Biol. Chem.* **2009**, *284*, 12328-12338.

180. Mann, R.; Mulligan, R. C.; Baltimore, D. Construction of a retrovirus packaging mutant and its use to produce helper-free defective retrovirus. *Cell* **1983**, *33*, 153–159.

181. Miller, A. D.; Buttimore, C. Redesign of retrovirus packaging cell lines to avoid recombination leading to helper virus production. *Mol. Cell. Biol.* **1986**, *6*, 2895–2902.

182. Morgenstern, J. P.; Land, H. Advanced mammalian gene transfer: high titer retroviral vectors with multiple drug selection markers and a complementary helper-free packaging cell line. *Nucleic Acids Res.* **1990**, *18*, 3587–3590.

183. Burns, J. C.; Friedmann, T.; Driever, W.; Burrascano, M.; Yee, J. K. Vesicular stomatitis virus G glycoprotein pseudotyped retroviral vectors: concentration to very high titer and efficient gene transfer into mammalian and nonmammalian cells. *Proc. Natl. Acad. Sci. USA* **1993**, *90*, 8033–8037.

184. Emi, N.; Friedmann, T.; Yee, J.-K. Pseudotyped formation of murine leukemia virus with G protein of vesicular stomatitis virus. *J. Virol.* **1991**, *65*, 1202–1207

185. Markowitz, D.; Goff, S.; Bank, A. Construction and use of a safe and efficient amphoteric packaging cell line. *Virology* **1988**, *167*, 400-406.

186. Gorzalka, S. Neuartige G-Protein-gekoppelte Purinrezeptoren: Funktionelle Charakterisierung nativer Adeninrezeptoren und Evaluation neuer Purinrezeptor-Liganden. *Dissertation* **2006**, University of Bonn.

187. Schiedel, A. C.; Meyer, H.; Alsdorf, B. B.; Gorzalka, S.; Brüssel, H.; Müller, C. E. [^{3}H]Adenine is a suitable radioligand for the labeling of G protein-coupled adenine

receptors but shows high affinity to bacterial contaminations in buffer solutions. *Purinergic Signal.* **2007**, *3*, 347-358.

188. Müller C. E. Adenosine receptor ligands-recent developments part I. Agonists. *Curr. Med. Chem.* **2000**, *7*, 1269-1288.

189. Siddiqi, S. M.; Jacobson, K. A.; Esker, J. L.; Olah, M. E.; Ji, X. D.; Melman, N.; Tiwari, K. N.; Secrist, J. A. 3rd; Schneller, S. W.; Cristalli, G.; Stiles, G. L.; Johnson, C. R.; IJzerman, A. P. Search for new purine- and ribose-modified adenosine analogues as selective agonists and antagonists at adenosine receptors. *J. Med. Chem.* **1995**, *38*, 1174-1188.

190. Knospe, M. Klonierung, heterologe expression und charakterisierung von säugetier adeninrezeptoren. *Diplomarbeit* **2007**, University of Bonn.

191. Bussolari, J. C.; Ramesh, K.; Stoeckler, J. D.; Chen, S. F.; Panzica, R. P. Synthesis and biological evaluation of N^4-substituted imidazo- and v-triazolo[4,5-d]pyridazine nucleosides. *J. Med. Chem.* **1993**, *36*, 4113-4120.

192. Hillmann, P.; Ko, G. Y.; Spinrath, A.; Raulf, A.; von Kügelgen, I.; Wolff, S. C.; Nicholas, R. A.; Kostenis, E.; Höltje, H. D.; Müller, C. E. Key determinants of nucleotide-activated G protein-coupled $P2Y_2$ receptor function revealed by chemical and pharmacological experiments, mutagenesis and homology modeling. *J. Med. Chem.* **2009**, *52*, 2762-2775.

193. Müller, C. E.; Maurinsh, J.; Sauer, R. Binding of [^{3}H]MSX-2 (3-(3-hydroxypropyl)-7-methyl-8-(m-methoxystyryl)-1-propargylxanthine) to rat striatal membranes - a new, selective antagonist radioligand for A_{2A} adenosine receptors. *Eur. J. Pharm. Sci.* **2000**, *10*, 259-265.

194. Klotz, K. N.; Lohse, M. J.; Schwabe, U.; Cristalli, G.; Vittori, S.; Grifantini, M. 2-Chloro-N^6-[^{3}H]cyclopentyladenosine ([^{3}H]CCPA) - a high affinity agonist radioligand for A_1 adenosine receptors. *Naunyn. Schmiedebergs Arch. Pharmacol.* **1989**, *340*, 679-683.

195. Feoktistov, I.; Biaggioni, I. Adenosine A_{2B} receptors. *Pharmacol. Rev.* **1997**, *49*, 381-402.

196. Beukers, M. W., den Dulk, H.; van Tilburg, E. W.; Brouwer, J.; Ijzerman, A, P. Why are A_{2B} receptors low-affinity adenosine receptors? Mutation of Asn273 to Tyr increases affinity of human A_{2B} receptor for 2-(1-Hexynyl)adenosine. *Mol. Pharmacol.* **2000**, *58*, 1349-1356.

197. Baraldi, P. G.; Tabrizi, M. A.; Fruttarolo, F.; Romagnoli, R.; Preti, D. Recent improvements in the development of A$_{2B}$ adenosine receptor agonists. *Purinergic Signal.* **2008**, *4*, 287–303.

198. Kuno, A.; Critz, S. D.; Cui, L.; Solodushko, V.; Yang, X. M.; Krahn, T.; Albrecht, B.; Philipp, S.; Cohen, M. V.; Downey, J. M. Protein kinase C protects preconditioned rabbit hearts by increasing sensitivity of adenosine A$_{2b}$-dependent signaling during early reperfusion. *J. Mol. Cell Cardiol.* **2007**, *43*, 262-271.

199. Rosentreter, U.; Henning, R.; Bauser, M.; Krämer, T.; Vaupel, A.; Hübsch, W.; Dembowsky, K.; Salcher-schraufstätter, O.; Stasch, J. P.; Krahn, T.; Perzborn, E. Substituted 2-thio-3,5-dicyano-4-aryl-6-aminopyridines and the use thereof as adenosine receptor ligands. *WO Patent* **2001**, 025210.

200. Krahn, T.; Krämer, T.; Rosentreter, U.; Downey, J. M.; Solenkova, N. Use of substituted 2-thio-3,5-dicyano-4-phenyl-6-aminopyridines for the treatment of reperfusion injury and reperfusion damage. *WO Patent* **2006**, 099958.

201. Brooker, G.; Harper, J. F.; Terasaki, W. L.; Moylan, R. D. Radioimmunoassay of cyclic AMP and cyclic GMP. *Adv. Cyclic Nucleotide Res.* **1979**, *10*, 1-33.

202. Brown, B. L.; Albano, J. D.; Ekins, R. P.; Sgherzi, A. M. A simple and sensitive saturation assay method for the measurement of adenosine 3', 5'-cyclic monophosphate. *Biochem. J.* **1971**, *121*, 561-562.

203. Gilman, A. G. Regulation of cyclic AMP metabolism in cultured cells of the nervous system. *Adv. Cyclic Nucleotide Res.* **1972**, *1*, 389-410.

204. Doskeland, S. O.; Ueland, P. M. Binding proteins for adenosine 3':5'-cyclic monophosphate in bovine adrenal cortex. *Biochem. J.* **1977**, *165*, 561-573.

205. Nordstedt, C.; Fredholm, B. B. A modification of a protein-binding method for rapid quantification of cAMP in cell-culture supernatants and body fluid. *Anal. Biochem.* **1990**, *189*, 231-234.

206. Koetter, U.; Barrett, M.; Lacher, S.; Abdelrahman, A.; Dolnick, D. Interactions of Magnolia and Ziziphus extracts with selected central nervous system receptors. *J. Ethnopharmacol.* **2009**, *124*, 421-425.

207. Basheer, R.; Strecker, R. E.; Thakkar, M. M.; McCarley, R. W. Adenosine and sleep-wake regulation. *Prog. Neurobiol.* **2004**, *73*, 379-396.

208. Schellenberg, R.; Sauer, S.; Abourashed, E. A.; Koetter, U.; Brattström, A. The fixed combination of valerian and hops (Ze91019) acts via a central adenosine mechanism. *Planta. Med.* **2004**, *70*, 594-597.

209. Müller, C. E.; Schumacher, B., Brattström, A.; Abourashed, E. A.; Koetter, U. Interactions of valerian extracts and a fixed valerian-hop extract combination with adenosine receptors. *Life Sci.* **2002**, *71*, 1939-1949.

210. Lacher, S. K.; Mayer, R.; Sichardt, K.; Nieber, K.; Müller, C. E. Interaction of valerian extracts of different polarity with adenosine receptors: identification of isovaltrate as an inverse agonist at A_1 receptors. *Biochem. Pharmacol.* **2007**, *15,* 248-258.

211. Gachet, C.; Leon, C.; Hechler, B. The platelet P2 receptors in arterial thrombosis. *Blood Cell. Mol. Dis*. **2006**, *36*, 223-227.

212. Hollopeter, G.; Jantzen, H. M.; Vincent, D.; Li, G.; England, L.; Ramakrishnan, V.; Yang, R. B.; Nurden, P.; Nurden, A.; Julius, D.; Conley, P. B. Identification of the platelet ADP receptor targeted by antithrombotic drugs. *Nature* **2001**, *409*, 202-207.

213. El-Tayeb, A.; Griessmeier, K. J.; Müller, C. E. Synthesis and preliminary evaluation of [^{3}H]PSB-0413, a selective antagonist radioligand for platelet $P2Y_{12}$ receptors. *Bioorg. Med. Chem. Lett.* **2005,** *15*, 5450–5452.

214. K., Atzler. G-Protein-gekoppelte Rezeptoren als Arzneistoff-Targets: In-Vitro Charakterisierung neuer Liganden und Untersuchung der Wirkstoff-Rezeptor-Interaktion. *Dissertation.* **2006**, University of Bonn.

215. Adriouch, S.; Hubert, S.; Pechberty, S.; Koch-Nolte, F.; Haag, F.; Seman, M. NAD^+ released during inflammation participates in T cell homeostasis by inducing ART2-mediated death of naive T cells in vivo. *J. Immunol.* **2007**, *179*, 186–194.

216. Moreschi, I.; Bruzzone, S.; Nicholas, R. A.; Fruscione, F.; Sturla, L.; Benvenuto, F.; Usai, C.; Meis, S.; Kassack, M. U.; Zocchi, E.; De Flora, A. Extracellular NAD^+ is an agonist of the human $P2Y_{11}$ purinergic receptor in human granulocytes. *J. Biol. Chem.* **2006**, *281*, 31419-31429.

217. Klein, C.; Grahnert, A.; Abdelrahman, A.; Müller, C. E.; Hauschildt, S. Extracellular NAD^+ induces a rise in $[Ca^{2+}]_i$ in activated human monocytes via engagement of $P2Y_1$ and $P2Y_{11}$ receptors. *Cell Calcium* **2009**, *46*, 263-272.

218. Beigi, R. D.; Kertesy, S. B.; Aquilina, G.; Dubyak, G. R. Oxidized ATP (oATP) attenuates proinflammatory signaling via P2 receptor-independent mechanisms. *Br. J. Pharmacol*. **2003**, *140*, 507–519.

219. Khakh, B. S.; Humphrey, P. P.; Surprenant, A. Electrophysiological properties of P2X-purinoceptors in rat superior cervical, nodose and guinea-pig coeliac neurones. *J. Physiol. Lond.* **1995**, *484*, 385–395.

7. Abbreviations

A-317491	5-([(3-Phenoxybenzyl)[(1S)-1,2,3,4-tetrahydro-1-naphthalenyl]amino]carbonyl)-1,2,4-benzenetricarboxylic acid
AC	Adenylate cyclase
ADA	Adenosine deaminase
ADP	Adenosine diphosphate
AdeRs	Adenine receptors
AdoRs	Adenosine receptors
ALPHA screen	Amplified luminescent proximity homogeneous assay
AP-1	Activator protein 1
Ap_3A	Diadenosine triphosphate
A_3P_5PS	Adenosine-3'-phosphate-5'-phosphosulfate
ARC109318	2,3-Dihydroxy-4-(7-(2-phenylcyclopropylamino)-5-(propylthio)-3H-[1,2,3]triazolo[4,5-d]pyrimidin-3-yl)cyclopentanecarboxamide
ARC69931MX	N^6-(2-methylthioethyl)-2-(3,3,3-trifluoropropylthio)-β,γ-dichloromethylene ATP
ARC67085MX	2-Propylthio-D-β,γ-dichloromethylene-ATP
ATL146e	4-{3-[6-Amino-9-(5-ethylcarbamoyl-3,4-dihydroxytetrahydro-furan-2-yl)-9H-purin-2-yl]-prop-2-ynyl} cyclohexanecarboxylic acid methyl ester
ATP	Adenosine triphosphate
AZD	Astra-zene-ca drugs
AZD6140	3-{7-[2-(3,4-Difluoro-phenyl)-cyclopropylamino]-5-propylsulfanyl [1–3]triazolo[4,5-d]pyrimidin-3-yl}-5-(2-hydroxymethoxy)-cyclopentane-1,2-diol
BAY 60-6583	2-[6-Amino-3,5-dicyano-4-[4 (cyclopropylmethoxy)phenyl]pyridin-2-ylsulfanyl]acetamide
B_{max}	A measure of the density of the receptor in certain tissue
BSA	Bovine serum albumin
CADO	2-Chloroadenosine
cAMP	Cyclic adenosine-3´,5´-monophosphate
$[Ca^{2+}]_i$	Intracellular calcium concentration
$[Ca^{2+}]_c$	Cytosolic calcium concentration

CCPA	2-Chloro-N^6-cyclopentyladenosine
cDNA	Complementary DNA
GF/B	Glass fiber filter -type B
CGS 21680	2(4-((2-Carboxymethyl)phenyl)ethylamino)-5'-N-ethylcarboxamidoadenosine
Ci	Curie (1 Ci = 37 GBq)
Cl-IB-MECA	2-Chloro-N^6-(3-iodobenzyl)adenosine-5'-N methylcarboxamide
CPA	N^6-Cyclopentyladenosine
cpm	Counts per minute
CRE	cAMP response element
CREB	Response-element binding protein
CS-747	2-Acetoxy-5-(α-cyclopropylcarbonyl-2-fluorobenzyl)-4,5,6,7-tetrahydrothieno[3,2-c]pyridine hydrochloride
CVT-510	N-[3-(R)-tetrahydrofuranyl]-6-aminopurine riboside
CVT-3146	2-{4-[(Methylamino)carbonyl]- 1*H*-pyrazol-1-yl}adenosine
DAG	Diacylglycerol
DMSO	Dimethyl sulfoxide
DNA	Deoxyribonucleic acid
DPCPX	8-Cyclopentyl-1,3-dipropylxanthine
DRG	Dorsal root ganglion
EC_{50}	The molar concentration of an agonist, which produces 50% of the maximum possible response for that agonist (50 % Effective concentration)
E. coli	*Escherichia coli*
EDTA	Ethylene diamine tetra acetic acid
ELISA	Enzyme-linked immunosorbent assay
E-NTPD	Ecto-nucleoside triphosphate diphosphohydrolase
ERK	Extracellular-signal-regulated kinases
FCS	Fetal calf serum
FP	Fluorescence polarization
G418	Geneticin
GDP	Guanosine diphosphate
GFP	Green fluorescent protein
GPCRG	Protein-coupled receptors

GR79236	N-[(1S, trans)-2-hydroxycyclopentyl]adenosine
GTP	Guanosine triphosphate
h	Human
HBSS	Hanks buffer salt solution
HENECA	2-Hexynl-5'-N-ethylcarboxamidoadenosine
HEPES	4-(2-Hydroxyethyl)-1-piperazine ethanesulfonic acid
HS	Horse serum
HTRF	Homogeneous time-resolved fluorescence
HTS	High throughput screening assay
IBMX	Isobutylmethylxanthine
IC_{50}	The molar concentration of an antagonist, which produces 50 % of the maximum possible inhibitory response for that antagonist (50 % Inhibitory concentration)
IP_5I	Diinosine pentaphosphate
IP_3	Inositol 1,4,5-trisphosphate
IU	International units
K_A	Association binding constant
k_{+1}	Rate constant for association
k_{-1}	Rate constant of dissociation
K_b	The dissociation constant for the binding of the antagonist
K_D	Dissociation binding constant (is the affinity of the radioactive ligand for the receptor)
kDa	Kilo Dalton
K_i	Inhibition constant
K_D	Dissociation binding constant
KHP	Krebs-Hepes buffer
KO	Knockout
k_{ob}	The observed rate constant
KW-6002	(E)-8-(3,4-dimethoxystyryl)-1,3-diethyl-7-methyl-1*H*-purine-2,6(3*H*,7*H*)-dione
L-268605	(3-(4-Methoxyphenyl)-5-amino-7-oxothiazolo[3,2]pyrimidine
L	Ligand
LG-medium	Lysogeny broth-medium
LPS	Lipopolysaccharide

LR	Ligand-receptor complex
LSC	Liquid Scintillation Counter
M	Magnolia
m	Mouse
MAPK	Mitogen-activated protein kinases
min	Minutes
MRE 2029-F20	N-[1,3] benzodioxol -5-yl-2-[5-(2,6-dioxo-1,3-dipropyl-2,3,6,7-tetra hydro-1*H*-purin-8-yl)-1-methyl-1*H*-pyrazol-3-yloxy]-acetamide
mRNA	Messenger ribonucleic acid
MRS	Molecular recognition section
MRS2365	(1′S,2′R,3′S,4′R,5′S)-4-[(6-amino-2-methylthio-9Hpurin-9-yl)-1-diphosphoryloxymethyl]bicyclo[3.1.0]hexane-2,3-diol
MRS3997	2-(3′′-(6′′-Bromoindolyl)ethyloxy)adenosine
MRS2179	2'-Deoxy-N^6-methyladenosine 3',5'-bisphosphate
MRS2279	2-Chloro-N^6-methyl-(*N*) methanocarba-2'-deoxyadenosine-3',5'-bisphosphate
MRS1220	9-Chloro-2-(2-furyl) [1,2,4]triazolo[1,5-c]quinazolin-5-phenylacetamide
MRS1523	5-Propyl 2-ethyl-4-propyl-3-(ethylsulfanylcarbonyl)-6-phenylpyridine-5-carboxylate
MRS1191	3-Ethyl-5-benzyl-2-methyl-4-phenylethynyl-6-phenyl-1,4-(±)-dihydropyridine-3,5-dicarboxylate
MRS1706	N-(4-Acetylphenyl)-2-[4-(2,3,6,7-tetrahydro-2,6-dioxo-1 ,3-dipropyl-1*H*-purin-8-yl)phenoxy]acetamide
MRS1754	N-(4-Cyanophenyl)-2-[4-(2,3,6,7-tetrahydro-2,6-dioxo-1, 3-dipropyl-1*H*-purin-8-yl)phenoxy]-acetamide
MSX-2	3-(3-Hydroxypropyl)-7-methyl-8-(*m*-methoxystyryl)-1-propargyl-xanthine
MSX-3	3-(3-Hydroxypropyl)-8-(m-methoxystyryl)-7-methyl-1-propargylxanthine-phosphate-disodium salt
MSX-4	L-valine-3-{8-[(E)-2-[3-methoxyphenyl)ethenyl]-7-methyl-1-propargylxanthine-3-yl}propyl ester hydrochloride
NAD	Nicotinamide adenine dinucleotide

NECA	5′-N-ethylcarboxamidoadenosine
NF279	8,8'-(Carbonylbis(imino-4,1 -phenylenecarbonylimino-4,1-phenylenecarbonylimino))bis(1,3, 5-naphthalenetrisulfonic acid)
NF449	4,4',4'',4'''-[Carbonylbis(imino-5,1,3-benzenetriyl-bis (carbonylimino))]tetrakis-1,3-benzenedisulfonic acid, octasodium salt
NFAT-RE	Nuclear factor of activated T cells
NS	Non-specific binding
Orgen Green AM	Oregon Green acetoxymethylester
P2	Second pellet
PBS	Phosphate buffered saline
pEC_{50}	$-\log EC_{50}$
PEI	polyethyleneimine
PIA	N^6- Phenylisopropyl adenosine
PI3Kγ	Phosphoinositol 3-kinaseγ
PIP2	Phosphatidylinositol-4,5-bisphosphate
pK_B	$-\log K_B$
PKC	Protein kinase C
PLC	Phospholipase C
PDE	Phosphodiesterase
PMSF	Phenylmethanesulfonylfluoride
PPADS	Pyridoxal-phosphate-6-azophenyl-2´,4´-disulfonate
PPi	Pyrophosphate
PSB	Pharmaceutical Sciences Bonn
PSB-0413	2-Propylthioadenosine-5´-adenylic acid (1,1-dichloro-1-phosphonomethyl-1-phosphonyl) anhydride
PSB-10	8-Ethyl-1,4,7,8-tetrahydro-4-methyl-2-(2,3,5-trichlorop henyl)-5H-imidazo[2,1-i]purin-5-one monohydrochloride
PSB-11	3H-8-ethyl-4-methyl-2-phenyl-(8R)-4,5,7,8-tetrahydro-1*H*-imidazo[2.1-i]purin-5-one
PSB-298	(8-{4-[2-(2-Hydroxyethylamino)-2-oxoethoxy]phenyl}-1-propylxanthine
PSB-603	8-[4-[4-(4-Chlorophenzyl)piperazide-1-sulfonyl)phenyl]] -1-propylxanthine

PSB-36	1-Butyl-8-(hexahydro-2,5-methanopentalen-3a(1*H*)-yl)-3,7-dihydro-3-(3-hydroxypropyl)-1*H*-purine-2,6-dione
PSB-1115	1-Propyl-8-p-sulfophenylxanthine
PTX	Pertussis toxin
R	Receptor
r	Rat
RO-3	5-[[4,5-Dimethoxy-2-(methylethyl)phenyl]methyl]-2,4-pyrimidinediamine
Ro20-1724	4-(3-Butoxy-4-methoxyphenyl)methyl-2-imidazolidone
RT	Room temprature
RT-PCR	Reverse transcription polymerase chain reaction
SCG	Superior cervical ganglia
SCH420814	[7-[2-[4-2,4-Difluorophenyl]-1-piperazinyl]ethyl]-2-(2-furanyl)-7*H*-pyrazolo[4,3-e][1,2,4]triazolo[1,5-c]pyrimidin-5-amine]
SCH58261	2-(2-Furanyl)-7-(2-phenylethyl)-7*H*-pyrazolo[4,3-e][1,2,4]triazolo[1,5-c]pyrimidin-5-amine
s	Seconds
S-ENBA	S-N^6-(2-endo-norbornyl)adenosine
S.E.M	Standard error of the mean
SRE	Serum response element
TAE	Tris-acetate-EDTA buffer
TB	Total binding
TRIS	2-Amino-2-hydroxymethyl-propane-1,3-diol (Tris(hydroxyl methyl)amino methane)
TM	Transmembrane
Tm	Melting temperature
TNP-ATP	2′,3′-O-(2,4,6- trinitrophenyl)adenosine 5′-triphosphate
TR-FRET	Time-resolved fluorescence resonance energy transfer
Triton X-100	t-Octylphenoxypolyethoxyethanol
UDP	Uridine diphosphate
UTP	Uridine triphosphate
UV	Ultraviolet
vs.	Versus
VSV-G	Envelope glycoprotein from the vesicular stomatitis virus

VT160	N^6-methoxy-2-(2-pyridinyl)-ethynyl-5´-N methylcarboxamidoadenosine
VUF5574	N-(2-Methoxyphenyl)-N′-[2-(3-pyridinyl)-4-quinazolinyl]-urea
VUF8504	4-Methoxy-*N*-[2-(2-pyridinyl)quinazolin-4-yl]benzamide
WRC-0571	8-(N-methylisopropyl)amino-N^6-(5'-endohydroxy- endonorbornyl)-9-methyladenine
WT	Wild type
ZM241385	4-(2-[7-Amino-2-(2-furyl)[1,2,4]triazolo[2,3-a][1,3,5]triazin-5-ylamino]ethyl)phenol
Z	Ziziphus

8. Curriculum Vitae

1. *Scholarship:*

   DFG Scholarship (GRK 804) 01.10.06 - 30.09.09.

2. *Patent*

   Müller, C. E.; Borrmann, T.; **Abdelrahman, A.** Adenine receptor ligands. European patent office, Nr. 08011782.3, **2008**.

3. *List of publications*

   ❖ El-Tayeb, A.; **Abdelrahman, A.;** Müller C. E.; Baqi Y. Medicinal chemistry of P2Y$_{12}$ receptors. *Manuscript in preparation.*

❖ **Abdelrahman**, A.; Müller, C. E. et. al. Characterization of [^{3}H]PSB-0413, a selective radioligand for P2Y$_{12}$ receptors. *Manuscript in preparation*.

❖ **Abdelrahman**, A.; Müller, C. E. et. al. Development of potent agonists and the first antagonists for adenine receptors. *Manuscript in preparation*.

❖ Klein, C.; Grahnert, A.; **Abdelrahman, A.**; Müller, C. E.; Hauschildt, S. Extracellular NAD$^+$ induces a rise in [Ca^{2+}]$_i$ in activated human monocytes via engagement of P2Y$_1$ and P2Y$_{11}$ receptors. *Cell Calcium*. **2009**, *46*, 263-272.

❖ Borrmann, T.; **Abdelrahman, A.**; Volpini, R.; Lambertucci, C.; Alksnis, E.; Gorzalka, S.; Schiedel, A. C.; Cristalli, G.; Müller, C. E. Synthesis and characterization of adenine and deazaadenine derivatives as ligands for adenine receptors, a new purinergic receptor family. *J. Med. Chem*, **2009**, *52*, 5974-89.

❖ Koetter, U.; Barrett, M.; Lacher, S.; **Abdelrahman, A.**; Dolnick, D. Interactions of Magnolia and Ziziphus extracts with selected central nervous system receptors. *J. Ethnopharmacol.*, **2009**, *124*, 421-5.

❖ von Kügelgen, I.; Schiedel, A. C.; Hoffmann, K.; Alsdorf, B. B.; **Abdelrahman, A.**; Müller, C. E. Cloning and functional expression of a novel G$_i$ protein-coupled receptor for adenine from mouse brain. *Mol. Pharmacol.*, **2008**, *73*, 469-77.

❖ Zlotos, D. P.; Tränkle, C.; **Abdelrahman, A.**; Gündisch, D.; Radacki, K.; Braunschweig, H.; Mohr, K. 6*H*,13*H*-Pyrazino[1,2-a;4,5-a']diindole analogs: probing the pharmacophore for allosteric ligands of muscarinic M2 receptors. *Bioorg. Med. Chem. Lett.*, **2006**, *16*, 1481-5.

5. *List of poster presentations*

➢ Borrmann, T.; Bauer, L. M.; **Abdelrahman, A.**; Müller, E. C. Synthesis and pharmacological characterization of N^6- and 8-substituted adenine derivatives as ligands for the recently discovered adenine receptors. *Purines* 2010, 29 May-2 June **2010**, Tarragona, Spain (Poster).

➢ **Abdelrahman, A.**; Atzler, K.; El-Tayeb, A.; Müller, C. E. Characterization of [³H]PSB-0413, the first selective radioligand for P2Y$_{12}$ receptors. Third joint Italian-German purine club meeting, July **2009**, Camerino, Italy (Poster).

➢ Knospe, M.; Schiedel, C. A.; Alsdorf, B. B.; **Abdelrahman, A.**; Seifert, R.; I von Kügelgen, I.; Müller, C. E. Heterologous expression of adenine receptors in Sf9 cells. Third joint Italian-German purine club meeting, July **2009**, Camerino, Italy (Poster).

➢ Alsdorf, B. B.; Schiedel, A. C.; **Abdelrahman, A.**; Borrmann, T.; von Kügelgen, I.; Müller, C. E. Expression and characterization of a novel mouse adenine receptor (mAde2) in Sf21 insect cells. *GRK 677 Minisymposium* **2009**, Bonn (Poster).

➢ **Abdelrahman, A.**; Schiedel, C. A.; Bernt, B. A. A.; Hoffmann, H.; von Kügelgen, I.; Müller, C. E. Characterization of a novel mouse adenine receptor by radioligand binding and functional experiments. *DPhG Jahrestagung* **2008**, Bonn (Poster).

➢ Borrmann, T.; **Abdelrahman, A.**; Gorzalka, S.; Schiedel, A. C.; Müller, C. E. Synthesis and structure-activity relationships of new adenine derivatives as ligands for the rat adenine receptor. *DPhG Jahrestagung* **2008**, Bonn (Poster).

➢ Borrmann, T.; **Abdelrahman, A.**; Gorzalka, S.; Schiedel, A. C.; Müller, C. E. Synthesis and structure-activity relationships of new adenine derivatives as ligands for the rat adenine receptor. *Purines Meeting* **2008**, Copenhagen (Denmark) (oral presentation).

➢ **Abdelrahman, A.**; Schiedel, C. A.; Bernt, B. A. A.; Hoffmann, H.; von Kügelgen, I.; Müller, C. E. Characterization of a novel mouse adenine receptor by radioligand binding and functional experiments. *Purines Meeting* **2008**, Copenhagen (Denmark) (Poster). Abstract in: *Purinergic Signalling* **2008**, *4 (Suppl 1)*, 194

➢ Alsdorf, B. B. A.; Schiedel, A. C.; **Abdelrahman, A.**; Meyer, H.; Borrmann, T.; Gorzalka, S.; von Kügelgen, I.; Müller, C. E. Evaluation of adenine derivatives as ligands for the novel G proteincoupled adenine receptors. *Frontiers in Medicinal Chemistry* **2008**, Regensburg (Poster).

➢ Borrmann, T.; **Abdelrahman, A.**; Gorzalka, S.; Schiedel, A. C.; Müller, C. E. Synthesis and structure-activity relationships of new adenine derivatives as ligands for the rat adenine receptor. Abstract in: *Purinergic Signalling* **2008**, *4 (Suppl 1)*, 13.

➢ Konspe, M.; Alsdorf, B. B. A.; **Abdelrahman, A.;** Schiedel, A. C.; von Kügelgen, I.; Müller, C. E. Heterogeneous expression of adenine receptors in non-mammalian cells. Second joint Italian-German purine club meeting, September 2007, Leipzig, Germany.

➢ Von Kügelgen, I; Schiedel, A. C.; Hoffmann, K; Alsdorf, B. B. A; **Abdelrahman, A.;** Müller, C. E. Cloning and functional expression of a novel G_i protein-coupled receptor for adenine from mouse brain. Abstract in: *Naunyn-Schmiedeberg´s Arch Pharmacol* **2007**, 375 *(Suppl. 1),* 27.

➢ Heiko Meyer, H.; **Abdelrahman, A.;** Gorzalka, S.; Schiedel, A. C.; Müller, C. E. Labelling of rat and human adenine binding sites.*GRK 677 Minisymposium* **2006**, Bonn (Poster).

6. **Workshops**

➢ Database search strategies in molecular biology and 3D models. Dr. Anke Schiedel (November 2009).

➢ Ligand/receptor-interaction: parameters, computer-assisted data analysis and presentation organized by PD Dr. Christian Tränkle. (September 2009).

➢ Combinatorial biosynthesis and heterologous production of new natural products. Organized by Prof. Dr. Jörn piel (November 2008).

➢ Light and fluorescence microscopy. Workshop organized by Prof. Dr. Michael Hoch (June, 2008).

➢ 7-Transmembrane Receptors as Drug Targets Workshop organized by Prof. Dr. Christa E. Müller (May 31 – June 2, 2007).

➢ "Radiopharmazie I - Grundkurs zur Erlangung der Fachkunde im Strahlenschutz nach § 30 StrlSchV" der Rheinischen Friedrich-Wilhelms-Universität Bonn (Wintersemester 2005).

➢ „Rezeptor-Bindungsuntersuchungen – Theorie und Praxis" (Wintersemester 2005).

9. Acknowledgment